
THE UNIVERSITY *of* EDINBURGH

# *Gli3* regulates the proliferation and differentiation of progenitors in the developing neocortex

**Alexandra L Kelman**

**Thesis submitted for the degree of**

**Doctor of Philosophy**

**The University of Edinburgh**

**2019**

*“Learning never exhausts the mind”*

**Leonardo da Vinci**

## Disclaimer

I (Alexandra Kelman) declare that this thesis has been composed solely by myself and that it has not been submitted, in whole or in part, in any previous application for a degree. Except where states otherwise by reference or acknowledgment, the work presented is entirely my own.

Signed……

Date……

## Contents

## List of figures

## List of tables

## Acknowledgements

Firstly, I would like to extend my greatest thanks to my supervisors Thomas Theil and John Mason. Without their help, I would never have arrived at this point and I am hugely grateful for everything they have done and for their massive patience with me. They have helped me in all aspects of my project, from practical work to my writing to allowing me to vent my frustrations.

I would also like to thank Kerstin Hasenpusch-Theil for all her help both in the lab and out. Her help has been invaluable to me and I couldn't have completed my project without her. Stephen West, Da Mi, Eamon Fitzgerald, Jini Basu, Mike Molinek, Vivian Alison, Louise Dunn, Hannah Parkin, Jim Clegg, Vassiliki Fotaki and Andrew Jarman have all helped me enormously as well, for which I'm grateful.

I've had great support from everyone in the DBUG labs, who have all given me good feedback on my work and made really useful suggestions. Altogether, the huge input I've received shaped my project and allowed me to finish.

Finally, I want to thank my family and friends, in particular my fiancé James for putting up with me for the last few years and supporting me to finally arrive at this point.

## Abstract

The cerebral cortex is a highly complex, layered, grey matter structure which plays major roles in processes such as consciousness, memory, and perception. In humans, it is the cortex which bestows us with cognitive abilities unique to our species, in part due to the massive expansion of cortical progenitors during embryonic development. The mature cortex of mammals is composed of a highly heterogenous population of cells, however only the glutamatergic projection neurons are generated within the embryonic neocortex itself. These cells are formed from apical and basal cortical progenitors in the developing dorsal telencephalon, and in the mouse cortical neurogenesis begins at approximately embryonic day 10.5 (E10.5).

Regulation of the differentiation of progenitors into neurons is a tightly regulated process, under the control of a strict interplay between signalling molecules and transcription factors. The zinc-finger transcription factor *Gli3* plays established roles in regulating the development of the dorsal telencephalon. Through the evaluation of a number of mutants, *Gli3* has been shown to function in patterning, the production and fate of cortical neurons, lamination, and axon tract formation, amongst other things. It is shown here that Gli3 is highly expressed in $Pax6^{+}$ apical progenitors in the dorsal telencephalon, the largest population of progenitors between E11.5 and E12.5. The aim of this thesis was to evaluate how *Gli3* regulates the proliferation and differentiation of cortical progenitors into neurons during these time points in the mouse.

Embryos of the $Gli3^{Xt/Pdn}$ mutant, which exhibit a reduction in Gli3, were used. At E11.5, the proportions of apical, basal, and early-born cortical neurons were altered in the dorsal telencephalon of the mutant. Microarray analysis revealed an up-regulation of *Cdk6* in $Gli3^{Xt/Pdn}$ embryos compared to control. Cdk6 is required for the transition from G1-phase into S-phase during the cell cycle, and shortening of G1-phase has been shown to correlate with progenitors self-renewing instead of differentiating. In agreement with the function of Cdk6, G1-phase and the length of the total cell cycle were shortened in the E11.5 $Gli3^{Xt/Pdn}$ mutant. At E12.5, the length of G1-phase and total cell cycle length were also shortened, and the proportion of apical and basal progenitors and early-born neurons were altered. It appears as though there is a delay in apical progenitor differentiation into basal progenitors and

neurons in the *Gli3*$^{Xt/Pdn}$ embryo, which correlates with the shortening of G1-phase observed. Interestingly, the length of S-phase was also decreased in the mutant at both E11.5 and E12.5, despite no obvious candidates indicative of S-phase regulation being identified in the microarray screen. Taken together, the evidence demonstrates that Gli3 plays a key role in regulating the differentiation of cortical progenitors at the correct time, likely in part due to regulation of the cell cycle, in order to regulate growth of the cerebral cortex.

## Abbreviations

| | |
|---|---|
| BrdU | 5-Bromo-2′-deoxyuridine |
| Cdks | Cyclin-dependent kinases |
| CdkIs | Cyclin-dependent kinase inhibitors |
| ChIP | Chromatin immunoprecipitation |
| CNS | Central nervous system |
| CP | Cortical plate |
| CR cells | Cajal-Retzius cells |
| Ctx | Cortex |
| G0-phase | Gap 0-phase |
| G1-phase | Gap 1-phase |
| G2-phase | Gap 2-phase |
| GO | Gene ontology |
| hESCs | Human embryonic stem cells |
| IdU | 5-Iodo-2′-deoxyuridine |
| IZ | Intermediate zone |
| LGE | Lateral ganglionic eminence |
| MGE | Medial ganglionic eminence |
| M-phase | Mitosis |
| MZ | Marginal zone |
| NE | Neuroepithelium |
| NeSCs | Neuroepithelial stem cells |
| PSPB | Pallial-subpallial boundary |
| PNS | Peripheral nervous system |

| | |
|---|---|
| RGCs | Radial glia cells |
| RNAseq | RNA sequencing |
| S-phase | Synthesis phase |
| SVZ | Subventricular zone |
| VZ | Ventricular zone |

# Chapter 1: Introduction

## 1.1 Early embryogenesis

The mature mammalian nervous system can be subdivided into two main components: the central nervous system (CNS), comprising the brain and spinal cord, and the peripheral nervous system (PNS), comprising all nervous tissue outside of the CNS. The PNS receives information from within and without the body and transmits it to the CNS, which collates and processes that information. The CNS then determines an appropriate response, which it transmits back to the PNS to produce that response (Purves *et al.*, 2008). Development of both the CNS and PNS occurs in the womb, and failure in this process can have major implications postnatally resulting in intellectual and physical disabilities. Therefore, study of embryonic nervous system development is vital.

The focus of this thesis is development of the cerebral cortex, the most anterior part of the brain. The mature cerebral cortex is a six-layered structure comprised of glutamatergic projection neurons, GABAergic interneurons and glia (Molyneaux *et al.*, 2007) , and plays major roles in consciousness, memory, attention, language, and thought. Whilst the focus here will be development of the cortex *in utero*, it is important to remember that postnatal modifications including the production of new neurons and neuronal cell death will occur throughout an organism's lifetime (Lindsey *et al.*, 2018). Development of the cortex was studied using the mouse as a model.

Following fertilisation of an egg by a sperm cell, a zygote is formed which will go on to form the embryo. The fertilised cell will divide within the zona pellucida, a membrane which surrounds the egg until implantation. The fertilised egg will undergo multiple rounds of division within the confines of the zona pellucida, during a process called cleavage, to form a morula (Maître, 2017). Following cleavage, the cells begin to cluster in the middle of the zona pellucida and the cells on the outside differentiate. The outer layer is comprised of cells known as trophoblasts, whilst the cells in the middle are known as embryoblasts. Between embryonic days 3.0-4.0 (E3.0-4.0) in the mouse the embryoblasts begin to cluster at one end of the morula, forming the

inner cell mass. This leaves a cavity at the other end called the blastocoel, creating a structure called the blastocyst. During this process, the zona pellucida degenerates, leaving the trophoblasts as the outer layer of cells and allowing implantation into the uterine wall to occur (Price *et al.*, 2011; Yamanaka *et al.*, 2006).

At E5.0 in the mouse, the inner cell mass restructures to form the amniotic cavity in the middle, and the layer of embryoblasts bisecting the middle of the trophoblast outer layer differentiate to form hypoblasts and epiblasts. Collectively, the two layers of epiblasts and hypoblasts form the bilaminar disc (Morris *et al.*, 2010). Following this, the process of gastrulation occurs at around E6.0. Cells along the centre of the epiblast layer begin to migrate forming a line known as the primitive streak, which is first recognisable at E6.5, through which they pass to form a layer of cells between the hypoblasts and epiblasts (Tam *et al.*, 1993). A trilaminar disc has now formed composed of the three germ layers. The layer formed from epiblasts is now known as the ectoderm, the newly formed middle layer is the mesoderm and the layer formed from hypoblasts is the endoderm. The ectoderm will give rise to the surface ectoderm, which will develop into for example skin and hair, the neural crest, which will give rise to the PNS, and the neural tube, which will form the CNS (Favarolo & López, 2018).

After gastrulation, neurulation begins at approximately E7.0. Underneath where the primitive streak was located, cells in the mesoderm begin to differentiate and form a chord-like structure known as the notochord, which expresses Sonic Hedgehog (Shh). Bone morphogenetic proteins (BMP) and Wingless-Type MMTV Integration Site Family Members (Wnt) inhibitors expressed in the node of the primitive streak prevent the ectoderm from taking on a surface ectoderm fate, instead inducing a neuroectodermal fate. The neuroectoderm thickens and flattens, forming the neural plate. The mediolateral, dorsoventral, and rostrocaudal/anteroposterior axes of the embryo are formed, with the notochord running down the midline at the ventral surface of the forming neural tube, and the notochord running along the anteroposterior axis. The midline of the neural plate anchors to the notochord whilst the lateral edges of the plate begin to fold dorsally. In the mouse, the lateral edges of the neural plate first fuse together at the hindbrain/cervical boundary. This fusion then runs both anteriorly and posteriorly, resulting in the neural tube. The anterior most end of the neural tube closes around E8.0-E8.5, where the forebrain and eventual cerebral cortex will form (Vermeren & Keynes, 2010, Colas & Schoenwolf, 2001) (figure 1.1).

The anterior end of the neural tube begins to bulge and can be subdivided into three primary brain vesicles anteroposteriorly; the prosencephalon (forebrain), mesencephalon (midbrain), and rhombencephalon (hindbrain). The posterior end of the neural tube will form the spinal cord. The primary brain vesicles will develop further into the secondary brain vesicles. The prosencephalon will subdivide to form the telencephalon, giving rise to the cerebrum, and the diencephalon, giving rise to the hypothalamus, thalamus, and optic vesicles. The mesencephalon will give rise to the midbrain. Finally, the rhombencephalon will subdivide into the metencephalon, giving rise to the cerebellum and pons, and the myelencephalon, giving rise to the medulla oblongata (Ishikawa *et al.*, 2012; Kiecker & Lumsden, 2005) (figure 1.2). The focus of this thesis is development of the early dorsal telencephalon into the cortex.

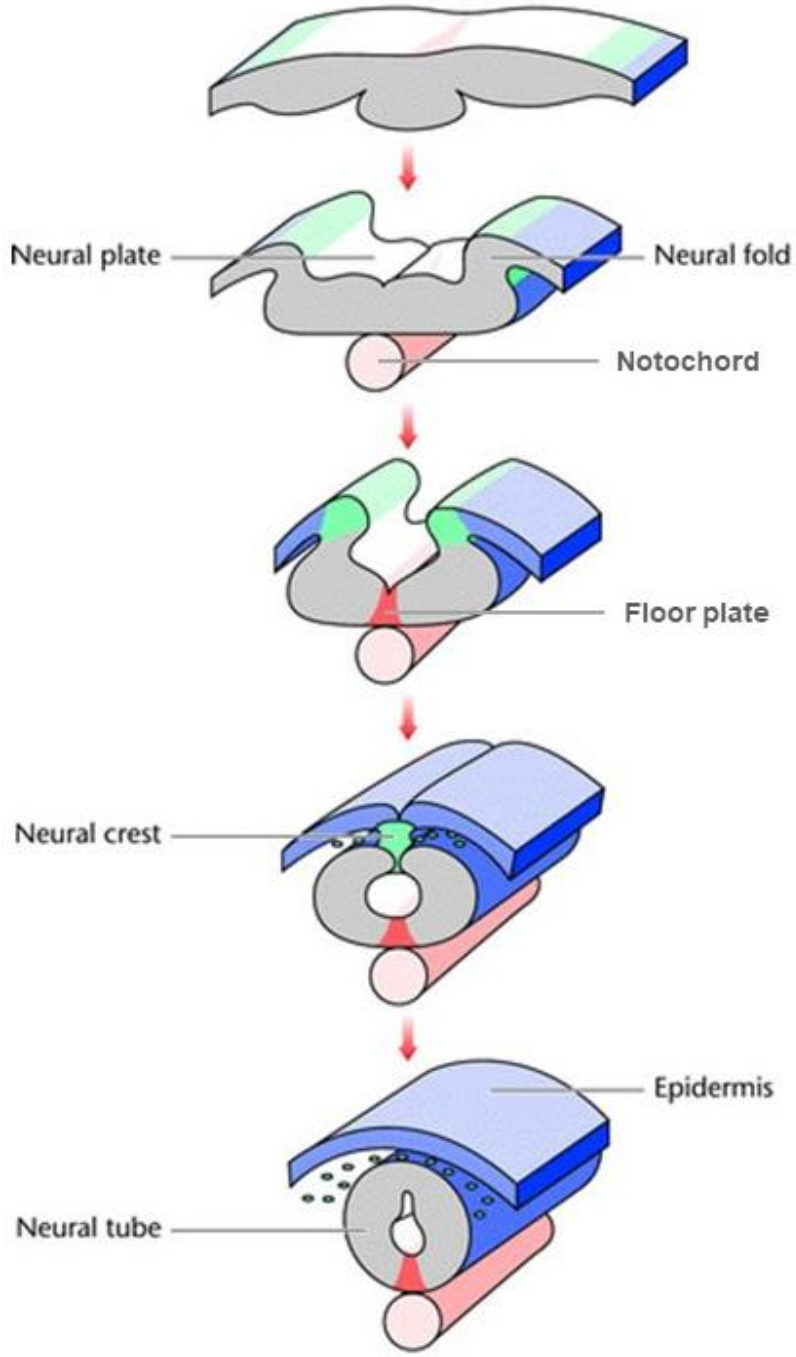


**Figure 1.1: Primary neurulation.** A schematic showing the process of neural tube formation in a transverse section through the anteroposterior axis. Neural crest cells are shown in green, neuroectoderm and surface ectoderm are shown in blue, and the notochord and floor plate are shown in orange. Modified from Vermeren & Keynes (2010).

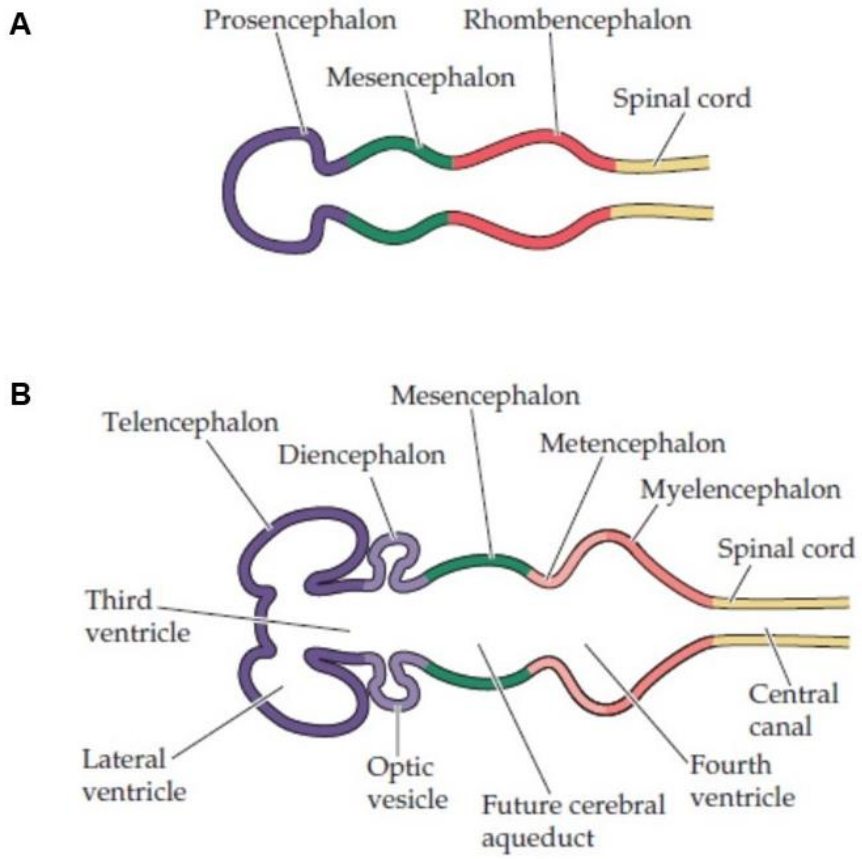


**Figure 1.2: Brain vesicles. A.** Schematic showing the primary brain vesicles, prosencephalon in blue, mesencephalon in green, and rhombencephalon in red, with the spinal cord shown in yellow. **B.** Schematic showing the secondary brain vesicles, telencephalon and diencephalon in blue and light blue, mesencephalon in green, metencephalon and myelencephalon in red and pink, with the spinal cord in yellow. Purves *et al.* (2008).

## 1.2 Telencephalic patterning

The mechanisms by which the neural tube becomes regionalised into the brain vesicles, which then further differentiate into different brain regions, are complex. The homogenous population of neuroectodermal cells of the neural tube must somehow form the wide variety of cells which make up the mature brain. This is regulated by the interplay of both cell intrinsic and extrinsic factors, which are in part determined by the location of a cell and so which signalling molecules it is being exposed to, the duration that that cell is exposed to the signals it is receiving, and the competency of that cell to respond to those signals.

The telencephalon can be divided into two parts, the dorsal telencephalon or pallium, which gives rise to the cerebral cortex, and the ventral telencephalon or subpallium, which gives rise to the basal ganglia. Throughout the dorsal and ventral telencephalon, there are a number of major signalling centres which secrete morphogens to assist in patterning the forebrain. Beginning in the ventral telencephalon, whilst the notochord does not extend so far rostrally into the telencephalon, a homologous tissue known as the prechordal plate exits in the ventral telencephalon which expresses *Shh* and noggin, a BMP inhibitor. The prechordal plate induces *Shh* expression in the ventral telencephalon, creating a high-ventral to low-dorsal *Shh* gradient. Conversely, the roof plate is formed where the two lateral edges of the neural plate fused, along the dorsal midline (Chizhikov & Millen, 2004). The non-neural/epidermal ectoderm which flanks the roof plate is a source of BMPs, which in turn induce expression of *BMP4* in the roof plate, creating a high-dorsal to low-ventral expression pattern, complimentary to that of *Shh*. The roof plate is also a source of Wnts (Chizhikov & Millen, 2004). As forebrain development progresses, the cells of the roof plate begin to invaginate as the two cerebral hemispheres form. The roof plate specifies a new signalling centre in the midline of the cortical hemispheres ventral to the hippocampus primordium and dorsal to the choroid plexus (Grove *et al.*, 1998), the cortical hem (Gupta & Sen, 2016). The cortical hem is identifiable from E9.5 in the mouse and is defined by the expression of *Wnt3a, Wnt5a*, and *Wnt2b* (Grove *et al.*, 1998) and a number of BMPs (Furuta *et al.*, 1997). It is required for mediolateral dorsal telencephalon patterning. Rostrally, the anterior neural ridge (ANR) is a major source of Fibroblast Growth Factors (Fgfs), which regulate the

anteroposterior patterning of the dorsal telencephalon (Shimamura & Rubenstein, 1997). Finally, located in the lateral telencephalon at the boundary between the dorsal and ventral telencephalons, also known as the pallial/subpallial boundary, is the antihem. This forms later, at approximately E12.5-E13.5 and expresses *Fgf7*, *Fgf15*, *Sfrp2* (a secreted *Wnt* antagonist), and three members of the Epidermal Growth Family (*EGF*) *Tgf*$\alpha$, *Neuregulin 1* and *Neuregulin 3* (Borello *et al.*, 2008; Assimacopoulos *et al.*, 2003). At the moment, the function of the antihem in patterning remains unclear. (Figure 1.3).

The secreted molecules produced by these signalling molecules each create a high-to-low gradient of expression as distance from their source is increased, creating highly regulated spatial patterning across the developing telencephalon. Cells in discrete locations will be exposed to differing concentrations of morphogens, thereby allowing them to express specific transcription factors. These transcription factors are then able to regulate the progression of neuronal development, allowing the differentiation of progenitors to form the heterogeneous populations of cells which comprise the mature brain.

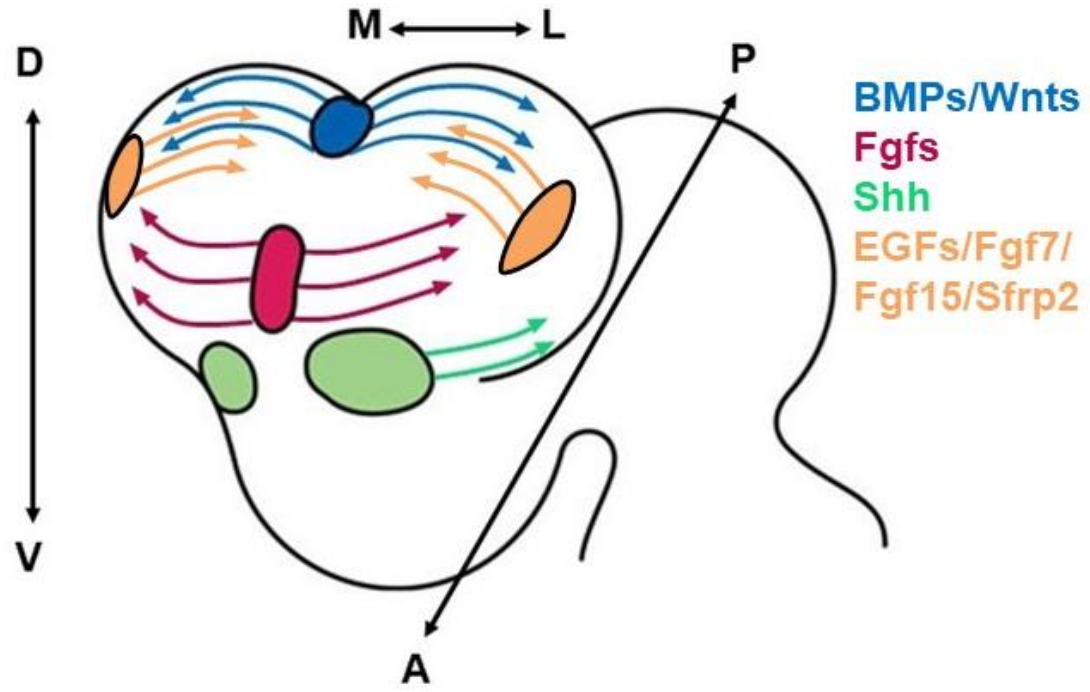


**Figure 1.3: Signalling centres of the developing telencephalon.** A schematic showing an E12.5 mouse telencephalon with the signalling centres depicted with the morphogens they secrete and the anteroposterior (A-P), dorsoventral (D-V) and mediolateral (M-L) axes. The cortical hem is shown in blue in the midline of the dorsal telencephalon where the neural tube invaginates to create the two cerebral hemispheres, from which BMPs and Wnts are secreted. The antihem (yellow) is located along the lateral edge of the telencephalon at the pallial/subpallial boundary, which secretes EGFs, Fgf7, Fgf15, and Sfrp2. The anterior neural ridge is shown in red at the rostral end of the dorsal telencephalon, from where Fgfs are secreted. Finally, the floor plate is shown in the ventral telencephalon in green from which Shh is secreted. Modified schematic from Thomas Theil.

### *1.2.1 Shh*

*Shh* is a member of the Hedgehog family of signalling proteins, alongside Desert Hedgehog and Indian Hedgehog, and mediates signalling from the notochord, prechordal plate and floor plate. Expression of *Shh* is first detectable in the primitive streak during the late stages of gastrulation in the midline of the mesoderm. From here the notochord forms and continues to express *Shh*, which then diffuses into the overlying ectoderm promoting ventralisation of the neural plate. A subset of cells within the neural plate lying directly above the notochord will differentiate into the floor plate and begin to express *Shh* in what will become the ventral midline of the CNS (Echelard *et al.*, 1993). By E9.5, the medial ganglionic eminences (MGEs) highly express *Shh* in the ventral telencephalon (Shimamura *et al.*, 1995), creating its characteristic high-ventral to low-dorsal expression pattern.

After excretion from a cell, *Shh* diffuses away from that cell and binds to its receptor Patched1 (*Ptch1*) on a target cell. This prevents *Ptch1* from inhibiting Smoothened (*Smo*), which is then able to accumulate in the primary cilium and activate signalling through the *Gli* family of transcription factors. In the absence of *Shh*, *Ptch1* inhibits *Smo* accumulation in the primary cilium, thereby allowing Gli3, and to a lesser extent Gli2, transcription factors to undergo processing into transcriptional repressors (Goodrich *et al.*, 1996).

In the forebrain, *Shh* is most well known for its role in patterning of the ventral telencephalon, where high levels of Shh signalling regulate expression of the transcription factors *Nkx2.1* and *Gsx2* (Fuccillo *et al.*, 2004; Corbin *et al.*, 2003). *Nkx2.1* is required for the correct specification of the MGE (Sussel *et al.*, 1999), which during early neurogenesis is the primary source of cortical interneurons which will migrate tangentially into the cortex (Gelman & Marín, 2010; Marín & Rubenstein, 2001). *Gsx2* is however required for the correct specification of the lateral ganglionic eminence (LGE) (Hsieh-Li *et al.*, 1995). In the mature brain, the MGE will have given rise to the globus pallidus, whilst the LGE will have given rise to the striatum. Differing temporal exposure to Shh and competence to respond to it allows for the MGE and LGE to generate an array of ventral cell types (Kohtz *et al.*, 1998). Rash & Grove, (2007) reported that in the Shh null mutant mouse $Shh^{-/-}$, cortical primordium developed in both the dorsal and ventral telencephalon, resulting in the ventral telencephalon differentiating into cortical layers. Again, this highlighted that *Shh* is required in the ventral differentiation programme in the ventral telencephalon.

However, *Shh* also contributes to the development of the dorsal telencephalon. In the developing cortex, Komada *et al.*, (2008) detected Shh protein in apical and basal progenitors and neurons at E13.5 and E15.5 in the mouse. In the *Shh*$^{-/-}$ mutant Rash & Grove (2007) revealed that contrary to previous reports (Chiang *et al*., 1996) the dorsal telencephalon divided into two cerebral hemispheres, apart from in the rostral-most telencephalon, and that the forebrain of these mutants was smaller than their wild-type littermates. When Shh signalling was knocked out specifically in the dorsal telencephalon through the use of *Emx1Cre* conditional mutants, cortical progenitor proliferation was reduced and the formation of the cortical layers was impaired (Komada *et al.*, 2008). Furthermore, conditional deletion of *Smo* thereby blocking Shh signalling in cortical progenitors resulted in abnormally small brains with defective cortical layering (Wang *et al.*, 2016).

Conversely, ectopic activation of Shh signalling in the cortex by inactivating *Ptch1* using *NestinCre* led to an increase in cortical progenitor proliferation, likely through the Notch signalling pathway, which also led to alterations in cortical layering (Dave *et al.*, 2011). *In utero* electroporation of a *Shh* expression vector into E12.5 dorsal telencephalon resulted in a larger and thicker cortex at E18.5 (Komada *et al.*, 2008). Finally, conditional activation of Shh signalling in *GFAP::Cre* cortical progenitors through constitutive *Smo* expression expanded cortical progenitor populations, resulting in a larger cortex and leading to cortical folding (Wang *et al*., 2016).

Taken together, *Shh* plays a role in the correct development of the dorsal telencephalon into the cerebral cortex. It acts to promote the proliferation of cortical progenitors, as evidenced by the reduction in cortex size when *Shh* is reduced and the increase in cortex size when *Shh* is ectopically activated.

### *1.2.2 BMPs*

BMPs constitute a large family of growth factors belonging to the Transforming Growth Factor beta (*TGFβ*) superfamily (Gámez *et al.*, 2013). Early in development, BMPs are expressed in the lateral edges of the neural plate which will fuse to form the neural tube. However, *BMP* inhibition is required to specify neuroectodermal tissue from ectodermal tissue, which is accomplished by the *BMP4* antagonists *noggin* and

*chordin*. *BMP4* expression instructs ectoderm cells to develop into non-neural ectoderm cells which will form the skin, but *noggin* and *chordin* expression in the node inhibit *BMP4* and allow the overlying ectoderm to develop into neural tissue. As development continues, the rostral-most region of the dorsal neural tube invaginates to form the cerebral hemispheres, and the cortical hem becomes specified in the dorsomedial telencephalon, which expresses *BMP2*, *4*, *5*, *6* and *7* (Furuta *et al.*, 1997).

BMPs are secreted before diffusing to target cells where they bind to cell surface BMP receptors (BMPRs). This binding results in the activation of the *Smad* family of proteins, which are then able to either active or repress transcription (Derynck & Zhang, 2003). Saxena *et al.* (2018) reported the presence of phosphorylated Smad1/5/8 in the ventricular zone (VZ) of the E11.5 cortex, where cortical progenitors reside, as well as in early-born neurons, indicating active BMP signalling.

Due to the expression of BMPs in the midline of the dorsal telencephalon, they have been implicated in mediolateral patterning of the dorsal telencephalon. Upon conditional inactivation of the BMPR *Bmpr1a* in the telencephalon the choroid plexus, which produces cerebrospinal fluid to fill the ventricles, failed to form. Choroid plexus precursors however did not change their fate to become lateral telencephalic cells and instead remained proliferative, indicating a more localised role for BMP signalling (Hébert *et al.*, 2002). Additionally, *Bmpr1a* and *Bmpr1b* inactivation in the forebrain specifically led to a loss of dorsal midline cell types leading to holoprosencephaly, a failure of the two cerebral hemispheres to separate (Fernandes *et al.*, 2007).

In explant culture, ectopic application of beads soaked in *BMP4* and *BMP2* to the lateral telencephalon induced dorsomedial cell fate. Furthermore in the dorsomedial telencephalon in the cortical hem, where BMPs are most highly expressed, the neuroectoderm experienced limited growth, alongside a reduction in cell proliferation and increased cell death (Furuta *et al*., 1997). When *Bmpr1a* is activated proliferation of dorsal progenitors is induced. *Bmpr1a* activation also leads to *Bmpr1b* expression, which induces progenitor mitotic arrest resulting in apoptosis. *BMP* activation also resulted in the cortical primordium being re-specified into choroid plexus (Panchision *et al.*, 2001).

Overall, during early neurogenesis in the dorsal telencephalon BMP signalling promotes neuronal differentiation and inhibits progenitor proliferation.

### *1.2.3 Wnts*

Wnts constitute a large protein ligand family which are first expressed in the primitive streak, yet for the correct specification of neural ectoderm rostrally the head mesoderm expresses *Wnt* antagonists (Litsiou *et al.*, 2005). *Wnt* expression continues in the roof plate, and as development continues in the dorsal telencephalon *Wnt2b*, *3a*, *5a*, *7b* and *8b* expression is found in the cortical hem, with different *Wnts* ranging in expression from E9.5 to E13.5 (Grove *et al*., 1998).

Wnts can act as morphogens through secretion by a cell followed by binding to *Frizzled*/*LRP* cell surface receptors on a target cell, where the signal is passed intracellularly to *Dishevelled*. Wnt signalling can then be transduced by three different pathways; canonical Wnt/β-catenin, noncanonical planar cell polarity (PCP), and noncanonical Wnt/$Ca^{2+}$. The canonical Wnt/β-catenin pathway regulates transcription of Tcf/LEF target genes. The noncanonical PCP pathway regulates the cell's cytoskeleton and the noncanonical Wnt/$Ca^{2+}$ pathway regulates intracellular $Ca^{2+}$, although the noncanonical pathways can also antagonise the canonical pathway. Canonical Wnts include *Wnt1*, *Wnt3a* and *Wnt8*, whereas noncanonical Wnts include *Wnt4*, *Wnt5a* and *Wnt11* (Kawano & Kypta, 2003; Kühl *et al.*, 2000).

The roles of Wnt signalling in the dorsal telencephalon are pleiotropic, although they are particularly important in hippocampus development. When *Wnt3a* was knocked out in mice, cortical progenitor cells appeared to be normally specified, but their proliferation was severely impaired, leading to almost complete loss of the hippocampus (Lee *et al.*, 2000). A similar hippocampal defect was also observed when *LEF1*, a transcriptional mediator of the canonical Wnt/β-catenin pathway, was mutated, due to defects in hippocampal field patterning and proliferation (Galceran *et al.*, 2000). Furthermore, when the *Wnt* surface receptor *LRP6* was mutated, there was reduced production of dentate granule neurons of the hippocampus due to a decrease in the number of dentate granule progenitors (Zhou *et al.*, 2004). In the developing cortex, Woodhead *et al.* (2006) achieved loss of β-catenin in a subset of cortical

progenitors by electroporation of a Cre recombinase expression plasmid into the cortex of β-catenin$^{flox/flox}$ embryos. This resulted in cortical progenitor cell cycle exit and differentiation into neurons.

On the other hand, when stabilised β-catenin was expressed in neural progenitors of mice there was an expansion of the progenitor population due to increased progenitor proliferation instead of differentiation and increased cell cycle re-entry after mitosis. This led to enlarged brains due to an increase in the surface area of the cortex (Woodhead *et al.*, 2006; Chenn & Walsh, 2002). When *Wnt3a* was ectopically expressed in the developing cortex thereby up-regulating Wnt/β-catenin signalling, there was an expansion of cortical progenitors leading to large neuronal heterotopias (Munji *et al.*, 2011).

Collectively, Wnt signalling in the early cortex promotes the proliferation of progenitors at the expense of progenitor differentiation, a role opposite to that of BMPs but reflecting that of *Shh*.

### *1.2.4 Fgfs*

The *Fgf* family of proteins contains 22 members in humans and mice that can be subdivided into seven subfamilies (Itoh & Ornitz, 2004). Fgf signalling first plays roles from very early on in development, regulating the differentiation of the inner cell mass into epiblasts and primitive endoderm (Krawchuk *et al.*, 2013). Later in development, the ANR is a major source of Fgfs in the telencephalon, located at the rostromedial pole of the telencephalon. *Fgf8*, *Fgf15*, *Fgf17* and *Fgf18* are all expressed here from as early as E8.5 and are able to impart anteroposterior information to the developing cortex (Borello *et al.*, 2008; Crossley *et al.*, 2001; Fukuchi-Shimogori & Grove, 2001, 2003). *Fgf15* is also expressed in the antihem and shows wide expression in the ventral telencephalon, whilst another *Fgf*, *Fgf2*, is expressed by cortical progenitors themselves (Hasenpusch-Theil *et al.*, 2017; Borello *et al.*, 2008; Vaccarino *et al.*, 1999).

There are 18 Fgfs which are secreted and able to interact with the four Fgf receptors (Fgfrs), whilst the remaining four members of the *Fgf* family are intracellular non-signalling proteins. When a secreted *Fgf* binds to an *Fgfr*, specific cytoplasmic

tyrosine residues of the receptor are phosphorylated, which triggers the activation of cytoplasmic STAT, PI3K-AKT, RAS-MAPK and PLCγ signalling pathways (Ornitz & Itoh, 2015).

As with many of the signalling molecules mentioned here, Fgfs play many roles in dorsal telencephalon development. When *Fgfr3c*, a receptor which sequesters Fgf proteins thereby by inhibiting their diffusion, was overexpressed close to the anterior *Fgf8* source it resulted in a shifting of the anteroposterior boundary anteriorly, although there was no difference in hemisphere size (Fukuchi-Shimogori & Grove, 2001). Further, in an *Fgf8* hypomorphic mouse mutant the anteroposterior boundary also shifts anteriorly, resulting in an expansion of caudal cortical domains at the expense of rostral domains. This was in part due to a change in the molecular identity of rostral cortical progenitors (Garel *et al.*, 2003). When the function of all Fgfrs was lost, cortical progenitors underwent accelerated differentiation and exit from the cell cycle, resulting in a depleted progenitor pool and reduction in cortical surface area as early as E11.5 (Rash *et al.*, 2011). In contrast, when *Fgf8* was overexpressed by *in utero* electroporation at E11.5 the anteroposterior boundary shifted posteriorly and the rostral cortex was expanded whilst the caudal cortex was reduced (Fukuchi-Shimogori & Grove, 2001).

When taken together, it would appear the primary function of Fgfs in the dorsal telencephalon is to promote cortical progenitor proliferation, and also to establish and maintain cortical anteroposterior identity. However, the role of Fgf signalling in the dorsal telencephalon is not so straight forward. Through the use of *Fgf15*$^{-/-}$ mutant mice, Borello *et al.* (2008) showed that *Fgf15* actually suppresses proliferation and promotes neural differentiation, resulting in a caudoventral fate in the rostral telencephalon.

### *1.2.5 Transcription factors*

Expression of the signalling molecules described above will influence progenitor cells in the developing dorsal telencephalon in different ways, based on the precise concentration and duration of morphogen exposure and the interactions of those morphogens. Upon binding of a morphogen to a progenitor which is competent to respond to it, intracellular signalling cascades are activated and influence

transcription factors. These transcription factors are then able to influence a progenitor's activity and ultimately fate. As with signalling molecules, transcription factor expression is often in a gradient. Some of the transcription factors involved in dorsal telencephalon development and expressed in the early cortical primordium include *Emx1*, *Emx2*, *Pax6*, *COUP-TF1*, *Foxg1* and *Gli3* ( Yip *et al.*, 2012; Sansom *et al.*, 2009; Theil *et al.,* 2002; Zhou *et al.*, 2001; Bishop *et al.*, 2000; Mallamaci *et al.*, 2000).

*Emx2* and *Pax6* display opposing gradients in the dorsal telencephalon, with *Emx2* displaying a high caudo-medial to low rostro-lateral gradient, whilst *Pax6* displays a high rostro-lateral to low caudo-medial gradient. These transcription factors are both involved in cortical regionalisation but in contrasting ways. In *Emx2* null mutants the rostral telencephalon was expanded at the expense of the caudal telencephalon, yet in the *Pax6* null mutant the caudal telencephalon was expanded at the expense of the rostral telencephalon, indicating shifts in the anteroposterior and mediolateral axes (Bishop *et al.,* 2000; Mallamaci *et al.*, 2000). This highlighted that during normal cortical development, an antagonism between *Emx2* and *Pax6* is required for the correct regionalisation of the cortex.

In *Emx2* null mutants, Shimogori *et al.* (2004) reported there was an increase in *Fgf8* expression, whilst *Wnt* expression was reduced. As the *BMP* inhibitor *noggin* can induce *Fgf8* expression, BMP signalling in *Emx2*$^{-/-}$ mutants was also investigated, and *noggin* expression was found to be increased and *BMP* activity decreased, which may have contributed to the *Fgf8* up-regulation. Fgfs are also able to suppress *Emx2* expression (Fukuchi-Shimogori & Grove, 2003). Furthermore, Theil *et al*. (2002) identified Tcf and Smad binding sites in an *Emx2* enhancer, allowing for regulation of *Emx2* by the Wnt and BMP pathways, respectively, showing further the complexities of the interactions between multiple signalling molecules and just one transcription factor.

In addition to its role in cortical region fate, *Pax6* is able to positively regulate genes which influence both progenitor self-renewal and neurogenesis. These opposing influences on progenitors are likely mediated through its interactions with other transcription factors, for example *Neurog2* and *Hes1*, and linked to the relative level of *Pax6* and other transcription factors. A loss of Pax6 causes a decrease in cortical progenitor self-renewal leading to early cell cycle exit which depletes the progenitor

pool, alongside a loss of cortical Ngn2 and down-regulation of Tbr2 expression (Sansom *et al*., 2009; Holm *et al.*, 2007; Quinn *et al*., 2007; Scardigli *et al.*, 2003; Estivill-Torrus *et al.*, 2002). The effect of Pax6 loss varies in progenitors based upon their wild-type expression levels, so that in regions which would normally express high levels of Pax6 the loss of Pax6 has a larger influence on their proliferation as opposed to progenitors which would normally express low Pax6 levels (Mi *et al.*, 2013). On the other hand, an increase in the level of Pax6 leads to increased cortical neurogenesis by also increasing cell cycle exit, whilst cortical Ngn2 and Tbr2 expression are increased (Sansom *et al*., 2009; Quinn *et al*., 2007; Scardigli *et al.*, 2003; Estivill-Torrus *et al.*, 2002).

Another transcription factor involved in the regionalisation of the developing cortex is the orphan nuclear receptor *COUP-TF1*. It is expressed in the cortex in a high caudo-lateral to low rostro-medial gradient, and Zhou *et al.* (2001) reported that in *COUP-TF1* null mice there was disruption in region specific and cortical layer specific gene expression.

*Foxg1* expression begins very early in the neural plate at E8.5, but by E9.5 after neural tube closure has occurred, it is expressed throughout most of the telencephalon (Kumamoto *et al*., 2013). *Foxg1* null mutants display a loss of ventral telencephalic structures and also display smaller cerebral hemispheres, likely due to reduced progenitor proliferation and increased differentiation *(*Martynoga *et al.,* 2005; Xuan *et al.*, 1995). There was also a reduction in Fgf8 signalling in *Foxg1* mutants, whilst *BMP2*, *4*, *6*, and *7* expression domains were expanded (Martynoga *et al*., 2005; Hanashima *et al.*, 2004; Dou *et al.*, 1999). Finally, Danesin *et al.* (2009) reported that *Foxg1* can coordinate the activity of the roof and floor plate, as it is a downstream effector of the Shh signalling pathway which inhibits the Wnt/β-catenin pathway.

Overall, there are many transcription factors that play key roles in dorsal telencephalon development, and it is important not to consider these in isolation. Complex neural networks exist highlighting the high level of interactions between transcription factors and signalling molecules in defined spatial and temporal settings, acting together for the correct formation of the cortex.

*Gli3* is another transcription factor which is extremely important in dorsal telencephalon development and will be the focus of this thesis.

### 1.3 The *Gli3* transcription factor

*Gli3* encodes a transcription factor of the *Gli* family, of which there are three members, *Gli1*, *Gli2*, and *Gli3*. All members of the family contain a conserved DNA binding domain consisting of five zinc fingers (Hui *et al.*, 1994), which was confirmed through crystallographic studies (Pavletich & Pabo, 1993). The Gli proteins share a similar zinc-finger domain with the Drosophila segment polarity gene *cubitus interruptus* (*ci*) (Orenic *et al.*, 1990), and with the sex-determining gene *tra-1* of *C. elegans* (Zarkower & Hodgkin, 1992). In the dorsal telencephalon, Gli3R is able to act as a major hub connecting Wnt, BMP and Fgf expression (Hasenpusch-Theil *et al.*, 2015).

In the developing mouse spinal cord and brain, *Gli3* mRNA expression can first be detected at around E8.5 and continues until around E16.5 in a high-dorsal to low-ventral pattern, complimentary to that of *Shh* (Hui *et al.*, 1994) (figure 1.4). In particular, in the developing dorsal telencephalon expression of *Gli3* mRNA was noted in the cortex and cortical hem (Grove *et al.*, 1998) in the VZ, where mitotically active cortical progenitors reside (Amaniti *et al.*, 2013; Hui *et al*., 1994). Gli3 protein has also been described to be expressed in the VZ as well as the subventricular zone (SVZ), where different subtypes of cortical progenitors reside, at E16.5 (Yabut *et al.*, 2016). Yabut *et al.* (2016) reported Gli3 expression in both the nucleus and cytoplasm.

Gli3 can function as either a full-length transcriptional activator or a truncated N-terminal fragment transcriptional repressor. In the dorsal telencephalon where *Shh* levels are low, the full length Gli3 activator protein can be processed into a repressor form. In the absence of Shh, it is thought that at the base of the primary cilium full-length Gli3 is phosphorylated by PKA, GSK3β and CKI, allowing for ubiquitination and processing of the protein into the truncated repressor form, which then likely translocates to the nucleus (Kawano *et al.*, 2017; Wen *et al.*, 2010). The full length Gli3 protein only acts as a weak activator, and when Shh signalling is active undergoes rapid proteosomal degradation.

Mice exhibiting mutations in *Gli3* have played key roles in determining the functions of *Gli3 in vivo*. The homozygous mutant *Gli3*$^{XtH/XtH}$ was first described by Johnson, (1967), called *extra-toes* due to polydactyly of the toes, and is a null mutant which

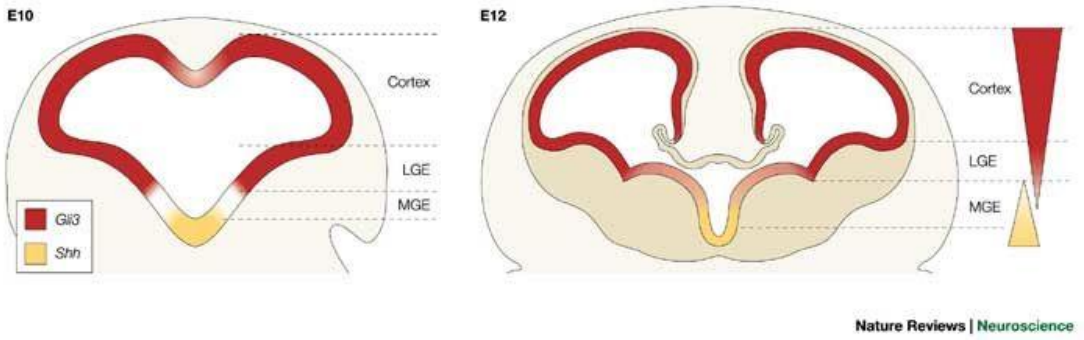


**Figure 1.4: *Gli3* and *Shh* expression in the developing dorsal and ventral telencephalon.** Schematics showing the complimentary expression patterns of *Gli3* and *Shh* at E10 (left) and E12 (right). *Gli3* shows a high-dorsal to low-ventral pattern and *Shh* shows a low-dorsal to high-ventral pattern. LGE; lateral ganglionic eminence, MGE; medial ganglionic eminence. (Rallu *et al.*, 2002).

exhibits deletion of the 5' end of *Gli3*. *Gli3*$^{XtJ/XtJ}$ embryos are also null mutants exhibiting an identical phenotype but due to a deletion of all sequences 3' of the second zinc-finger domain (Büscher *et al.*, 1998; Hui & Joyner, 1993). There are severe defects in the dorsal telencephalon of these mutants, including a decrease in the size of the neocortex and loss of the hippocampus and choroid plexus due to disruption to the cortical hem. Cells with ventral telencephalic identity were located in the dorsal telencephalon, cortical layering was disrupted, and *BMP*, *Wnt* and *Fgf* expression were altered (Fotaki *et al.*, 2006; Theil, 2005; Tole *et al.*, 2000; Theil *et al.*, 1999 figure 1.5 D). *Shh* and *Gli3* null mutants exhibit opposing effects on telencephalon development, yet in *Shh/Gli3* double mutants the dorsalisation of the *Shh* mutant ventral telencephalon was not rescued completely whilst *Gli3* patterning defects like loss of the hippocampus (Rallu *et al.*, 2002) and ectopic Fgf8 and Fgf15 expression alongside loss of dorsal telencephalic Emx1 expression were also not rescued (Rash & Grove, 2007). This indicated the involvement of other factors, with Fgfs being a viable candidate, as in the *Shh*$^{-/-}$ mutant the expression of multiple Fgfs is reduced, yet when *Gli3* is also reduced or abolished *Fgf* expression is partially restored (Rash & Grove, 2007). Indeed, Kuschel *et al.* (2003) previously provided the first evidence that Fgf signalling might be a candidate by showing that Fgf8 ectopic application in

wild-type embryos resulted in repression of dorsal telencephalic gene expression in the dorsal telencephalon and induction of ventral telencephalic genes. Furthermore, Hasenpusch-Theil *et al*. (2015) reported a functional Ets binding site in an enhancer of *Wnt8b*, indicating Fgf signalling is required for *Wnt8b* expression in the cortical hem. Conversely, *Fgf17* expression is repressed by Wnt/β-catenin signalling in the dorsomedial telencephalon (Hasenpusch-Theil *et al.*, 2017). In turn, *Gli3* expression is regulated cooperatively by the action of Fgf and Wnt/β-catenin signalling.

The hypomorphic *Polydactyly Nagoya* (*Gli3*$^{Pdn/Pdn}$) (Hayasaka *et al.,* 1980) mouse has also given great insight into the endogenous functions of *Gli3*. The integration of a retrotransposon into intron 3 of *Gli3*, upstream of the zinc-finger domain, leads to alternative splicing resulting in three different transcripts being produced. The first transcript is formed due to an out-of-frame insertion resulting in a truncated protein which is regarded as non-functional due to the loss of the zinc-finger domain. The second transcript results from an in-frame insertion causing the addition of approximately 60 extra amino acids, the consequences of which remain unclear. In the final situation, where there is no alternative splicing, wild-type Gli3 protein is produced thereby leaving cells with a reduced level of functional Gli3 (Kuschel *et al.*, 2003; Naruse *et al.*, 2000; Thien & Rüther, 1999). The amount of functional Gli3 protein in *Gli3*$^{Pdn/Pdn}$ embryos is reduced by approximately three-fold at E12.5 (Magnani *et al.*, 2010). These mutants also display alterations in Fgf, BMP and Wnt signalling (figure 1.5 B), resulting in ventralisation of the dorsal telencephalon and defects in midline formation though in milder form (Kuschel *et al*., 2003).

*Gli3*$^{Xt/Pdn}$ embryos generated by intercrossing *Gli3*$^{Xt/+}$ and *Gli3*$^{Pdn/+}$ mice display *Gli3* expression levels intermittent to *Gli3*$^{Xt/Xt}$ and *Gli3*$^{Pdn/Pdn}$ embryos (Magnani *et al.*, 2013), and whilst the disruption to dorsal telencephalon development is not as severe as in the *Gli3*$^{Xt/Xt}$ mutant, it is more severe than in the *Gli3*$^{Pdn/Pdn}$ embryo. Kuschel *et al*. (2003) described ventralisation of the dorsal telencephalon in *Gli3*$^{Xt/Pdn}$ embryos, due to ectopic activation of *Fgf8* expression, as well as abolishment of *Wnt2b*, *Wnt3a* and *Bmp4* expression in the cortical hem (figure 1.5 C). *Emx1* expression was abolished by E10.5, with a reduction in *Emx2*, followed by a loss of the distinct high-lateral to low-medial *Pax6* gradient by E12.5. This coincides with an up-regulation of the ventral telencephalon markers *Dlx2* and *Mash1* in a characteristic inverted “V” shape along the rostral most midline. This indicates a reduction in *Gli3* leads to a ventral

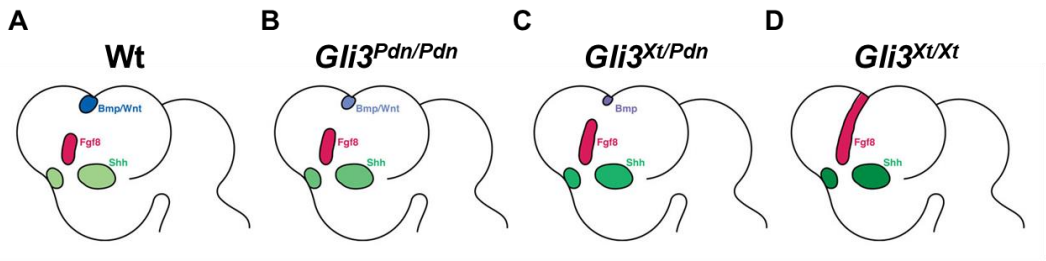


**Figure 1.5: Disruption to the signalling centres of the *Gli3*$^{Pdn/Pdn}$, *Gli3*$^{Xt/Pdn}$ and *Gli3*$^{Xt/Xt}$ developing telencephalon. A.** Schematic showing an E11.5 wild-type (Wt) mouse telencephalon with the signalling centres depicted with the morphogens they secrete. **B.** Schematic showing an E11.5 *Gli3*$^{Pdn/Pdn}$ telencephalon with reduced *Wnt/BMP* expression and increased *Shh* expression. **C.** Schematic showing an E11.5 *Gli3*$^{Xt/Pdn}$ telencephalon with reduced *BMP* and abolished *Wnt* signalling, alongside an increased *Fgf8* expression domain and increased *Shh* expression. **D.** Schematic showing an E11.5 *Gli3*$^{Xt/Xt}$ telencephalon with abolished *Wnt/BMP* expression, an increased *Fgf8* expression domain and increased *Shh* expression. These schematics have been simplified for comparison between the changes in signalling, and do not show the differences in brain morphology due to the mutations. Modified schematic from Thomas Theil.

differentiation programme being at least partially adopted by some dorsal progenitors in the rostral most telencephalon. This was shown to be independent of Shh signalling and instead due to ectopic Fgf activity combined with reduced BMP/Wnt signalling (Kuschel *et al.*, 2003).

Following the disruption in patterning of the dorsal telencephalon, Friedrichs *et al.* (2008) provided evidence of disruption to lamination of the *Gli3*$^{Xt/Pdn}$ dorsal telencephalon. The secreted protein reelin is required for lamination of the cortex (Goffinet, 1979), and a major source of reelin$^{+}$ Cajal-Retzius (CR) cells is the cortical hem, which is abolished in *Gli3*$^{Xt/Pdn}$ embryos. However, other sources of CR cells are the Dbx1$^{+}$ progenitor pools in the septum and ventral pallium (Bielle *et al*., 2005), and these pools are expanded in *Gli3*$^{Xt/Pdn}$ embryos. However, these expanded populations

are not sufficient to allow for lamination to proceed undisturbed. Furthermore, the reelin$^{+}$ cells present in the *Gli3*$^{Xt/Pdn}$ dorsal telencephalon form clusters, disrupting the radial glia scaffold along which newly differentiated cortical neurons migrate.

Further defects in the dorsal telencephalon of *Gli3*$^{Xt/Pdn}$ embryos were described by Magnani *et al*. (2013). Here, it was shown that *Gli3*$^{Xt/Pdn}$ embryos largely lack subplate neurons, an early-born neuronal population formed primarily from cortical progenitors (Price *et al.*, 1997), which pioneer the projection of corticofugal axons and the corpus callosum (Jacobs *et al*., 2007; De Carlos & O'Leary, 1992; McConnell *et al.*, 1989). In the rostral and intermediate cortex of *Gli3*$^{Xt/Pdn}$ embryos, cortical projection neurons do not express Neurofilament, a pan-axonal marker. Although these neurons are able to form axons, the axons are stunted and form fasciculated bundles. By transplanting *Gli3*$^{Xt/Pdn}$ tissue into slices of control tissue, and vice versa, Magnani *et al*. (2013) demonstrated that it is the environment through which the axons grow that result in defects in axon outgrowth and pathfinding, as axon outgrowth was possible when mutant tissue was transplanted into control, yet axons of control tissue were unable to grow in the mutant environment.

Defects in cortical neurogenesis have been identified in the *Gli3*$^{Xt/Xt}$ and *Gli3*$^{Xt/Pdn}$ embryos. In *Gli3*$^{Xt/Xt}$ embryos, there was a delay in neurogenesis at E11.5 as identified by a reduction in Tbr1 expression, yet it appeared to be unaffected at E12.5 (Theil, 2005). In *Gli3*$^{Xt/Pdn}$ embryos, there was a near complete loss of subplate neurons (Magnani *et al*., 2013). However, in *Gli3*$^{Pdn/Pdn}$ embryos neurogenesis was unaffected (Magnani *et al.*, 2010). Altogether, it would appear early neurogenesis is affected dependent upon the level of *Gli3* expression in the cortex.

Taken together, it is clear that *Gli3* is required in cortical progenitors for the correct development of the dorsal telencephalon. Figure 1.5 summarises how the cortical hem, anterior neural ridge and floor plate are altered in the *Gli3*$^{Pdn/Pdn}$, *Gli3*$^{Xt/Pdn}$ and *Gli3*$^{Xt/Xt}$ embryos.

## 1.4 Cortical neurogenesis

The complex interplay between signalling molecules and transcription factors allow for the development of the cortex by cortical progenitors, via the process of cortical neurogenesis. The mature mammalian cortex is comprised of a heterogenous populations of cells, including neurons and glia. The neuronal population can be broadly split into two subtypes of cells; glutamatergic projection neurons and GABAergic inhibitory neurons. Whilst GABAergic neurons are generated in the ventral telencephalon and migrate into the dorsal telencephalon through tangential migration (Sultan & Shi, 2018), the glutamatergic projection neurons are generated in the dorsal telencephalon from cortical progenitors (Paridaen & Huttner, 2014). In order for the mature cortex to form the appropriate number of neurons and hence the correct size, these progenitors must divide at the correct time in the correct way.

In the mouse, cortical neurogenesis begins after neural tube closure at approximately E10. Until then, neuroepithelial stem cells (NeSCs), which line the edge of the ventricle, undergo symmetric, self-renewing division to form two NeSCs. When neurogenesis begins, they begin to transform into radial glia cells (RGCs) which will undergo asymmetric division to produce one RGC and one neuron (Haubensak *et al.*, 2004; Noctor *et al.*, 2004). RGCs extend a process radially to span the ventricular to pial surface, which will aid in the migration of neurons to their final position (Haubensak *et al*., 2004). RGCs are the predominant cortical progenitor subtype early in neurogenesis but will go on to produce a number of other cortical progenitors, which can largely be subdivided into two major categories; apical progenitors and basal progenitors. Apical progenitors, which includes RGCs, reside in the VZ closest to the ventricular surface. These progenitors express the transcription factor Pax6 and are able to undergo three modes of division: symmetrical division forming two apical progenitors, symmetrical division forming two basal progenitors, or asymmetrical division forming one apical progenitor and either one neuron (direct neurogenesis) or one basal progenitor (indirect neurogenesis) (Englund *et al.*, 2005; Miyata *et al.*, 2001; Götz *et al.*, 1998). From approximately E11.5, basal progenitors are present and can be characterised by their expression of the transcription factor Tbr2. Whilst these progenitors are formed in the VZ from apical progenitors, they migrate radially to form another proliferative compartment dorsally to the VZ, known as the SVZ. By

approximately E14.5, basal progenitors overtake apical progenitors to become the predominant cortical progenitor subtype. Basal progenitors are more committed and are only able to undergo two modes of division: a small number of symmetrical divisions forming two basal progenitors, or more often, symmetrical division forming two neurons (Englund *et al.*, 2005; Noctor *et al*., 2004) (figure 1.6).

The mature cortex is a layered structure. The first-born neurons migrate away from the VZ along the radial fibres of RGCs, and subsequently born neurons migrate past these to more basal positions. The earliest-born neurons form a layer known the preplate at about E11.5 which is located basally to the VZ and eventually to the SVZ and consists of subplate neurons and CR cells. As more neurons are born, these migrate radially to form a new layer known as the cortical plate by about E12.5, which splits the preplate into the subplate layer, overlying the SVZ and below the cortical plate, and the marginal zone, overlying the cortical plate at the pial surface. Subplate neurons are confined to the subplate layer and CR cells to the marginal zone. As neurogenesis proceeds, the distinct cortical layers start to form beginning with the deep layer VI and finishing with the superficial layers II-III, with the marginal zone becoming layer I (Molyneaux *et al*., 2007), so that the cortex forms in an inside-out manner. Following neurogenesis, RGCs give rise to glial cells, first astrocytes followed by oligodendrocytes, and will eventually transform into ependymal cells (MuhChyi *et al*., 2013).

The formation of the cortical layers is a complex, highly regulated process, and the birthdate of neurons corresponds with their final laminar position. As neurogenesis proceeds, cortical progenitors become more restricted so that they progress from being able to produce deep layer VI-V neurons before being able to produce only upper layer IV-II neurons. When progenitors harvested from young donors which were giving rise to deep layer neurons were transplanted into older host brains, they were able to switch to upper layer neuron production. However, when progenitors harvested from older donors which were giving rise to upper layer neurons were transplanted into younger host brains at the time of deep layer neuron production, they were unable to generate deep layer neurons, showing their commitment to upper layer neuron production (Frantz & McConnell, 1996; McConnell & Kaznowski, 1991). It was further demonstrated *in vitro* that this timing mechanism is cell intrinsic (Shen *et al.*, 2006).

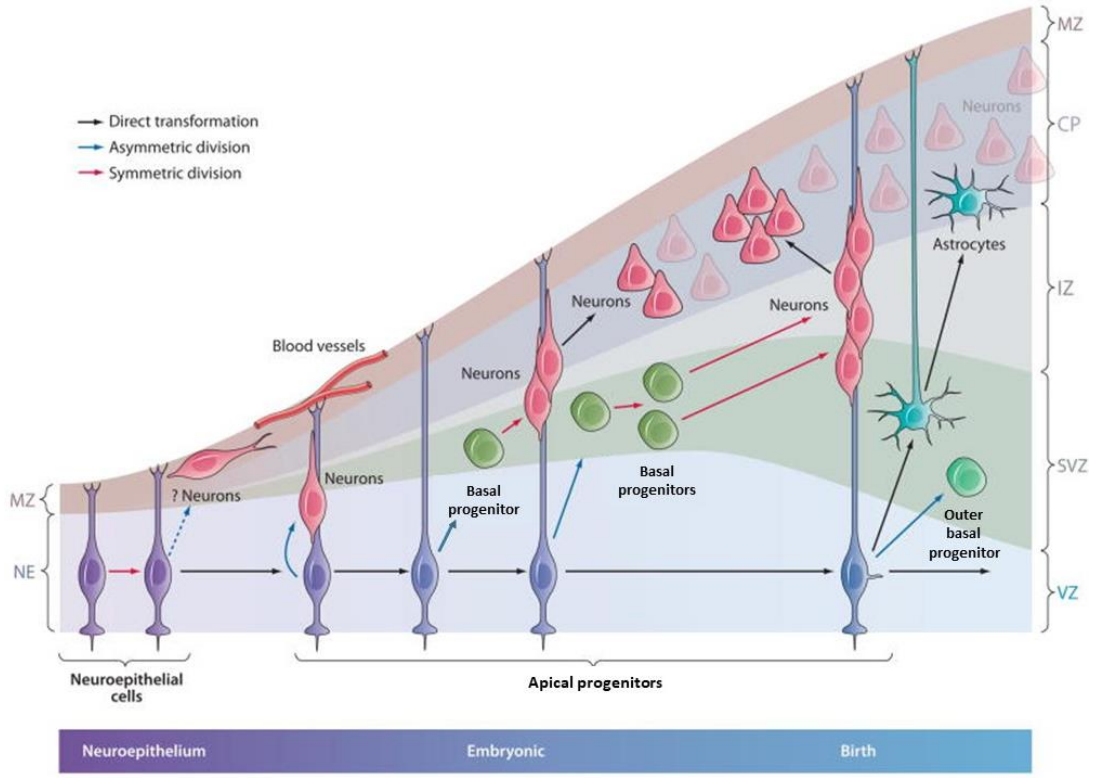


**Figure 1.6: Cortical neurogenesis.** Schematic showing the production of glutamatergic cortical neurons from neuroepithelial cells followed by apical progenitors, located in the VZ, and basal progenitors, located in the SVZ. Apical progenitors undergo symmetric division to form two new apical progenitors, symmetric division to form two basal progenitors, or asymmetrical division to form one apical progenitor and one basal progenitor or neuron. Basal progenitors undergo symmetrical division to form two new basal progenitors or symmetrical division to form two neurons. CP; cortical plate, IZ; intermediate zone, MZ; marginal zone, NE; neuroepithelium, SVZ; subventricular zone, VZ; ventricular zone. Modified schematic from Kriegstein & Alvarez-Buylla (2009).

Aside from the age of the embryo, exposure to signalling molecules and the transcription factors expressed by a cell, and its position within the cortex, many factors can influence the mode of division a cortical progenitor will undergo. For example, post-translational gene modifications affect apical progenitor differentiation into basal progenitors via microRNA-92 silencing of Tbr2 (Nowakowski et al., 2013). Post mitotic neurons are also able to signal back to cortical progenitors and influence their division. The transcriptional repressor Sip1 is expressed in postmitotic neurons and signals via the neurotrophin Ntf3 to promote apical progenitor to basal progenitor and deep layer to upper layer fate changes (Parthasarathy *et al*., 2014; Seuntjens *et al.*, 2009). Furthermore, epigenetic modifications can alter the balance between cortical progenitor proliferation and differentiation. For example, Pereira *et al*. (2010) deleted Ezh2, which represses transcription through histone H3 modification, in cortical progenitors before the beginning of cortical neurogenesis. This loss of function resulted in gene expression up-regulation which promoted cortical progenitor differentiation as opposed to proliferation, causing an overproduction of basal progenitors and neurons. In addition to these factors, the cell cycle of a progenitor has a large influence over the manner in which a progenitor will divide and will be discussed in detail below.

## 1.5 Cell cycle

The cortical progenitor cell cycle is a complex process beginning in a daughter cell following division of the parent cell. After mitosis and division of the parent, each daughter cell will enter gap 1-phase (G1-phase) of the cell cycle. Here, each cell is able to weigh up cell intrinsic and extrinsic signals, which will determine if the cell will continue on through the cell cycle as a progenitor and complete another round of cell division or if it will exit the cell cycle and differentiate, thereby entering gap 0-phase (G0-phase). If the cell is to continue on as a progenitor it must pass through the mid G1-restriction point, which is determined based on the level of cell cycle dependent protein expression. Once the checkpoint has been passed, the cell will then pass from G1-phase into synthesis phase (S-phase), during which DNA is replicated. After DNA replication, the cell will pass into gap 2-phase (G2-phase), where the cell prepares itself for mitosis through protein synthesis and rapid cell growth. A second checkpoint, the G2/M checkpoint, is reached just before the cell progresses from G2-phase into the final phase, mitosis (M-phase). Here, the level of DNA damage is assessed allowing a cell to repair damaged DNA before initiating mitosis. If damaged DNA is not allowed to repair before mitosis, the cell will undergo cell death following division. During the final phase, M-phase, the cell will divide to form two new progeny which will enter G1-phase and begin a new cell cycle.

A number of protein families are key to either allowing or disallowing the cell to progress through the cell cycle. In general, cyclin-dependent kinases (Cdks) and their binding partners the cyclins cause progression through the cell cycle or through specific cell cycle phases. Conversely the Cdk inhibitors (CdkIs) act to inhibit Cdks and result in exit from the cell cycle or prevent a cell from progressing to the next cell cycle phase. With regard to G1-phase, there is sequential expression of Cdk6 and Cdk4 which bind to D-type cyclins, acting to progress the cell past the checkpoint, followed by Cdk2 binding to E-type cyclins to progress the cell from G1-phase into S-phase. The Cdk/cyclin complex acts to hyperphosphorylate Rb, thereby preventing it from binding to and sequestering the E2F family of transcription factors (Dyson, 1998). These transcription factors promote transcription of genes which will cause progression into S-phase and ultimately DNA replication (Harbour & Dean, 2000). Progression through S-phase is mediated by Cdk2 binding with cyclin A, followed by

cyclin A and Cdk1 mediating progression through G2-phase. Finally, Cdk1 and cyclin B mediate progression through M-phase (Suryadinata *et al*., 2010) (figure 1.7). The levels of Cdks, cyclins and CdkIs are dependent on both intrinsic and extrinsic cell features. Intrinsic features include factors such as the size of the cell and the cell fate determinants inherited from the mother cell, which can influence if the cell will pass the checkpoint and continue to cell division, whilst extrinsic factors include proliferative or differentiative signals a cell receives from its environment. With regards to whether a progenitor will undergo proliferative or differentiation division, the most scrutinised cell cycle phase is G1-phase. During this phase, a cell will resolve the intrinsic and extrinsic factors acting upon it to determine the mode of division undertaken. The length of G1-phase has been shown to be critically important in the determination of which type of division will take place.

With regards to cell intrinsic mechanisms, Calegari & Huttner (2003) used the pharmacological non-specific Cdk inhibitor olomoucine to lengthen G1-phase, resulting in an induction of cell differentiation at the expense of proliferation. From here they proposed the “cell cycle length” model, in which they suggested lengthening of G1-phase is sufficient to cause neurogenesis, as the cell has longer to respond to cell fate determinants and so cell fate will change. Lange *et al*. (2009) overexpressed Cdk4/cyclin D1 to promote progression from G1- into S-phase and a shortening of G1-phase, which resulted in an inhibition of neurogenesis leading to increased basal progenitor production and expansion. Furthermore, Pilaz *et al.* (2009) overexpressed either cyclin D1 or cyclin E1, also leading to a shorter G1-phase, promoting the proliferation of apical and basal progenitors at the expense of differentiation into neurons. Moreover, when G1-phase is shorter preceding a proliferative division, Cdk levels rise more quickly and are able to phosphorylate Ngn2, a regulator of neuronal differentiation, whilst at the same time $p27^{Kip1}$, a CdkI, will be present at lower levels and therefore unavailable to stabilise Ngn2 (Nguyen *et al.*, 2006). The result of this is an inability of Ngn2 to promote neuronal differentiation. When G1-phase is longer, there is less Ngn2 phosphorylation and CdkI levels are higher, resulting in an increased ability of Ngn2 to activate the expression of its target genes key to differentiation (Ali *et al.*, 2011). Cell extrinsic factors which can affect the length of G1-phase include exposure to signalling molecules such as *Wnts*. For example, Shtutman *et al*. (1999) and Tetsu & McCormick (1999) revealed cyclin D1 to be a direct target of the β-catenin/LEF-1 pathway, and β-catenin overexpression induced cyclin D1 expression whilst expression of a Tcf/LEF dominant/negative construct

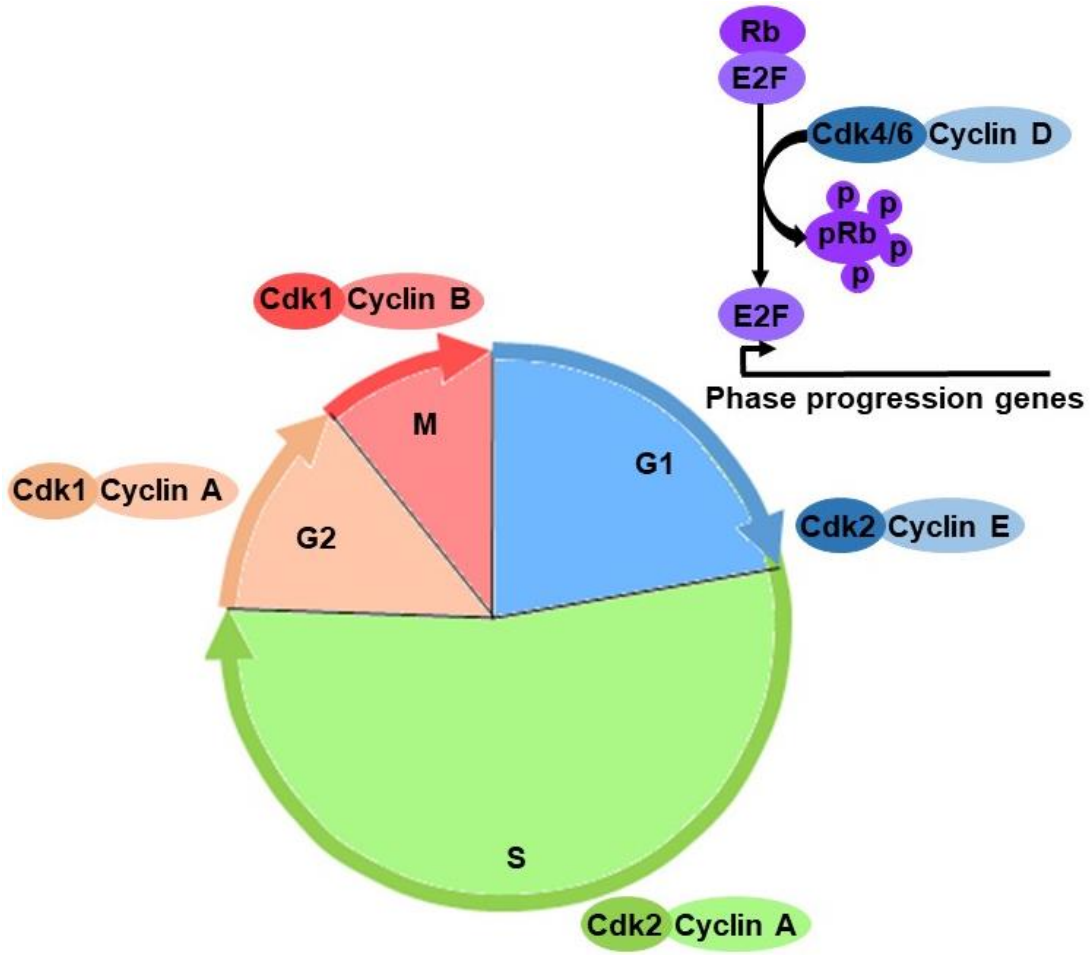


**Figure 1.7: Cell cycle progression.** Schematic showing progression through each phase of the cell cycle mediated by Cdks and cyclins. In G1-phase, Cdk4/6 in concert with D-type cyclins hyperphosphorylate pRb, easing repression of E2F transcription factors and allowing for transcription of phase progression genes. Cdk2 and Cyclin E then promote transition from G1-phase to S-phase, before Cdk2 and Cyclin A mediate progression through S-phase. Cdk1 and Cyclin A allow progression through G2-phase, before finally Cdk1 and cyclin B progress the cell through M-phase.

resulted in G1-phase arrest. Collectively, these studies provide evidence that the length of G1-phase is causal to the decision to proliferate or differentiate, with a

shorter G1-phase causing proliferative division and a longer G1-phase causing differentiative division.

Conversely, a longer S-phase is considered to correlate with proliferative divisions, with S-phase becoming shorter as cells become more differentiated. Arai *et al*. (2011) compared the cell cycle phase lengths of $Tis21^{+}$ and $Tis21^{-}$ progenitors. If a cell is to undergo a proliferative division, it will not express Tis21, but upon commitment to differentiation Tis21 expression is up-regulated during G1-phase (Iacopetti *et al*., 1999). They revealed that S-phase length was significantly shorter in $Tis21^{+}$ cells which are about to undergo differentiation, associated with a down-regulation of genes which would be expected to increase S-phase length in $Tis21^{+}$ cells and an up-regulation of genes which would reduce S-phase length in $Tis21^{-}$ cells. They propose the fidelity of DNA replication and time spent on DNA repair must be longer in proliferative cells which are expected to produce many more cells, than in differentiative cells which will produce comparatively less cells and so any mistakes will not be transmitted to as many progeny. In contrast to the Ali *et al*. (2011); Arai *et al.* (2011); Lange *et al.*, (2009); Pilaz *et al*., (2009); Calegari & Huttner (2003) studies which were undertaken in mouse, Gonzales *et al*. (2015) investigated the role of different phase lengths in human embryonic stem cells (hESCs) *in vitro*. Here, they showed that in hESCS by decreasing S-phase length both genetically and pharmacologically, the pluripotent state is dissolved, meaning the cell will undergo differentiation. Building on the “cell cycle length” model of Calegari & Huttner (2003), they suggest that G1-phase is primed to respond to differentiation cues, whilst S-phase is primed to respond to pluripotency maintenance. Taken together, whilst G1-phase lengthens as cells differentiate, S-phase length is longer when a cell will undergo proliferative division and is shorter when a cell will undergo differentiative division.

As to the final two phases, G2- and M-phase, much less is known about how the length of these phases may affect proliferation and differentiation. In the above study, Gonzales *et al*. (2015) also revealed that in hESCs G2-phase shortening may be linked to differentiation. The group undertook an RNAi screen in differentiating hESCs to identify pathways regulating dissolution of the pluripotent state. Cyclin B1 was identified in the screen, and when knocked down in hESCs led to pluripotency marker downregulation, indicating differentiation. Conversely when overexpressed, cyclin B1 led to a delay in pluripotency state dissolution, indicating a maintenance of the

pluripotent state. Taken together, the study indicated that as with S-phase, G2-phase length may be longer when a cell will undergo proliferative division so the cell can respond to pluripotency maintenance.

In a recent study, Pilaz *et al*. (2016) investigated the role of M-phase length on progenitor proliferation/differentiation using the *Magoh*$^{+/-}$ mutant mouse and two pharmacological inhibitors of M-phase. In the *Magoh*$^{+/-}$ mutant, microcephaly, a reduction in brain size, is exhibited due to defective mitosis resulting in basal progenitor depletion and neuronal apoptosis (Silver *et al*., 2010). Using live imaging, Pilaz *et al.* (2016) recorded that mitotic delay in the *Magoh*$^{+/-}$ mutant correlated with neuronal production at the expense of progenitor proliferation. To further investigate this finding, two pharmacological inhibitors of M-phase were employed, S-trityl-L-cysteine (STLC) and nocodazole. E13.5 cortical brain slices incubated with both inhibitors showed a 50% increase in neurons compared to control and a 25% decrease in basal progenitors. Furthermore, slices incubated with STLC also showed a significant reduction in apical progenitors. Overall, this would indicate that a lengthening of M-phase length leads to decreased progenitor proliferation and increased progenitor differentiation, as has been reported for G1-phase length.

In summary, proliferative division may correlate with a shorter G1-phase followed by longer S- and G2-phases and a shorter M-phase. On the contrary, differentiative division may correlate with a longer G1-phase followed by shorter S- and G2-phases and a longer M-phase. However, the evidence underlying the contribution of each phase length to the mode of division a progenitor will undergo varies greatly, and whilst there is good evidence that the length of G1-phase is critical, more research is required to establish the role of other phases in cortical progenitor division.

One factor shown to impact upon the cell cycle is *Gli3*. Besides regulating the development of the cortex, *Gli3* also regulates development of the limbs. Vokes *et al.* (2008) conducted a genome-wide chromatin immunoprecipitation (ChIP)-on-chip analysis and transcriptional profiling for regulatory regions to which *Gli3* binds and revealed a potential *Gli3* binding site in the *Cdk6* promoter. Building upon this, Lopez-Rios *et al*. (2012) also conducted ChIP analysis using conditional *Gli3* knockout limb buds. They showed that *in vivo Gli3* binds to the *Cdk6* promoter region with ~4-fold enrichment in wild-type limb buds and no interaction in conditional *Gli3* knockout limb

buds. They suggested *Gli3* acts as a negative regulator of the G1- to S-phase transition causing progenitors to cycle faster, likely through *Cdk6* regulation.

The role of *Gli3* in cortical cell cycle regulation has also been investigated. Wang *et al*. (2011) used *NestinCre* to conditionally delete *Gli3* in the cortex after patterning, with complete *Gli3* deletion by E14.5. As described previously in other *Gli3* mutants (Friedrichs *et al*., 2008; Theil, 2005; Tole *et al*., 2000), lamination was disrupted in the cortex of *NestinCre* conditional *Gli3* knockouts. In these mutants, the loss of *Gli3* led to an increased production of deeper layer neurons and decreased upper layer neuron production. Additionally, there was a decrease in apical progenitor proliferation and increased cell cycle exit of these progenitors, leading to a decreased basal progenitor population which also exited the cell cycle prematurely. The group suggested that *Gli3* is required to maintain progenitors in the cell cycle, and that as progenitors progress from apical to basal progenitors to neurons the level of *Gli3* decreases, allowing them to become more differentiated. However, the role of *Gli3* in early neurogenesis and particularly in apical progenitors is hard to assess from this study, due to the lateness at which *Gli3* expression was deleted. Indeed, here the group reported that deletion was only complete by E14.5, whereas cortical neurogenesis begins at approximately E10. Further, they did not investigate the cell cycle, leaving an open question regarding the role of *Gli3* in the cell cycle in cortical progenitors. Friedrichs *et al*. (2008) indicated a reduction in the Tbr1 expression domain dorsomedially at E12.5 in the $Gli3^{Xt/Pdn}$ mutant, indicating a disruption in neurogenesis prior to the time point reported by Wang *et al*. (2011).

Whilst a link has been made already between *Gli3,* proliferation/differentiation of cortical progenitors, and the cell cycle in the limb bud and in late cortical neurogenesis, this has not yet been investigated for cortical progenitors at the onset of neurogenesis, nor has the role of the cell cycle in mutant cortical progenitors here. Therefore, due to the copious amount of evidence linking the cell cycle, and in particular G1-phase, to the proliferation/differentiation of cortical progenitors in early neurogenesis, it is important to study the role of *Gli3* with respect to the cell cycle here.

## 1.6 Aims and hypothesis of this thesis

The focus of this thesis is the role *Gli3* plays between E11.5-E12.5 in the developing dorsal telencephalon, and how its regulation of the cell cycle may impact upon apical and basal progenitor proliferation/differentiation, leading to alterations in the neuronal population. I hypothesise that early neurogenesis is disrupted in the *Gli3*$^{Xt/Pdn}$ mutant due to a disruption in the cell cycle, caused by a reduction in *Gli3*. The aims of this thesis were:

1. To examine the expression of the Gli3 protein in apical and basal progenitors and assess the impact of reduced *Gli3* expression levels on the apical and basal progenitor and early-born neuronal populations.

2. To examine apical and basal progenitor cell cycle exit/re-entry in the *Gli3*$^{Xt/Pdn}$ dorsal telencephalon followed by detailed investigation of the individual cell cycle phase lengths in these progenitors.

3. Using microarray analysis data from the *Gli3*$^{Xt/Pdn}$ mutant, identify potential candidate genes underlying *Gli3's* regulation of the cell cycle and to begin to investigate the mechanisms by which *Gli3* may regulate the cell cycle.

# Chapter 2: Materials and Methods

## 2.1 Animals

### *2.1.1 Husbandry*

Procedures were carried out and mice kept in accordance with Home Office regulations and the University of Edinburgh's Policy on the Use of Animals in Research.

To obtain *Gli3*$^{Xt/Pdn}$ embryos, *Gli3*$^{Xt/+}$ mice, maintained on a mixed C56Bl6 x C3H background, were interbred with *Gli3*$^{Pdn/+}$ mice, maintained on a C3H background. Wild-type (wt), *Gli3*$^{Pdn/+}$ and *Gli3*$^{Xt/+}$ embryos were used as control as they exhibited no distinct phenotype. To obtain *Emx1Cre;Gli3*$^{fl/fl}$ embryos, *Emx1Cre;Gli3*$^{fl/+}$ mice were mated with *Gli3*$^{fl/fl}$ mice, and *Emx1Cre;Gli3*$^{+/+}$ and *Emx1Cre;Gli3*$^{fl/+}$ embryos were used as control as no observable phenotype was displayed. *Gli3-FLAG* embryos were also used for antibody testing (Nishi *et al*., 2015). To obtain *Gli3*$^{Xt/Pdn}$*;Tis21GFP* embryos, *Gli3*$^{Xt+}$ animals were interbred with *Tis21*-GFP animals (Haubensak *et al.*, 2004) (a kind gift from W. Huttner). *Gli3*$^{Xt/+}$*;Tis21GFP* animals were then interbred with *Gli3*$^{Pdn/+}$ animals. *Gli3*$^{+/+}$*;Tis21GFP*, *Gli3*$^{Pdn/+}$*;Tis21GFP* and *Gli3*$^{Xt/+}$*;Tis21GFP* were used as control.

Food and water were available to all mice *ad libitum*, and mice were kept in a 14/10-hour light/dark cycle. Timed matings occurred overnight, with E0.5 classified as the morning of vaginal plug discovery. For each experiment, between 3 and 5 embryos were analysed.

### *2.1.2 Administration of BrdU and IdU*

10mg/ml 5-Bromo-2′-deoxyuridine (BrdU) (Sigma) or 5-Iodo-2′-deoxyuridine (IdU) (Sigma) were dissolved in 0.007M NaOH and 0.154M NaCl at 37°C (BrdU) and 70°C (IdU) with shaking in an Eppendorf Thermomixer at 1,400rpm for 20-30 mins just prior to use.

To calculate the length of S-phase and the length of the total cell cycle, 10mg/kg IdU was injected intraperitoneally (IP) into pregnant dams at E11.5 or E12.5. 1.5 hrs later, 10mg/kg BrdU was injected IP into the dams, followed by sacrifice of the mice and harvesting of the embryos 30 mins after BrdU injection.

To calculate the length of G2-phase, 10mg/kg BrdU was injected IP into pregnant dams at E11.5 or E12.5 1 hr, 1.5 hrs or 2 hrs before sacrifice and embryo isolation.

To calculate cell cycle exit, 10mg/kg BrdU was injected IP into pregnant dams at E10.5 or E11.5, and embryos were collected 24 hrs later.

### *2.1.3 Tissue preparation*

Pregnant dams were culled via anaesthetic overdose with IsoFlo 100% w/v isoflurane (Zoetis) followed by cervical dislocation when embryos reached E11.5 – E13.5. The uterus was dissected from the dams and transferred into ice cold 1x phosphate buffered saline (PBS) (table 2.6) except for during preparation for slice culture, in which uteri were transferred into ice cold 1x Krebs (table 2.6). Whole embryos were then dissected from the uterus, before the whole head was removed from the embryo. Heads to be used for histochemistry were transferred into 4% paraformaldehyde in PBS (PFA) (table 2.6) and fixed overnight at 4°C. For slice cultures, the brain was dissected from the embryos and embedded in 3-4% SeaKem LE agarose (Lonza) in sterile 1x PBS. Tail tips were removed from embryos and used for genotyping.

### *2.1.4 Genotyping*

Tail tips were digested at 55°C and 1,400rpm for 2 hrs in a thermomixer (Eppendorf) with 100μl DirectPCR lysis reagent (tail) (Viagen) containing 200μg/ml proteinase K (Sigma). The enzyme was denatured following digestion at 85°C for 50 mins.

Genotyping reactions were carried out in a total volume of 25μl (except *Xt* which was carried out in a total volume of 50μl) using the reagents and oligonucleotides shown in table 2.1 and table 2.2. PCRs were then performed using the programmes as shown in table 2.3.

PCR products were separated on 2% (w/v) agarose gels containing 1x TAE buffer (table 2.6) and GelRed Nucleic Acid Gel Stain (Biotium) or ethidium bromide (Sigma) (for Pdn reactions only) before visualisation with UV light.

**Table 2.1: PCR reaction mixtures**

| | 5x Green Go Taq Reaction Buffer (Promega) (μl) | dNTPs (0.5mM) (Promega) (μl) | Oligonuc-leotides (10μM) (Sigma) (μl) | Taq DNA polymerase (5μg/μl) (Promega) (μl) | $dH_2O$ (μl) | DNA (μl) |
|---|---|---|---|---|---|---|
| *Emx1Cre* | 5 | 0.5 | 1 | 0.1 | 16.4 | 1 |
| *Gli3 Flox* | 5 | 0.5 | 0.75 | 0.1 | 16.9 | 1 |
| *Pdn* | 5 | 1 | 0.75 | 0.2 | 15.55 | 1 |
| *Xt* | 10 | 1 | 2 | 0.2 | 29.9 | 1 (diluted 1:1 with $dH_2O$) |

**Table 2.2: PCR primers**

| Allele | Primer | Sequence (5'-3') | Band size (bp) |
|---|---|---|---|
| *Emx1Cre* | CreF | -ACCTGATGGACATGTTCAGGGA- | Cre: 308 |
| | CreR | -TCCGGTTATTCAACTTGCACCA- | |
| *Gli3 Flox* | Gli3-S1 | -CTGGATGAACCAAGCTTTCCATC- | Flox: 500 Wt: 200 |
| | Gli3-AS3 | -CTGCTCAGTGCTCTGGGCTCC- | |
| *Pdn* | Pdn Etn 11F | -TTGAGCCTTGATCAGAGTAACTGTC- | Pdn/+: 180 Wt: 220 |
| | PdnR6 | -TGTTTCCCATTGTCCAACCCTACCC- | |
| | PdnF5 | -GTTCAAGTTGGTGCATAGCTACCAGGTTCC- | |
| *Xt* | C3f | -GGCCCAAACATCTACCAACACATAG- | Wt: 180 |
| | C3r | -GTTGGCTGCTGCATGAAGACTGAC- | |
| | Xt580f | -TACCCCAGCAGGAGACTCAGATTAG- | Xt/+: 580 |
| | Xt580r | - AAACCCGTGGCTCAGGACAAG- | |

**Table 2.3: Genotyping programmes**

| Genotype | Reaction conditions |
|---|---|
| *Emx1Cre* | Maintained at 94°C for 5 mins, then 30 cycles were performed of 94°C for 30 secs denaturing, 61°C for 45 secs annealing and 72°C for 45 secs extension. The reaction was then held 72°C for 5 mins. |
| *Flox* | Maintained at 95°C for 2 mins, then 30 cycles were performed of 95°C for 30 secs denaturing, 61°C for 45 secs annealing and 72°C for 45 secs extension. The reaction was then held 72°C for 5 mins. |
| *Pdn* | Maintained at 95°C for 3 mins, then 30 cycles were performed of 94°C for 1 min denaturing, 55°C for 1 min annealing and 72°C for 1 min extension. The reaction was then held at 72°C for 7 mins. |
| *Xt* | Maintained at 94°C for 2 mins, then 35 cycles were performed of 94°C for 15 secs denaturing, 62°C for 30 secs annealing and 72°C for 30 secs extension. The reaction was then held 72°C for 5 mins. |

### *2.1.5 Tissue sectioning*

**Cryostat**

Heads were washed in 1x PBS following overnight fixation before being transferred into 30% sucrose (Fischer Scientific) in 1x PBS (w/v) and stored on a rotator at 4°C overnight. Heads were then incubated in 30% sucrose/OCT (VWR) (1:1) for 30 mins before embedding in 30% sucrose/OCT (1:1) and stored at -80°C. 10μm coronal sections were cut on a CM3050S cryostat (Leica) and adhered to Superfrost Plus slides (VWR). Slides were stored at 4°C overnight, with long-term storage at -20°C.

**Microtome**

Heads were washed in 1x PBS overnight following fixation, before being dehydrated in 70% ethanol (Fischer) and embedded in paraffin wax through an automated tissue processor (Tissue-Tek, VIP, Sakura). 10μm coronal sections were cut on an RM2245 microtome (Leica) and mounted on Superfrost Plus slides. Slides were incubated at 37°C overnight before being stored at 4°C.

**Vibratome**

Heads were removed from embryos and from these the brains were dissected out in ice cold 1x Krebs + antibiotics (table 2.6). The brains were then transferred to molten LE agarose kept at 43°C, and stirred in the agarose for approximately 4-5 mins to allow for the tissue to adhere with the agarose. The agarose was then allowed to solidify on ice, and 300μm coronal sections were cut on a Leica VT1000S vibratome in ice cold 1x Krebs. Sections were collected in 1x Krebs + antibiotics and kept on ice before being put into culture.

## 2.2 Immunofluorescence

### *2.2.1 Cryostat sections*

Slides were acclimatised to room temperature for approximately 30 mins before washing 3x 20 mins each on a rocker in 1x PBS to rehydrate the tissue. Sections being stained for primary antibodies which require antigen retrieval were rested in 10mM sodium citrate buffer for 5 mins (pH6) (table 2.6) before being either

microwaved for 4x 5 mins each or incubated in a water bath at 80°C for 30 mins. The sections were rested in the sodium citrate buffer for approximately 20 mins, before being washed for 5 mins in 1x PBS. All slides were then encircled with an ImmEdge Hydrophobic Barrier Pen (Vector Laboratories), before blocking in 20% goat serum (Sigma) in 1x PBS for 2 hrs at room temperature. Subsequently, slides were incubated overnight at room temperature with primary antibodies (table 2.4) diluted in 10% goat serum. Slides were then washed 3x 10 mins each in 1x PBS, before secondary antibodies (table 2.5) and either TOPRO-3 (Invitrogen) or DAPI (Life Technologies) (table 2.5) were added to the sections for 2 hrs. Slides were again washed 3x 10 mins each in 1x PBS before mounting with mowiol (table 2.6).

**Amplification**

Slides were processed as above, however on the second day of the protocol after washing slides 3x 10 mins each in 1x PBS, slides were incubated for 1.5 hrs with a biotinylated secondary antibody (table 2.5) in 10% goat serum in 1x PBS with either TOPRO-3 or DAPI (table 2.5). Secondary antibodies required for primary antibodies which did not need amplification were included in this step. Slides were washed for 3x 10 mins in 1x PBS, before incubation with a streptavidin-conjugated secondary antibody (table 2.5) diluted in 10% goat serum in 1x PBS for 30 mins. Slides were washed 3x 10 mins each in 1x PBS, before mounting with mowiol.

### *2.2.2 Paraffin sections*

Dewaxing of paraffin sections was achieved by washing slides 3x 7 mins each in xylene (ThermoFisher Scientific), followed by 2 mins in EtOH (ThermoFisher Scientific)/xylene (1:1), 2x 2 mins each in 100% EtOH, and 1 min in each of 96% EtOH, 90% EtOH, 70% EtOH and 50% EtOH. Sections then underwent antigen retrieval by incubating the slides in 10mM sodium citrate buffer (pH6) for 5 mins at room temperature before microwaving 4x 5 mins each. Sections were then rested in the sodium citrate buffer for 20 mins at room temperature before washing in 1x PBST (table 2.6) for 5 mins. Sections were encircled with an ImmEdge Hydrophobic Barrier Pen and blocked for 2 hrs in blocking solution (20% goat serum in 1x PBST). Slides were incubated overnight at room temperature with primary antibodies (table 2.4) diluted in blocking solution. Slides were washed 3x 10 mins each in 1x PBST, followed by incubation for 2 hrs with secondary antibodies (table 2.5) diluted in 10% goat serum

in 1x PBST with TOPRO-3 or DAPI (table 2.5). Finally, slides were washed 3x 10 mins each in 1x PBST before mounting with mowiol.

**Amplification**

Slides were treated as above on the first day, however on the second day after washing 3x 10 mins each in 1x PBST, slides were incubated for 1.5 hrs with a biotinylated secondary antibody (table 2.5) in 10% goat serum in PBST with TOPRO-3 or DAPI (table 2.5). Any other secondary antibodies required were included in this step. Slides were washed 3x 10 mins each in 1x PBST, followed by incubation for 30 mins with a streptavidin-conjugated secondary antibody (table 2.5) diluted in 10% goat serum in PBST. Slides were washed again 3x 10 mins each in PBST and mounted with mowiol.

**Table 2.4: Primary antibodies**

| Primary antibody | Dilution | Citrate buffer treatment | Specific protocol required | Origin | Manufacturer |
|---|---|---|---|---|---|
| BrdU | 1:50 | Required | - | Rat | Abcam |
| GFP | 1:1000 | - | Cryostat sections | Chicken | Abcam |
| Gli3 | 1:100 | Required | Citrate buffer treatment performed in water bath | Goat | R & D Systems |
| IdU/BrdU | 1:50 | Required | - | Mouse | Becton Dickinson |
| Pax6 | 1:400 | - | - | Rabbit | BioLegend |
| PCNA | 1:500 | - | - | Mouse | Santa-Cruz |
| pHH3 | 1:100 | - | - | Rabbit | Millipore |
| pRb S780 | 1:200 | - | - | Rabbit | Cell signalling |
| Tbr1 | 1:400 | Required | Amplification | Rabbit | Abcam |
| Tbr2 | 1:1000 | - | - | Rabbit | Abcam |

**Table 2.5: Secondary antibodies**

| Secondary antibody | Dilution | Origin | Conjugated to | Manufacturer |
|---|---|---|---|---|
| Anti-chicken IgG | 1:100 | Donkey | DyLight488 | JacksonImmuno Research |
| Anti-mouse IgG | 1:200 | Goat | Alexa488 | Invitrogen |
| Anti-mouse IgG | 1:100 | Donkey | Cy2 | Jackson/Dianova |
| Anti-rabbit IgG | 1:200 | Goat | Alexa647 | Invitrogen |
| Anti-rabbit IgG | 1:400 | Goat | Biotin | DAKO |
| Anti-rabbit IgG | 1:100 | Donkey | Cy3 | Jackson/Dianova |
| Anti-rat IgG | 1:100 | Donkey | Cy3 | Jackson/Dianova |
| DAPI | 1:2000 | - | - | Life Technologies |
| Streptavidin | 1:100 | - | AlexaFluorA568 | ThermoFisher Scientific |
| TOPRO-3 | 1:2000 | - | - | Invitrogen |

## 2.3 Slice culture

300μm coronal vibratome slices of E11.5, E12.5 and E13.5 brains were cultured for 24 hrs in 15mm centre well organ culture dishes (BD Falcon by Corning). The slices were cultured on 8μm Whatman nucleopore track-etched membranes, on 1ml of pre-warmed (37°C) Minimum Essential Medium (MEM) (Invitrogen) with serum (table 2.6). Slices were placed in a 37°C 5% $CO_2$ Panasonic MCO-170AICUV-PE incubator for 1 hr. MEM was removed, and 1ml of pre-warmed (37°C) neurobasal medium (Invitrogen) supplemented (table 2.6) was added. At this point, either palbociclib (Selleck Chemicals, varying concentrations, dissolved in DMSO (Sigma)) or DMSO were added to slices.

The following day, the medium was removed and slices were fixed overnight with 4% PFA at 4°C. Slices were washed 3x 15 mins each with 1x PBS, before 30% sucrose in 1x PBS was added to the wells and left overnight at 4°C. The 30% sucrose solution was replaced with 30% sucrose/OCT (1:1) for approximately 30 mins, before slices were embedded in 30% sucrose/OCT (1:1) and stored at -80°C. Slices were then cut to 10μm thick coronal sections via cryostat, as outlined in section 2.1.5.

## 2.4 Microscopy

Fluorescent images were captured with a Leica DMLB upright compound microscope fitted with a Leica DSC480 digital camera using 2.5x, 5x, 10x, 20x and 40x lenses. Bright field images were taken using a Leica M165C microscope with a Leica DFC420 digital camera using 2.5x, 5x and 10x lenses. Images were processed with LAS AF Lite software and Adobe Photoshop CS6 software, adjusting images equally for contrast and brightness.

## 2.5 Quantification and analysis

### *2.5.1 Quantification of cells*

For all cell counts, cells within a 175μm wide box parallel to the ventricular surface and spanning the width of the cortex (apical to basal surfaces) were counted (figure 3.5). Three consecutive coronal sections were counted per embryo, at the level where the epithalamus first appeared. Both hemispheres were counted, and boxes were placed laterally across the cortex close to the pallial-subpallial boundary (PSPB) or medially close to the midline region.

Cell counts were performed using the Cell Counter plugin in ImageJ. Statistical analyses were conducted and graphs produced using GraphPad Prism 6.

### *2.5.2 Statistics*

Quantitative results are quoted throughout as mean ± 95% confidence interval. Graphs depict mean ± 95% confidence interval. Significance was calculated either via the Mann-Whitney U-test or, for slice culture only, the Kruskal-Wallis test followed by Dunn's post-hoc test. A significance level of 0.05 was used, $p<0.05$ is indicated by one asterisk, $p<0.01$ is indicated by two asterisks.

**Table 2.6: Solutions used in this thesis**

| Solution | Preparation |
|---|---|
| 10x Krebs (pH 7.2) | To prepare 1l:<br>• Dissolve dry ingredients in a small volume of $dH_2O$, and once dissolved increase volume to 1l with further $dH_2O$:<br>○ 73.6g NaCl (ThermoFisher Scientific)<br>○ 1.87g KCl (ThermoFisher Scientific)<br>○ 1.66g $NaH_2PO_4.H_2O$ (ThermoFisher Scientific)<br>○ 2.44g $MgCl_2.6H_2O$ (ThermoFisher Scientific)<br>○ 3.68g $CaCl_2.2H_2O$ (ThermoFisher Scientific)<br>• Adjust pH to 7.2 and autoclave |
| 1x Krebs + antibiotics | To prepare 50ml:<br>• To 49ml 1x Krebs add:<br>○ 500µl 1M HEPES buffer solution (Invitrogen)<br>○ 500µl penicillin streptomycin (Invitrogen)<br>○ 100µl 50mg/ml gentamicin (Gibco)<br>• Can be stored at 4°C for up to 2 weeks |
| MEM supplemented with serum | To prepare 50ml:<br>• To 44ml MEM (Invitrogen) add:<br>○ 5ml foetal calf serum (Sigma)<br>○ 500µl D-(+)-glucose solution 45% (Sigma)<br>○ 500µl penicillin streptomycin (Invitrogen)<br>• Can be stored at 4°C for up to 2 weeks |
| Mowiol | To prepare 24ml:<br>• Mix together overnight at room temperature:<br>○ 12ml $dH_2O$ |

| | |
|---|---|
| | ○ 2.4g mowiol (Fluka Analytical)<br>○ 6g glycerol (Melford)<br>• Heat for 1-2 hrs at 60°C with:<br>○ 12ml 0.2M Tris (pH8.5) (Sigma)<br>• Centrifuge for 15 mins at 2,000rpm before adding:<br>○ 2.5% DABCO (Sigma)<br>• Store at -20°C for long-term storage, store at 4°C for short-term storage |
| Neurobasal medium (supplemented) | To prepare 50ml:<br>• To 47.5ml neurobasal medium (Invitrogen) add:<br>○ 1ml B27 50x supplement (Invitrogen)<br>○ 500µl D-(+)-glucose solution 45% (Sigma)<br>○ 500µl penicillin streptomycin (Invitrogen)<br>○ 500µl l-glutamine solution (Invitrogen)<br>• Can be stored at 4°C for up to 2 weeks |
| 10x PBS (pH 7.4) | To prepare 2l:<br>• Dissolve dry ingredients in a small volume of $dH_2O$, and once dissolved increase volume to 2l with further $dH_2O$:<br>○ 160.2g NaCl (ThermoFisher Scientific)<br>○ 4.0g KCl (ThermoFisher Scientific)<br>○ 4.0g $KH_2PO_4$ (ThermoFisher Scientific)<br>○ 23.2g $Na_2HPO_4.2H_2O$ (ThermoFisher Scientific)<br>• Adjust pH to 7.4 before dilution to 1x working stock |
| 1x PBST (0.1% Triton-X) | To prepare 1l:<br>• To 1l 1x PBS add: |

| | |
|---|---|
| | ○ 1ml Triton-X (Acros Organics) |
| 4% PFA | To prepare 1l:<br>• Heat together until dissolved:<br>○ 1l 1xPBS<br>○ 40g paraformaldehyde (ThermoFisher Scientific)<br>• Store at -20°C for long-term storage, store at 4°C for short-term storage |
| 100mM sodium citrate buffer (pH 6) | To prepare 1l:<br>• Dissolve dry ingredient in a small volume of $dH_2O$ and adjust pH to 6.0 with 1M citric acid, before increasing volume to 1l with further $dH_2O$:<br>○ 29.4g $C_6H_6Na_3O_7$ (ThermoFisher Scientific) |
| 50x TAE buffer | To prepare 2l:<br>• Dissolve dry ingredients in a small volume of $dH_2O$ before increasing volume to 2l with further $dH_2O$:<br>○ 100ml 0.5M EDTA (pH8.0) (ThermoFisher Scientific)<br>○ 60ml acetic acid (ThermoFisher Scientific)<br>○ 242g Tris Base (Sigma) |

# Chapter 3: Gli3 is primarily expressed in apical progenitors of the developing neocortex, and reduction in Gli3 expression alters apical progenitor, basal progenitor and cortical neuron production

## 3.1 Introduction

Neurogenesis within the developing neocortex is a highly controlled process leading to the production of glutamatergic projection neurons. The layers of the mature cortex are formed in an inside-out manner, with the deeper layers being formed first from early-born neurons followed by the upper, more superficial layers being formed subsequently from later-born neurons. For this process to occur correctly, distinct subtypes of cortical progenitors must divide at the correct time and in the correct manner. In general, rodent cortical neurogenesis begins when neuroepithelial cells switch from self-renewing, proliferative divisions to asymmetric, differentiative divisions at approximately E10. These asymmetric divisions lead to the formation of apical progenitors and the earliest-born neurons (Haubensak *et al*., 2004; Noctor *et al.*, 2004). In early neurogenesis apical progenitors are the predominant cortical progenitor subtype and are characterised by their expression of the paired homeodomain transcription factor Pax6. These progenitors reside in the ventricular zone (VZ) and undergo three types of division: symmetrical division to form two apical progenitors, symmetrical division to form two basal progenitors, or asymmetrical division to form one apical progenitor and either one basal progenitor or one neuron (Miyata *et al.*, 2001; Götz *et al.*, 1998). The second major subdivision of cortical progenitor are basal progenitors, which are formed from apical progenitors only and become the predominant cortical progenitor subtype later in neurogenesis, at approximately E14.5. Conversely, basal progenitors express the T-domain transcription factor Tbr2, reside in the subventricular zone (SVZ), and undergo two types of division: a limited number of symmetrical division to form two basal progenitors or, most commonly, symmetrical division to form two neurons (Englund *et al.*, 2005; Noctor *et al.*, 2004).

The manner in which apical and basal progenitors divide and the timing of these divisions is critical to the correct formation of the cortex. As such, it is a tightly controlled process involving the interaction of a number of different signalling molecules and transcription factors. Of note, mutations in the transcription factor *Gli3* have long been shown to result in severe developmental defects in the cortex, since Johnson (1967) first reported that the *Gli3*$^{Xt/Xt}$ null mutant exhibited small cerebral hemispheres and some animals were hydrocephalic.

*Gli3* mRNA expression is first detectable at E8.5 in the mouse, and expression continues until approximately E16.5. In general, it is expressed in a high-dorsal to low-ventral pattern throughout the developing spinal cord and brain, in particular in the forebrain and hindbrain (Hui *et al*., 1994). In the presence of Shh, full length Gli3 protein acts as a transcriptional activator, but in the absence of Shh, as in the dorsal telencephalon, Gli3 is proteolytically cleaved at the base of the primary cilium into a transcriptional repressor (Fotaki *et al.*, 2006). In the dorsal telencephalon, *Gli3* mRNA is expressed in the neocortex and cortical hem (Grove *et al.*, 1998) and appears to be localised to the VZ (Amaniti *et al*., 2013; Hui *et al*., 1994), hinting at a role in mitotically active cells. Furthermore, single-cell mRNA sequencing of cells from the developing human telencephalon revealed *GLI3* to be expressed in radial glial cells, a subset of apical progenitors (Pollen *et al*., 2014). Recently Yabut *et al*. (2016) described that at E16.5 Gli3 protein was localised in the VZ, but they also described expression in the SVZ. However, as they did not use markers of apical or basal progenitors, they were unable to say in which progenitor subtype(s) Gli3 was expressed. They noted that along the ventricular surface, Gli3 expression was largely cytoplasmic, yet expression was more localised to the nucleus as cells reached the SVZ. Neither the *in situ* nor immunofluorescence studies were able to reveal whether Gli3 protein is expressed within apical and/or basal progenitors, only that it is expressed in the progenitor zones.

The functions in which *Gli3* regulates the development of the dorsal telencephalon have primarily been evaluated through the use of *Gli3* mutant mice. The focus of this thesis will be the *Gli3*$^{Xt/Pdn}$ mutant, a compound mutant formed by the crossing of the heterozygotes of the null *Gli3*$^{Xt/Xt}$ mutant and the hypomorphic *Gli3*$^{Pdn/Pdn}$ mutant (Kuschel *et al*., 2003). *Gli3*$^{Xt/Pdn}$ pups die shortly after birth and exhibit clear defects in the dorsal telencephalon. The signalling centres of the dorsal telencephalon are disrupted, leading to some dorsal progenitors implementing a ventral differentiation

programme in the rostral most telencephalon due to disruption of Fgf, BMP and Wnt signalling (Kuschel *et al.*, 2003). Lamination of the cortex is disturbed in *Gli3*$^{Xt/Pdn}$ mice due to the loss of the cortical hem, a major source of Wnt signalling and a source of reelin, which is essential for lamination (Friedrichs *et al.*, 2008). Furthermore, Magnani et al. (2013) demonstrated that subplate neurons are largely absent in these embryos. Subplate neurons are very early-born neurons produced mainly between E10.5 and E12.5 (Price *et al*., 1997), and the lack of subplate neurons in *Gli3*$^{Xt/Pdn}$ embryos indicates there may be a defect in cortical neurogenesis. Taken together, it is clear that *Gli3* is required for the proper formation of the cortex.

The focus of this chapter therefore will be the localisation of the Gli3 protein in the developing dorsal telencephalon as identified by immunofluorescence. I will show that, in alignment with mRNA sequencing, Gli3 protein is principally expressed in apical progenitors. I will then go on to evaluate the effect of Gli3 reduction on apical and basal progenitors and early-born cortical neurons in the *Gli3*$^{Xt/Pdn}$ dorsal telencephalon.

## 3.2 Gli3 is primarily expressed in apical progenitors

### *3.2.1 Specificity of the Gli3 antibody*

While *Gli3* expression has been extensively studied at the mRNA level, there is very limited published data showing Gli3 protein expression in embryos *in situ*. At the protein level, only Yabut *et al*. (2016) have begun to elucidate where the protein is situated, however as stated above they only examined E16.5 and did not combine Gli3 with any other markers. I tested the specificity of a GIi3 antibody in immunofluorescence on cryostat sections of *Emx1Cre;Gli3$^{fl;/fl}$* embryos and littermate controls at E12.5 and E17.5. In *Emx1Cre;Gli3$^{fl/fl}$* embryos, *Gli3* is inactivated in the cortex between E10.5 and E12.5 in a medial to lateral gradient (Amaniti *et al.*, 2013). These embryos were used to examine the specificity of the antibody as *Gli3* expression is unaffected in the lateral ganglionic eminence (LGE), which served as a positive control. At E12.5, in control embryos Gli3 protein expression was clearly visible in the VZ of the cortex (figure 3.1 A-A", B-B"), in agreement with published *Gli3* mRNA data (Amaniti *et al*., 2013; Hui *et al*., 1994). Gli3 is also expressed in the hippocampal primordium and in the cortical hem. As the antibody recognises the Gli3 N-terminus, it recognises both the activator and repressor forms, hence it detects Gli3 expression in the LGE (figure 3.1 E-E", 3.2 A-A", C-C", E-E", G-G"). However, in *Emx1Cre;Gli3$^{fl;/fl}$* embryos Gli3 protein was greatly reduced in neocortex (figure 3.1 C-C", D-D"), consistent with the loss of *Gli3* mRNA (Amaniti *et al.*, 2013). This specific loss of Gli3 protein was also observed in E17.5 Gli3 conditional mutants. In E17.5, in control embryos Gli3 was still expressed in the cortex and LGE (figure 3.1 E-E", F-F") yet it was absent in the cortex of *Emx1Cre;Gli3$^{fl;/fl}$* embryos (figure 3.1 G-G", H-H").

In both control and mutant embryos at E12.5, Gli3 appeared to be mostly localised to the nucleus with some cytoplasmic staining visible along the very edge of the ventricle (figure 3.1 A-D"), in agreement with the observations of Yabut *et al.* (2016) at E16.5. However, at E17.5 Gli3 expression appeared to be more diffuse and showed more cytoplasmic staining (figure 3.1 E-H"). This is noteworthy, as although Gli3 functions as a transcription factor and so expression would be primarily expected in the nucleus, it is processed in and at base of the primary cilium, and so higher resolution images are needed to further resolve where the protein is localised. Overall though, the antibody showed good protein specificity and was clear at the cellular level, and so was further used in this thesis.

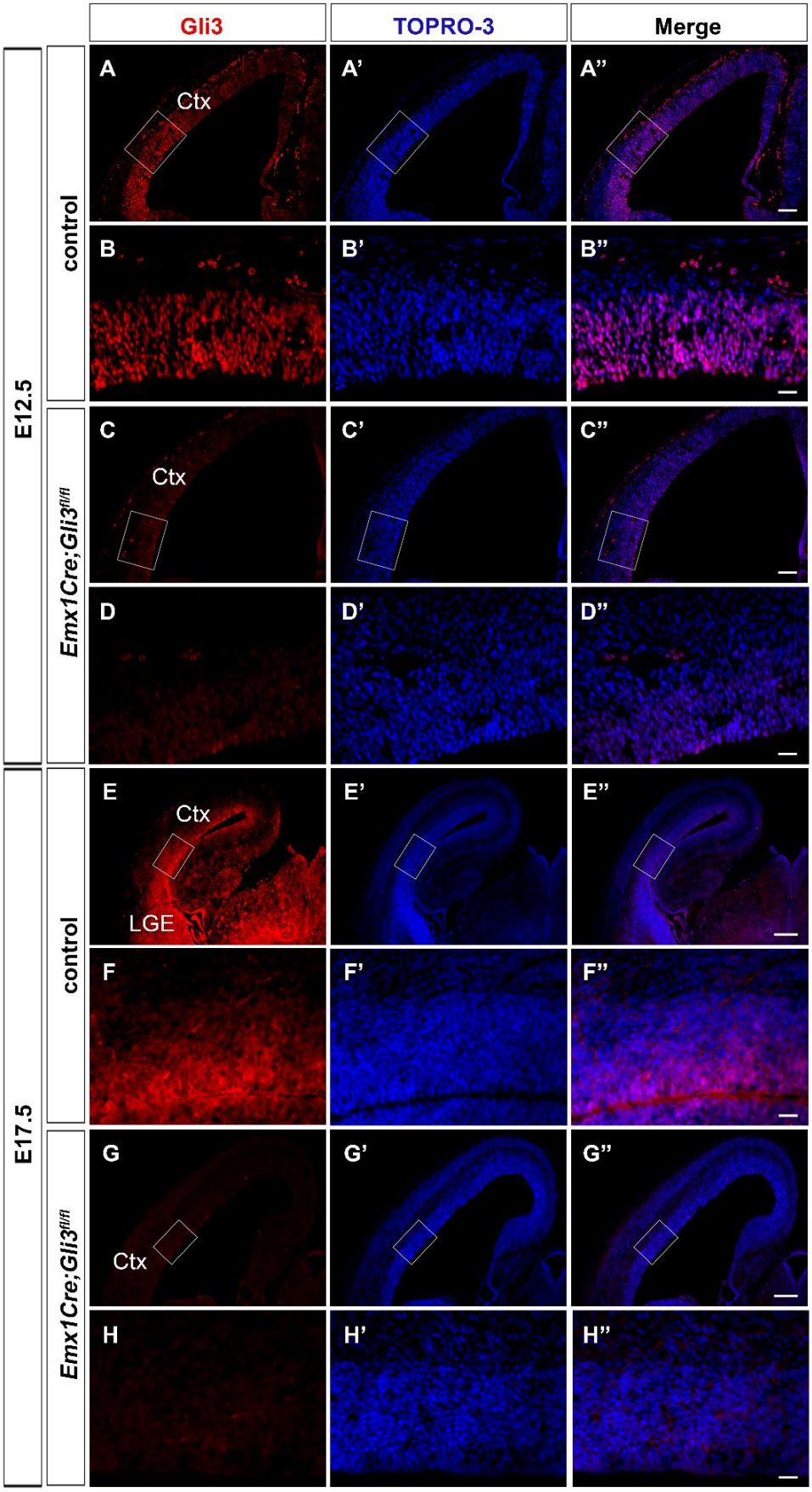
Gli3
TOPRO-3
Merge
E12.5
control
Emx1Cre;Gli3fl/fl
E17.5
control
Emx1Cre;Gli3fl/fl
A
A'
A''
B
B'
B''
C
C'
C''
D
D'
D''
E
E'
E''
F
F'
F''
G
G'
G''
H
H'
H''
Ctx
LGE

**Figure 3.1: Gli3 and TOPRO-3 expression in the E12.5 and E17.5 cortex.** Comparison between control and *Emx1Cre;Gli3*$^{fl/fl}$ embryos showing the specificity of the Gli3 antibody. Boxes on A, C, E, G represent area shown in B, D, F, H, respectively. **A-D".** Gli3/TOPRO-3 immunofluorescence on coronal sections of E12.5 cortex from control and *Emx1Cre;Gli3*$^{fl/fl}$ telencephalon. **E-H".** Gli3/TOPRO-3 immunofluorescence on coronal sections of E17.5 cortex from control and *Emx1Cre;Gli3*$^{fl/fl}$ telencephalon. Ctx; cortex, LGE; lateral ganglionic eminence. Scale bars = 25μm (B", F", D", H"), 100μm (A", C"), 500μm (E", G").

### *3.2.2 Gli3 is expressed in apical progenitors with minimal expression in basal progenitors in the early developing dorsal telencephalon*

Several groups have reported *Gli3* mRNA to be expressed in the VZ in the mouse (Amaniti *et al.*, 2013; Grove *et al*., 1998; Hui *et al*., 1994), and in humans, *GLI3* mRNA was found to be co-expressed with *PAX6* in radial glia cells (Pollen *et al.*, 2014). I therefore examined Gli3 protein distribution between apical and basal progenitors in E11.5 and E12.5 control embryos to determine if Gli3 was expressed in apical and/or basal progenitors. At E11.5, Gli3 showed expression in the VZ of the cortex and there was clear coexpression with Pax6, used as a marker of apical progenitors (figure 3.2 A-B"). However, there was very little expression outside of the VZ and little overlap between Gli3 and Tbr2, which labels basal progenitors (figure 3.2 C-D"). There were a few cells which did express both Gli3 and Tbr2 (marked by arrows, figure 3.2 D-D"), and it is possible that these were newly formed basal progenitors which had not yet fully switched off Gli3 expression. At E12.5, Gli3 expression was clear in the VZ and overlapped with Pax6 as shown at E11.5 (figure 3.2 E-F"). There was less overlap between Gli3 and Tbr2 than Pax6, although it was not as clear as at E11.5. There were more basal progenitors expressing both Gli3 and Tbr2 at E12.5, and these $Gli3^{+}Tbr2^{+}$ cells were mainly located in the VZ, lending credence to the hypothesis that these cells were newly formed basal progenitors which may not have downregulated Gli3 expression completely or may have inherited Gli3 protein from their parent cell (arrows, figure 3.2 H-H"). The expression of Gli3 protein mimics that of *Gli3* mRNA, and Gli3 showed higher expression in apical progenitors than in basal progenitors.

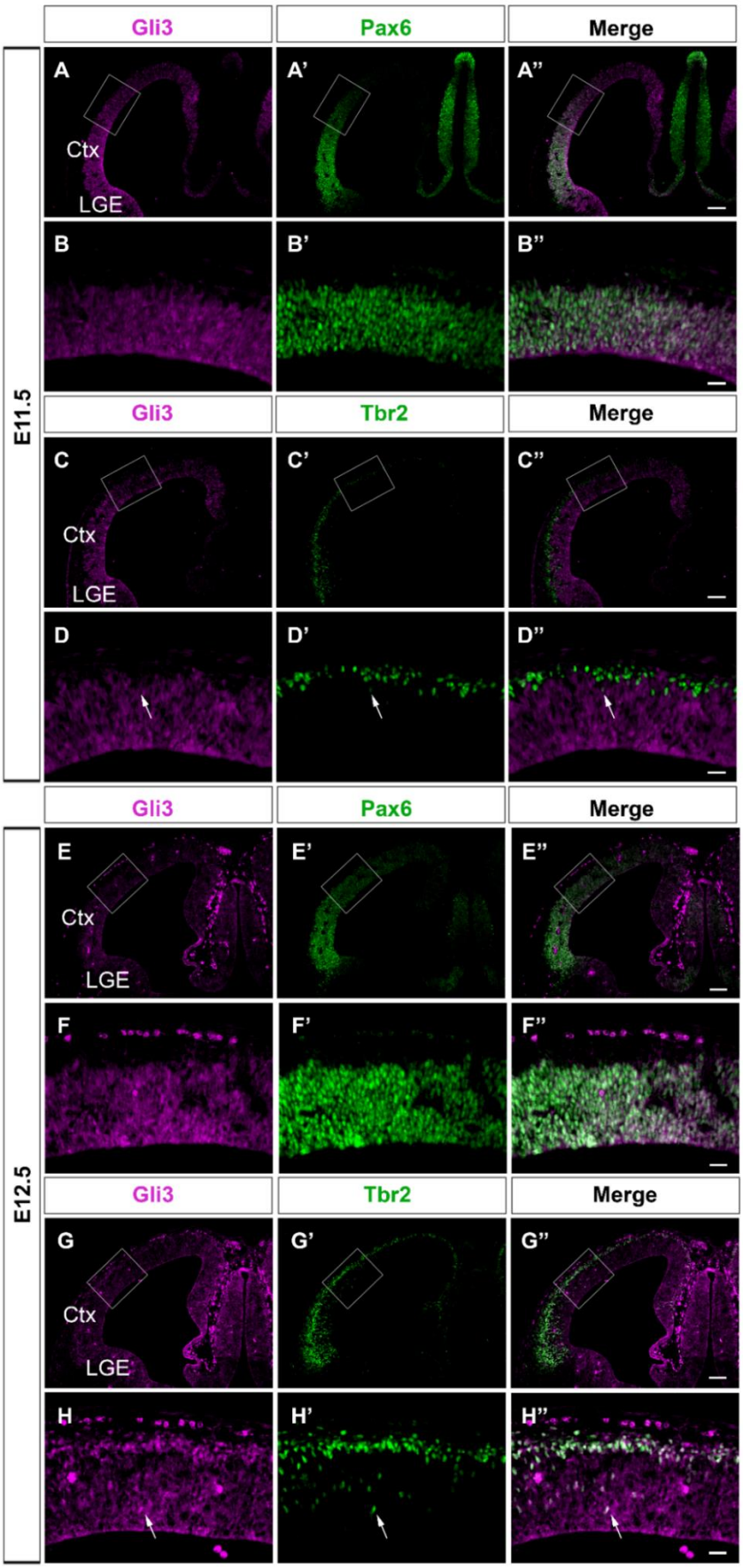
Gli3
Pax6
Merge
A
A'
A''
Ctx
LGE
B
B'
B''
E11.5
Gli3
Tbr2
Merge
C
C'
C''
Ctx
LGE
D
D'
D''
Gli3
Pax6
Merge
E
E'
E''
Ctx
LGE
F
F'
F''
E12.5
Gli3
Tbr2
Merge
G
G'
G''
Ctx
LGE
H
H'
H''

**Figure 3.2: Gli3, Pax6 and Tbr2 expression in E11.5 and E12.5 wild-type cortex.** Boxes on A, C, E, G represent area shown in B, D, F, H, respectively. White arrows denote co-labelled cells. **A-B".** Gli3 and Pax6 expression in the E11.5 cortex. **C-D".** Gli3 and Tbr2 expression in the E11.5 cortex. **E-F".** Gli3 and Pax6 expression in the E12.5 cortex. **G-H".** Gli3 and Tbr2 expression in the E12.5 cortex. Ctx; cortex, LGE; lateral ganglionic eminence. Scale bars = 25μm (B", F", D", H"), 100μm (A", C", E", G").

### *3.2.3 Gli3 protein is reduced in Gli3$^{Xt/Pdn}$ embryos at E11.5 and E12.5*

*Gli3*$^{Xt/Pdn}$ embryos are a widespread tool for evaluating the result of reduced *Gli3* function on the development of the telencephalon. I used the Gli3 antibody to assess protein levels and distribution at E11.5 and E12.5 in these embryos. Immunofluorescence was carried out together with either Pax6 or Tbr2 to assess if the Gli3 expression pattern remained the same in these embryos.

At E11.5, Gli3 was expressed in the VZ of the cortex of control embryos in apical progenitors (figure 3.3 A-B") but in only a few basal progenitors (figure 3.3 C-D"). In *Gli3*$^{Xt/Pdn}$ mutant embryos, some Gli3 expression was still visible in the cortex but with a much reduced intensity. In the mutants, Gli3 expression again overlapped with Pax6 in apical progenitors (figure 3.3 E-F"), but very little with Tbr2 in basal progenitors (figure 3.3 G-H").

At E12.5, Gli3 expression was visible in the VZ of the cortex in control embryos and overlapped with Pax6 in apical progenitors (figure 3.4 A-B") but with only a few Tbr2$^{+}$ basal progenitors (figure 3.4 C-D"). In the *Gli3*$^{Xt/Pdn}$ embryos, Gli3 was expressed at a reduced level in the VZ overlapping with Pax6 in apical progenitors (figure 3.4 E-F"). There appeared to be more Gli3 expression in E12.5 mutant basal progenitors (figure 3.4 G-H") than at E11.5.

Overall, the immunofluorescent analyses reflected prior analyses of *Gli3* mRNA expression in *Gli3*$^{Xt/Pdn}$ embryos and support that there were reduced *Gli3* mRNA and Gli3 protein levels present in the cortex (Magnani *et al.*, 2013; Friedrichs *et al.*, 2008), although western blot analysis is required to accurately measure the amount of protein reduction.

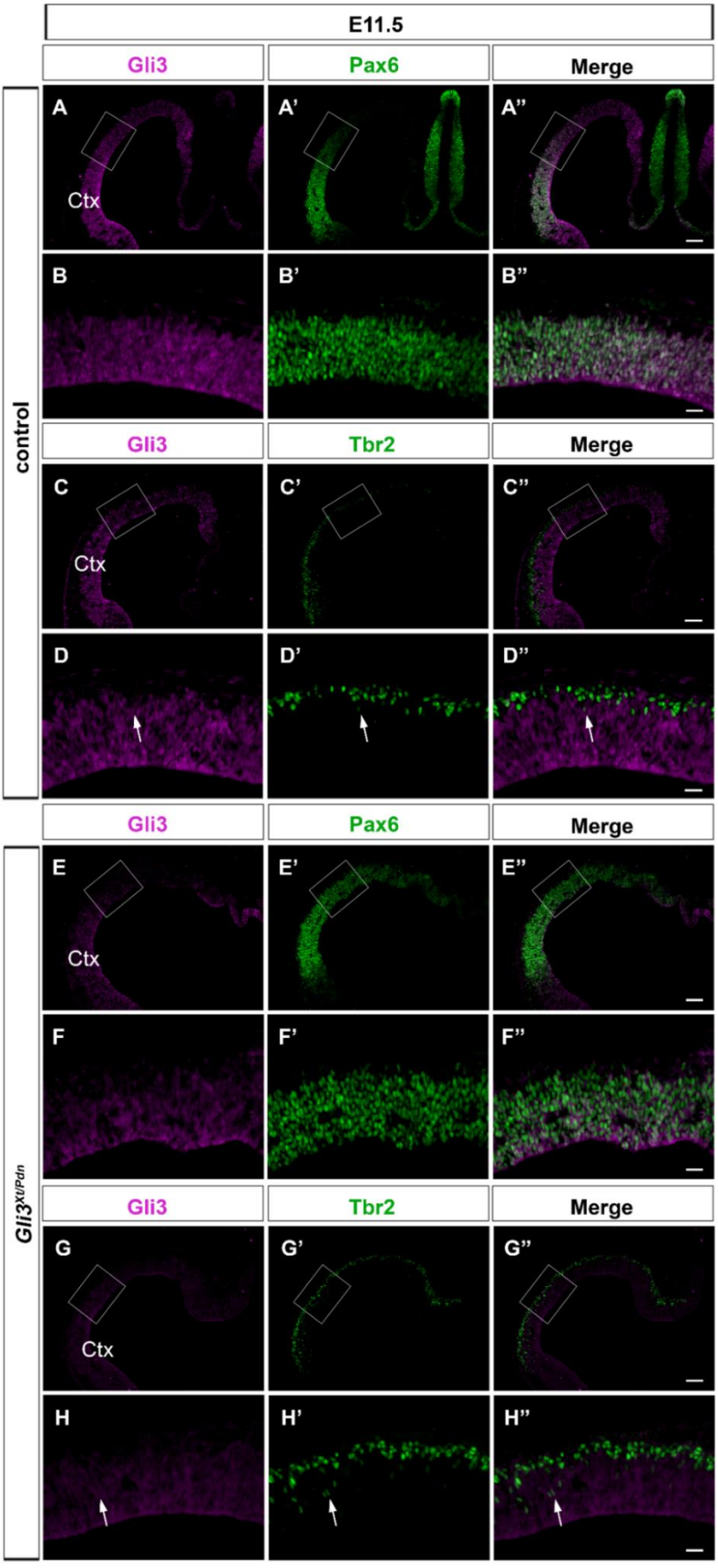
E11.5
Gli3
Pax6
Merge
control
A
A'
A''
Ctx
B
B'
B''
Gli3
Tbr2
Merge
C
C'
C''
Ctx
D
D'
D''
Gli3
Pax6
Merge
Gli3Xt/Pdn
E
E'
E''
Ctx
F
F'
F''
Gli3
Tbr2
Merge
G
G'
G''
Ctx
H
H'
H''

**Figure 3.3: Gli3 protein is reduced in *Gli3*$^{Xt/Pdn}$ embryos at E11.5.** Boxes on A, C, E, G represent area shown in B, D, F, H, respectively. White arrows denote co-labelled cells. **A-B".** Gli3 and Pax6 expression in the E11.5 wild-type cortex. **C-D".** Gli3 and Tbr2 expression in the E11.5 wild-type cortex. **E-F".** Gli3 and Pax6 expression in the E11.5 *Gli3*$^{Xt/Pdn}$ cortex. **G-H".** Gli3 and Tbr2 expression in the E11.5 *Gli3*$^{Xt/Pdn}$ cortex. Ctx; cortex. Scale bars = 25μm (B", F", D", H"), 100μm (A", C", E", G").

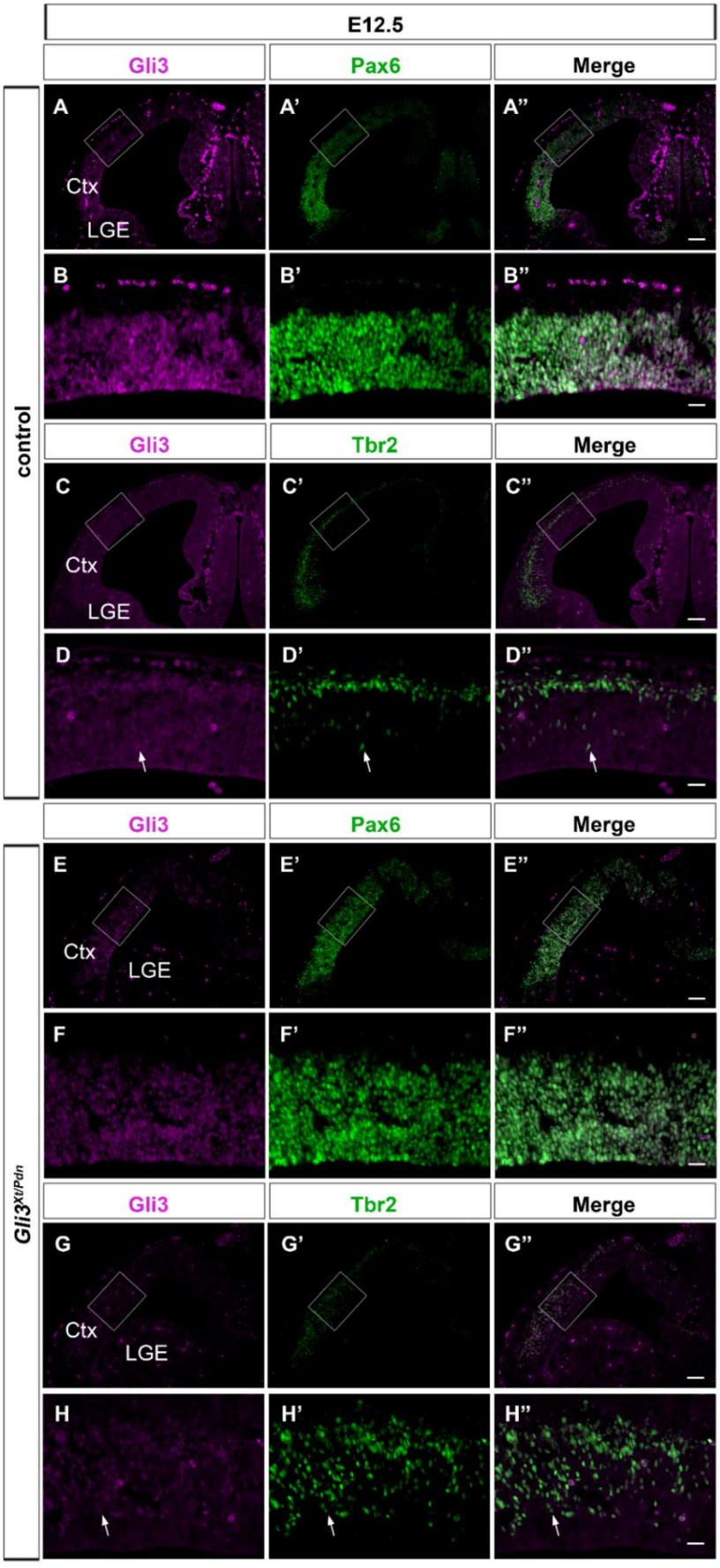
E12.5
Gli3
Pax6
Merge
control
A
A'
A"
Ctx
LGE
B
B'
B"
Gli3
Tbr2
Merge
C
C'
C"
Ctx
LGE
D
D'
D"
Gli3
Pax6
Merge
Gli3Xt/Pdn
E
E'
E"
Ctx
LGE
F
F'
F"
Gli3
Tbr2
Merge
G
G'
G"
Ctx
LGE
H
H'
H"

**Figure 3.4: Gli3 protein is reduced in *Gli3$^{Xt/Pdn}$* embryos at E12.5.** Boxes on A, C, E, G represent area shown in B, D, F, H, respectively. White arrows denote co-labelled cells. **A-B".** Gli3 and Pax6 expression in the E12.5 wild-type cortex. **C-D".** Gli3 and Tbr2 expression in the E12.5 wild-type cortex. **E-F".** Gli3 and Pax6 expression in the E12.5 *Gli3$^{Xt/Pdn}$* cortex. **G-H".** Gli3 and Tbr2 expression in the E12.5 *Gli3$^{Xt/Pdn}$* cortex. Ctx; cortex, LGE; lateral ganglionic eminence. Scale bars = 25μm (B", F", D", H"), 100μm (A", C", E", G").

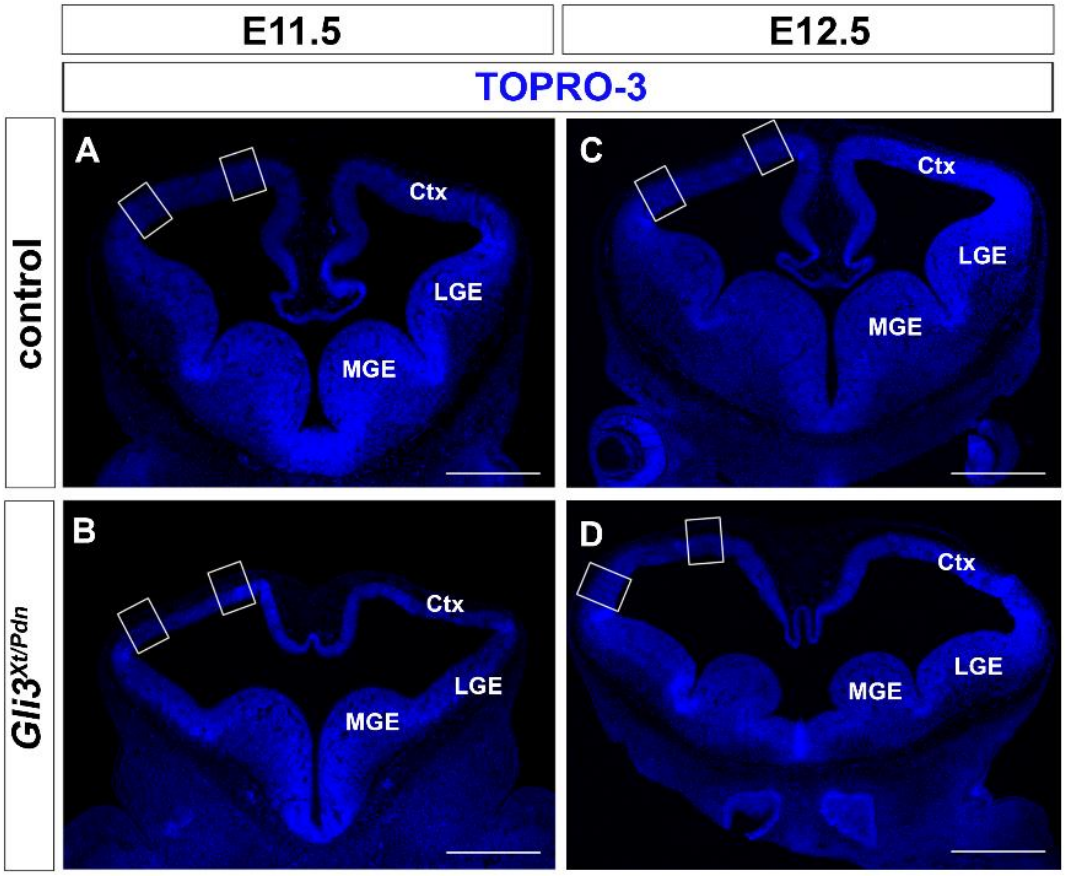


**Figure 3.5: Location of cell counts.** Placement of lateral and medial boxes for counting in E11.5 wild-type embryos **(A)**, E11.5 *Gli3*$^{Xt/Pdn}$ embryos **(B)**, E12.5 wild-type embryos **(C)** and E12.5 *Gli3*$^{Xt/Pdn}$ embryos **(D)**. Boxes were 175μm wide and spanned the ventricular to pial cortical surface and were aligned parallel with the cortical ventricular surface. Analyses in this thesis were conducted on three adjacent sections per embryo in both hemispheres. Ctx; cortex, LGE; lateral ganglionic eminence, MGE; medial ganglionic eminence. Scale bars = 500μm (A, B), 1,000μm (C, D).

### 3.3 Reduction in *Gli3* results in an increased apical progenitor population in *Gli3$^{Xt/Pdn}$* embryos at E11.5 and a decreased apical progenitor population in *Gli3$^{Xt/Pdn}$* embryos at E12.5

My Gli3 protein expression analyses revealed that Gli3 was primarily expressed in apical progenitors, and so the effect of reducing Gli3 levels on the formation of apical progenitors was examined. Immunofluorescence was carried out against Pax6 and PCNA, a marker of proliferating cells (Hall *et al*., 1990), and the proportion of apical progenitors to the total number of progenitors was calculated. As described in section 2.5.1 and as shown in figure 3.5, as neurogenesis progresses from lateral to medial cell counts were performed in boxes placed across the lateral and medial neocortex to compare the cortex in two slightly different stages of neurogenesis. These boxes were placed at the level where the epithalamus first appeared, to avoid the partial ventralisation of the rostral most *Gli3$^{Xt/Pdn}$* dorsal telencephalon. Laterally, the proportion of apical progenitors was increased 1.16-fold in *Gli3$^{Xt/Pdn}$* embryos from 74.65±1.57% in control to 86.76±2.40% in mutants (n=4, $p<0.05$) (figure 3.6 A, B, E). However, medially the proportion of apical progenitors was unchanged and remained relatively similar at 92.69±1.55% in control and 89.79±0.85% in mutant (n=4, $p>0.05$) (figure 3.6 C, D, E). This clearly indicated that the reduction in Gli3 expression had an effect on the proportion of apical progenitors laterally where neurogenesis was more advanced.

The effect on apical progenitor formation was also evaluated at E12.5 in the same manner as at E11.5 to assess if the defect remained 24 hrs later. At E12.5, laterally there was no difference in the proportion of apical progenitors between control and *Gli3$^{Xt/Pdn}$* (71.34±1.58% in control and 68.49±2.69% in mutant, n=4, $p<0.05$) (figure 3.7 A, B, E). However, medially there was a 1.22-fold decrease in the proportion of apical progenitors in the *Gli3$^{Xt/Pdn}$* mutant compared to control (89.98±1.56% in control and 74.05±4.13% in mutant, n=4, $p<0.05$) (figure 3.7 C, D, E).

Combined with the data from E11.5, over the course of 24 hrs the proportion of apical progenitors decreased. Laterally, there was an increased proportion at E11.5 but no difference between control and mutant at E12.5, and medially there was no difference between control and mutant at E11.5 to a decreased apical progenitor proportion at E12.5, which may have reflected the lateral to medial transmission of neurogenesis. Overall, in terms of Pax6 expression, this was in partial agreement with Kuschel *et al.*

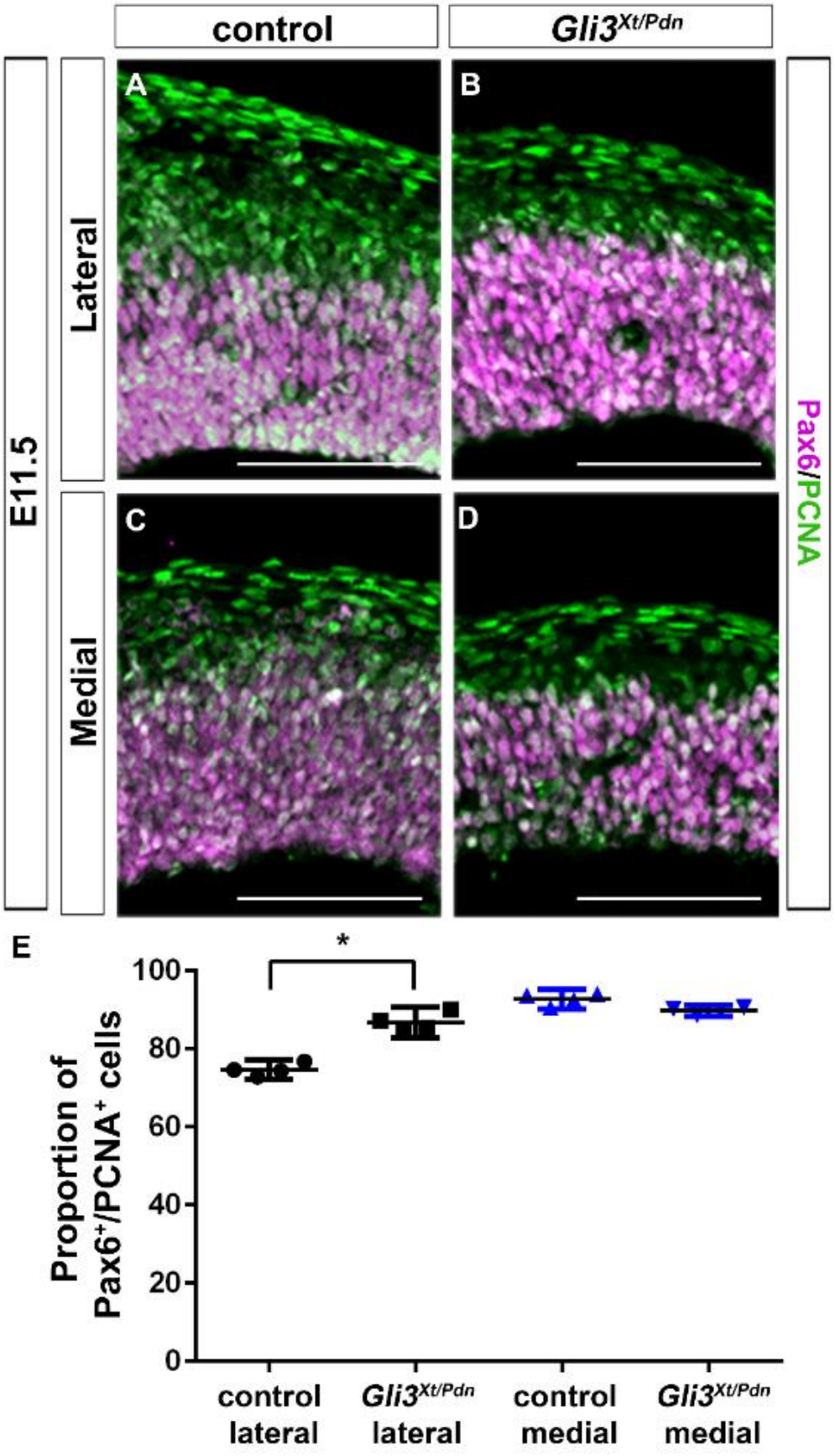
control
Gli3Xt/Pdn
E11.5
Lateral
Medial
A
B
C
D
Pax6/PCNA
E
*
Proportion of Pax6+/PCNA+ cells
100
80
60
40
20
0
control lateral
Gli3Xt/Pdn lateral
control medial
Gli3Xt/Pdn medial

**Figure 3.6: Reduction in *Gli3* resulted in an increased proportion of lateral apical progenitors in *Gli3*$^{Xt/Pdn}$ embryos at E11.5. A-D.** Pax6/PCNA immunofluorescence on sections of E11.5 cortex from control and *Gli3*$^{Xt/Pdn}$ embryos. **E.** Reduced *Gli3* significantly increased the proportion of lateral apical progenitors in *Gli3*$^{Xt/Pdn}$ mutants, whereas there was no effect on the proportion of medial apical progenitors. All statistical data represents mean ± 95% confidence interval; n=4; * = $p<0.05$; Mann-Whitney U-test. Scale bars = 100μm.

(2003) who reported that expression of *Pax6* was unaffected prior to E12.5, but was reduced at E12.5.

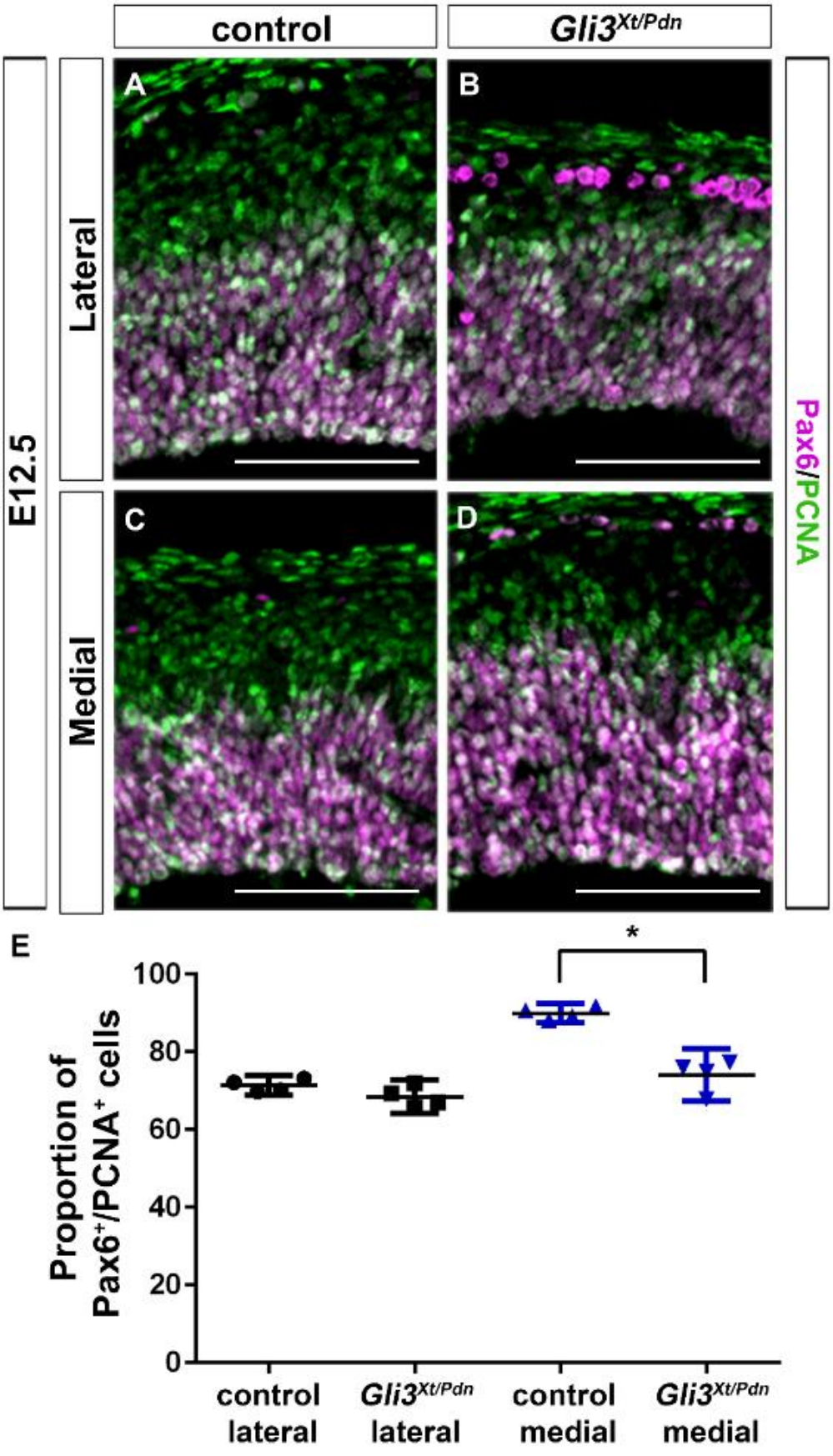
control
Gli3Xt/Pdn
E12.5
Lateral
Medial
A
B
C
D
Pax6/PCNA
E
*
Proportion of Pax6+/PCNA+ cells
100
80
60
40
20
0
control lateral
Gli3Xt/Pdn lateral
control medial
Gli3Xt/Pdn medial

**Figure 3.7: Reduction in *Gli3* resulted in a decreased proportion of medial apical progenitor in *Gli3*$^{Xt/Pdn}$ embryos at E12.5. A-D.** Pax6/PCNA immunofluorescence on sections of E12.5 cortex from control and *Gli3*$^{Xt/Pdn}$ embryos. **E.** Reduced *Gli3* significantly decreased the proportion of medial apical progenitors in *Gli3*$^{Xt/Pdn}$ mutants, whereas there was no effect on the proportion of lateral apical progenitors. All statistical data represents mean ± 95% confidence interval; n=4; * = p<0.05; Mann-Whitney U-test. Scale bars = 100μm.

### 3.4 *Gli3* reduction results in a reduced basal progenitor population in *Gli3*$^{Xt/Pdn}$ embryos at E11.5 and an increased basal progenitor population at E12.5

As basal progenitors are formed via the asymmetric divisions of apical progenitors, the proportion of basal progenitors present in the *Gli3*$^{Xt/Pdn}$ mutant was assessed to see if it was altered along with the proportion of apical progenitors. PCNA immunofluorescence was carried out alongside Tbr2 immunofluorescence and the proportion of basal progenitors present at E11.5 was calculated. Laterally, as opposed to Pax6, there was a 1.36-fold decrease in the proportion of basal progenitors formed in the mutant (29.72±3.59% in control and 21.91±1.34% in mutant, n=4, p<0.05) (figure 3.8 A, B, E). However medially, as with Pax6, there was no statistically significant difference in the proportion of basal progenitors (13.43±1.29% in control and 14.55±1.15% in mutant, n=4, p>0.05) (figure 3.8 C, D, E). It is evident that the Gli3 reduction caused disruption to the normal formation of basal progenitors, possibly as a consequence of the disruption in the apical progenitor population.

The same analyses on basal progenitors were repeated at E12.5 to measure if the disruption in basal progenitor production at E11.5 had a consequent effect 24 hrs later. Laterally, there was a 1.47-fold increase in the proportion of basal progenitors in the mutant compared to control (30.15±1.79% in control and 44.21±3.35% in mutant, n=4, p<0.05) (figure 3.9 A, B, E), and a 2.01-fold increase in basal progenitor proportion medially (14.45±2.86% in control and 30.04±3.79% in mutant, n=4, p<0.05) (figure 3.9 C, D, E). Taken together, the decreased proportion of basal progenitors laterally at E11.5 followed by an overproduction of basal progenitors both laterally and

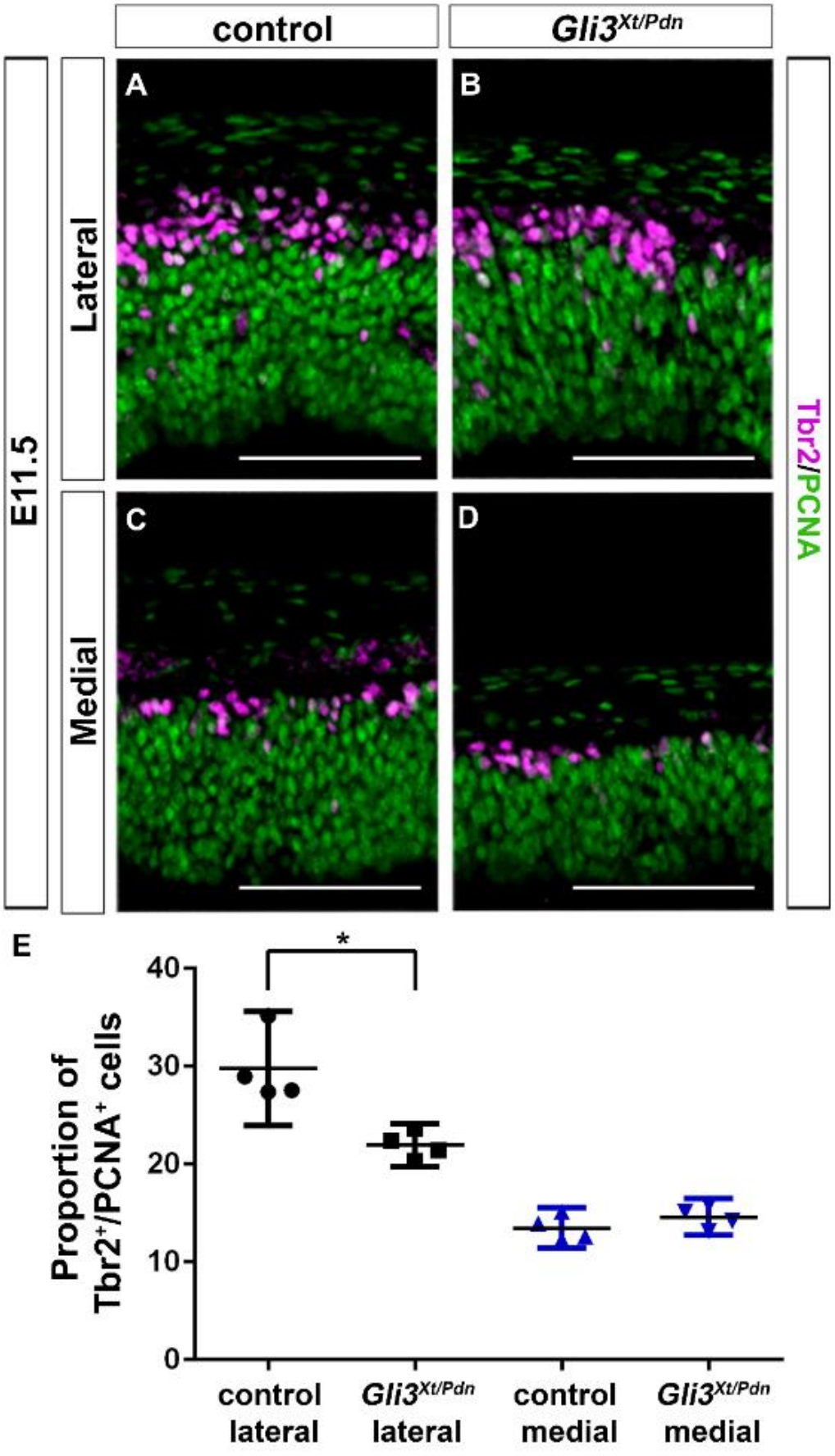
control
Gli3Xt/Pdn
E11.5
Lateral
Medial
A
B
C
D
Tbr2/PCNA
E
Proportion of Tbr2+/PCNA+ cells
40
30
20
10
0
*
control lateral
Gli3Xt/Pdn lateral
control medial
Gli3Xt/Pdn medial

**Figure 3.8: Reduction in *Gli3* resulted in a decreased proportion of lateral basal progenitors in *Gli3*$^{Xt/Pdn}$ embryos at E11.5. A-D.** Tbr2/PCNA immunofluorescence on sections of E11.5 cortex from control and *Gli3*$^{Xt/Pdn}$ embryos. **E.** Reduced *Gli3* significantly decreased the proportion of lateral basal progenitors in *Gli3*$^{Xt/Pdn}$ mutants, whereas there was no effect on the proportion of medial basal progenitors. All statistical data represents mean ± 95% confidence interval; n=4; * = $p<0.05$; Mann-Whitney U-test. Scale bars = 100μm.

medially at E12.5 indicate a possible delay in the normal timeline of progenitor formation.

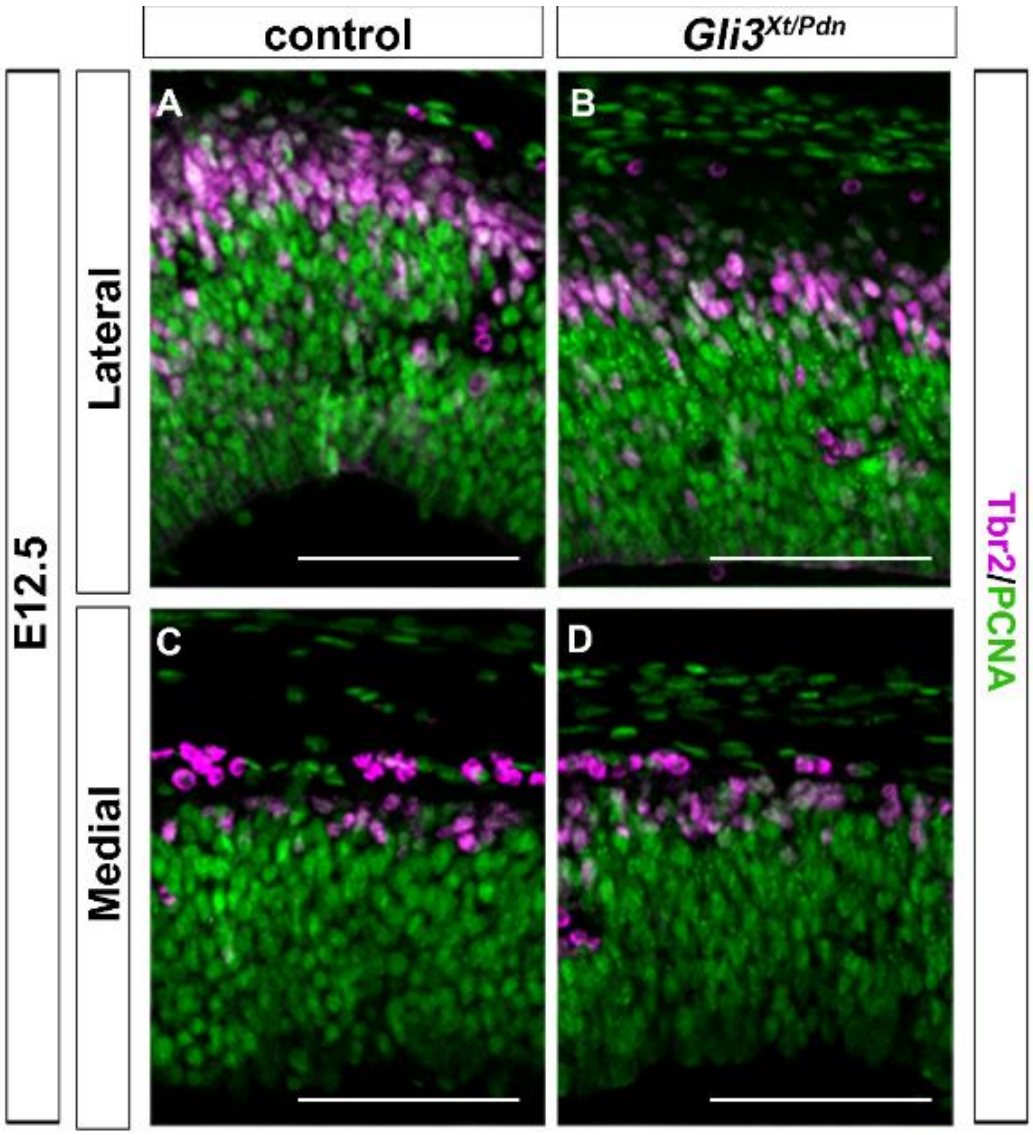
control
Gli3Xt/Pdn
E12.5
Lateral
Medial
A
B
C
D
Tbr2/PCNA

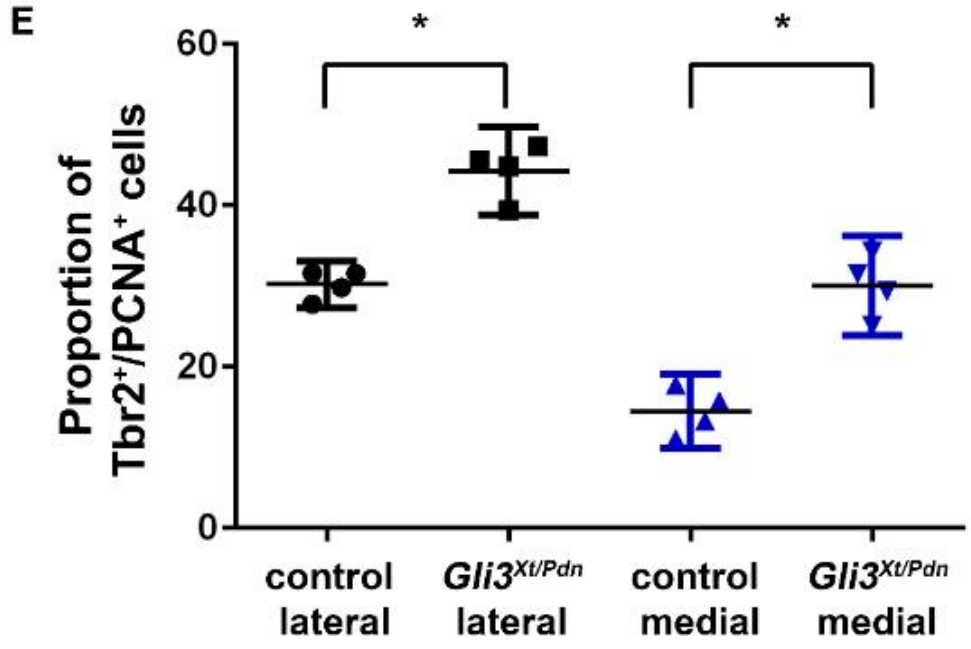
E
Proportion of Tbr2+/PCNA+ cells
60
40
20
0
*
*
control lateral
Gli3Xt/Pdn lateral
control medial
Gli3Xt/Pdn medial

**Figure 3.9: Reduction in *Gli3* resulted in increased proportions of lateral and medial basal progenitors in *Gli3*$^{Xt/Pdn}$ embryos at E12.5. A-D.** Tbr2/PCNA immunofluorescence on sections of E12.5 cortex from control and *Gli3*$^{Xt/Pdn}$ embryos. **E.** Reduced *Gli3* significantly increased the proportions of lateral and medial basal progenitors in *Gli3*$^{Xt/Pdn}$ mutants. All statistical data represents mean ± 95% confidence interval; n=4; * = $p<0.05$; Mann-Whitney U-test. Scale bars = 100μm.

### 3.5 *Gli3* reduction results in a decreased neuronal population in *Gli3*$^{Xt/Pdn}$ embryos at E11.5 and an increased neuronal population at E12.5

Due to the alterations in apical and basal progenitor proportions, the proportions of early-born neurons formed in the E11.5 and E12.5 neocortex were assessed. Immunofluorescence against Tbr1 was carried out using TOPRO-3 as a nuclear counterstain to determine the proportion of neurons compared to the total number of cells. At E11.5, laterally there was a nearly two-fold decrease in the proportion of neurons formed in the mutant compared to control (19.55±1.78% in control and 9.97±1.90% in mutant, n=4, $p<0.05$) (figure 3.10 A, B, E). This was in alignment with the increased proportion of apical progenitors which seemed to have reduced differentiation rates into basal progenitors and neurons. However, medially, following the same pattern as with apical progenitors and basal progenitors, there was no difference in neuron formation (8.44±1.08% in control and 8.87±1.92% in mutant, n=4, $p>0.05$) (figure 3.10 C, D, E).

The proportion of neurons formed was also assessed at E12.5 using Tbr1 and TOPRO-3. In the lateral cortex, the proportion of neurons formed in *Gli3*$^{Xt/Pdn}$ embryos was increased 1.16-fold compared to control (19.45±1.73% in control and 22.52±2.33% in mutant, n=4, $p<0.05$) (figure 3.11 A, B, E). Medially, there was a larger increase in neuron proportion in the mutant compared to control of 1.52-fold (9.40±0.64% in control and 14.30±2.56% in mutant, n=4, $p<0.05$) (figure 3.11 C, D, E). The differences in neuron formation again align with the differences in basal progenitor formation and are likely to be linked with the decrease in apical progenitors.

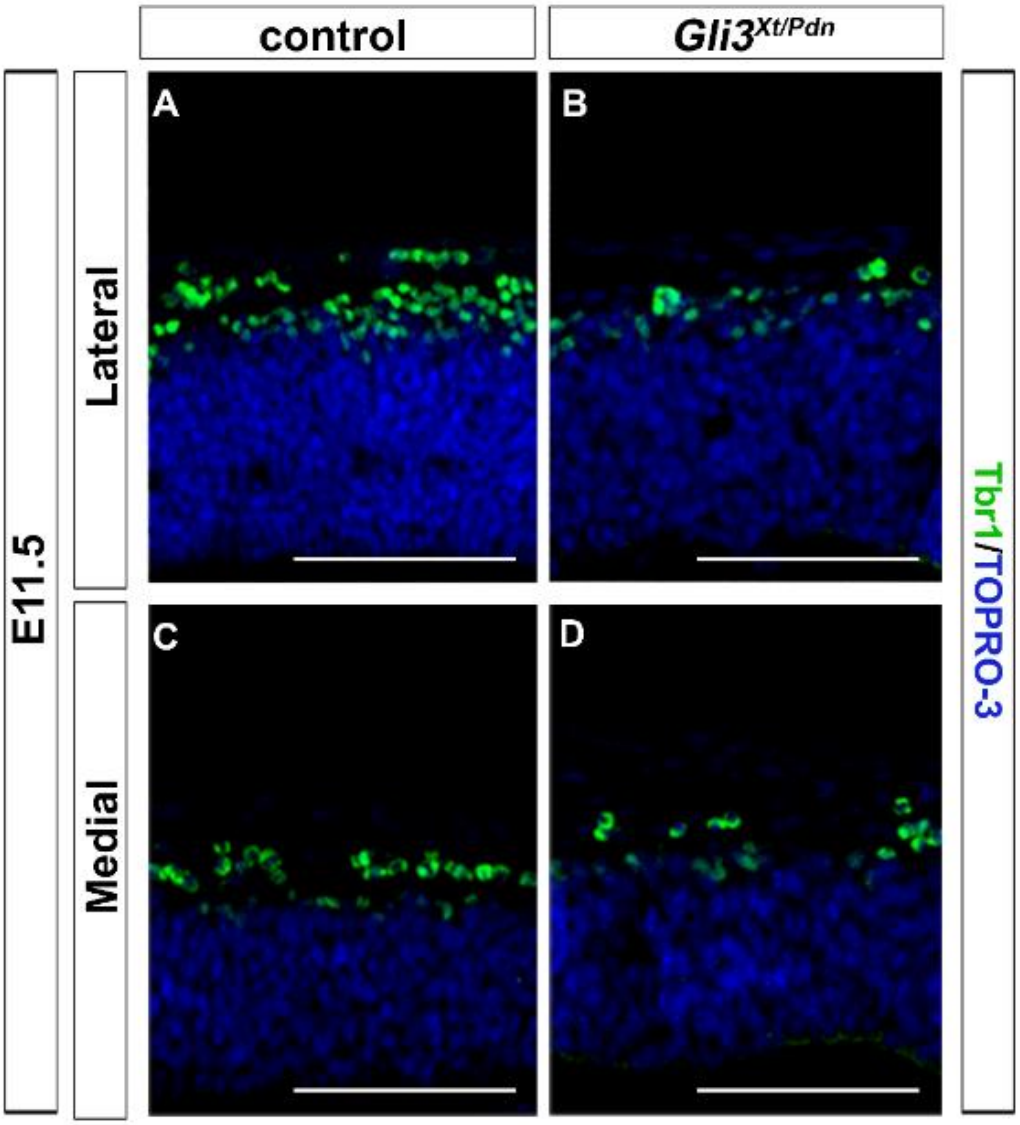
control
Gli3Xt/Pdn
E11.5
Lateral
Medial
A
B
C
D
Tbr1/TOPRO-3

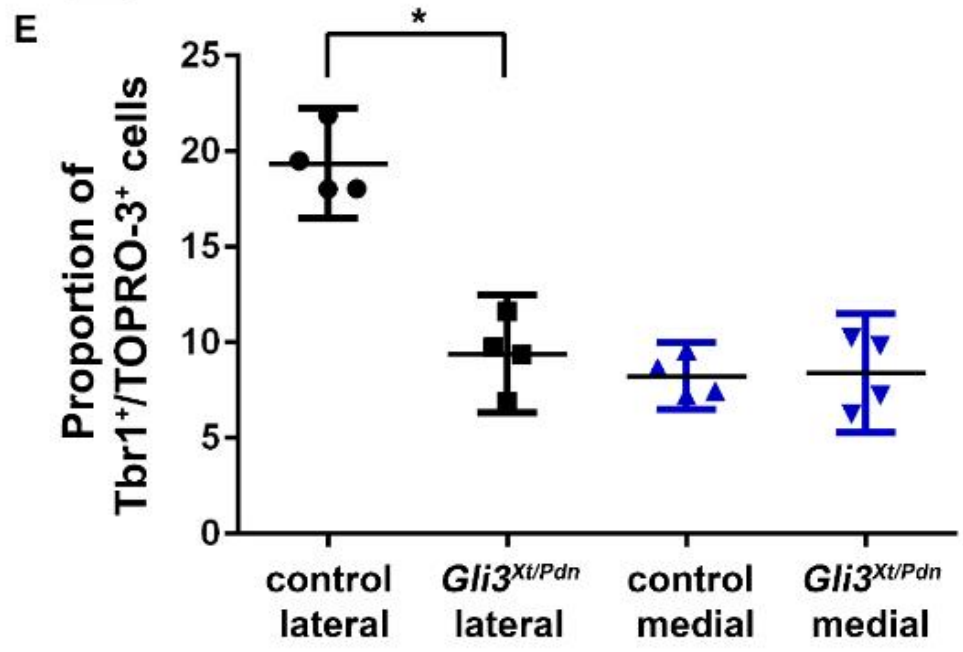
E
Proportion of Tbr1+/TOPRO-3+ cells
25
20
15
10
5
0
*
control lateral
Gli3Xt/Pdn lateral
control medial
Gli3Xt/Pdn medial

**Figure 3.10: Reduction in *Gli3* resulted in a decreased proportion of lateral early-born neurons in *Gli3*$^{Xt/Pdn}$ embryos at E11.5. A-D.** Tbr1/TOPRO-3 immunofluorescence on sections of E11.5 cortex from control and *Gli3*$^{Xt/Pdn}$ embryos. **E.** Reduced *Gli3* significantly decreased the proportion of lateral early-born neurons in *Gli3*$^{Xt/Pdn}$ mutants, whereas there was no effect on the proportion of medial early-born neurons. All statistical data represents mean ± 95% confidence interval; n=4; * = $p<0.05$; Mann-Whitney U-test. Scale bars = 100μm.

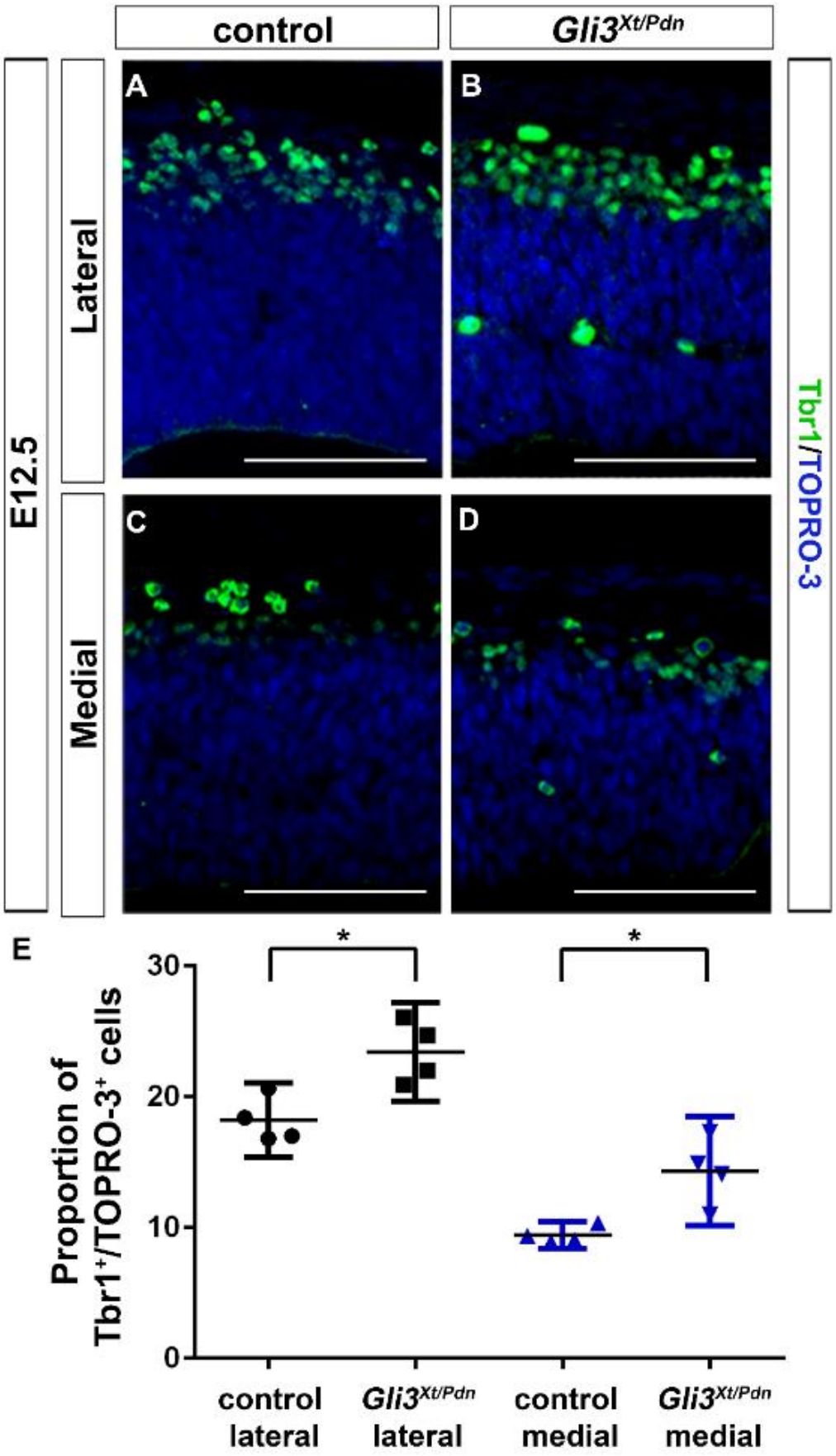
control
Gli3Xt/Pdn
E12.5
Lateral
Medial
A
B
C
D
Tbr1/TOPRO-3
E
Proportion of Tbr1+/TOPRO-3+ cells
30
20
10
0
*
*
control lateral
Gli3Xt/Pdn lateral
control medial
Gli3Xt/Pdn medial

**Figure 3.11: Reduction in *Gli3* resulted in increased proportions of lateral and medial early-born neurons in *Gli3*$^{Xt/Pdn}$ embryos at E12.5. A-D.** Tbr1/TOPRO-3 immunofluorescence on sections of E12.5 cortex from control and *Gli3*$^{Xt/Pdn}$ embryos. **E.** Reduced *Gli3* significantly increased the proportions of lateral and medial early-born neurons in *Gli3*$^{Xt/Pdn}$ mutants. All statistical data represents mean ± 95% confidence interval; n=4; * = $p<0.05$; Mann-Whitney U-test. Scale bars = 100μm.

### 3.6 Discussion

Gli3 protein is clearly expressed in the developing dorsal telencephalon at time points critical to the development of the cortex. The majority of Gli3 was expressed overlapping with Pax6 in apical progenitors, however there was also some expression in $Tbr2^{+}$ basal progenitors. There was a reduction in the intensity of the Gli3 staining in the E11.5 and E12.5 cortex of *Gli3*$^{Xt/Pdn}$ embryos, and these were used to further examine the role of Gli3 on neuron formation in the developing cortex.

At E11.5 in the lateral telencephalon, there was a larger proportion of apical progenitors to total progenitors in the *Gli3*$^{Xt/Pdn}$ mutant compared to control. At the same time, there was a smaller proportion of basal progenitors and a smaller proportion of neurons. By E12.5, the proportion of apical progenitors in the mutant was not significantly different to the proportion in control, effectively showing a decrease in the proportion of apical progenitors from E11.5 to E12.5 in the mutant. Conversely, the proportions of basal progenitors and neurons had both increased in the mutant. In the medial telencephalon at E11.5, there was no significant difference in the proportion of apical progenitors, basal progenitors or neurons in the mutant compared to control. However, by E12.5, there was a significantly smaller proportion of apical progenitors in the mutant, and significantly larger proportions of basal progenitors and neurons. At E11.5 there were differences measured in the progenitor and neuronal proportions laterally yet there were no differences measured medially. This may have been due to the progression of neurogenesis from lateral to medial, but it cannot be ruled out that altered signalling within the *Gli3*$^{Xt/Pdn}$ dorsal telencephalon may also have contributed, or possibly a mixture of both. However, the rostro-caudal level examined was chosen to minimise the impact of disrupted signalling centres. Taken together, the general trend for increased apical progenitors and decreased basal progenitors and neurons at E11.5 followed by decreased apical progenitors and increased basal progenitors and neurons at E12.5 would indicate an early delay in neurogenesis. As Gli3 showed the greatest expression in apical progenitors, it is likely that this delay was due to a cell-autonomous effect on the asymmetric division of apical progenitors which give rise to basal progenitors and neurons.

### *3.6.1 Gli3 protein is primarily expressed in apical progenitors*

Loss of Gli3 has been linked with disruptions to the developing telencephalon since Johnson (1967) described the *extra-toes* (*Gli3*$^{Xt/Xt}$) mouse, which carries a deletion of the 3' end of *Gli3* resulting in a null mutation. *Gli3* mRNA has been shown to be expressed in the dorsal telencephalon, particularly in the VZ at E11.5 and E12.5 (Amaniti *et al.*, 2013; Hui *et al.*, 1994), close to the beginning of neurogenesis in the cortex and important time points for the development of the final structure and function of the cortex (Martynoga *et al*., 2012). Furthermore, it has been confirmed by western blot that Gli3 is expressed in the developing telencephalon (Magnani *et al.*, 2013; Fotaki *et al*., 2006), but there is little published data showing the cellular location of the Gli3 protein in dorsal telencephalon at different ages. Here, in alignment with mRNA *in situ* (Amaniti *et al*., 2013), it was confirmed via immunofluorescence that Gli3 is expressed mostly in the VZ at E11.5 and E12.5 of the developing neocortex, showing mainly concomitant expression with Pax6 and so in apical progenitors. Indeed, in the developing human telencephalon, Pollen *et al.* (2014) carried out single-cell mRNA sequencing and also revealed that GLI3 clusters with PAX6 and is a marker of radial glial cells. Due to its high expression in apical progenitors, which are the source of basal progenitors and during early neurogenesis the main source of neurons, Gli3 is therefore in a prime position to regulate early neurogenesis.

There was much less overlap between Gli3 expression and Tbr2. The basal progenitors in which Gli3 expression was the most intense were located within the VZ, presumably moving basally on route to the forming SVZ. Englund *et al.* (2005) reported Tbr2$^{+}$ progenitors in the VZ commonly expressed Pax6 as well, although both were at lower levels than when either was expressed alone. It is likely that these progenitors which express both Pax6 and Tbr2 are newly formed basal progenitors moving from the ventricular surface through the VZ to the SVZ. Pax6 transcription has likely stopped but inherited mRNA and protein from the parent cell has not yet been fully broken down, and Tbr2 expression has already begun, resulting in dual expression. Based on their location, it is likely that the basal progenitors expressing Gli3 also belong to this population of basal progenitors newly formed from apical progenitors, and Gli3 has not fully cleared yet.

On a subcellular level, the localisation of Gli3 is interesting. Based on its role as a transcription factor, clearly expression would be expected in the nucleus. Indeed, I saw clear nuclear overlap between Gli3 and TOPRO-3 (figure 3.1). However it was

also abundantly evident that there was cytoplasmic expression which was particularly obvious at E17.5 (figure 3.1 E-H"), and which was also reported at E16.5 by Yabut *et al.* (2016), who described Gli3 expression to be cytoplasmic along the edge of the VZ. In the absence of Shh, the full-length Gli3 protein translocates to the base of the primary cilium, where it undergoes PKA phosphorylation triggering further phosphorylation by GSK3β and CK1. These phosphorylated residues result in a βTrCP binding site and subsequent $SCF^{\beta TrCP}$ ubiquitination (Tempe *et al.*, 2006). Via this mechanism, the C-terminus is cleaved from the full-length Gli3 protein via the ubiquitin-proteasome pathway and targeted for degradation. It is hypothesised that the N-terminus repressor form of Gli3 then translocates to the nucleus where it undertakes its role as a transcriptional repressor (Wen *et al.*, 2010). Clearly, there would be some cytoplasmic Gli3 expression expected, however it would be expected predominantly in the region of the primary cilium. Whilst in figure 3.1 F there appeared to be a band of stronger expression along the very edge of the ventricle where the primary cilium is located, Gli3 expression was widespread throughout the whole cytoplasm. It is possible that this expression is due to the processing and translocation of the protein from the cilium to the nucleus, however this may also indicate control over the nuclear localisation of Gli3 as a mechanism to regulate Gli3 repression. As stated before, higher resolution images of Gli3 expression are required, and it would be interesting to combine Gli3 staining with ciliary markers, such as Arl13b and gamma-tubulin.

Gli3 expression was also evaluated in the $Gli3^{Xt/Pdn}$ mutant embryo at E11.5 and E12.5. At E11.5, there was expression of Gli3 in the mutant dorsal telencephalon, however it was at a lower level than in control. Gli3 was chiefly expressed in the $Pax6^{+}$ apical progenitors of the mutant but was also expressed in some basal progenitors within the VZ as in control. At E12.5, again Gli3 was expressed in the dorsal telencephalon of the mutant in the VZ, but at a lower level than in control. Gli3 expression was more predominant in apical progenitors as opposed to basal progenitors. Whilst the intensity of the Gli3 staining in the $Gli3^{Xt/Pdn}$ dorsal telencephalon at E11.5 and E12.5 was reduced, quantification of the amount of Gli3 protein is still required, either by western blot or by measuring fluorescence levels.

In figure 3.3 it is also clear how the reduction in Gli3 affects the size and shape of the dorsal telencephalon. At E11.5, the cortex becomes thinner and longer in the mutants with expanded ventricles and obvious reduction in the size of the midline structures,

as has been reported previously (Friedrichs *et al*., 2008; Kuschel *et al.*, 2003). At E12.5, there is again a reduction of the midline structures, with a longer and thinner dorsal telencephalon. At both ages, the LGE is reduced in size.

Altogether, Gli3 protein expression was evident in the dorsal telencephalon at E11.5 and E12.5, coinciding mostly with Pax6 expression in apical progenitors. As shown here, in the *Gli3*$^{Xt/Pdn}$ embryo the pattern of Gli3 expression remains the same as in control embryos although at a lower level. It is clear that a reduction in *Gli3* affects both the size and shape of the dorsal telencephalon, making it evident that the level of Gli3 expression is critically important in the proper development of the cortex.

### *3.6.2 Gli3 reduction leads to alterations in the apical progenitor, basal progenitor and early neuronal populations*

Due to the abundance of Gli3 protein in the VZ of the E11.5 and E12.5 *Gli3*$^{Xt/Pdn}$ embryos, I assessed how the reduction of Gli3 in these mutant embryos would affect progenitors and subsequent cortical neurons. As stated, overall at E11.5 there was an increased apical progenitor proportion and decreased basal progenitor and neuronal proportion in the lateral cortex, whilst the medial cortex was unaffected. By E12.5, the apical progenitor proportions both laterally and medially had decreased compared to control with respect to the E11.5 measurements, and the basal progenitor and neuronal proportions had increased. Taken together, one possible explanation for the disruption to the progenitor and neuronal proportions at E12.5, is that the system attempted to rectify the increased proportion of apical progenitors present at E11.5 by differentiating a large proportion of them into basal progenitors and neurons in the 24 hrs between analyses, but did this overzealously, thereby surpassing the control levels of progenitors and neurons. In this scenario, these analyses could suggest that the timing of asymmetrical, differentiative divisions has been disrupted in the *Gli3*$^{Xt/Pdn}$ embryo, ultimately leading to a delay in neuron formation.

Haubensak *et al.* (2004) used *Tis21*-GFP knock-in mice to highlight the proportion of progenitors in the neocortex dividing asymmetrically to form more differentiated cells. They showed that at the beginning of neurogenesis at approximately E10.5, apical progenitors in the VZ were dividing asymmetrically and had already formed basal progenitors which were translocating basally and also expressing *Tis21*, indicating

they were ready to begin differentiative division. The larger proportion of apical progenitors present in *Gli3*$^{Xt/Pdn}$ embryos at E11.5 and concomitant smaller proportions of basal progenitors and neurons may indicate that there was a delay in the timing of when apical progenitors should begin to divide differentiatively into basal progenitors and neurons. At E12.5, the smaller proportion of apical progenitors and larger proportions of basal progenitors and neurons in the mutant may indicate the system attempting to overcome the delay by pushing for more asymmetrical, differentiative divisions of apical progenitors into basal progenitors and neurons in the 24 hrs between measurements, depleting the apical progenitor pool. One way to further examine this would be to look at Tis21 expression in *Gli3*$^{Xt/Pdn}$ embryos, which was carried out and will be discussed in section 5.6.

Another possible explanation for the decreased basal progenitor proportion observed laterally at E11.5 could be a decrease in basal progenitor proliferation, although the concomitant increase in apical progenitor proportion would argue for an alteration in asymmetric division of apical progenitors. Furthermore, as Gli3 protein was primarily expressed in apical progenitors, I would argue that it was more likely that Gli3 had a direct effect on apical progenitors, altering their balance between differentiative and proliferative division and therefore the amount of basal progenitors formed, rather than an effect on basal progenitor proliferation itself. Indeed, there was also a decrease in neuronal proportion at E11.5, which can only be attributed to alterations in neurogenic progenitor division, so if basal progenitors at E11.5 were failing to proliferate and differentiating instead, I would not have expected to see a nearly two-fold decrease in the proportion of neurons.

As well as Gli3 cell intrinsic effects on apical progenitors, the contribution from alterations to signalling in the *Gli3*$^{Xt/Pdn}$ dorsal telencephalon cannot be ruled out. Kuschel *et al*. (2003) revealed that in the rostral-most *Gli3*$^{Xt/Pdn}$ dorsal telencephalon there was ectopic activation of *Fgf8* expression. Furthermore, due to the reduction in the cortical hem, *Wnt2b*, *Wnt3a* and *Bmp4* expression are abolished. Although the rostro-caudal level at which the analyses were performed was carefully selected to minimise the impact of the disruption in signalling, it is likely that it still influenced the cell populations.

One caveat of using Pax6 and Tbr2 as markers of apical and basal progenitors is that there is not completely exclusive expression of the two markers between the two populations. The sum of Pax6$^{+}$ and Tbr2$^{+}$ cells across the four conditions examined

(E11.5 lateral and medial and E12.5 lateral and medial) totalled between 101% and 112%. However, as mentioned above, this is in line with previous studies which also found some double expression of the two proteins in single cells (Englund *et al.*, 2005), which were suggested to be newly formed basal progenitors which had inherited Pax6 protein from their parent cell. I would suggest that the Gli3 expression seen in a number of $Tbr2^+$ basal progenitors (section 3.2.2) reflects the same situation. It should also be noted that Tbr2 is expressed in some preplate neurons, including postmitotic Cajal-Retzius (CR) cells (Englund *et al*., 2005). However, as PCNA was used in conjunction with Tbr2, only those $Tbr2^+$ cells which were progenitors were counted.

Another caveat of the above experiments was the use of Tbr1 to measure the proportion of early-born neurons. In addition to being expressed in early-born neurons generated from apical and basal progenitors and which will populate layer VI, Tbr1 is also expressed in the marginal zone in CR cells, cells which are born outwith the cortex and so not from cortical apical and basal progenitors. In the lateral telencephalon CR cells derive from the ventral pallium, which is slightly expanded in $Gli3^{Xt/Pdn}$ embryos (Friedrichs *et al*., 2008). One would expect therefore to see an increase in the proportion of $Tbr1^+$ cells in the lateral measurements undertaken above, however, I observed a decrease at E11.5. This could indicate that the delay in neurogenesis is greater than was measured. Medially, CR cells derive from the cortical hem, which is severely reduced in the $Gli3^{Xt/Pdn}$ mutant, however at E11.5 there was no difference between the proportion of $Tbr1^+$ neurons in the mutant and control, and an increased proportion of neurons in the mutant compared to control at E12.5. Therefore, it is likely that the $Tbr1^+$ neurons counted at the level used here reflect early-born neurons derived from apical progenitors. However, in the future it may be important to repeat these counts using a different neuronal marker, or to carry out immunofluorescence against Tbr1 and reelin, to rule out the contribution from any CR cells.

### 3.7 Summary

It has been shown here that Gli3 protein expression aligns with *Gli3* mRNA expression patterns, and that Gli3 is expressed in the dorsal telencephalon at E11.5 and E12.5. Gli3 is primarily expressed in $Pax6^{+}$ apical progenitors, with co-expression in a very small subset of likely newly differentiated $Tbr2^{+}$ basal progenitors. Furthermore, Gli3 is greatly reduced in the neocortex of $Gli3^{Xt/Pdn}$ embryos. As Gli3 was shown to be primarily expressed in apical progenitors which give rise to basal progenitors and early-born cortical neurons, the impact of the reduction of *Gli3* to these populations was assessed. In the lateral cortex of E11.5 $Gli3^{Xt/Pdn}$ embryos, there was an increased proportion of apical progenitors alongside decreased proportions of basal progenitors and neurons. By E12.5 in the lateral cortex, the proportion of apical progenitors in the mutant compared to control was unaltered, yet the proportions of basal progenitors and neurons were increased. In the medial cortex, at E11.5 the apical and basal progenitor and neuronal populations were unchanged, but by E12.5 there was a decreased apical progenitor proportion and increased basal progenitor and neuronal proportions. These analyses revealed a delay in neurogenesis at E11.5 in the $Gli3^{Xt/Pdn}$ dorsal telencephalon which was overcome by E12.5. As Gli3 expression was mostly confined to apical progenitors, it is likely that this delay was the result of cell intrinsic properties of Gli3 mutant apical progenitors, altering the proliferative/differentiative balance of these progenitors. However, as signalling is also altered in the $Gli3^{Xt/Pdn}$ dorsal telencephalon, it cannot be ruled out that alterations in Fgf, Wnt and BMP signalling contributed to the defects presented.

# Chapter 4: Reduction in *Gli3* results in major alterations to cell cycle kinetics in the *Gli3*$^{Xt/Pdn}$ neocortex

## 4.1 Introduction

As revealed in chapter 3, Gli3 protein was primarily expressed in apical progenitors of the early developing cortex, with little expression in basal progenitors. In the *Gli3*$^{Xt/Pdn}$ cortex, Gli3 was expressed in apical progenitors but was reduced. In these embryos, the proportion of apical progenitors was increased at E11.5 in the lateral cortex, whilst the proportions of basal progenitors and early-born neurons were decreased. However, in the medial cortex the proportions of all three progenitor populations were unaltered. At E12.5, in the mutant lateral cortex, the proportion of apical progenitors was unchanged compared to control, yet the proportions of basal progenitors and early-born neurons were increased. By E12.5 in the medial cortex, the apical progenitor proportion was decreased compared to control whereas the basal progenitor and early-born neuron proportions were increased compared to control. In this chapter, I will explore the cell cycle as a mechanism through which the progenitor populations may have been altered, leading to a delay in neurogenesis in the lateral cortex.

In order for the adult brain to form appropriately, the correct number of neurons must be produced at the correct time. Glutamatergic projection neurons of the murine cortex are mainly formed from apical and basal cortical progenitors, which must exit the cell cycle at the appropriate time to correctly form the required number of neurons for each cortical layer. If there is an increase in the differentiative capacity of a progenitor population, despite an initial increase in the production of neurons, the progenitor population will become depleted. This will ultimately lead to a reduction in the total number of neurons formed compared to control as the progenitors are exhausted. Conversely, if there is an increase in the proliferative capacity of a progenitor population, whilst there will be an initial decrease in the number of neurons formed due their delayed production, the larger progenitor pool will ultimately give rise to a larger population of neurons as compared to control (Dehay & Kennedy, 2007). A delay in the division of progenitors at the appropriate time can result in neurons from the incorrect layer being produced, resulting in the over-proliferation of one layer

at the expense of another, and leading to cytoarchitectural differences in the adult brain (Lange *et al*., 2009; Pilaz *et al*., 2009). In a number of seminal studies performed over the last few decades, the importance of the cell cycle in the decision of proliferative versus differentiative division has become apparent.

When a daughter cell is produced from a dividing mother cell, the daughter will enter G1-phase. G1-phase is a growth phase, during which the cell makes the decision as to whether it will leave the cell cycle or if it will remain in the cell cycle and divide again. During G1-phase, a restriction point is reached. If the retinoblastoma (Rb) family of proteins are hypophosphorylated the cell will not progress past the checkpoint, in which case it will differentiate or remain in G1-phase. Upon Rb hyperphosphorylation, the cell will progress past the checkpoint and genes required for transition into the next phase of the cell cycle will be up-regulated (Blagosklonny & Pardee, 2002). The following stage, S-phase, sees replication of the DNA. From here, cells will progress into a second growth phase, G2-phase, followed by undergoing mitosis during M-phase.

When each cortical progenitor divides, it may undergo either proliferative or differentiative division. When apical and basal progenitors undergo proliferative division, they produce two new apical or two new basal progenitors, respectively. When apical progenitors undergo differentiative division, they produce either one apical progenitor and one basal progenitor or neuron, or two neurons. When basal progenitors undergo differentiative division, they may produce one basal progenitor and one neuron, or more commonly two neurons.

The length of G1-phase has been shown to have a tight correlation with whether a progenitor will undergo proliferative or differentiative division. A shorter G1-phase has been shown to correlate with proliferative division (Lange *et al*., 2009; Pilaz *et al*., 2009), whilst G1-phase lengthening is required for differentiative division (Calegari & Huttner, 2003). The “cell cycle length” model suggests that a longer G1-phase allows for progenitors to receive and respond to differentiative signals (Calegari & Huttner, 2003). Conversely, S-phase has been suggested to be longer when a progenitor will undergo proliferative division, allowing for extra time to be spent checking the fidelity of DNA replication (Gonzales *et al*., 2015; Arai *et al.*, 2011). S-phase then gets shorter as progenitors undergo differentiative division. As with S-phase, G2-phase has been reported to be shorter during proliferative division, so that longer S- and G2-phases allow for progenitors to respond to proliferative signals (Gonzales *et al.*, 2015). Finally,

Pilaz *et al*. (2016) revealed that lengthening of M-phase results in a decrease in progenitor proliferation and an increase in neuron formation, altering the balance in apical progenitor division. Altogether, a shorter G1-phase, longer S- and G2-phases, followed by a shorter M-phase appear to correlate with a proliferative division. However, a longer G1-phase, shorter S- and G2-phases, and longer M-phase appear to correlate with a differentiative division, with varying degrees of evidence to support the effect of altering each phase length.

Clearly, cell cycle length is important in the decision of proliferative or differentiative division. In the E11.5 and E12.5 *Gli3*$^{Xt/Pdn}$ cortex, I reported alterations to the apical and basal progenitor and early-born neuron populations, likely in part caused by differences in the proliferative and differentiative divisions of the progenitors. By deleting *Gli3* in the dorsal telencephalon later in neurogenesis using a *NestinCre* driver line, Wang *et al*. (2011) reported that basal progenitors were depleted due to a reduction of apical progenitor proliferation and increased differentiation of the basal progenitors themselves. Meanwhile, in the limb bud, *Gli3* has been shown to promote differentiation at the expense of proliferation by negatively regulating the G1- to S-phase promoting Cyclin dependent kinase 6, *Cdk6* (Lopez-Rios *et al*., 2012). This raises the possibility that *Gli3* also regulates the cell cycle in cortical progenitors, which will in turn influence its effect over proliferative and differentiative division.

This chapter will address if reducing *Gli3* in the *Gli3*$^{Xt/Pdn}$ cortex affects the cell cycle. Firstly, I measured if there was an alteration in cell cycle re-entry/cell cycle exit at E11.5 and E12.5 in the lateral and medial cortex. Following this, I measured the length of each phase of the cell cycle in the total progenitor population to determine if cell cycle length was altered in the mutant. I found that it was reduced at both E11.5 and E12.5, and as Gli3 was primarily expressed in apical progenitors, I then measured each phase length in both apical and basal progenitors separately. In the *Gli3*$^{Xt/Pdn}$ neocortex, there was a decrease in the total cell cycle length, and in particular a shortening of both G1- and S-phases in apical progenitors, with very little effect on basal progenitors.

## 4.2 Cell cycle exit is decreased in the *Gli3*$^{Xt/Pdn}$ mutant at E11.5 but increased at E12.5

At E11.5, in the *Gli3*$^{Xt/Pdn}$ lateral cortex there was an increased apical progenitor proportion and decreased basal progenitor and neuronal proportions, whilst these remained unchanged in the medial cortex. Laterally, basal progenitors and neurons may have undergone apoptosis, and/or apical progenitors may have divided proliferatively, re-entering the cell cycle to produce new apical progenitors at the expense of basal progenitors and neurons. By E12.5, the apical progenitor proportion was unchanged and the basal progenitor and neuronal proportions were increased laterally, whilst medially there was a decrease in apical progenitor proportion and increased basal progenitor and neuronal proportions. Here both laterally and medially, apical progenitors may have undergone cell death and/or there was an increase in apical and basal progenitor cell cycle exit, followed by differentiation of both apical and basal progenitors into neurons.

I therefore examined progenitor cell cycle exit at these time points in the *Gli3*$^{Xt/Pdn}$ neocortex. In order to assess cell cycle exit, pregnant females were injected intraperitoneally (IP) with BrdU and sacrificed 24 hrs later. BrdU is a thymidine analogue which is incorporated into synthesising DNA, and so labels proliferating cells in S-phase of the cell cycle (Gratzner, 1982). Immunofluorescence against BrdU and PCNA was carried out, and the proportions of BrdU$^+$/PCNA$^+$ and BrdU$^+$/PCNA$^-$ cells were counted. Cells which were in S-phase at the time of BrdU injection became BrdU$^+$, and would also be PCNA$^+$ if, 24 hrs later, these cells had not exited the cell cycle and so remained as progenitors. In contrast, if they had exited the cell cycle and differentiated into neurons, they would be PCNA$^-$. Embryos were dosed with BrdU at E10.5 and sacrificed at E11.5 to assess the cell cycle exit of progenitors in the 24 hrs preceding E11.5, and dosed with BrdU at E11.5 before sacrifice at E12.5 to assess cell cycle exit in the 24 hrs preceding E12.5. As with previous analyses, the lateral and medial neocortex were examined (figure 4.1 A).

In the lateral E11.5 neocortex, the proportion of BrdU$^+$/PCNA$^-$ neurons that had formed following a differentiative division, was decreased in the *Gli3*$^{Xt/Pdn}$ embryo compared to control (15.77±0.86% in control and 7.20±1.13% in mutant, n=4, $p<0.05$) (figure 4.1 B, C, F), indicating mutant progenitor cell cycle re-entry. This agrees with the previously performed analyses suggesting that laterally at E11.5 there was a

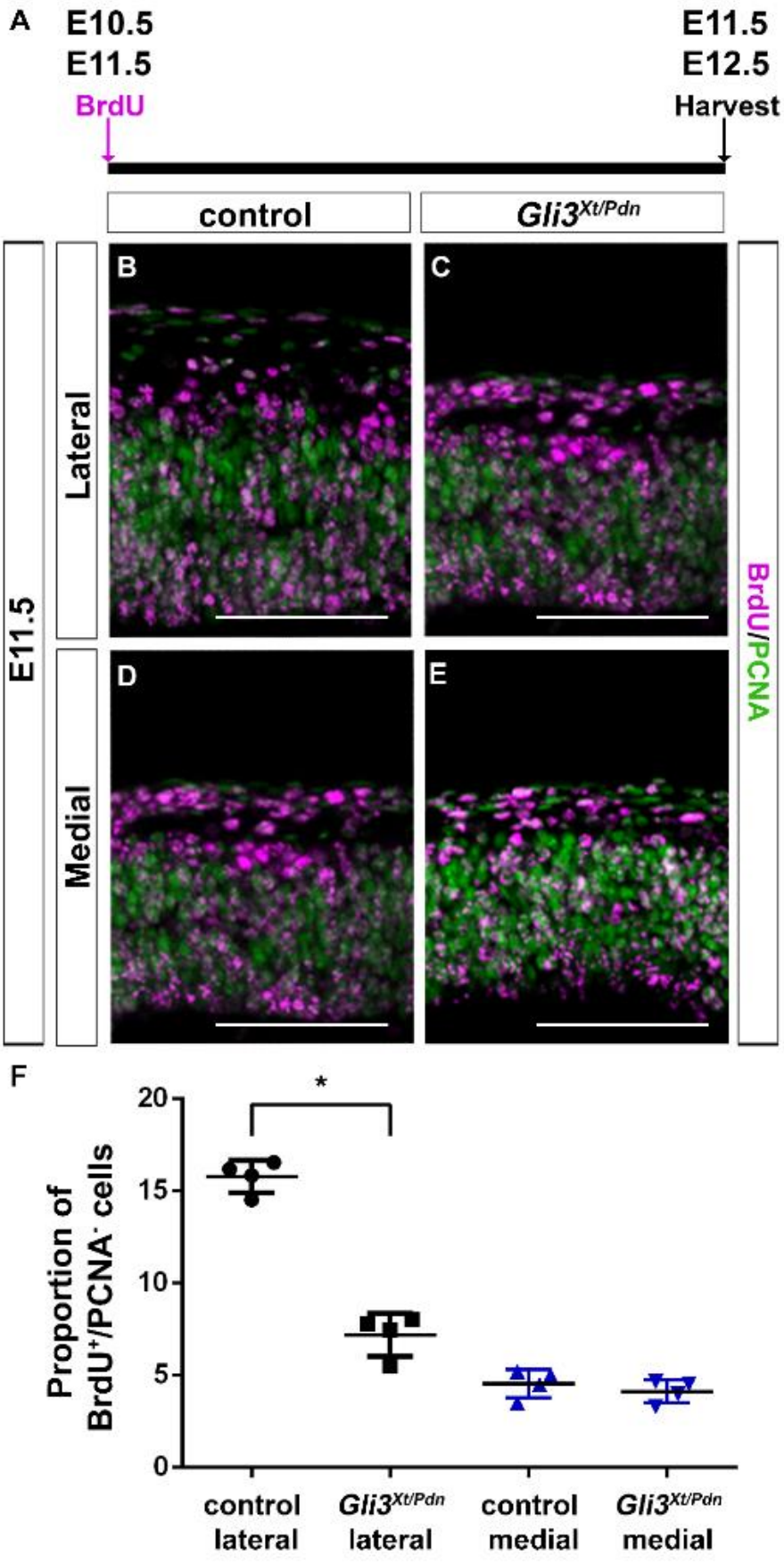
A
E10.5
E11.5
BrdU
E11.5
E12.5
Harvest
control
Gli3Xt/Pdn
E11.5
Lateral
Medial
B
C
D
E
BrdU/PCNA
F
Proportion of BrdU+/PCNA- cells
20
15
10
5
0
*
control lateral
Gli3Xt/Pdn lateral
control medial
Gli3Xt/Pdn medial

**Figure 4.1: Cell cycle exit was decreased laterally in the *Gli3*$^{Xt/Pdn}$ mutant at E11.5. A.** Schematic depicting the experimental BrdU paradigm used to measure cell cycle exit. BrdU was injected into pregnant dams at either E11.5 or E12.5 and embryos were harvested 24 hrs later. **B-E.** BrdU/PCNA immunofluorescence on sections of E11.5 cortex from control and *Gli3*$^{Xt/Pdn}$ embryos. **F.** The proportion of BrdU$^{+}$/PCNA$^{-}$ cells was significantly decreased in the *Gli3*$^{Xt/Pdn}$ lateral cortex. There was no significant difference between control and mutant in the medial cortex. All statistical data represents mean ± 95% confidence interval; n=4; * = $p<0.05$; Mann-Whitney U-test. Scale bars = 100μm.

larger apical progenitor population and smaller basal progenitor and early-born neuron populations, indicating a delay in the onset of differentiative divisions. In the medial neocortex, there was no change between the proportion of BrdU$^{+}$/PCNA$^{-}$ cells in the mutant compared to control (4.55±0.86% in control and 4.13±1.13% in mutant, n=4, $p>0.05$) (figure 4.1 D, E, F). Indeed, the analyses of apical and basal progenitors and early-born neurons also did not show any differences in the medial E11.5 cortex.

This analysis was repeated at E12.5. At this timepoint in the lateral neocortex, there was an increase in the proportion of BrdU$^{+}$/PCNA$^{-}$ cells in the *Gli3*$^{Xt/Pdn}$ embryo compared to control (12.03±2.05% in control and 18.56±2.75% in mutant, n=4, $p<0.05$) (figure 4.2 A, B, E), indicating a shift towards differentiative divisions and cell cycle exit at the expense of proliferative divisions in the mutant in the 24 hrs time interval. In the medial neocortex at E12.5, again there was an increase in the proportion of differentiative to proliferative divisions in the mutant compared to control (11.25±1.25% in control and 15.27±1.32% in mutant, n=4, $p<0.05$) (figure 4.2 C, D, E). Further, this was reflected as a decreased proportion of apical progenitors and increased proportions of basal progenitors and neurons. Altogether, there was an increase in cell cycle re-entry in the E11.5 lateral cortex, followed by increased cell cycle exit in the E12.5 lateral and medial cortex.

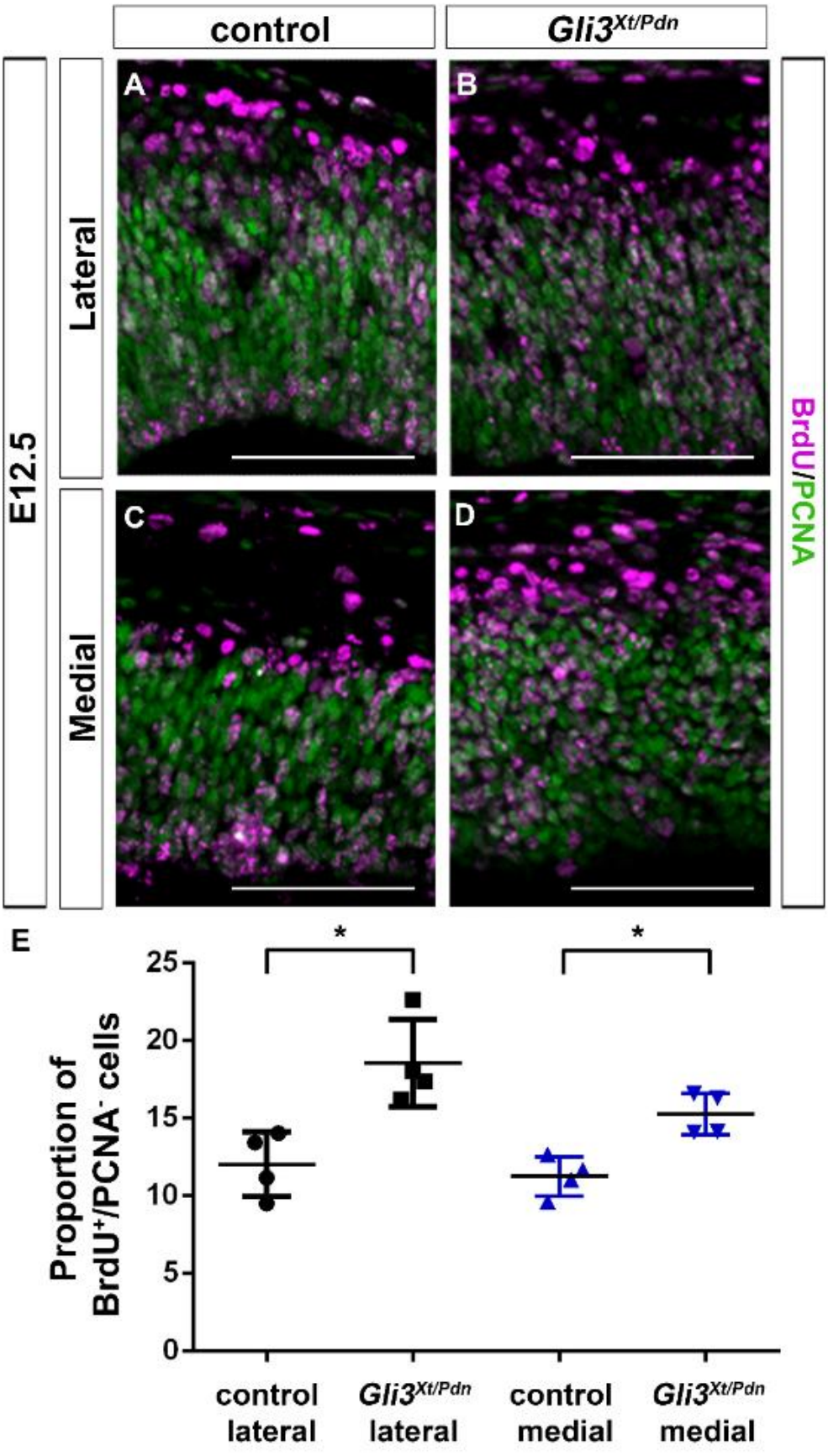
control
Gli3Xt/Pdn
E12.5
Lateral
Medial
A
B
C
D
BrdU/PCNA
E
Proportion of BrdU+/PCNA- cells
25
20
15
10
5
0
*
*
control lateral
Gli3Xt/Pdn lateral
control medial
Gli3Xt/Pdn medial

**Figure 4.2: Cell cycle exit was increased in the *Gli3*$^{Xt/Pdn}$ mutant at E12.5. A-D.** BrdU/PCNA immunofluorescence on sections of E12.5 cortex from control and *Gli3*$^{Xt/Pdn}$ embryos. **E.** The proportion of BrdU$^{+}$/PCNA$^{-}$ cells was significantly increased in the *Gli3*$^{Xt/Pdn}$ lateral and medial cortex. All statistical data represents mean ± 95% confidence interval; n=4; * = p<0.05; Mann-Whitney U-test. Scale bars = 100μm.

## 4.3 Cell cycle phase lengths are altered in the total cortical progenitor population of E11.5 and E12.5 *Gli3*$^{Xt/Pdn}$ embryos

As mentioned before, the cell cycle is critical to the decision of which mode of division a progenitor will undertake. *Cdk6*, a gene critical to the progression of progenitors from G1-phase into S-phase, is directly regulated by *Gli3* (Lopez-Rios *et al.*, 2012; Vokes *et al*., 2008). As cell cycle re-entry/exit were shown to be disrupted in the *Gli3*$^{Xt/Pdn}$ cortex at E11.5 and E12.5, resulting in an alteration in proliferative/differentiative division, the length of the cell cycle was examined. Decreased G1- and M-phases and increased S- and G2-phases would indicate increased progenitor proliferation, whilst longer G1- and M-phases and shorter S- and G2-phases would indicate increased differentiative division. Before undertaking extensive analyses of the cell cycle in apical and basal progenitors separately, I examined both progenitor populations together. Cell cycle phase lengths were found to be altered, and as Gli3 expression is mainly restricted to apical progenitors, I examined both populations separately to determine if *Gli3* acted cell-autonomously.

### *4.3.1 Determination of the length of each phase of the cell cycle*

To begin with, S-phase length was measured and from here total cell cycle length was calculated. IdU, a thymidine analogue distinguishable from BrdU (Gratzner, 1982), was injected IP into E11.5 and E12.5 pregnant females, followed by IP injection of BrdU 1.5 hrs later. Females were sacrificed 30 mins after BrdU injection, and embryos were harvested (figure 4.3 A). IdU and BrdU were used as they label cells in S-phase at the time of administration of each substance. The fraction of cells in S-phase compared to the total number of proliferative cells within the population measured, is

proportional to the length of S-phase ($T_S$) as compared to the length of the total cell cycle ($T_C$), according to Nowakowski *et al.* (1989). As the progenitors of a population exhibit asynchronous progression through the cell cycle, by administering IdU and BrdU sequentially it is to possible to distinctly label different proportions of the progenitors. A small proportion will be labelled with IdU only; those cells were in S-phase at the time of IdU administration but have progressed into G2-phase by the time of BrdU administration. These cells are referred to as “leaving-cells”, or “L-cells”. The majority of cells which are labelled following this protocol will be in S-phase at the time of IdU administration and will still be in S-phase at the time of BrdU administration, and so become double-labelled by both substances. These cells are referred to the “staying-cells”, or “S-cells” (Martynoga *et al.*, 2005). Therefore, following the logic of Nowakowski *et al.* (1989) above and as determined by Shibui *et al.* (1989) and Martynoga *et al.*, (2005), the ratio of L-cells to S-cells is equal to the ratio of the length of time allowed for IdU incorporation ($T_I$ here equal to 1.5 hrs) compared to $T_S$:

$T_I$ / $T_S$ = L-cells / S-cells

Therefore:

$T_S = T_I$ / (L-cells / S-cells)

Furthermore, the same concept can be extrapolated to calculate $T_C$ using $T_S$ and the total number of proliferative cells within the population under measure (P-cells):

$T_S$ / $T_C$ = S-cells / P-cells

Therefore:

$T_C = T_S$ / (S-cells / P-cells)

In the data presented in chapter 4, $T_S$ and $T_C$ were first calculated for all cortical progenitors combined. Therefore, the number of P-cells was determined by counting the number of TOPRO-$3^+$ cells within the ventricular zone, as Caviness *et al.* (1995) and Estivill-Torrus *et al*. (2002) estimated that between 98% and 100% of progenitors located here at the ages examined are proliferative.

In order to calculate G2-phase length ($T_{G2}$), BrdU was administered to pregnant dams 1 hr, 1.5 hrs or 2 hrs before sacrificing and harvesting embryos (figures 4.5 and 4.6).

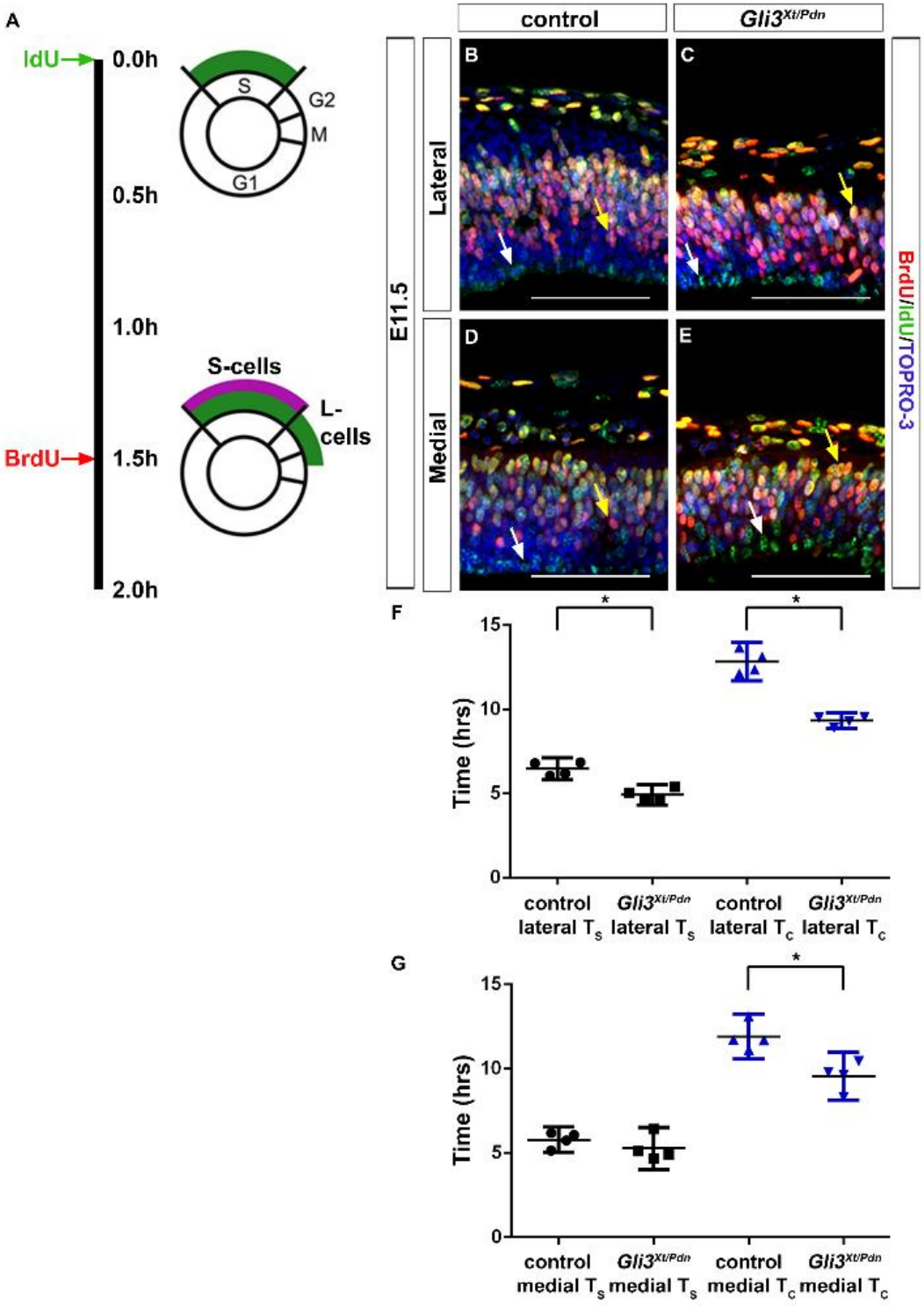
A
IdU
0.0h
S
G2
M
G1
0.5h
1.0h
S-cells
L-cells
BrdU
1.5h
2.0h
control
Gli3Xt/Pdn
E11.5
Lateral
Medial
B
C
D
E
BrdU/IdU/TOPRO-3
F
Time (hrs)
15
10
5
0
control lateral Ts
Gli3Xt/Pdn lateral Ts
control lateral Tc
Gli3Xt/Pdn lateral Tc
G
Time (hrs)
15
10
5
0
control medial Ts
Gli3Xt/Pdn medial Ts
control medial Tc
Gli3Xt/Pdn medial Tc

**Figure 4.3: S-phase and total cell cycle length were decreased in the *Gli3*$^{Xt/Pdn}$ total cortical progenitor population at E11.5. A.** Schematic depicting the experimental BrdU/IdU injection paradigm used to measure S-phase and total cell cycle length. **B-E.** BrdU/IdU/TOPRO-3 immunofluorescence on sections of E11.5 cortex from control and *Gli3*$^{Xt/Pdn}$ embryos. White arrows depict IdU/TOPRO-3 co-labelled L-cells, yellow arrows depict BrdU/IdU/TOPRO-3 co-labelled S-cells. **F.** S-phase and total cell cycle length were significantly decreased in the lateral *Gli3*$^{Xt/Pdn}$ cortex. **G.** Total cell cycle length was significantly decreased in the medial *Gli3*$^{Xt/Pdn}$ cortex whilst there was no effect on S-phase length. All statistical data represents mean ± 95% confidence interval; n=4; * = $p<0.05$; Mann-Whitney U-test. Scale bars = 100μm.

Sections from the embryos were stained for BrdU as a marker of S-phase and pHH3 as a marker of M-phase. The number of double-labelled cells was quantified and plotted as a fraction of the total number of pHH3$^+$ cells against the defined time-points. $T_{G2}$ was designated as the time at which 50% of cells in M-phase were in S-phase at the time of BrdU administration and so were BrdU$^+$ (Arai *et al.*, 2011). To calculate $T_{G2}$ for all progenitors combined, all pHH3$^+$ cells were counted together irrespective of their position at the ventricular surface or in an aventricular position.

To calculate the length of M-phase ($T_M$), sections from embryos were stained with pHH3 and PCNA. Thereby, the proportion of cells in M-phase compared to the total proliferative population could be calculated, and extrapolating from the method used to calculate $T_S$ as above, $T_M$ could be calculated from $T_C$:

$T_M = T_C$ (pHH3$^+$ cells / PCNA$^+$ cells)

To calculate $T_M$ for all progenitors combined, the total number of pHH3$^+$ cells present in the box counted was used.

Finally, the length of G1-phase has been shown to be critically important in the decision of a progenitor to divide proliferatively or differentiatively (Calegari & Huttner, 2003). In the *Gli3*$^{Xt/Pdn}$ mutant, a disruption in proliferative/differentiative division may have, at least in part, underlaid the disruption in both cell cycle exit and apical/basal progenitor and early-born neuron proportions. Therefore, it was important to measure

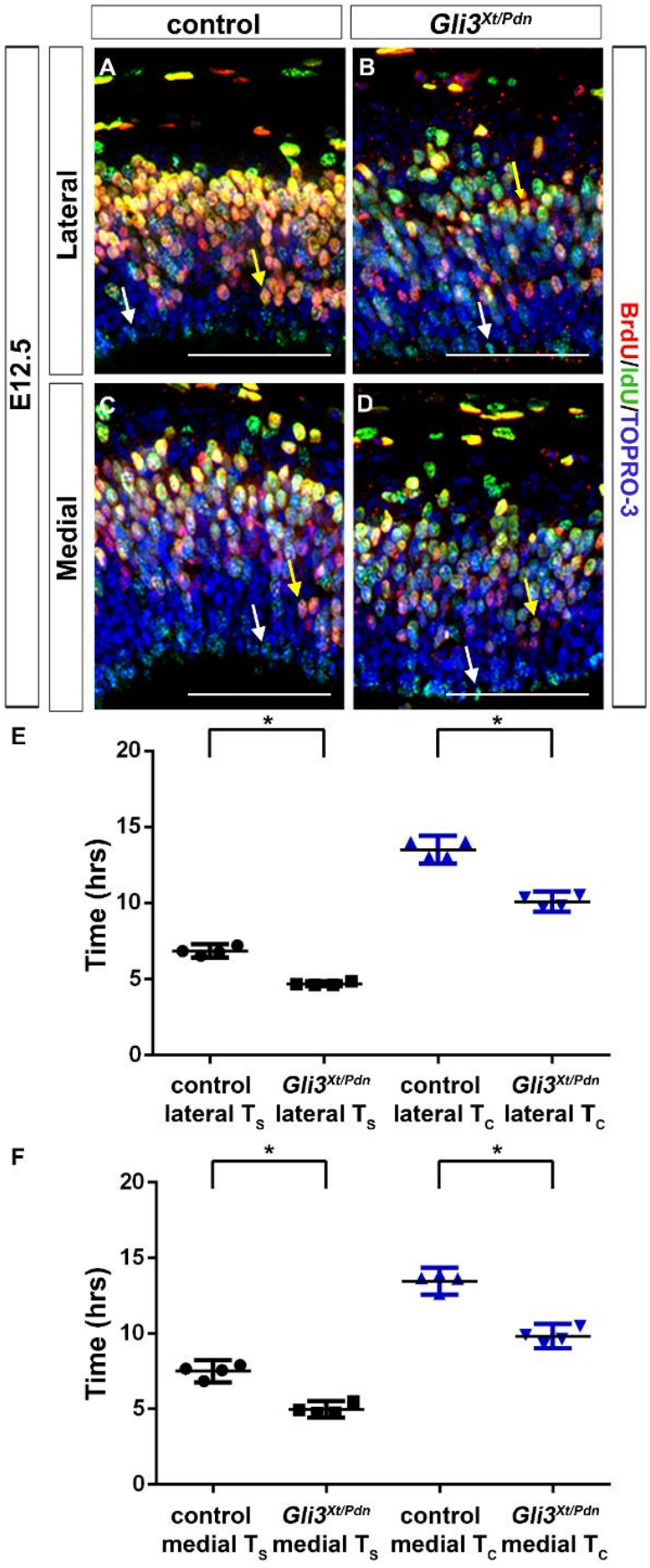
control
Gli3Xt/Pdn
E12.5
Lateral
Medial
A
B
C
D
BrdU/IdU/TOPRO-3
E
Time (hrs)
20
15
10
5
0
*
*
control lateral Ts
Gli3Xt/Pdn lateral Ts
control lateral Tc
Gli3Xt/Pdn lateral Tc
F
Time (hrs)
20
15
10
5
0
*
*
control medial Ts
Gli3Xt/Pdn medial Ts
control medial Tc
Gli3Xt/Pdn medial Tc

**Figure 4.4: S-phase and total cell cycle length were decreased in the *Gli3*$^{Xt/Pdn}$ total cortical progenitor population at E12.5. A-D.** BrdU/IdU/TOPRO-3 immunofluorescence on sections of E12.5 cortex from control and *Gli3*$^{Xt/Pdn}$ embryos. White arrows depict IdU/TOPRO-3 co-labelled L-cells, yellow arrows depict BrdU/IdU/TOPRO-3 co-labelled S-cells. **E.** S-phase and total cell cycle length were significantly decreased in the lateral *Gli3*$^{Xt/Pdn}$ cortex. **F**. S-phase and total cell cycle length were significantly decreased in the medial *Gli3*$^{Xt/Pdn}$ cortex. All statistical data represents mean ± 95% confidence interval; n=4; * = p<0.05; Mann-Whitney U-test. Scale bars = 100μm.

G1-phase length ($T_{G1}$). It was not possible to directly measure $T_{G1}$ in these embryos, but as $T_C$, $T_S$, $T_{G2}$ and $T_M$ had already been measured, it was possible to indirectly calculate $T_{G1}$ by subtracting the sum of $T_S$, $T_{G2}$ and $T_M$ from $T_C$. Again, this measurement was carried out at E11.5 and E12.5, both laterally and medially for all cortical progenitors combined.

### *4.3.2 G1-, S- and M-phase and total cell cycle length were reduced in the total progenitor population in the Gli3*$^{Xt/Pdn}$ *cortex at E11.5 and E12.5*

In the E11.5 lateral neocortex, $T_C$ was shortened in the *Gli3*$^{Xt/Pdn}$ mutant compared to control, from 12.83±0.70 hrs in the control to 9.33±0.28 hrs in the mutant (n=4, p<0.05) (figure 4.3 B, C, F). Furthermore, $T_S$ was also shortened in the mutant from 6.48±0.40 hrs in control to 4.93±0.37 hrs in the mutant (n=4, p<0.05) (figure 4.3 B, C, F). In the control medial neocortex $T_C$ was 11.91±0.83 hrs, yet it was shorter in the mutant at only 9.56±0.87 hrs (n=4, p<0.05) (figure 4.3 D, E, G). However, $T_S$ was unaffected in the mutant medial neocortex (5.80±0.46 hrs in control and 5.28±0.77 hrs in mutant, n=4, p>0.05) (figure 4.3 D, E, G).

At E12.5, in the lateral neocortex $T_C$ was again shorter in the mutant than in control (13.51±0.56 hrs in control and 10.08±0.40 hrs in mutant, n=4, p<0.05) (figure 4.4 A, B, E), as was $T_S$ (6.84±0.27 hrs in control and 4.68±0.11 hrs in mutant, n=4, p<0.05) (figure 4.4 A, B, E). Medially, $T_C$ was also shorter in the mutant compared to control (13.46±0.56 hrs in control and 9.83±0.49 hrs in control, n=4, p<0.05) (figure 4.4 C,

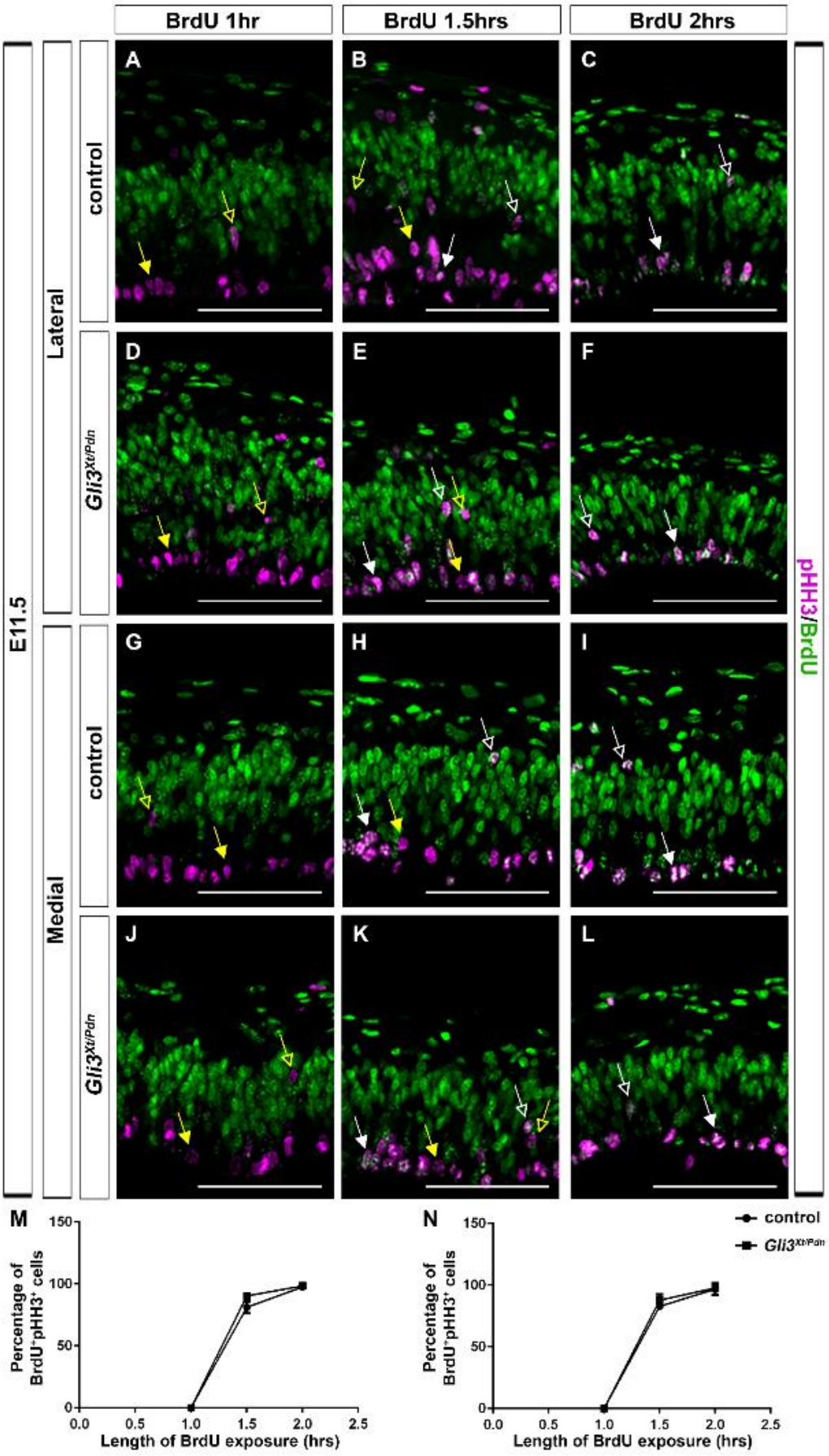
BrdU 1hr
BrdU 1.5hrs
BrdU 2hrs
E11.5
Lateral
Medial
control
Gli3Xt/Pdn
pHH3/BrdU
A
B
C
D
E
F
G
H
I
J
K
L
M
N
Percentage of BrdU+pHH3+ cells
Length of BrdU exposure (hrs)
control
Gli3Xt/Pdn

**Figure 4.5: G2-phase was unaltered in the *Gli3*$^{Xt/Pdn}$ total cortical progenitor population at E11.5. A-L.** pHH3/BrdU immunofluorescence on sections of E11.5 cortex from control and *Gli3*$^{Xt/Pdn}$ embryos. Solid yellow arrows depict BrdU single-labelled apical progenitors, solid white arrows depict pHH3/BrdU co-labelled apical progenitors, empty yellow arrows depict BrdU single-labelled basal progenitors, and empty white arrows depict pHH3/BrdU co-labelled basal progenitors. **M.** There was no effect on G2-phase length in the lateral **(M)** or medial **(N)** *Gli3*$^{Xt/Pdn}$ cortex. Error bars represent mean ± 95% confidence interval; n=11. Scale bars = 100μm.

D, F), as was $T_S$ (7.50±0.45 hrs in control and 4.98±0.35 hrs in mutant, n=4, $p<0.05$) (figure 4.4 C, D, F). Taken together, the reduction in *Gli3* at both E11.5 and E12.5 resulted in a decrease in S-phase and total cell cycle length.

At E11.5, $T_{G2}$ was of similar length in the mutant compared to control both laterally and medially (lateral: 1.31 hrs in control and 1.27 hrs in mutant, medially: 1.29 hrs in control and 1.29 hrs in mutant, n=11) (figure 4.5 M, N). Moreover, $T_{G2}$ was also largely unaffected at E12.5 both laterally and medially (lateral: 1.28 hrs in control and 1.31 hrs in mutant, medially: 1.29 hrs in control and 1.29 hrs in mutant, n=12 in control and n=11 in mutant) (figure 4.6 M, N). As $T_{G2}$ was calculated from a curve containing multiple embryos from multiple litters, statistical analyses were not conducted. However, it is clear that the reduction in *Gli3* had very little if any effect on the length of G2-phase.

Both laterally and medially at E11.5 $T_M$ was unaffected in the mutant compared to control (lateral: 0.89±0.09 hrs in control and 0.81±0.03 hrs in mutant, n=4, $p>0.05$, medially: 0.90±0.08 hrs in control and 0.80±0.04 hrs in mutant, n=4, $p>0.05$) (figure 4.7 E). However, by E12.5 in the lateral neocortex, $T_M$ was shorter in the mutant compared to control (1.10±0.05 hrs in control and 0.93±0.09 hrs in mutant, n=5, $p<0.05$) (figure 4.8 A, B, E). Likewise, medially $T_M$ was reduced in the mutant compared to control (1.09±0.11 hrs in control and 0.77±0.08 hrs in mutant, n=4, $p<0.05$) (figure 4.8 C, D, E). Altogether, the reduction in *Gli3* had little effect on M-phase length at E11.5, yet it was shorter in the mutant at E12.5.

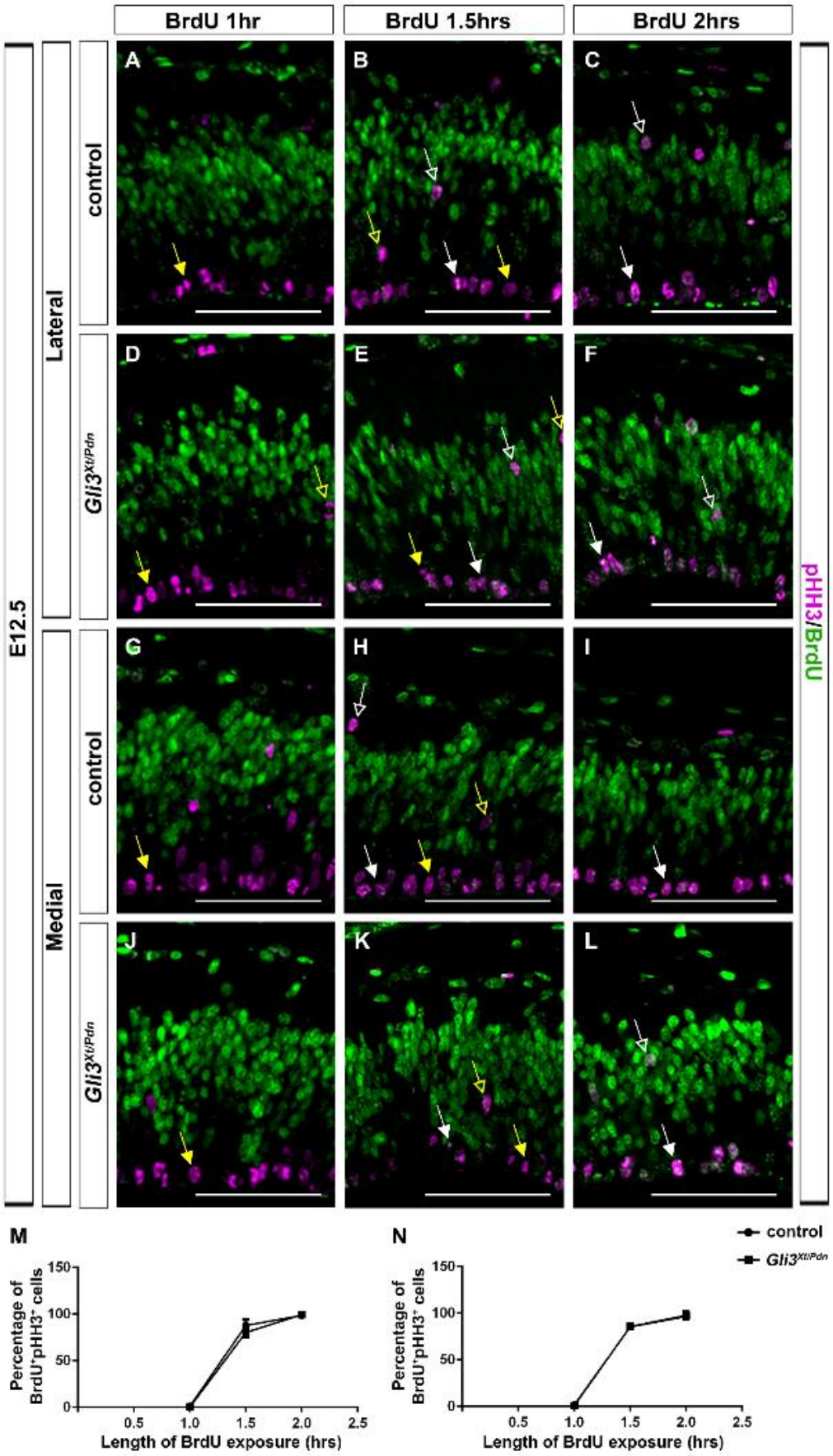
BrdU 1hr
BrdU 1.5hrs
BrdU 2hrs
E12.5
Lateral
Medial
control
Gli3Xti/Pdn
pHH3/BrdU
A
B
C
D
E
F
G
H
I
J
K
L
M
N
control
Gli3Xti/Pdn
Percentage of BrdU+pHH3+ cells
Length of BrdU exposure (hrs)
0
50
100
150
0.5
1.0
1.5
2.0
2.5

**Figure 4.6: G2-phase was unaltered in the *Gli3*$^{Xt/Pdn}$ total cortical progenitor population at E12.5. A-L.** pHH3/BrdU immunofluorescence on sections of E12.5 cortex from control and *Gli3*$^{Xt/Pdn}$ embryos. Solid yellow arrows depict BrdU single-labelled apical progenitors, solid white arrows depict pHH3/BrdU co-labelled apical progenitors, empty yellow arrows depict BrdU single-labelled basal progenitors, and empty white arrows depict pHH3/BrdU co-labelled basal progenitors. **M.** There was no effect on G2-phase length in the lateral **(M)** or medial **(N)** *Gli3*$^{Xt/Pdn}$ cortex. Error bars represent mean ± 95% confidence interval; n=12 in control and n=11 in mutant. Scale bars = 100μm.

With respect to all progenitors combined, in the lateral neocortex at E11.5 $T_{G1}$ was shortened in *Gli3*$^{Xt/Pdn}$ mutants compared to control (4.14±0.80 hrs in control and 2.33±0.21 hrs in mutant, n=4, $p<0.05$) (figure 4.9). In the medial neocortex, $T_{G1}$ was also shorter in the mutant compared to control (3.93±0.83 hrs in control and 2.19±0.51 hrs in mutant, n=4, $p<0.05$) (figure 4.9).

At E12.5, in the lateral cortex, $T_{G1}$ was unaltered in the mutant compared to control (4.29±0.66 hrs in control and 3.17±0.46 hrs in mutant, n=4, $p>0.05$) (figure 4.10). In the medial cortex, $T_{G1}$ was decreased in the mutant (3.58±0.14 hrs in control and 2.79±0.20 hrs in mutant, n=4, $p<0.05$) (figure 4.10). This would indicate that *Gli3* regulates G1-phase length at both E11.5 and E12.5. A summary of the length of each phase and total cell cycle length is given in table 4.1 below.

**Table 4.1: Cell cycle phase lengths for all cortical progenitors combined**

| | | | Cell cycle phases | | | | |
|---|---|---|---|---|---|---|---|
| | | | $T_{G1}$ | $T_S$ | $T_{G2}$ | $T_M$ | $T_C$ |
| **E11.5** | **Lateral** | **Control** | 4.14 | 6.48 | 1.31 | 0.89 | 12.83 |
| | | ***Gli3*$^{Xt/Pdn}$** | **2.33** | **4.93** | 1.27 | 0.81 | **9.33** |
| | **Medial** | **Control** | 3.93 | 5.80 | 1.29 | 0.90 | 11.91 |
| | | ***Gli3*$^{Xt/Pdn}$** | **2.19** | 5.28 | 1.29 | 0.80 | **9.56** |
| **E12.5** | **Lateral** | **Control** | 4.29 | 6.84 | 1.28 | 1.10 | 13.51 |
| | | ***Gli3*$^{Xt/Pdn}$** | 3.17 | **4.68** | 1.31 | **0.93** | **10.08** |
| | **Medial** | **Control** | 3.58 | 7.50 | 1.29 | 1.09 | 13.46 |
| | | ***Gli3*$^{Xt/Pdn}$** | **2.79** | **4.98** | 1.29 | **0.77** | **9.83** |

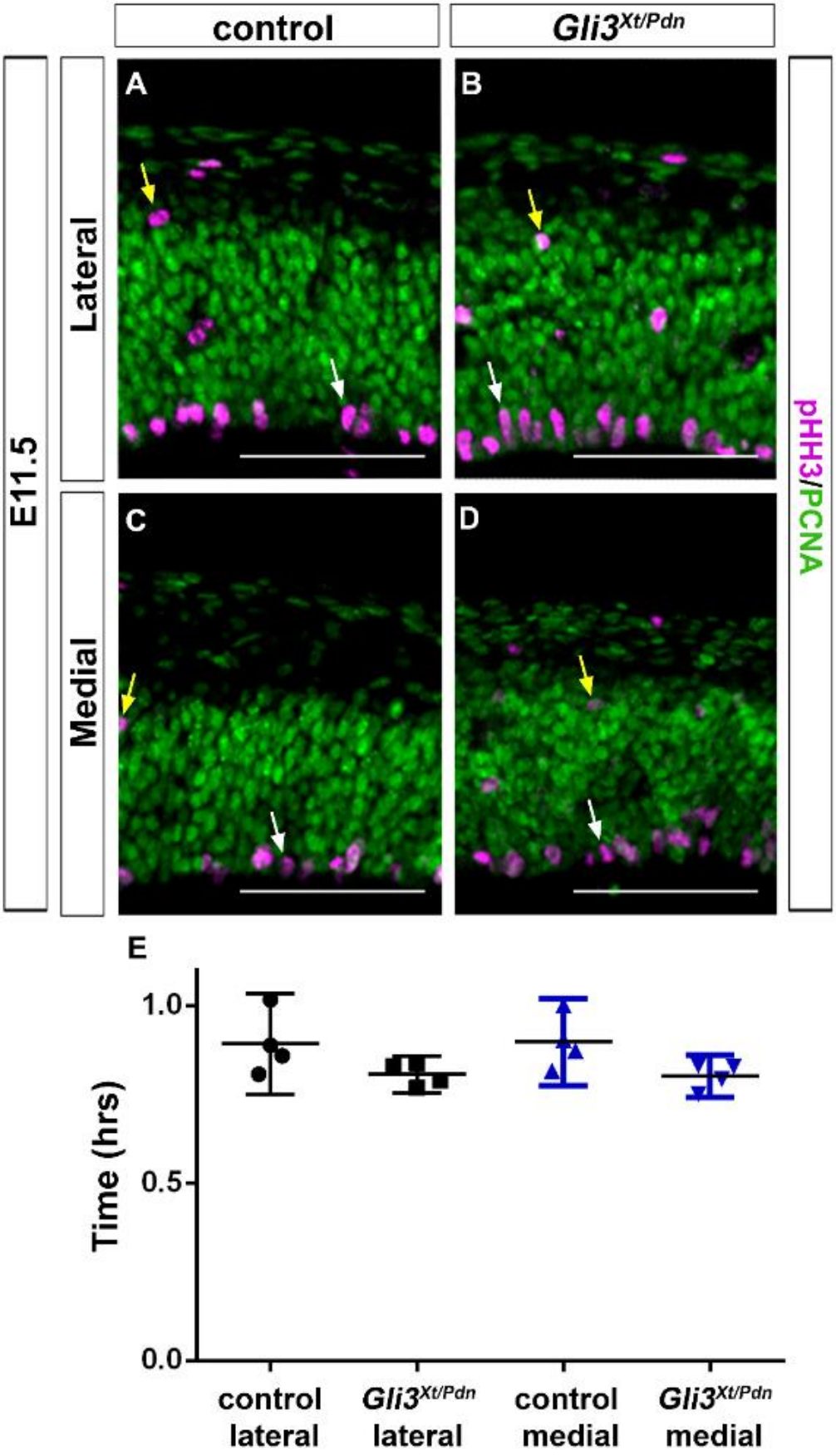
control
Gli3Xt/Pdn
E11.5
Lateral
Medial
A
B
C
D
pHH3/PCNA
E
Time (hrs)
1.0
0.5
0.0
control lateral
Gli3Xt/Pdn lateral
control medial
Gli3Xt/Pdn medial

**Figure 4.7: M-phase length was unaltered in the *Gli3*$^{Xt/Pdn}$ total cortical progenitor population at E11.5. A-D.** pHH3/PCNA immunofluorescence on sections of E11.5 cortex from control and *Gli3*$^{Xt/Pdn}$ embryos. White arrows depict apical progenitors, yellow arrows depict basal progenitors **E.** There was no effect on M-phase length in the lateral and medial *Gli3*$^{Xt/Pdn}$ cortex. All statistical data represents mean ± 95% confidence interval; n=4; * = $p<0.05$; Mann-Whitney U-test. Scale bars = 100μm.

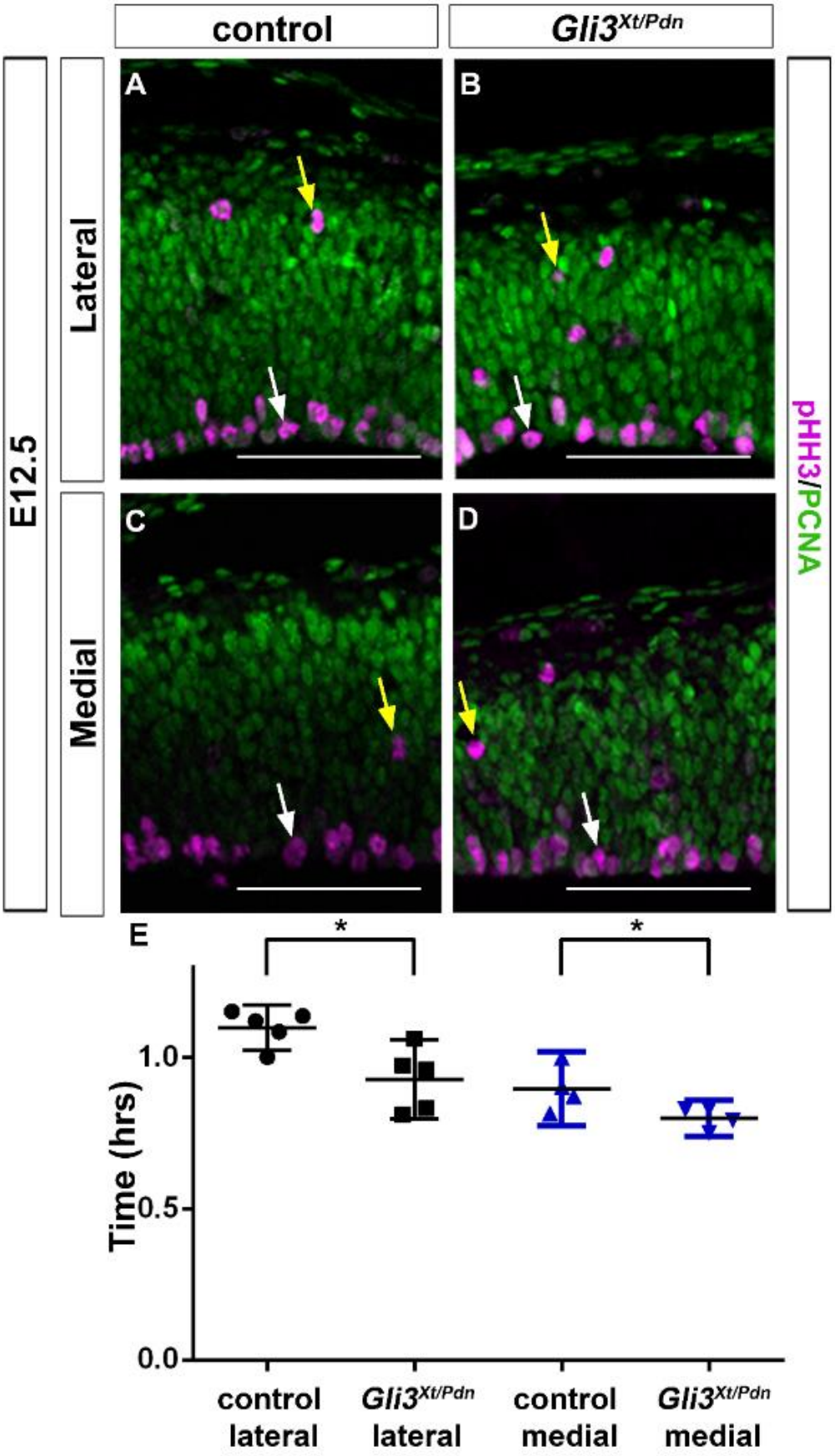
control
Gli3Xt/Pdn
E12.5
Lateral
Medial
A
B
C
D
pHH3/PCNA
E
*
*
Time (hrs)
1.0
0.5
0.0
control lateral
Gli3Xt/Pdn lateral
control medial
Gli3Xt/Pdn medial

**Figure 4.8: M-phase length was reduced in the *Gli3*$^{Xt/Pdn}$ total cortical progenitor population at E12.5. A-D.** pHH3/PCNA immunofluorescence on sections of E12.5 cortex from control and *Gli3*$^{Xt/Pdn}$ embryos. White arrows depict apical progenitors, yellow arrows depict basal progenitors **E.** M-phase length was significantly decreased in the lateral and medial *Gli3*$^{Xt/Pdn}$ cortex. All statistical data represents mean ± 95% confidence interval; n=5 in control and n=4 in mutant; * = $p<0.05$; Mann-Whitney U-test. Scale bars = 100μm.

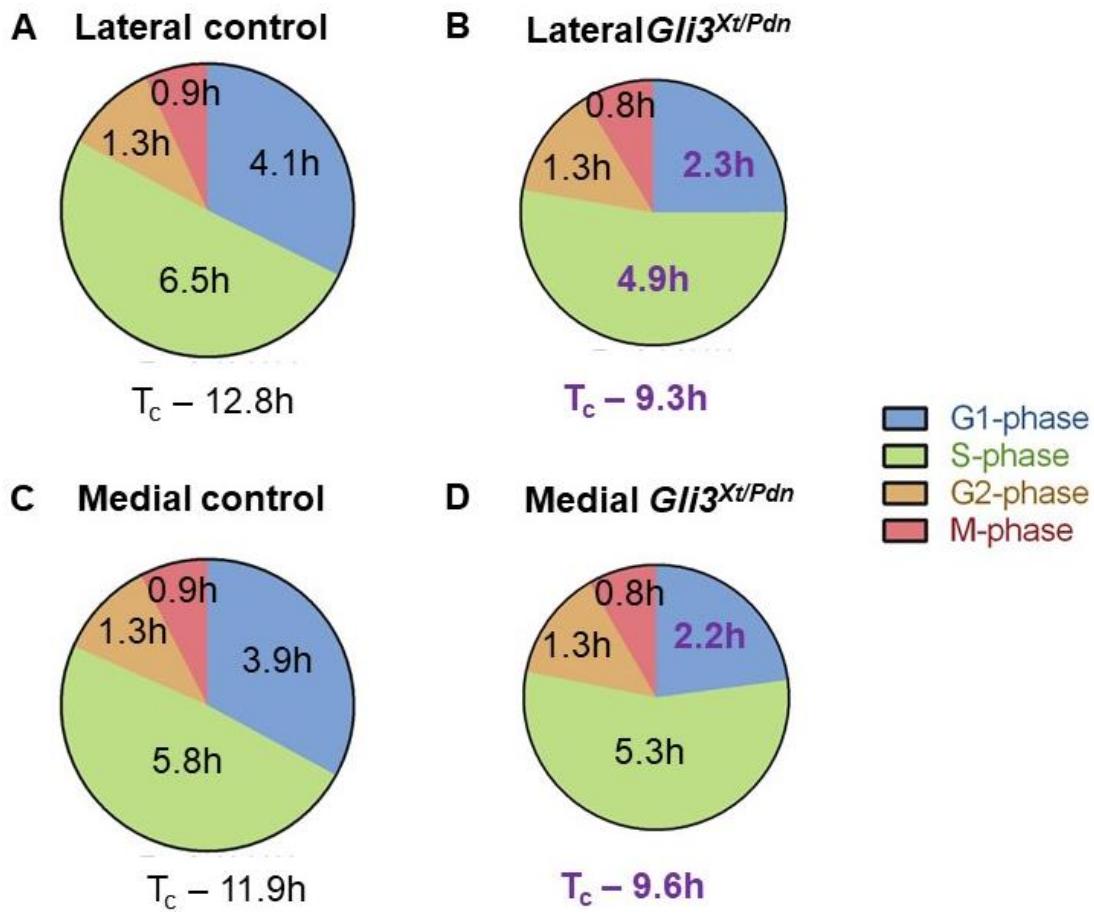


**Figure 4.9: G1-phase length was reduced in the lateral and medial *Gli3*$^{Xt/Pdn}$ total cortical progenitor population at E11.5.** Schematics showing the length of each cell cycle phase and total cell cycle length in lateral control **(A)**, lateral *Gli3*$^{Xt/Pdn}$ **(B)**, medial control **(C)** and medial *Gli3*$^{Xt/Pdn}$ **(D)** embryos. In **B** and **D** significantly altered phase lengths are shown in bold purple text and note reduced total circle size representing reduced total cell cycle length. All statistical data represents mean; n=4; * = $p<0.05$; Mann-Whitney U-test.

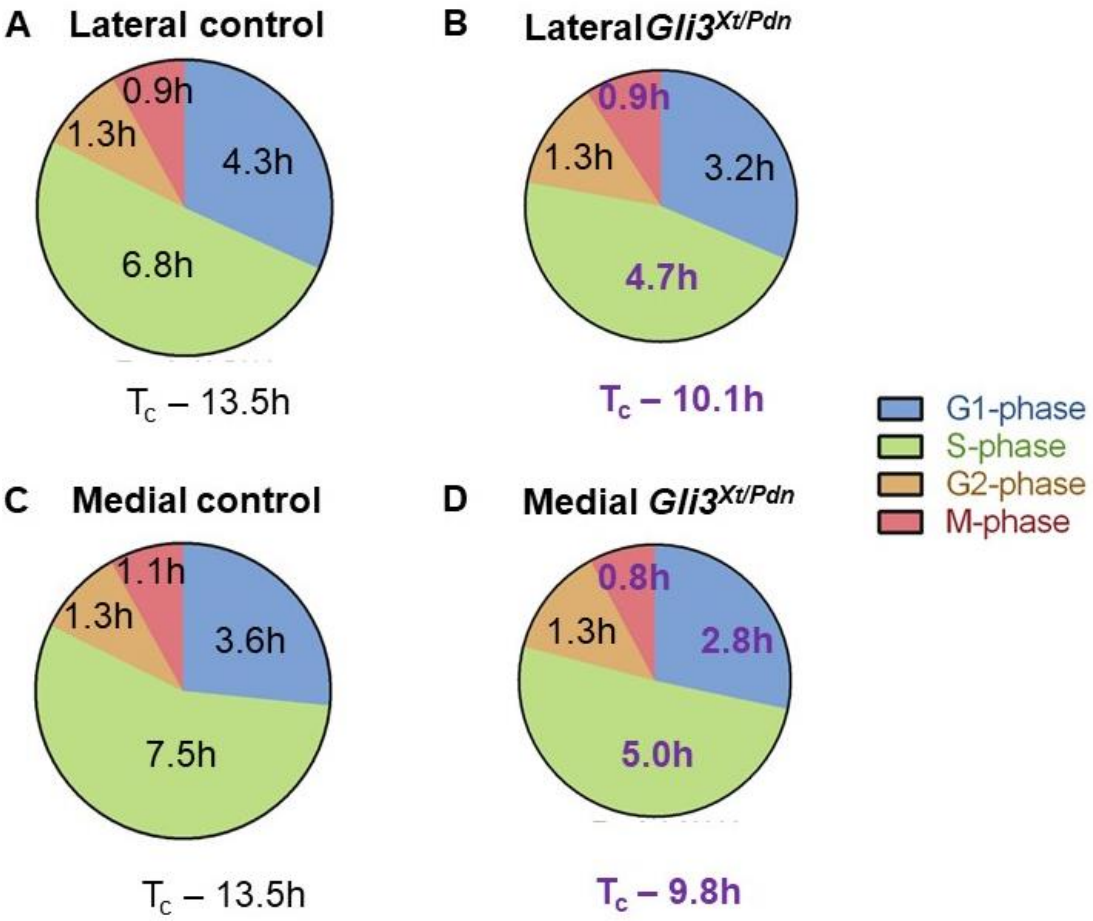


**Figure 4.10: G1-phase length was reduced in the medial *Gli3*$^{Xt/Pdn}$ total cortical progenitor population at E12.5.** Schematics showing the length of each cell cycle phase and total cell cycle length in lateral control **(A)**, lateral *Gli3*$^{Xt/Pdn}$ **(B)**, medial control **(C)** and medial *Gli3*$^{Xt/Pdn}$ **(D)** embryos. In **B** and **D** significantly altered phase lengths are shown in bold purple text and note reduced total circle size representing reduced total cell cycle length. All statistical data represents mean; n=4; * = $p<0.05$; Mann-Whitney U-test.

### 4.4 G1-, S- and M-phase and total cell cycle length were reduced in apical progenitors of E11.5 and E12.5 *Gli3*$^{Xt/Pdn}$ embryos

The reduction in *Gli3* resulted in a shortening of the total cell cycle length and of G1-, S- and M-phase in the *Gli3*$^{Xt/Pdn}$ mutant, when examining the total cortical progenitor population. At E11.5 and E12.5, apical progenitors are the main progenitor subtype, and Gli3 expression is mainly confined to this population. Therefore, the analyses of cell cycle lengths outlined above were repeated in the apical progenitor population alone.

To calculate $T_S$ and $T_C$, the same analyses on cell cycle parameters as carried out on all progenitors were conducted. Using BrdU and IdU as described in section 4.3.1 the length of S-phase and the total cell cycle length were measured in E11.5 and E12.5 apical progenitors in the lateral and medial cortex, however the number of P-cells was determined based on the number of apical progenitors expressing Pax6 within the area counted.

At E11.5 in the lateral cortex, $T_S$ was significantly shorter in the *Gli3*$^{Xt/Pdn}$ mutant as compared to control (5.08±0.21 hrs in control and 4.61±0.21 hrs in mutant, n=4, $p<0.05$) (figure 4.11 A, B, E), as was $T_C$ (8.28±0.27 hrs in control and 6.87±0.14 hrs in mutant, n=4, $p<0.05$) (figure 4.11 A, B, E). In the medial cortex, $T_S$ was unaltered in the mutant compared to control (4.09±0.66 hrs in control and 4.23±0.60 hrs in mutant, n=4, $p>0.05$) (figure 4.11 C, D, F), as was $T_C$ (6.79±0.54 hrs in control and 6.41±0.59 hrs in mutant, n=4, $p>0.05$) (figure 4.11 C, D, F).

In the E12.5 lateral neocortex, $T_S$ was significantly shorter in the mutant compared to control (5.82±0.37 hrs in control and 4.80±0.34 hrs, n=4, $p<0.05$) (figure 4.12 A, B, E) and $T_C$ was also significantly reduced (12.71±0.61 hrs in control and 9.48±0.29 hrs in mutant, n=4, $p<0.05$) (figure 4.12 A, B, E). Medially, $T_S$ was shorter in the mutant compared to control (6.03±0.53 hrs in control and 4.78±0.61 hrs in mutant, n=4, $p<0.05$) (figure 4.12 C, D, F) along with $T_C$ (12.71±0.61 hrs in control and 9.48±0.29 hrs in mutant, n=4, $p<0.05$) (figure 4.12 C, D, F). Taken together, the reduction in *Gli3* in apical progenitors in *Gli3*$^{Xt/Pdn}$ mutants reduced both S-phase and total cell cycle laterally at E11.5 and both laterally and medially at E12.5.

As with all progenitors combined, the length of G2-phase was measured in the apical progenitor population alone. BrdU was administered as described in section 4.3.1,

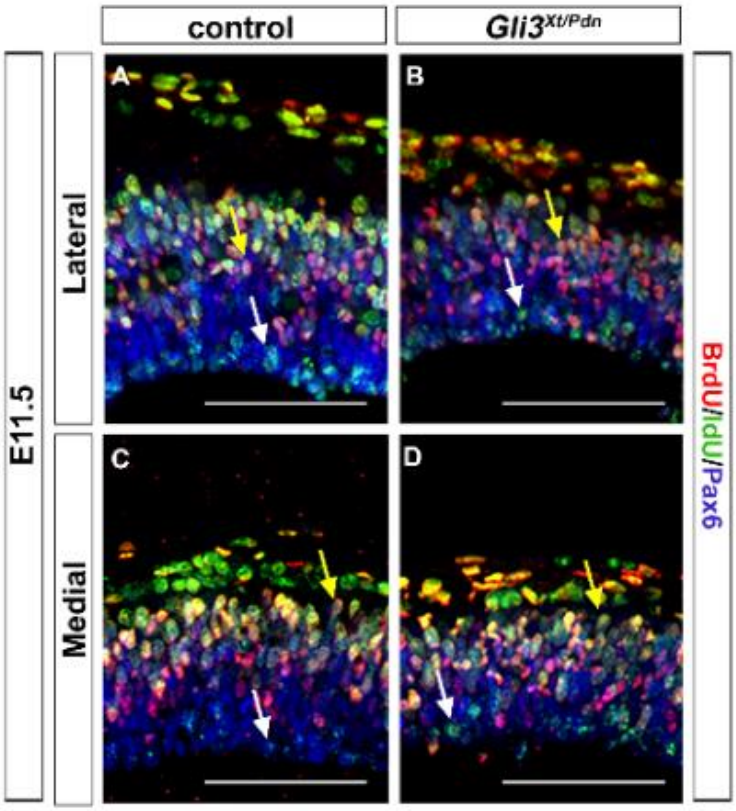
control
Gli3Xt/Pdn
E11.5
Lateral
Medial
A
B
C
D
BrdU/IdU/Pax6

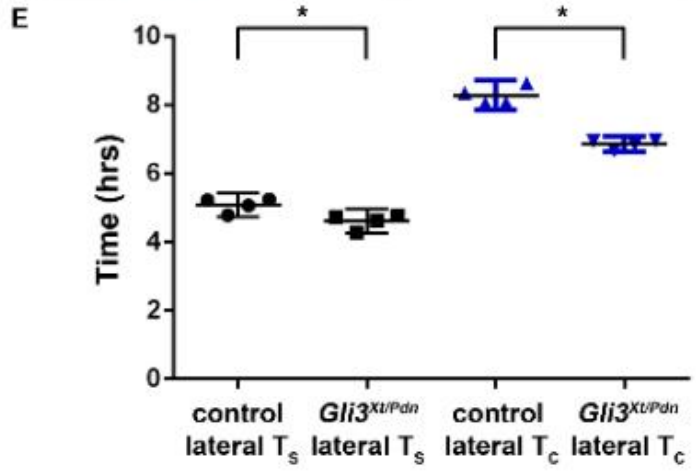
E
Time (hrs)
0
2
4
6
8
10
*
*
control lateral Ts
Gli3Xt/Pdn lateral Ts
control lateral Tc
Gli3Xt/Pdn lateral Tc

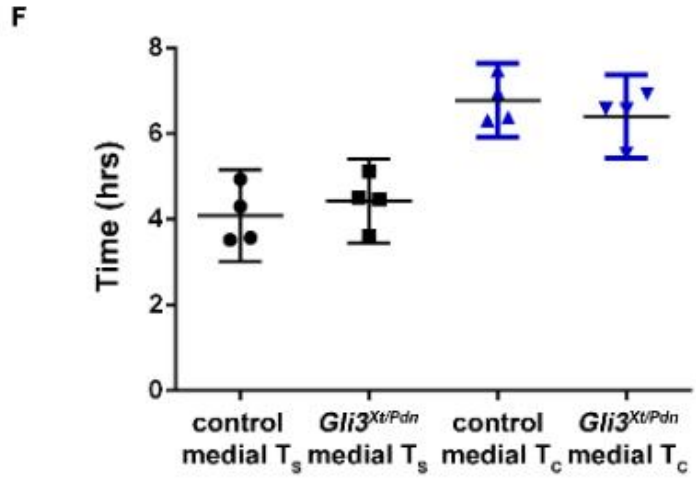
F
Time (hrs)
0
2
4
6
8
control medial Ts
Gli3Xt/Pdn medial Ts
control medial Tc
Gli3Xt/Pdn medial Tc

**Figure 4.11: S-phase and total cell cycle length were reduced in lateral *Gli3*$^{Xt/Pdn}$ apical progenitors at E11.5. A-D.** BrdU/IdU/Pax6 immunofluorescence on sections of E11.5 cortex from control and *Gli3*$^{Xt/Pdn}$ embryos. White arrows depict IdU/Pax6 co-labelled L-cells, yellow arrows depict BrdU/IdU/Pax6 co-labelled S-cells. **E.** S-phase and total cell cycle length were significantly decreased in the lateral *Gli3*$^{Xt/Pdn}$ cortex. **F.** S-phase and total cell cycle length were unaltered in the medial *Gli3*$^{Xt/Pdn}$ cortex. All statistical data represents mean ± 95% confidence interval; n=4; * = p<0.05; Mann-Whitney U-test. Scale bars = 100μm.

and only pHH3$^+$ cells along the ventricular zone were counted. In the E11.5 lateral neocortex the length of G2-phase was very similar in the *Gli3*$^{Xt/Pdn}$ mutant compared to control (1.31 hrs in control and 1.26 hrs in mutant, n=11) (figure 4.13 M), and $T_{G2}$ was also unaltered in the medial cortex (1.29 hrs in control and 1.29 hrs in mutant, n=11) (figure 4.13 N).

At E12.5, $T_{G2}$ was a similar length in both the mutant and control in the lateral cortex (1.27 hrs in control, n=12, and 1.31 hrs in mutant, n=11) (figure 4.14 M), and was unaltered in the medial cortex (1.29 hrs in control, n=12, and 1.29 hrs in mutant, n=11) (figure 4.14 N). Overall, it appears that *Gli3* has little impact on the length of G2-phase in apical progenitors.

M-phase length was also measured as described in section 4.3.1 but in the apical progenitor population alone, using the proportion of pHH3$^+$ cells located along the edge of the ventricle. At E11.5 in the lateral cortex, $T_M$ was unaltered in the *Gli3*$^{Xt/Pdn}$ mutant compared to control (0.76±0.05 hrs in control and 0.62±0.03 hrs in mutant, p=4, p>0.05) (figure 4.15 A, B, E). In the medial cortex, the length of M-phase was also unchanged in the mutant compared to control (0.86±0.07 hrs in control and 0.70±0.07 hrs in mutant, n=4, p>0.05) (figure 4.15 C, D, E).

In the E12.5 lateral neocortex, $T_M$ was shorter in mutant apical progenitors than in control (0.82±0.03 hrs in control and 0.69±0.07 hrs in mutant, n=5, p<0.05) (figure 4.16 A, B, E). Furthermore, $T_M$ was also shorter in the medial mutant cortex compared to control (1.04±0.11 hrs in control and 0.66±0.08 hrs in mutant, n=4, p<0.05) (figure 4.16 C, D, E). Combined, *Gli3* reduction in the mutant did not alter M-phase length significantly at E11.5 but acted to reduced it at E12.5, in both the lateral and medial

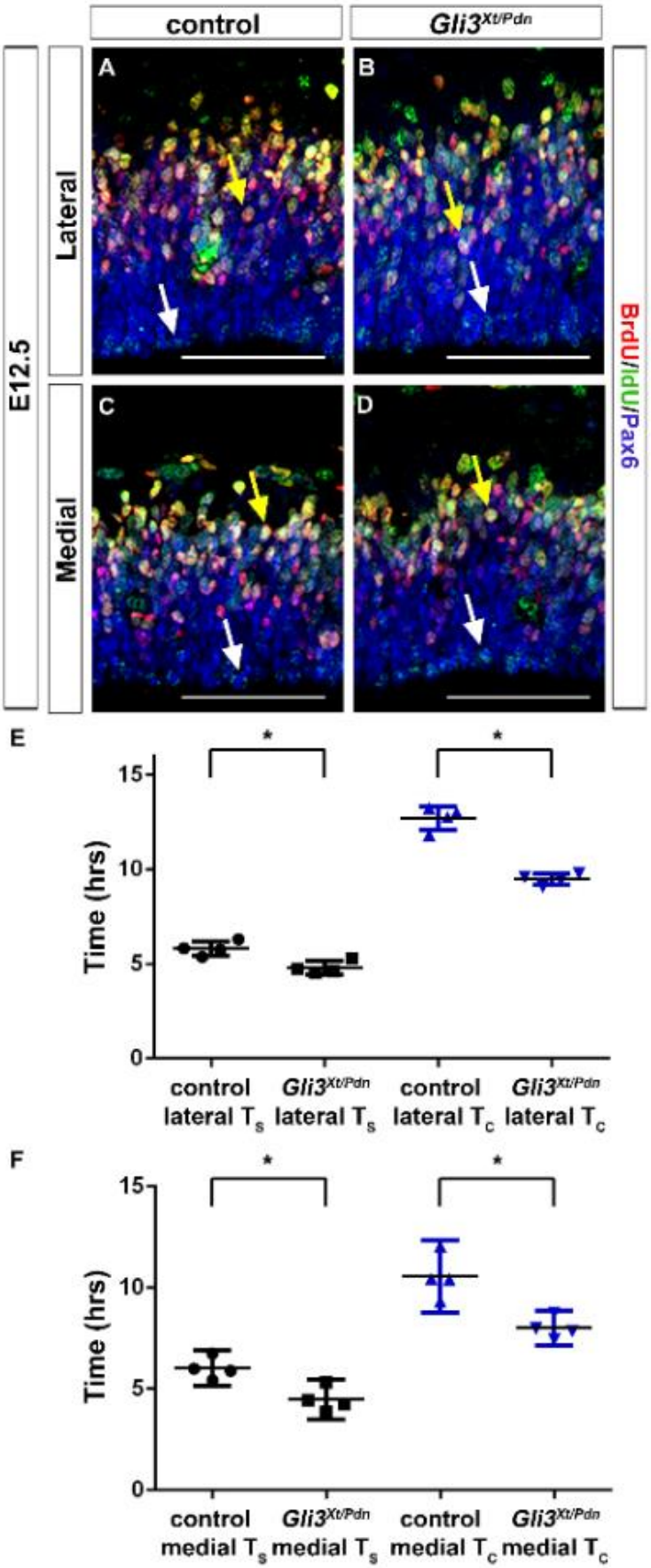
control
Gli3Xt/Pdn
E12.5
Lateral
Medial
A
B
C
D
BrdU/IdU/Pax6
E
Time (hrs)
15
10
5
0
*
*
control lateral Ts
Gli3Xt/Pdn lateral Ts
control lateral Tc
Gli3Xt/Pdn lateral Tc
F
Time (hrs)
15
10
5
0
*
*
control medial Ts
Gli3Xt/Pdn medial Ts
control medial Tc
Gli3Xt/Pdn medial Tc

**Figure 4.12: S-phase and total cell cycle length were reduced in *Gli3*$^{Xt/Pdn}$ apical progenitors at E12.5. A-D.** BrdU/IdU/Pax6 immunofluorescence on sections of E12.5 cortex from control and *Gli3*$^{Xt/Pdn}$ embryos. White arrows depict IdU/Pax6 co-labelled L-cells, yellow arrows depict BrdU/IdU/Pax6 co-labelled S-cells. **E.** S-phase and total cell cycle length were significantly decreased in the lateral *Gli3*$^{Xt/Pdn}$ cortex. **F.** S-phase and total cell cycle length were significantly decreased in the medial *Gli3*$^{Xt/Pdn}$ cortex. All statistical data represents mean ± 95% confidence interval; n=4; * = p<0.05; Mann-Whitney U-test. Scale bars = 100μm.

cortex, indicating that *Gli3* may regulate the length of M-phase in apical progenitors at E12.5 but not E11.5.

Finally, due the reported significance of the length of G1-phase in the decision for a progenitor to divide either proliferatively or differentiatively, as described for the total progenitor population (section 4.3.1) $T_{G1}$ was calculated from $T_S$, $T_{G2}$, $T_M$ and $T_C$ for apical progenitors alone. In the lateral cortex of E11.5 embryos $T_{G1}$ was significantly shortened in *Gli3*$^{Xt/Pdn}$ mutant compared to control (1.13±0.17 hrs in control and 0.37±0.08 hrs in mutant, n=4, p<0.05) (figure 4.17). In the medial neocortex, $T_{G1}$ was 0.55±0.13 hrs in control embryos but could not be calculated in the mutant (figure 4.17). Due to inaccuracies in the measurements of $T_S$, $T_{G2}$, $T_M$ and $T_C$, the length of $T_{G1}$ was calculated as 0 hrs in the mutant. It is very unlikely that medial mutant apical progenitors did not have a G1-phase, and so due to imprecision in the measurements of the other phases I was unable to calculate the correct length of G1-phase.

24 hrs later, in the E12.5 lateral neocortex, $T_{G1}$ was significantly shorter in *Gli3*$^{Xt/Pdn}$ compared to control (4.82±0.33 hrs in control and 2.67±0.34 hrs in mutant, n=4, p<0.05) (figure 4.18). Medially, there was no significant difference between $T_{G1}$ in control and mutant (2.21±0.57 hrs in control and 1.59±0.40 hrs in mutant, n=4, p>0.05) (figure 4.18). Taken together, *Gli3* had an influence on the length of G1-phase in the apical progenitor population at both E11.5 and E12.5, acting to shorten it. A summary of the length of each phase within apical progenitors is shown in table 4.2.

**Table 4.2: Cell cycle phase lengths of apical progenitors**

| | | | Cell cycle phases | | | | |
|---|---|---|---|---|---|---|---|
| | | | $T_{G1}$ | $T_S$ | $T_{G2}$ | $T_M$ | $T_C$ |
| **E11.5** | **Lateral** | **Control** | 1.13 | 5.08 | 1.31 | 0.76 | 8.28 |
| | | ***Gli3*$^{Xt/Pdn}$** | **0.37** | **4.61** | 1.27 | 0.62 | **6.87** |
| | **Medial** | **Control** | 0.55 | 4.09 | 1.29 | 0.86 | 6.76 |
| | | ***Gli3*$^{Xt/Pdn}$** | **ND** | 4.43 | 1.29 | 0.70 | 6.41 |
| **E12.5** | **Lateral** | **Control** | 4.82 | 5.82 | 1.27 | 0.80 | 12.71 |
| | | ***Gli3*$^{Xt/Pdn}$** | **2.67** | **4.80** | 1.31 | **0.69** | **9.46** |
| | **Medial** | **Control** | 2.21 | 6.03 | 1.29 | 1.04 | 10.56 |
| | | ***Gli3*$^{Xt/Pdn}$** | 1.56 | **4.48** | 1.29 | **0.67** | **8.01** |

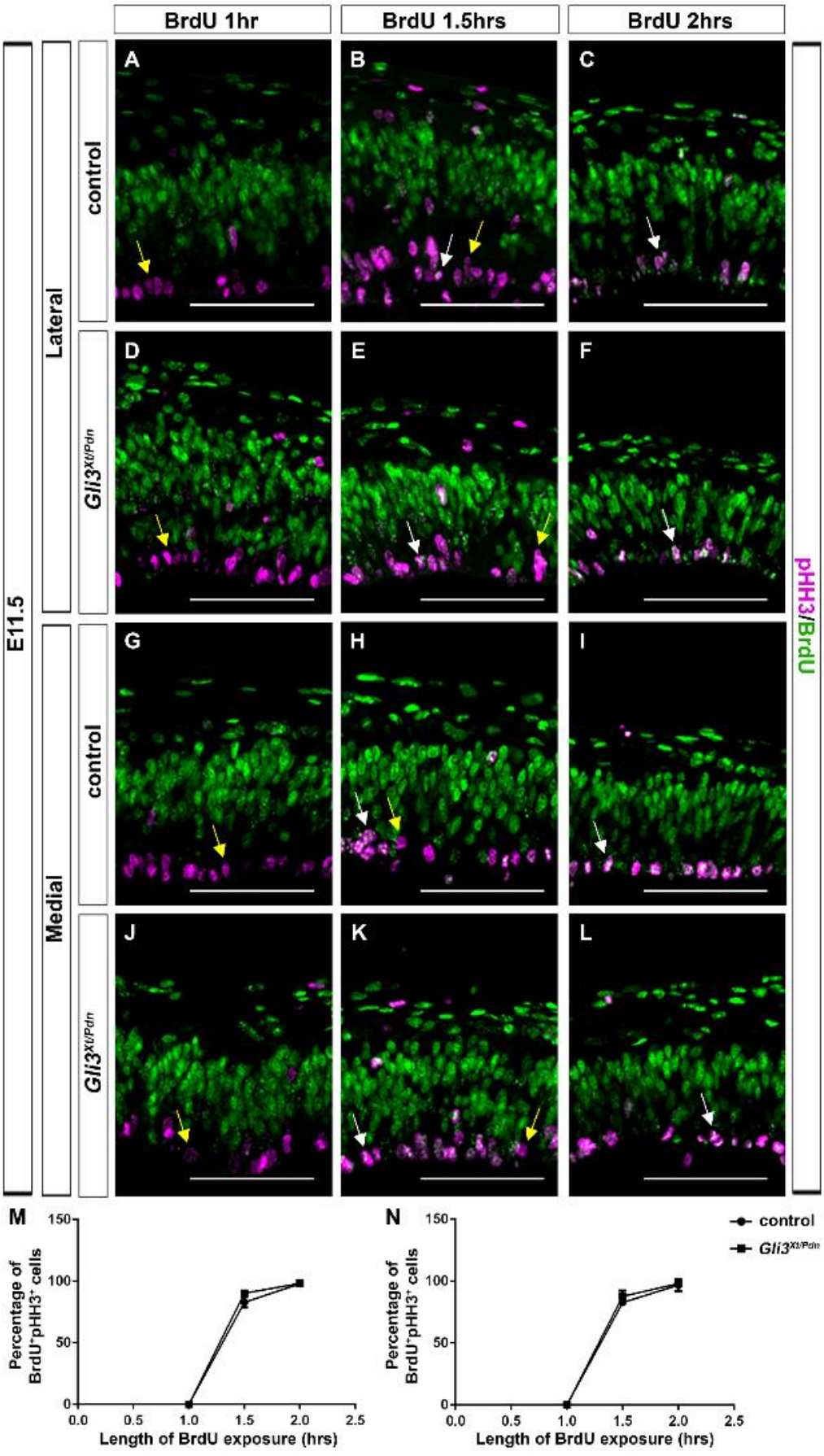
BrdU 1hr
BrdU 1.5hrs
BrdU 2hrs
E11.5
Lateral
Medial
control
Gli3Xt/Pdn
pHH3/BrdU
A
B
C
D
E
F
G
H
I
J
K
L
M
N
Percentage of BrdU+pHH3+ cells
Length of BrdU exposure (hrs)
control
Gli3Xt/Pdn

**Figure 4.13: G2-phase was unaltered in the *Gli3*$^{Xt/Pdn}$ apical progenitor population at E11.5. A-L.** pHH3/BrdU immunofluorescence on sections of E11.5 cortex from control and *Gli3*$^{Xt/Pdn}$ embryos. Yellow arrows depict BrdU single-labelled apical progenitors, white arrows depict pHH3/BrdU co-labelled apical progenitors. **M.** There was no effect on G2-phase length in the lateral **(M)** or medial **(N)** *Gli3*$^{Xt/Pdn}$ cortex. Error bars represent mean ± 95% confidence interval; n=11. Scale bars = 100μm.

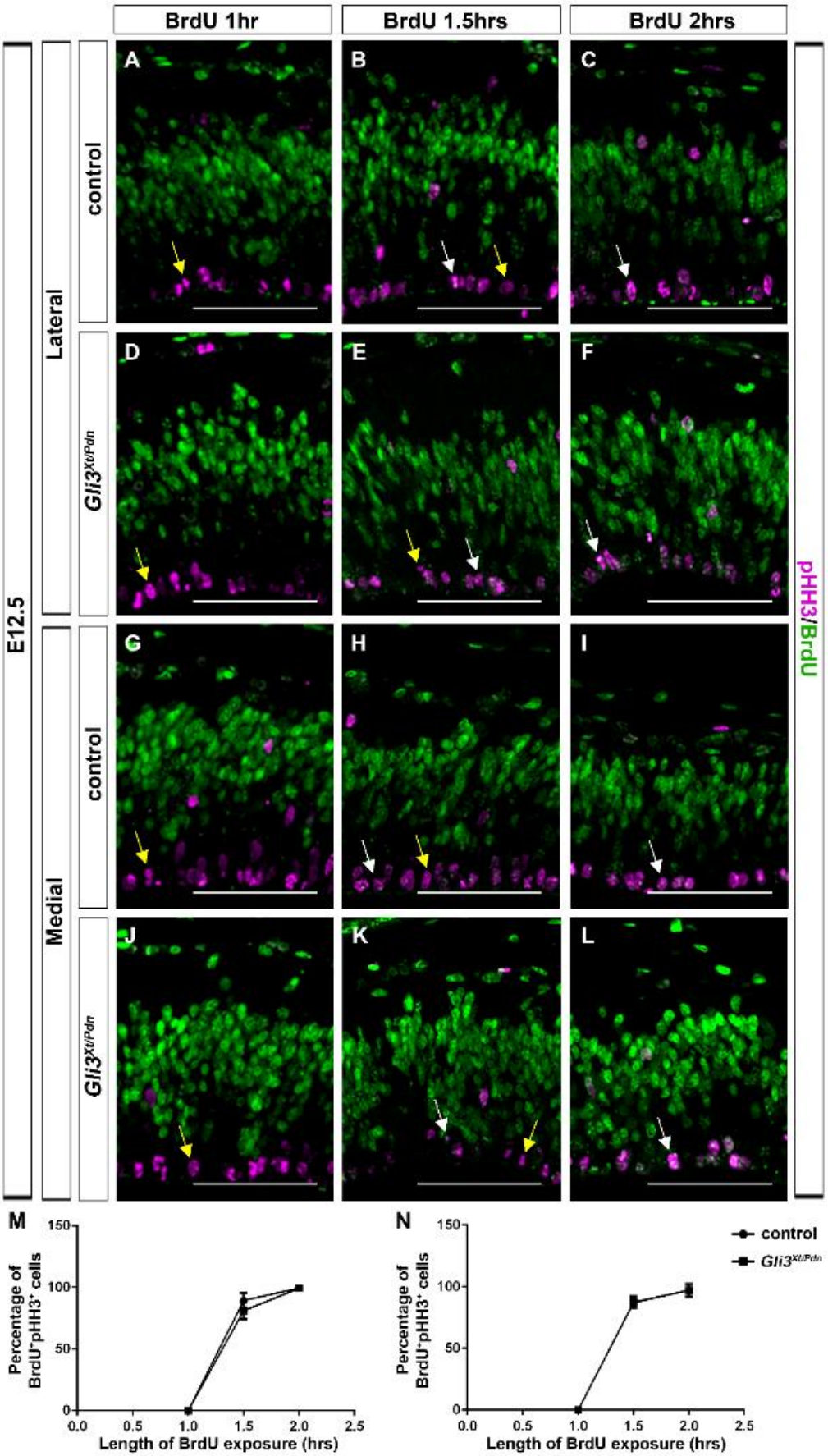
BrdU 1hr
BrdU 1.5hrs
BrdU 2hrs
E12.5
Lateral
Medial
control
Gli3Xt/Pdn
pHH3/BrdU
A
B
C
D
E
F
G
H
I
J
K
L
M
N
Percentage of BrdU⁻pHH3⁺ cells
Length of BrdU exposure (hrs)
control
Gli3Xt/Pdn

**Figure 4.14: G2-phase was unaltered in the *Gli3*$^{Xt/Pdn}$ apical progenitor population at E12.5. A-L.** pHH3/BrdU immunofluorescence on sections of E12.5 cortex from control and *Gli3*$^{Xt/Pdn}$ embryos. Yellow arrows depict BrdU single-labelled apical progenitors, white arrows depict pHH3/BrdU co-labelled apical progenitors. **M.** There was no effect on G2-phase length in the lateral **(M)** or medial **(N)** *Gli3*$^{Xt/Pdn}$ cortex. Error bars represent mean ± 95% confidence interval; n=12 in control and n=11 in mutant. Scale bars = 100μm.

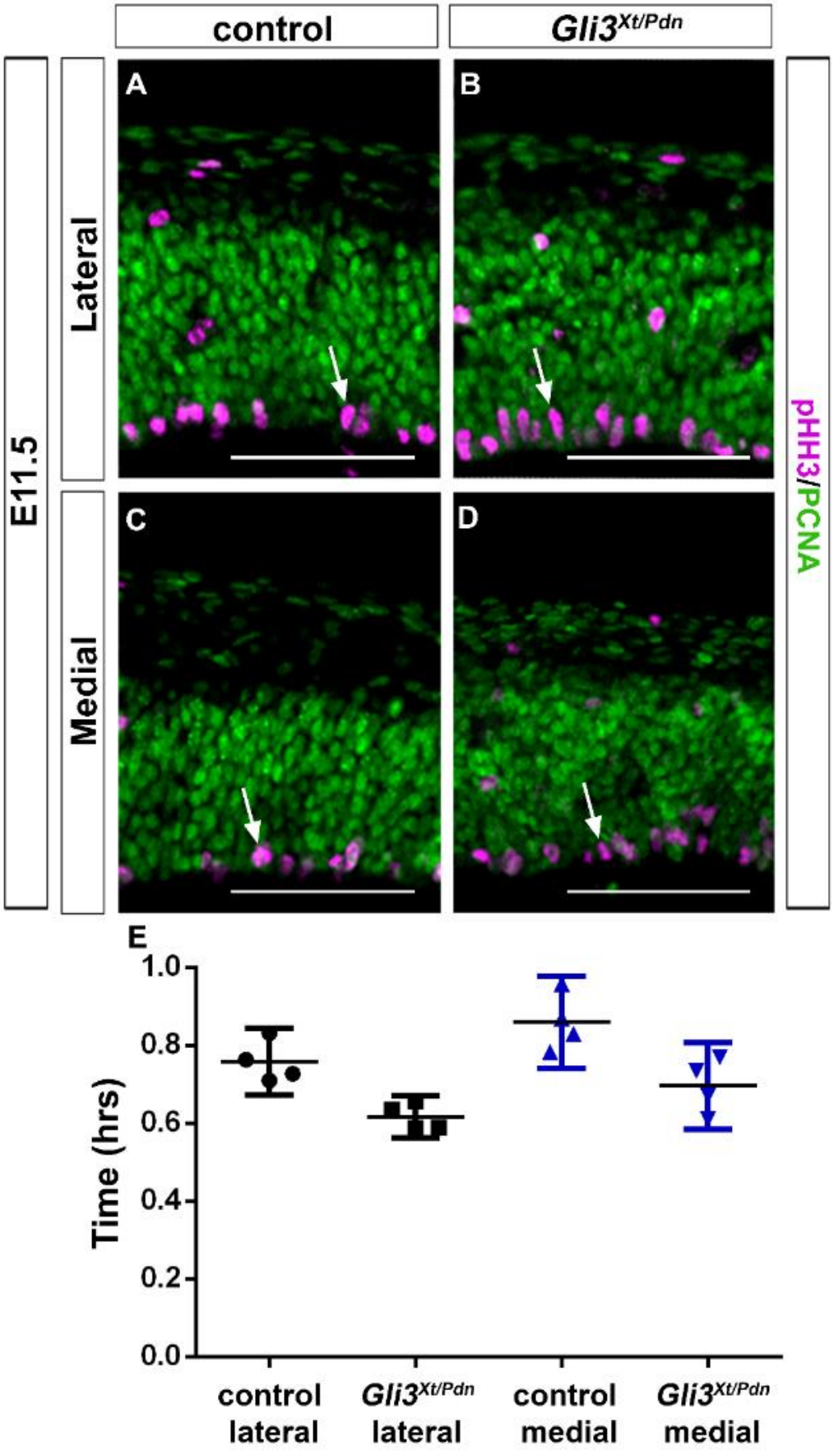
control
Gli3Xt/Pdn
E11.5
Lateral
Medial
A
B
C
D
pHH3/PCNA
E
Time (hrs)
1.0
0.8
0.6
0.4
0.2
0.0
control lateral
Gli3Xt/Pdn lateral
control medial
Gli3Xt/Pdn medial

**Figure 4.15: M-phase length was unaltered in the *Gli3*$^{Xt/Pdn}$ apical progenitor population at E11.5. A-D.** pHH3/PCNA immunofluorescence on sections of E11.5 cortex from control and *Gli3*$^{Xt/Pdn}$ embryos. Arrows depict pHH3/PCNA co-labelled apical progenitors. **E.** There was no effect on M-phase length in the lateral and medial *Gli3*$^{Xt/Pdn}$ cortex. All statistical data represents mean ± 95% confidence interval; n=4; * = $p<0.05$; Mann-Whitney U-test. Scale bars = 100μm.

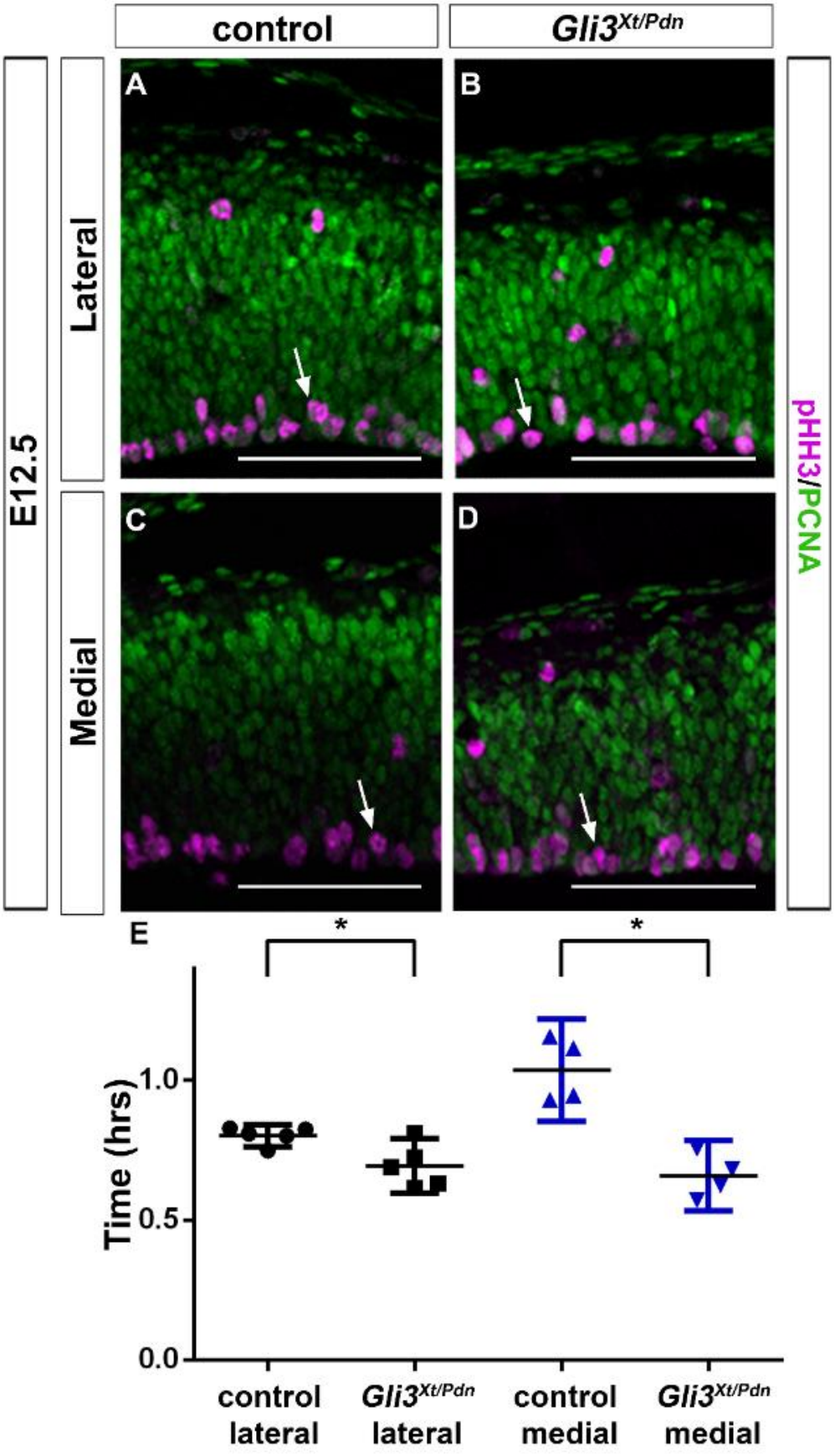
control
Gli3Xt/Pdn
E12.5
Lateral
Medial
A
B
C
D
pHH3/PCNA
E
*
*
Time (hrs)
1.0
0.5
0.0
control lateral
Gli3Xt/Pdn lateral
control medial
Gli3Xt/Pdn medial

**Figure 4.16: M-phase length was shorter in the *Gli3*$^{Xt/Pdn}$ apical progenitor population at E12.5. A-D.** pHH3/PCNA immunofluorescence on sections of E12.5 cortex from control and *Gli3*$^{Xt/Pdn}$ embryos. Arrows depict pHH3/PCNA co-labelled apical progenitors. **E.** There was a significant reduction in M-phase length in the lateral and medial *Gli3*$^{Xt/Pdn}$ cortex. All statistical data represents mean ± 95% confidence interval; n=4; * = $p<0.05$; Mann-Whitney U-test. Scale bars = 100μm.

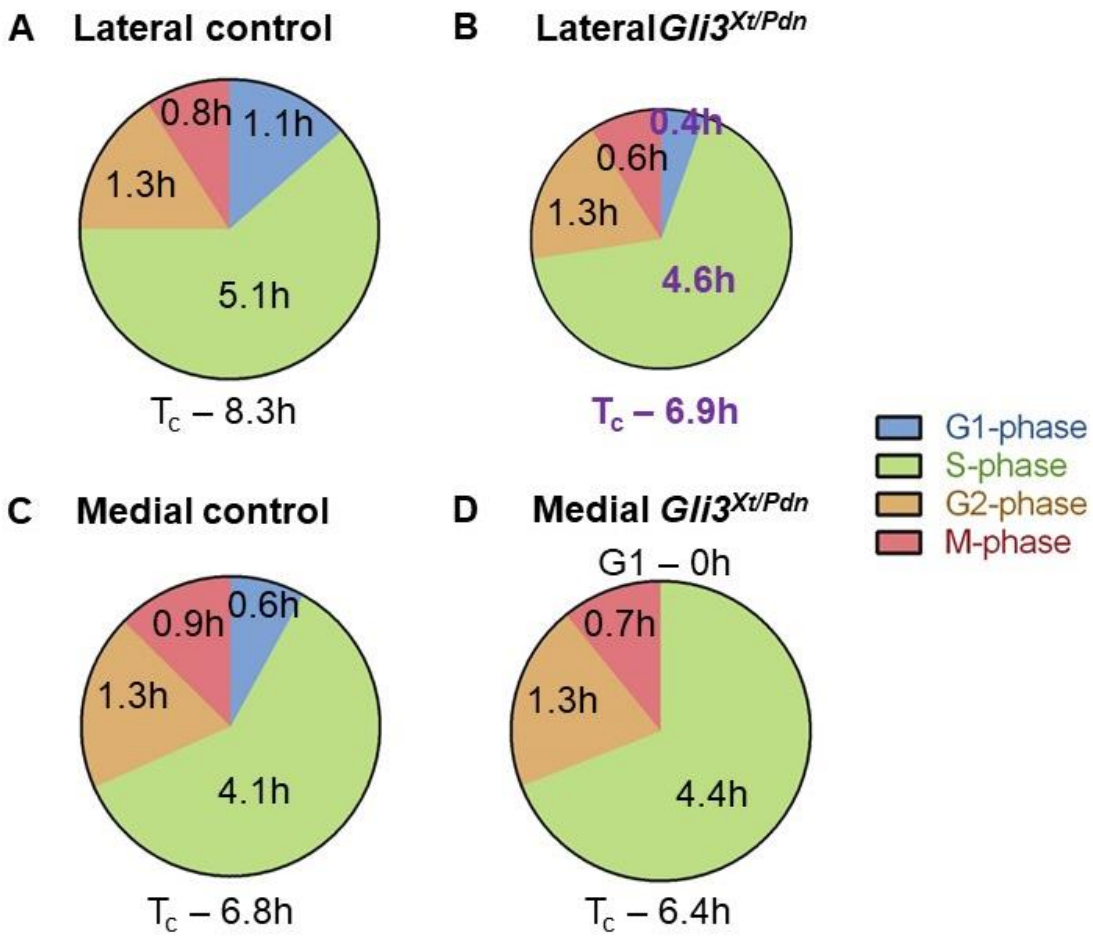


**Figure 4.17: G1-phase length was reduced in the lateral *Gli3*$^{Xt/Pdn}$ apical progenitor population at E11.5.** Schematics showing the length of each cell cycle phase and total cell cycle length in lateral control **(A)**, lateral *Gli3*$^{Xt/Pdn}$ **(B)**, medial control **(C)** and medial *Gli3*$^{Xt/Pdn}$ **(D)** embryos. In **B** and **D** significantly altered phase lengths are shown in bold purple text and note reduced total circle size **(B)** representing reduced total cell cycle length. All statistical data represents mean; n=4; * = $p<0.05$; Mann-Whitney U-test.

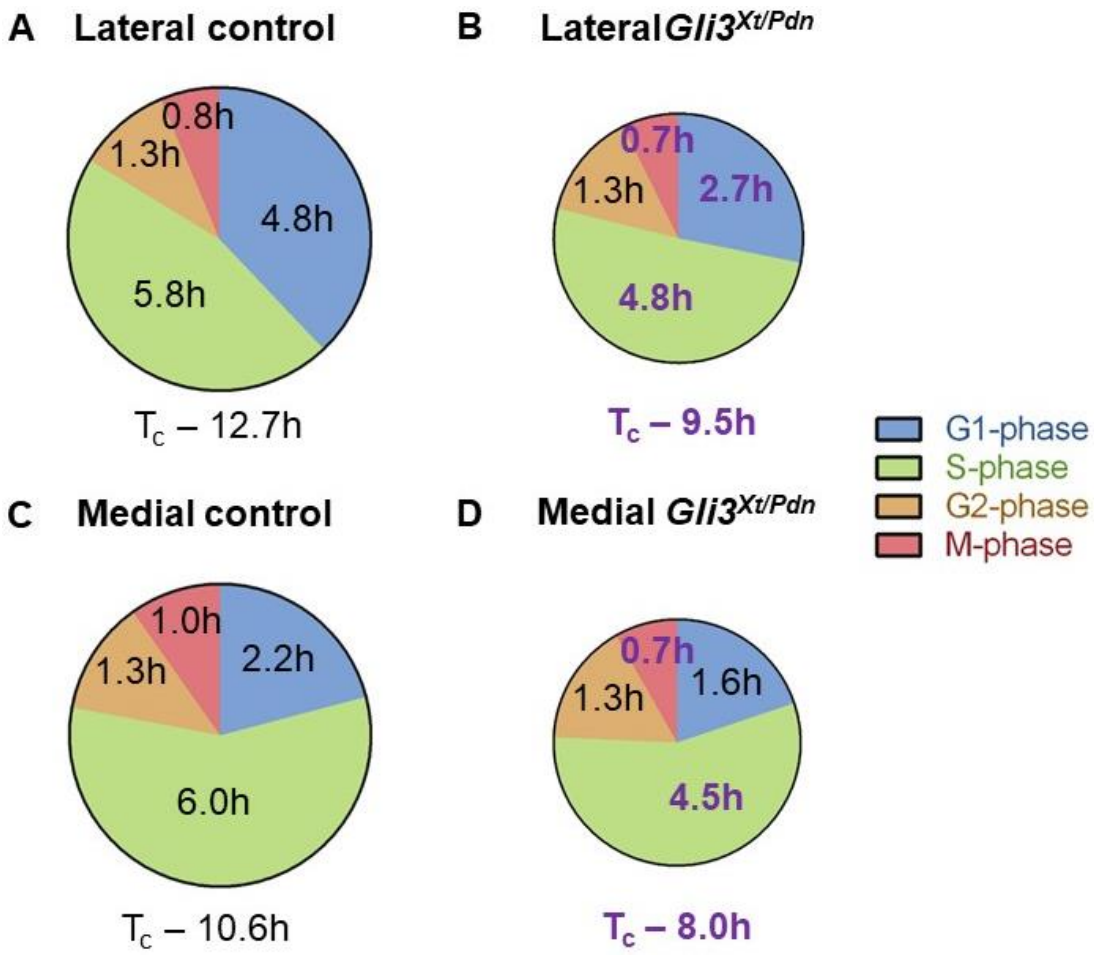


**Figure 4.18: G1-phase length was reduced in the *Gli3*$^{Xt/Pdn}$ apical progenitor population at E12.5.** Schematics showing the length of each cell cycle phase and total cell cycle length in lateral control **(A)**, lateral *Gli3*$^{Xt/Pdn}$ **(B)**, medial control **(C)** and medial *Gli3*$^{Xt/Pdn}$ **(D)** embryos. In **B** and **D** significantly altered phase lengths are shown in bold purple text and note reduced total circle size representing reduced total cell cycle length. All statistical data represents mean; n=4; * = $p<0.05$; Mann-Whitney U-test.

### 4.5 S- and M-phase length and total cell cycle length were altered in basal progenitors of the E11.5 and E12.5 *Gli3*$^{Xt/Pdn}$ neocortex

As above, analyses of the cell cycle phase lengths and of total cell cycle length were conducted in the basal progenitor population alone. Due to the lack of expression of Gli3 in these progenitors, any alterations to the cell cycle were thought unlikely. In the medial *Gli3*$^{Xt/Pdn}$ cortex at E11.5 and E12.5, there were too few basal progenitors present, and so analyses of the cell cycle were only conducted laterally.

Total cell cycle length and the length of S-phase were calculated using BrdU and IdU as described in section 4.3.1 using Tbr2 to define the number of P-cells. At E11.5 in the lateral cortex, $T_S$ was significantly shorter in *Gli3*$^{Xt/Pdn}$ embryos compared to control (8.52±1.23 hrs in control and 5.82±0.48 hrs in mutant, n=4, $p<0.05$) (figure 4.19 A, B, C), as was $T_C$ (16.35±1.08 hrs in control and 13.65±0.73 hrs in mutant, n=4, $p<0.05$) (figure 4.19 A, B, C).

At E12.5, $T_S$ was unchanged in the mutant compared to control (7.47±0.97 hrs in control and 7.25±0.84 hrs in mutant, n=4, $p>0.05$) (figure 4.20 A, B, C), as was $T_C$ (17.00±2.16 hrs in control and 16.79±1.32 hrs in mutant, n=4, $p>0.05$) (figure 4.20 A, B, C). As in the lateral cortex at E11.5, the reduction in *Gli3* affected both S-phase and total cell cycle length of basal progenitors as it did in apical progenitors, however 24 hrs later it appears that the reduction in *Gli3* did not affect $T_S$ and $T_C$.

$T_{G2}$ of basal progenitors was measured at both E11.5 and E12.5 in the lateral cortex as described in section 4.3.1, using only pHH3$^+$ cells in an aventricular position. At E11.5, there was little difference in $T_{G2}$ in the *Gli3*$^{Xt/Pdn}$ embryo compared to control (1.34 hrs in control and 1.26 hrs in mutant, n=11) (figure 4.21 G). 24 hrs later, $T_{G2}$ was similar to E11.5 and unchanged between control and mutant (1.31 hrs in control, n=12, and 1.31 hrs in mutant, n=11) (figure 4.22 G). Therefore, as in the apical progenitor population, *Gli3* reduction had little effect on the length of G2-phase.

As described in section 4.3.1, M-phase length was measured in the basal progenitor population at both E11.5 and E12.5 by counting the pHH3$^+$ cells away from the ventricular surface. At E11.5, $T_M$ was unchanged in *Gli3*$^{Xt/Pdn}$ basal progenitors compared to control (0.13±0.04 hrs in control and 0.19±0.01 hrs in mutant, n=4, $p>0.05$) (figure 4.23 A, B, C). At E12.5, surprisingly there was a 2.55-fold increase in $T_M$ in the mutant compared to control (0.09±0.09 hrs in control and 0.23±0.03 hrs in

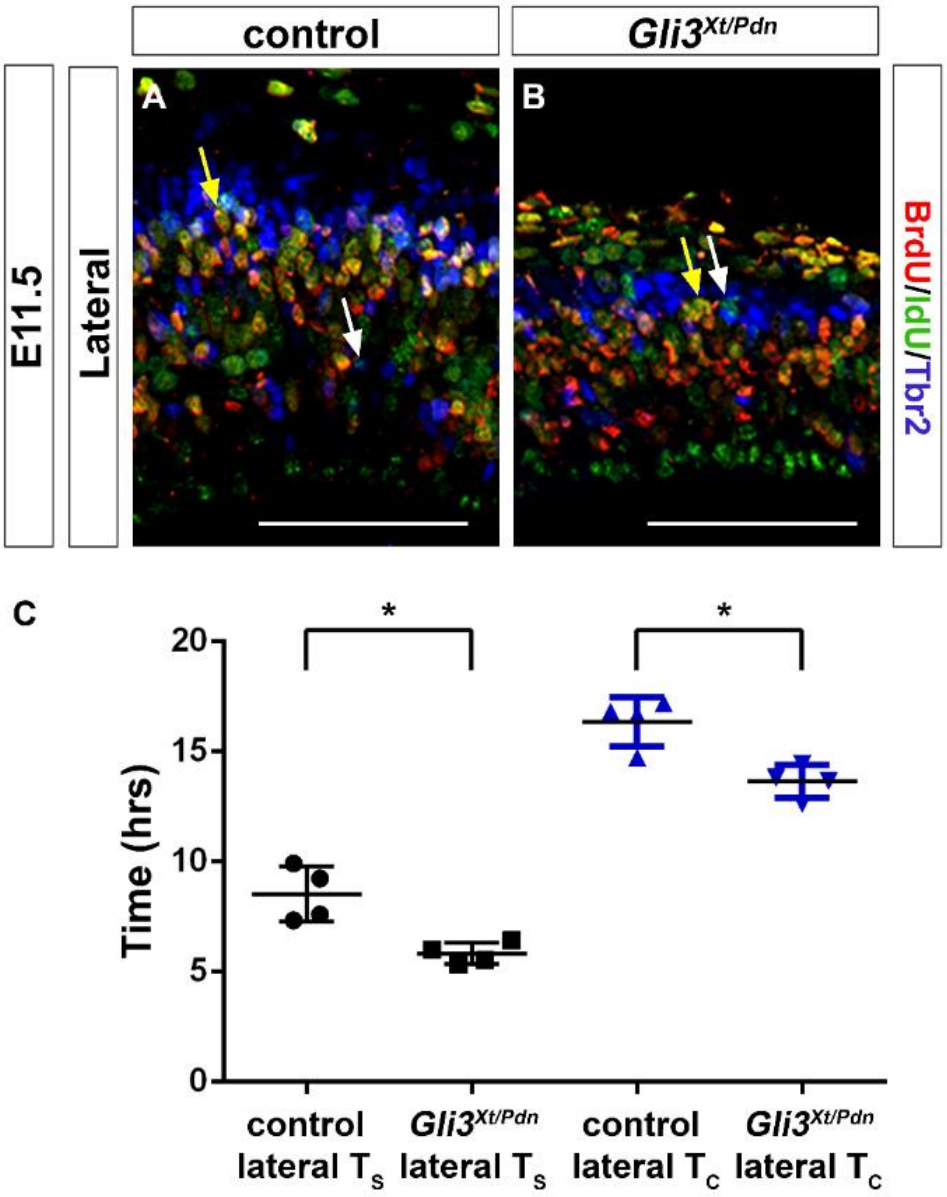


**Figure 4.19: S-phase and total cell cycle length were reduced in lateral *Gli3*$^{Xt/Pdn}$ basal progenitors at E11.5. A, B.** BrdU/IdU/Tbr2 immunofluorescence on sections of E11.5 cortex from control and *Gli3*$^{Xt/Pdn}$ embryos. White arrows depict IdU/Tbr2 co-labelled L-cells, yellow arrows depict BrdU/IdU/Tbr2 co-labelled S-cells. **C.** S-phase and total cell cycle length were significantly decreased in the lateral *Gli3*$^{Xt/Pdn}$ cortex. All statistical data represents mean ± 95% confidence interval; n=4; * = p<0.05; Mann-Whitney U-test. Scale bars = 100μm.

mutant, n=5, p<0.05) (figure 4.24 A, B, C). Altogether, as in apical progenitors, *Gli3* had no effect on $T_M$ at E11.5. However, in apical progenitors at E12.5 the reduction in *Gli3* resulted in a shortened $T_M$, yet in E12.5 basal progenitors the reduction in *Gli3* resulted in a statistically significant lengthening of $T_M$.

The length of G1-phase was calculated as in section 4.3.1 from the measurements of the other phase lengths and total cell cycle length in basal progenitors. In the lateral E11.5 cortex, the $T_{G1}$ was unaltered in mutant basal progenitors compared to control (6.35±0.81 hrs in control and 6.38±0.65 hrs in mutant, n=4, p>0.05) (figure 4.25), as was $T_{G1}$ 24 hrs later in the E12.5 cortex (8.13±1.53 hrs in control and 8.00±1.34 hrs in mutant, n=4, p>0.05) (figure 4.26). Unlike in apical progenitors $T_{G1}$ was unchanged in basal progenitors at both E11.5 and E12.5. Shown below in table 4.3 is a summary of the cell cycle phase lengths of basal progenitors.

**Table 4.3: Cell cycle phase lengths of basal progenitors**

| | | | Cell cycle phases | | | | |
|---|---|---|---|---|---|---|---|
| | | | **$T_{G1}$** | **$T_S$** | **$T_{G2}$** | **$T_M$** | **$T_C$** |
| **E11.5** | **Lateral** | **Control** | 6.35 | 8.52 | 1.34 | 0.13 | 16.35 |
| | | ***Gli3*$^{Xt/Pdn}$** | 6.37 | **5.82** | 1.26 | 0.19 | **13.65** |
| **E12.5** | **Lateral** | **Control** | 8.13 | 7.47 | 1.31 | 0.09 | 17.00 |
| | | ***Gli3*$^{Xt/Pdn}$** | 8.00 | 7.25 | 1.31 | **0.23** | 16.79 |

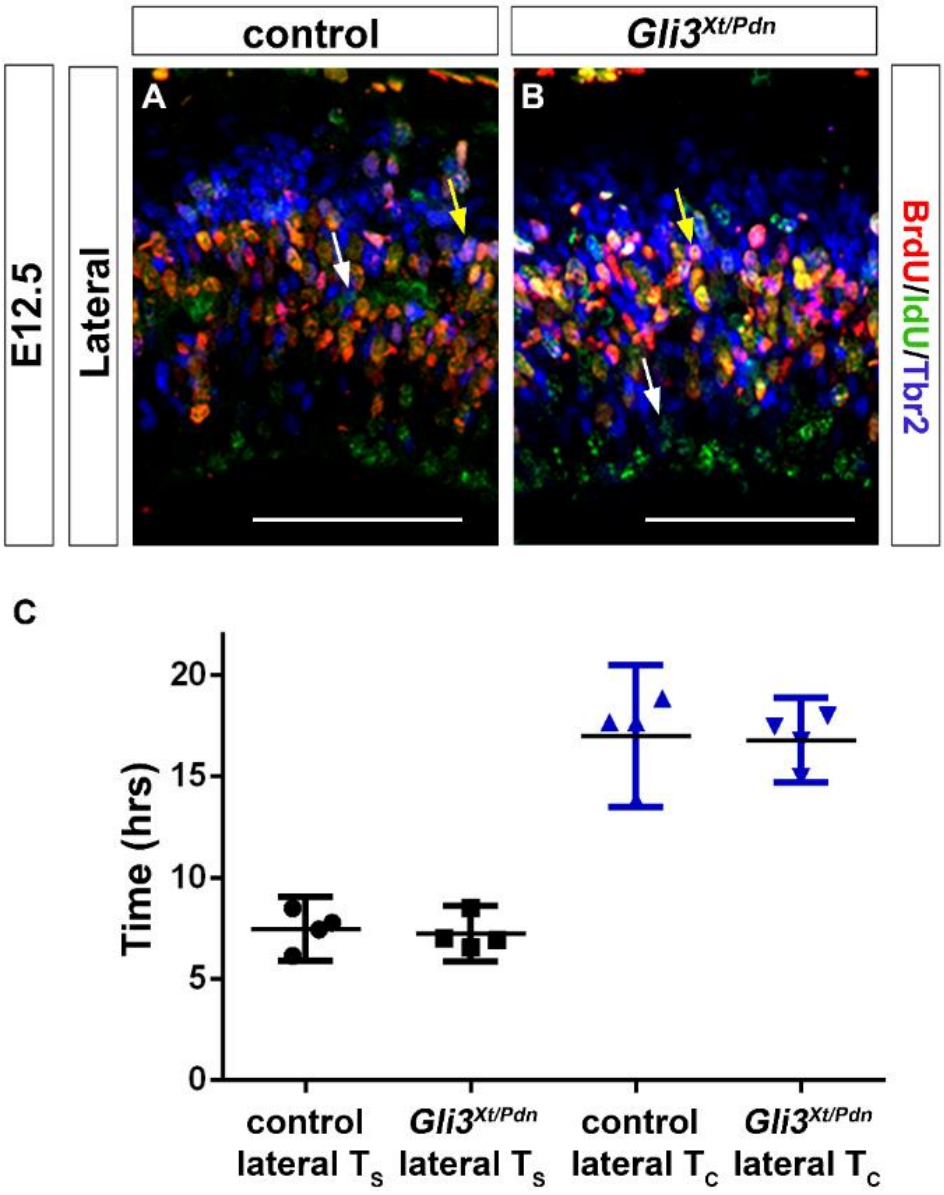


**Figure 4.20: S-phase and total cell cycle length were unaltered in lateral *Gli3*$^{Xt/Pdn}$ basal progenitors at E12.5. A, B.** BrdU/IdU/Tbr2 immunofluorescence on sections of E12.5 cortex from control and *Gli3*$^{Xt/Pdn}$ embryos. White arrows depict IdU/Tbr2 co-labelled L-cells, yellow arrows depict BrdU/IdU/Tbr2 co-labelled S-cells. **C.** S-phase and total cell cycle length were unaffected in the lateral *Gli3*$^{Xt/Pdn}$ cortex. All statistical data represents mean ± 95% confidence interval; n=4; * = $p<0.05$; Mann-Whitney U-test. Scale bars = 100μm.

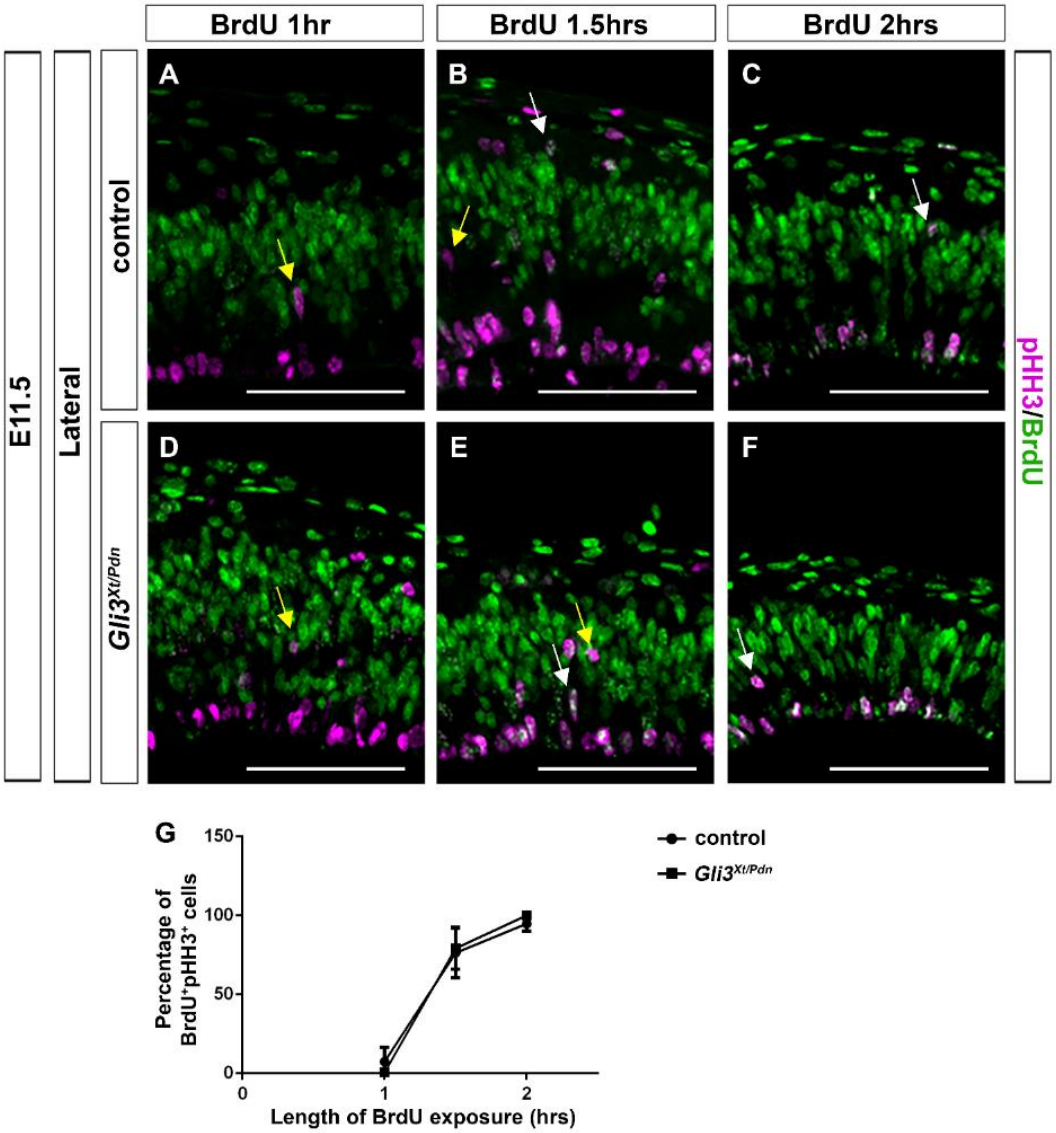


**Figure 4.21: G2-phase was unaltered in the lateral *Gli3*$^{Xt/Pdn}$ basal progenitor population at E11.5. A-F.** pHH3/BrdU immunofluorescence on sections of E11.5 cortex from control and *Gli3*$^{Xt/Pdn}$ embryos. Yellow arrows depict BrdU single-labelled basal progenitors, white arrows depict pHH3/BrdU co-labelled basal progenitors. **G.** There was no effect on G2-phase length in the lateral *Gli3*$^{Xt/Pdn}$ cortex. Error bars represent mean ± 95% confidence interval; n=11. Scale bars = 100μm.

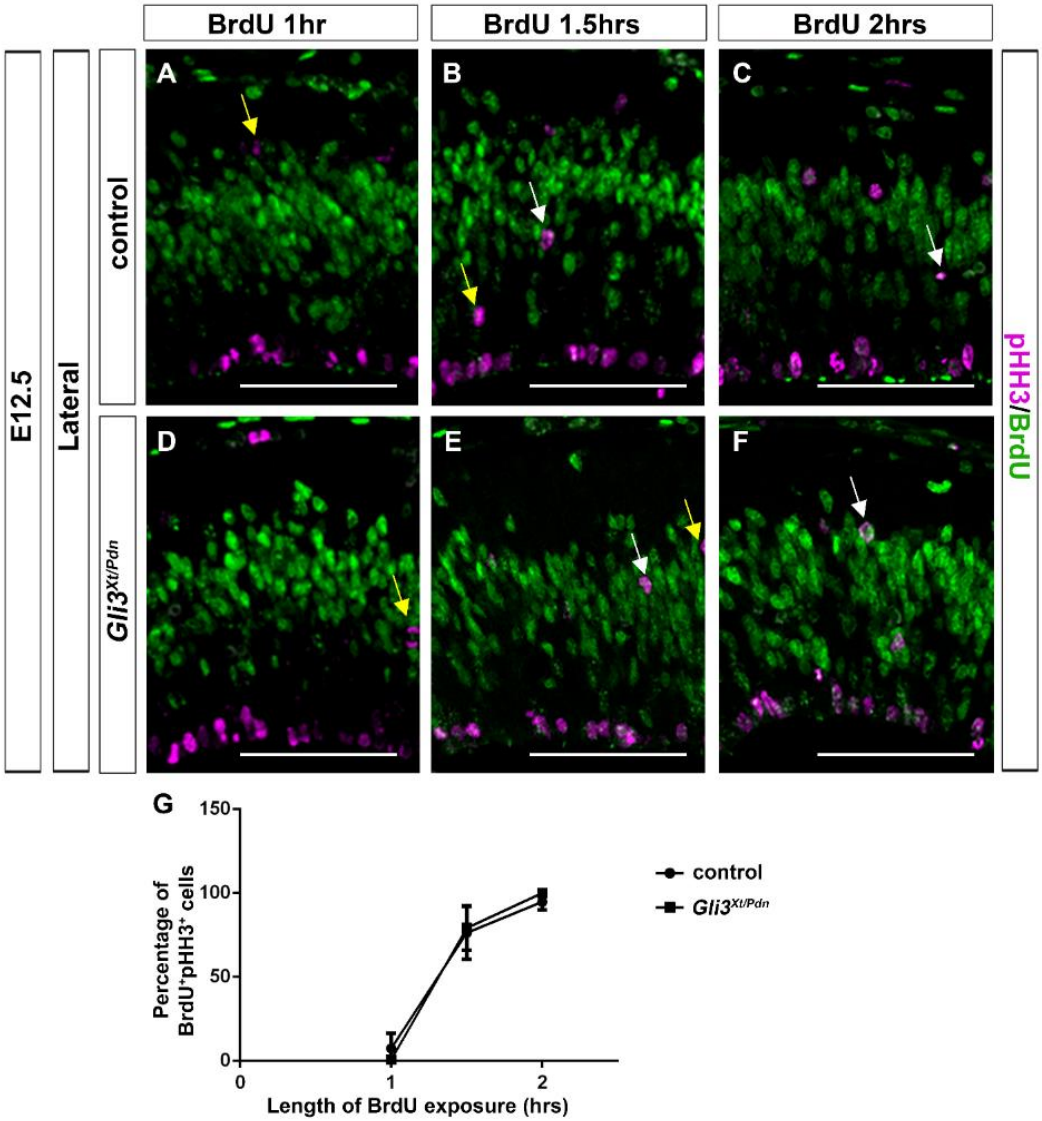


**Figure 4.22: G2-phase was unaltered in the lateral *Gli3*$^{Xt/Pdn}$ basal progenitor population at E12.5. A-F.** pHH3/BrdU immunofluorescence on sections of E12.5 cortex from control and *Gli3*$^{Xt/Pdn}$ embryos. Yellow arrows depict BrdU single-labelled basal progenitors, white arrows depict pHH3/BrdU co-labelled basal progenitors. **G.** There was no effect on G2-phase length in the lateral *Gli3*$^{Xt/Pdn}$ cortex. Error bars represent mean ± 95% confidence interval; n=11. Scale bars = 100μm.

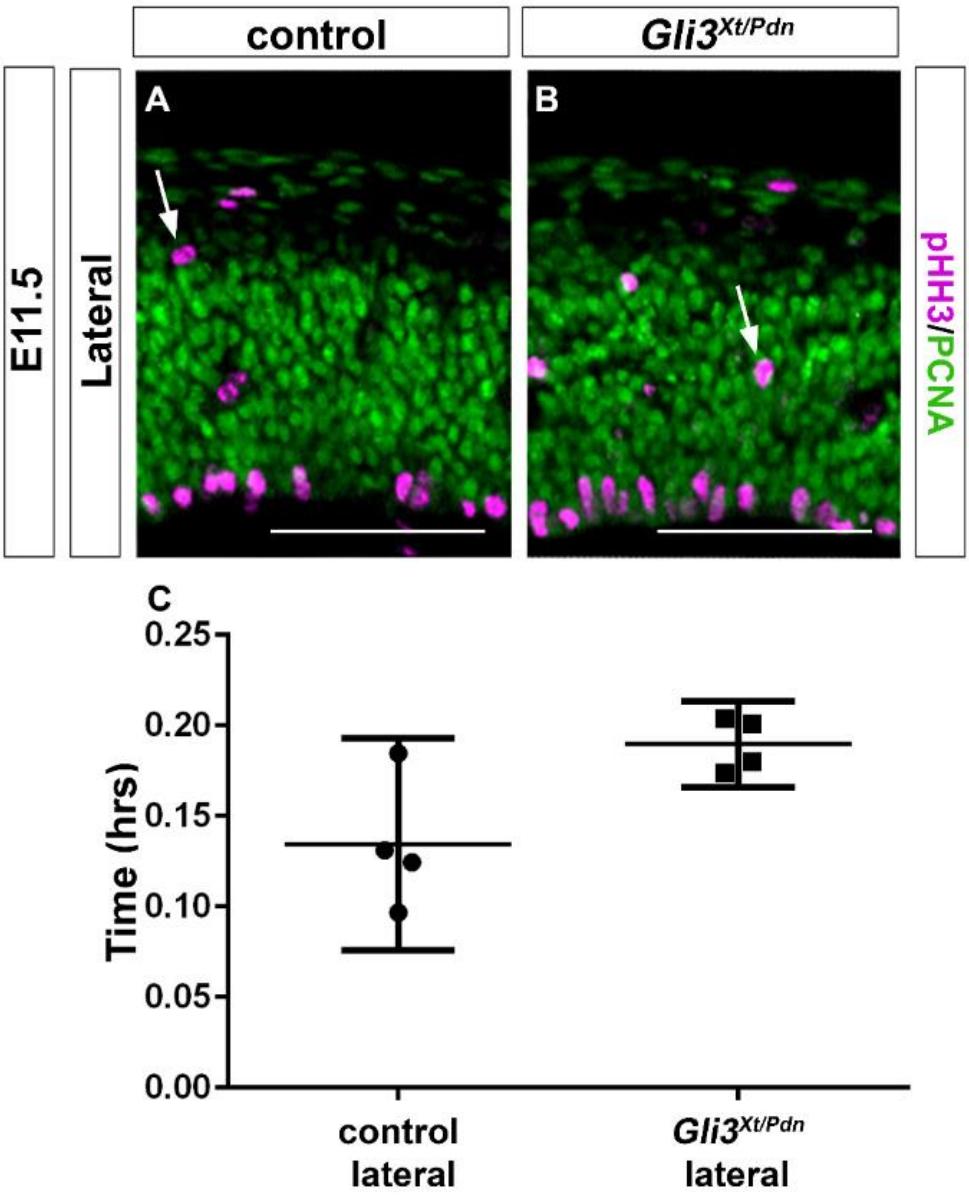


**Figure 4.23: M-phase length was unaltered in the lateral *Gli3*$^{Xt/Pdn}$ basal progenitor population at E11.5. A, B.** pHH3/PCNA immunofluorescence on sections of E11.5 cortex from control and *Gli3*$^{Xt/Pdn}$ embryos. Arrows depict pHH3/PCNA co-labelled basal progenitors. **C.** There was no effect on M-phase length in the lateral *Gli3*$^{Xt/Pdn}$ cortex. All statistical data represents mean ± 95% confidence interval; n=4; * = p<0.05; Mann-Whitney U-test. Scale bars = 100μm.

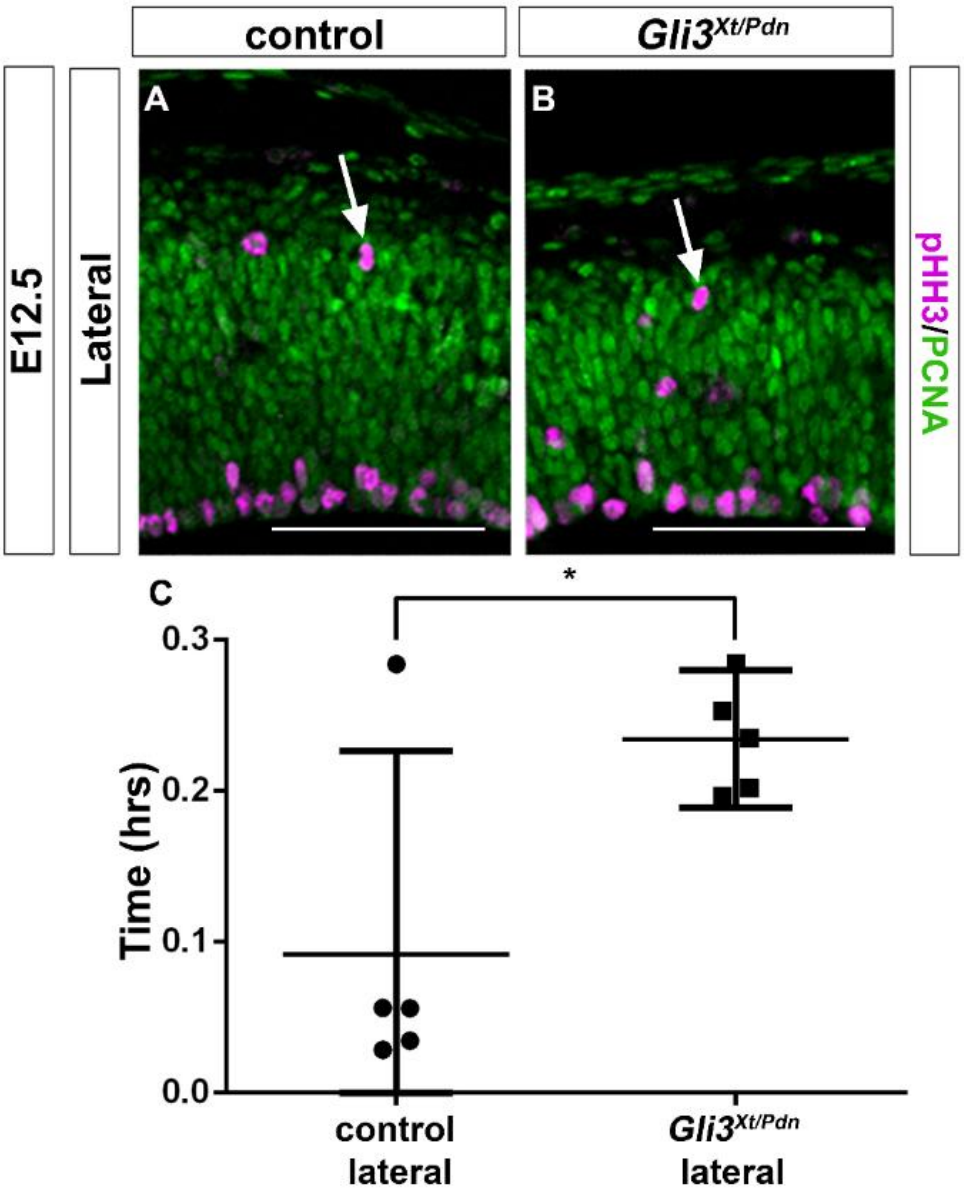


**Figure 4.24: M-phase length was increased in the lateral *Gli3*$^{Xt/Pdn}$ basal progenitor population at E12.5. A, B.** pHH3/PCNA immunofluorescence on sections of E12.5 cortex from control and *Gli3*$^{Xt/Pdn}$ embryos. Arrows depict pHH3/PCNA co-labelled basal progenitors. **C.** There was a significant increase in M-phase length in the lateral *Gli3*$^{Xt/Pdn}$ cortex. All statistical data represents mean ± 95% confidence interval; n=5; * = $p<0.05$; Mann-Whitney U-test. Scale bars = 100μm.

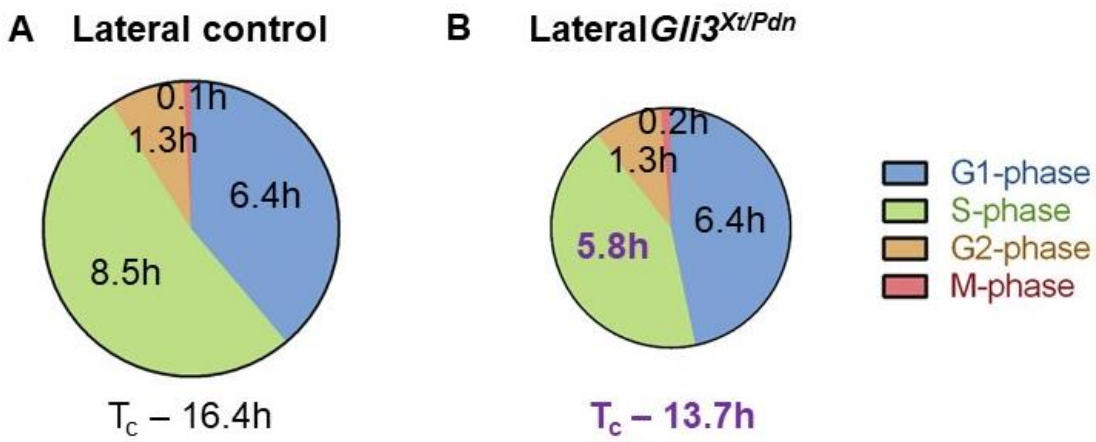


**Figure 4.25: G1-phase length was unaltered in the lateral *Gli3*$^{Xt/Pdn}$ basal progenitor population at E11.5.** Schematics showing the length of each cell cycle phase and total cell cycle length in lateral control **(A)** and lateral *Gli3*$^{Xt/Pdn}$ **(B)** embryos. In **B** significantly altered phase lengths are shown in bold purple text and note reduced total circle size representing reduced total cell cycle length. All statistical data represents mean; n=4; * = p<0.05; Mann-Whitney U-test.

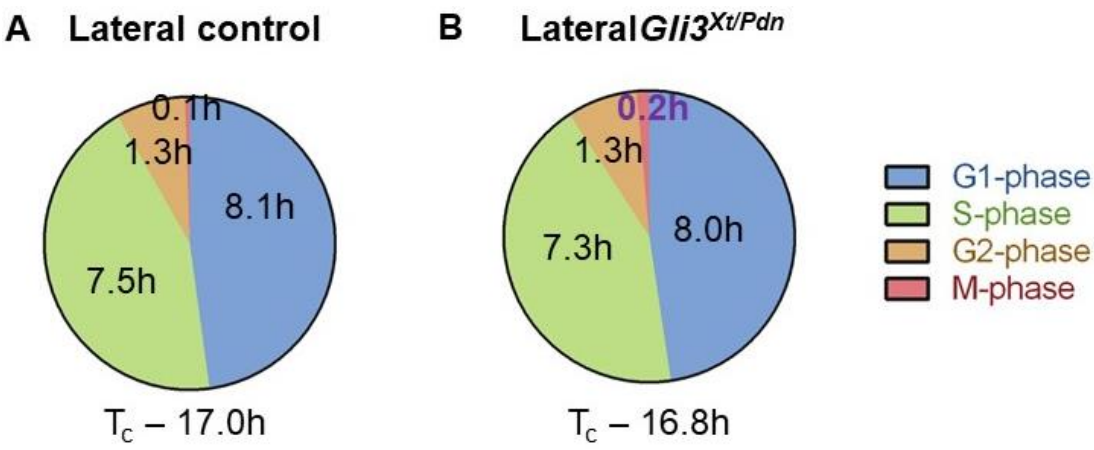


**Figure 4.26: G1-phase length was unaltered in the lateral *Gli3*$^{Xt/Pdn}$ basal progenitor population at E12.5.** Schematics showing the length of each cell cycle phase and total cell cycle length in lateral control **(A)** and lateral *Gli3*$^{Xt/Pdn}$ **(B)** embryos. In **B** significantly increased M-phase length is shown in bold purple text. All statistical data represents mean; n=4; * = p<0.05; Mann-Whitney U-test.

## 4.6 Discussion

The aim of this chapter was to begin to understand why the proportions of apical and basal progenitors and early-born neurons were altered in the *Gli3*$^{Xt/Pdn}$ cortex. One major factor known to impact upon the proliferation and differentiation of progenitors, which can alter progenitor and neuronal proportions, is the cell cycle (Lange *et al.*, 2009; Pilaz *et al*., 2009). Here, exit from the cell cycle and therefore differentiation into neurons was evaluated in the *Gli3*$^{Xt/Pdn}$ mutant, followed by examination of the length of each phase in the progenitor populations. I shall first discuss the lateral cortex, starting with apical progenitors at E11.5 and E12.5, then basal progenitors at E11.5 and E12.5. I will then discuss the medial cortex, focussing on apical progenitors at E11.5 and E12.5. As I was unable to make measurements in the medial basal progenitor population due to the low number of cells present at both E11.5 and E12.5, I will not discuss this population. I will consider how the changes observed in cell cycle re-entry/exit and in cell cycle phase lengths may have affected the proliferation/differentiation defects observed.

### *4.6.1 In Gli3*$^{Xt/Pdn}$ *lateral apical progenitors, cell cycle phase lengths were reduced at E11.5 and E12.5, whilst cell cycle exit was reduced at E11.5 and increased at E12.5*

At E11.5 in the lateral cortex, cell cycle re-entry for the total progenitor population was increased 2.19-fold in the *Gli3*$^{Xt/Pdn}$ mutant, indicating a tip towards proliferative divisions at the expense of differentiative divisions. Indeed, here apical progenitors, the largest progenitor population, showed an increased proportion whilst there were decreases in the proportions of basal progenitors and early-born neurons. This would indicate that the increase in cell cycle re-entry measured reflected an increase in apical progenitor proliferation instead of differentiation.

Concurrently, in the apical progenitor population, G1-phase, S-phase and total cell cycle length were shorter in the mutant compared to control. G2- and M-phase were unaltered in the mutant, suggesting *Gli3* does not regulate these phases here. The “cell cycle length” model proposes that G1-phase lengthening is required for progenitors to act upon differentiation cues (Calegari & Huttner, 2003). Here, as G1-phase length was shorter in the mutant apical progenitors, it would suggest a drive

towards proliferative divisions at the expense of differentiative divisions. Indeed, this was also suggested by the increase in cell cycle re-entry. Furthermore, the larger apical progenitor proportion and smaller basal progenitor and early-born neuron proportions also indicated that apical progenitors had undergone proliferative, self-renewing divisions to increase their pool instead of differentiating into basal progenitors and neurons. As Gli3 expression was primarily confined to this progenitor population, *Gli3's* regulation of G1-phase was likely direct. A likely candidate by which *Gli3* regulates G1-phase length is *Cdk6*, as it has been shown to bind to the *Cdk6* promoter and thereby negatively regulate the cell cycle (Lopez-Rios *et al.*, 2012; Vokes *et al*., 2008).

Whilst a lengthening of G1-phase has been shown to be required for progenitors to switch from proliferative to differentiative division (Lange *et al.*, 2009; Pilaz *et al*., 2009; Calegari & Huttner, 2003), shortening of S-phase length has been associated with the switch from proliferative to differentiative division (Gonzales *et al*., 2015; Arai *et al.*, 2011). Therefore, it was surprising to find a shortening of G1-phase length and simultaneous shortening of S-phase length. As these analyses were conducted at the population level instead of an individual cell level, there may have been a larger proportion of progenitors undergoing differentiative division. This was unlikely however, based on the measurements of apical and basal progenitor and early-born neuron proportions and cell-cycle exit, which pointed to increased proliferative division at E11.5. To directly examine the proportion of progenitors which were undergoing proliferative versus differentiative division, Tis21 expression was examined. When a progenitor will undergo differentiative division, *Tis21* mRNA is up-regulated during G1-phase, and protein expression continues throughout S-, G2- and M-phases (Iacopetti *et al.*, 1999). As I will show in section 5.6.1, the proportion of $Tis21^{+}$ apical progenitors was unaltered in the mutant compared to control in the E11.5 lateral cortex.

Taken together, perhaps *Gli3* regulates S-phase length directly, acting to shorten it, yet the length of G1-phase is a more critical factor regulating proliferative versus differentiative division in E11.5 lateral apical progenitors. Unlike G1-phase lengthening, S-phase shortening has not been shown to be causative in the switch from proliferative to differentiative division in the mouse. Furthermore, cell cycle length is not the only element influencing mode of division, and the impact of these other elements likely contribute to the decision of how to divide.

In the *Gli3*$^{Xt/Pdn}$ mutant, there are many defects contributing to the alteration in cortical development, such as alterations in signalling (Kuschel *et al*., 2003), all of which complicate the analyses of these embryos. In order to assess if and how *Gli3* regulates the cell cycle directly, examination of cell cycle phase lengths was also undertaken in the *Emx1Cre;Gli3*$^{fl;/fl}$ embryo in the rostro-medial telencephalon (Hasenpusch-Theil *et al*., 2018). At E11.5, there were few Tbr2$^{+}$ basal progenitors, and so analyses were conducted at the total progenitor population level which primarily reflected the apical progenitor population. Here, G1- and S-phase and total cell cycle length were also decreased in the *Emx1Cre;Gli3*$^{fl;/fl}$ mutant compared to control. As *Gli3* has only recently been deleted here (Amaniti *et al.*, 2013), it is likely that *Gli3* therefore directly regulates both G1- and S-phase length.

In the E12.5 lateral cortex of the *Gli3*$^{Xt/Pdn}$ mutant, there was a 1.54-fold increase in cell cycle exit. Here, the apical progenitor population still made up the majority of cortical progenitors. As opposed to E11.5, the proportion of apical progenitors was unchanged in the mutant compared to control at E12.5, and there were larger proportions of basal progenitors and neurons. This would suggest that in the time interval between analyses, there was a switch from apical progenitor proliferative division to differentiative division into neurons, decreasing their proportion from E11.5 to E12.5, and increasing the proportion of early-born neurons.

As at E11.5, G1-phase length was significantly shorter in the E12.5 mutant apical progenitors, implying *Gli3* directly affects G1-phase length. The analyses of apical and basal progenitors and early-born neurons outlined before suggests there was an early delay in neurogenesis at E11.5 caused by an increase in proliferative divisions that was overcome at E12.5, due to an increase in differentiative division. Therefore, the question is raised in that if there was a decrease in proliferative divisions and an increase in differentiative divisions between E11.5 and E12.5 in the mutant, why was G1-phase length shorter in the mutant at E12.5? Factors other than the cell cycle are known to regulate neurogenesis, and so it is possible that at E12.5, the length of G1-phase is less important in the mutant. For example, *Wnt* and *Fgf* signalling are disrupted in the *Gli3*$^{Xt/Pdn}$ mutant (Kuschel *et al.*, 2003), although these are more influential in the medial cortex. It is also conceivable that *Gli3* regulates factors which inhibit proliferation. RNA sequencing was performed in the E11.5 and E12.5 *Emx1Cre;Gli3*$^{fl;/fl}$ dorsal telencephalon. In these embryos, at E11.5 the Cdk inhibitors *Cdkn1a, b* and *c* were down-regulated at E11.5 yet were unaltered at E12.5

(Hasenpusch-Theil *et al.*, 2018). In these mutants, G1-phase length was reduced compared to control at E11.5, yet unaffected at E12.5.

In the *Gli3*$^{Xt/Pdn}$ mutant, at E12.5 S-phase was also shorter compared to control in apical progenitors. As a shortened S-phase has been shown to correlate with differentiative division as opposed to proliferative division (Gonzales *et al*., 2015; Arai *et al*., 2011), at E12.5 this links to the alterations in progenitor and neuronal proportions. Three possible explanations could be suggested to explain why both S-phase and G1-phase were reduced in mutant apical progenitors compared to control at E12.5, although it is likely other factors also contribute to these observations. Firstly, the length of S-phase may be more critical to the mode of division which mutant apical progenitors will undertake than the length of G1-phase. Secondly, the reduced S-phase length measured at E11.5 might already indicate a switch towards apical progenitor differentiative division in the mutant, the result of which (a relative reduction in apical progenitor proportion and increase in neuronal proportion from E11.5 to E12.5), was only obvious 24 hrs later. Thirdly, it is possible that G1-phase lengthening is required for the switch from proliferative to differentiative division, yet it was artificially blocked possibly due to a reduction in *Cdk6* inhibition by the reduction in *Gli3* in the mutant. S-phase shortening may then have occurred to compensate for the block on G1-phase lengthening.

Unlike at E11.5, M-phase length was shorter in *Gli3*$^{Xt/Pdn}$ lateral apical progenitors at E12.5, where there was an increase in cell cycle exit indicating an increase in differentiation. However, Pilaz *et al*. (2016) reported that a longer M-phase length correlates with an increase in neurogenesis. As was seen with G1-phase, perhaps the length of M-phase was not as critical to the decision to undergo proliferative as opposed to differentiative division in these progenitors at this time.

### *4.6.2 In lateral basal progenitors of the Gli3*$^{Xt/Pdn}$ *mutant, S-phase and total cell cycle length were reduced at E11.5, whilst M-phase was increased at E12.5*

Cell cycle was also examined in basal progenitors to reveal if there were any cell non-autonomous effects of the reduction of *Gli3* in the *Gli3*$^{Xt/Pdn}$ mutant. As before, cell cycle re-entry/exit was evaluated at the total progenitor population level. In the E11.5 lateral cortex, there was an increase in cell cycle re-entry. Whilst there was an increased apical progenitor proportion, there were decreased basal progenitor and

neuronal proportions. The decreased basal progenitor proportion may have been due to decreased basal progenitor production from apical progenitors or increased basal progenitor cell death. I suggest that the increased cell cycle re-entry measured indicated an increase in apical progenitor proliferation, at the expense of differentiation into basal progenitors, but cannot rule out that there was decreased basal progenitor apoptosis. It would therefore be important to examine cell death in the *Gli3*$^{Xt/Pdn}$ cortex. Furthermore, these analyses were conducted at the total progenitor population level by combining BrdU with PCNA. In the future, cell cycle re-entry/exit should be examined at the apical and basal progenitor levels by combining BrdU with Pax6 and Tbr2. This would confirm if the alterations seen in the total progenitor population reflects primarily the apical progenitor proportion, and/or if the basal progenitor proportion was also affected.

In E11.5 lateral basal progenitors, S-phase was significantly shorter in the mutant compared to control, resulting in a significantly reduced total cell cycle length. As in the apical progenitors, G2- and M-phase were unaltered, suggesting *Gli3* does not regulate these phase lengths in the E11.5 lateral cortex. However, unlike apical progenitors G1-phase was unaltered, indicating as hypothesised above that *Gli3* directly regulates the length of G1-phase in the lateral cortex. The change in S-phase length could reflect indirect regulation of *Gli3* over this phase length, or possibly an increase in the differentiation of basal progenitors. Tis21 immunostaining revealed a small, yet significant 1.09-fold increase in basal progenitor differentiation here (section 5.6.2). However, it is unlikely this accounted for the 1.46-fold decrease in S-phase length, so arguably *Gli3* regulates S-phase length on a cell non-autonomous level also.

By E12.5 in the lateral neocortex, there had been a switch from cell cycle re-entry in the mutant to increased cell cycle exit. Whilst the mutant apical progenitor proportion was unchanged in comparison with control, the basal progenitor and early-born neuron proportions were increased. The switch from cell cycle re-entry to cell cycle exit therefore likely reflected either an increase in apical progenitor differentiation into neurons and/or an increase in basal progenitor differentiation into neurons. If there had been a considerable increase in basal progenitor differentiation, I would suggest that the basal progenitor proportion would not have been so significantly increased (by 1.47-fold) compared to control in the mutant. Therefore, the increased cell cycle exit recorded at the total progenitor population level probably indicated an alteration

in apical progenitors, highlighting the need to repeat cell cycle exit analyses with Pax6 and Tbr2 instead of PCNA.

Unexpectedly in the E12.5 lateral basal progenitor population all cell cycle length measurements including total cell cycle length were unaltered in the *Gli3*$^{Xt/Pdn}$ mutant compared to control, apart from M-phase. As the total cell cycle length of basal progenitors was unaffected yet these cells appeared to spend more time in M-phase, this reflects a larger proportion of basal progenitors in mitosis. The increased basal progenitor proportion measured here may therefore be due to an increase in basal progenitor production from apical progenitors differentiating between E11.5 and E12.5, combined with a larger proportion of basal progenitors dividing proliferatively. Eventually, this would be expected to lead to an increase in basal progenitors followed by an increase in subsequently born deeper-layer neurons when these basal progenitors divide differentiatively, resulting in disruption to the cortical layers. Friedrichs *et al.* (2008) reported that in newborn P0 *Gli3*$^{Xt/Pdn}$ animals, ER81 (layer V) and RORβ (layer IV) neurons were scattered throughout the cortical layers in the lateral neocortex, including near to the ventricular surface, indicating disruption to the generation of these neurons.

Together, the reduction in *Gli3* had little effect on the cell cycle of the basal progenitor population at both ages. This was unsurprising, as Gli3 was primarily expressed in apical progenitors. Therefore, *Gli3* likely primarily regulates the cell cycle directly, although alterations to the cell cycle and to the balance between proliferative and differentiative division also probably occurred due to alterations in signalling and other factors disrupted in the *Gli3*$^{Xt/Pdn}$ mutant.

### *4.6.3 In the Gli3$^{Xt/Pdn}$ medial apical progenitor population, cell cycle exit and cell cycle phase lengths were unaffected at E11.5, yet cell cycle exit was increased and cell cycle phase lengths were shorter at E12.5*

In the medial neocortex, there were very few Tbr2$^{+}$ basal progenitors at both E11.5 and E12.5, thereby skewing the calculation of the length of each phase of the cell cycle. As such, I did not measure the cell cycle phase lengths of medial basal progenitors at E11.5 and E12.5, and so will only discuss the medial apical progenitor population.

In the E11.5 medial mutant cortex, the proportions of apical and basal progenitors and early-born neurons were unaltered. In conjunction, cell cycle exit was also unaffected, indicating that at this early age medially the reduction in *Gli3* had little effect on progenitor division.

S-, G2- and M-phase of the cell cycle, as well as total cell cycle length, were unaltered in the mutant compared to control at this time. However, I was unable to accurately measure G1-phase length and so cannot comment on whether or not G1-phase was altered in mutant medial apical progenitors. It is unlikely that these cells did not have a G1-phase, as an extremely short, negligible G1-phase is associated with embryonic stem cells, which are much less differentiated than apical progenitors (Soufi & Dalton, 2016). A calculated length of 0 hrs for G1-phase of these cells is likely due to inaccurate measurement of the other cell cycle phase lengths, particularly an overestimation of G2-phase length. However, using this methodology to indirectly measure G1-phase length made this error unavoidable. In the future, measurement of G1-phase length directly would be valuable. As apical progenitors comprised the majority of progenitors, the reduction seen in G1-phase length when apical and basal progenitors were combined was likely due to a reduction of G1-phase length in apical progenitors. This would indicate increased apical progenitor proliferative division and reduced differentiative division, although these changes were not recognised in the progenitor and neuronal proportions. As neurogenesis progresses from lateral to medial, the decrease in G1-phase length may precede alterations in the progenitor and neuronal proportions.

Although I was unable to determine if G1-phase length was significantly altered in the apical progenitor population, it was reduced in the E11.5 $Gli3^{Xt/Pdn}$ medial cortex when all progenitors were examined together. A shorter G1-phase is associated with proliferative division (Lange *et al*., 2009; Pilaz *et al*., 2009), yet there were no alterations in the apical and basal progenitor and neuronal proportions. This indicates that although G1-phase was reduced, it did not have a substantial effect on the cell populations.

All other phase lengths were unaltered in the mutant E11.5 medial cortex compared to control. This reflects the lack of alteration to the neuronal and progenitor proportions, suggesting that in the E11.5 medial cortex *Gli3* has little effect on this very early stage of neurogenesis. This is in contrast to the lateral cortex, where the reduction in *Gli3* has a significant effect on the mutant cell cycle, as well as on the

progenitor and neuronal proportions. Perhaps as neurogenesis in the lateral cortex is more advanced than in the medial cortex, this underlies the importance of *Gli3* to neurogenesis as the reduction of it in the *Gli3*$^{Xt/Pdn}$ mutant results in increasing disruption to the cortex following the progression of neurogenesis.

By E12.5, the apical progenitor proportion had decreased in the mutant compared to control, and the basal progenitor and early-born neuron proportions had increased. In the medial E12.5 cortex in both control and mutant embryos, apical progenitors still represented the largest progenitor population, and there was a 1.36-fold increase in cell cycle exit. Therefore, here the reduction in *Gli3* caused an increase in apical progenitor differentiation into early-born neurons, as was happening in the lateral cortex, although possibly basal progenitor differentiation into neurons also occurred.

Here in the apical progenitor population, S-phase, M-phase and total cell cycle length were reduced in the mutant compared to control. A shorter S-phase length correlates with differentiative division (Gonzales *et al*., 2015; Arai *et al.*, 2011), which would fit with the increase seen in apical progenitor differentiation into basal progenitors and neurons observed between E11.5 and E12.5 in the mutant. A reduction in *Gli3* resulting in a shorter S-phase may therefore contribute to the mutant phenotype, but it is likely that factors other than cell cycle length, such as alterations in signalling, also contributed to the changes in progenitor and neuronal proportions. One major factor likely to have had a large impact in the *Gli3*$^{Xt/Pdn}$ mutant is alterations in signalling. In the medial cortex, *Wnt2b* and *Wnt3a* gene expression is abolished in the mutant (Kuschel *et al.*, 2003). Wnt signalling has been shown to delay basal progenitor formation by encouraging proliferative division (Wrobel *et al.*, 2007), and so the abolition of *Wnt* signalling in the medial cortex may contribute to apical progenitor differentiative division and basal progenitor formation at E12.5.

Finally, as in the lateral cortex, M-phase length was also reduced in the medial *Gli3*$^{Xt/Pdn}$ apical progenitor population compared to control. Again, this contradicts the report from (Pilaz *et al.*, 2016) who stated that a longer M-phase is associated with increased neurogenesis, as I measured a shorter M-phase whilst the early-born neuronal proportion was increased. This could indicate that *Gli3* regulates M-phase length, yet the decrease in M-phase length was not influential enough to prolong the delay in neurogenesis observed at E11.5. Instead, the reduction in S-phase length and differences in signalling led to the increased basal progenitor and early-born neuron proportions.

Altogether, *Gli3* clearly plays a role in the regulation of the cell cycle, which likely contributes to the alterations observed in the progenitor and neuronal proportions, although these alterations are complex. At E11.5, the reduction in G1-phase in the mutant apical progenitors correlates with the "cell cycle length" model, as I reported a larger proportion of apical progenitors and concomitant smaller proportions of basal progenitors and neurons. Therefore, the reduced G1-phase length would indicate that apical progenitors are undergoing increased self-renewing divisions, reflecting their larger proportion, at the expense of differentiative divisions, reflecting the smaller basal progenitor and neuronal proportions. Conversely, shorter S-phase length is linked with differentiative division, yet S-phase length was shorter in the mutant compared to control. It would seem in the E11.5 cortex, G1-phase length was critically important in the decision as to which mode of division to undergo. However, by E12.5, both G1-phase and S-phase length were still reduced in the mutant yet the progenitor and neuronal proportions would indicate a switch in apical progenitors from proliferative to differentiative division. Thus, at E12.5, G1-phase length seemed to be less critical, and S-phase length more critical in the *Gli3*$^{Xt/Pdn}$ cortex, in order to correct the delay in neurogenesis. Overall, I hypothesise that in the *Gli3*$^{Xt/Pdn}$ mutant, particularly in the lateral cortex, there is competition between the influence of G1-phase shortening and S-phase shortening, with G1-phase length more important at E11.5 whilst S-phase length is more important at E12.5.

In the future, it would be useful to directly measure the length of G1-phase to avoid the complication observed in the E11.5 medial G1-phase measurement. It is now possible to do this with the use of transgenic mouse mutants such as FUCCI mice. In these mice, for example, Cdt1 is tagged to a red fluorescent marker thereby labelling progenitors only when they are in G1-phase, and Geminin is tagged to a green fluorescent marker and is only expressed when those same progenitors are in S/G2/M-phase (Roccio *et al.*, 2013). Using time lapse microscopy or live imaging, it is possible to directly measure how long individual cells remain in G1-phase, and it would be very interesting to cross these into *Gli3*$^{Xt/Pdn}$ embryos to give a more accurate measurement of the length of G1-phase.

Furthermore, when measuring the length of M-phase, I classified pHH3$^{+}$ cells along the ventricular edge as apical progenitors and those away from the ventricular edge as basal progenitors, yet I used PCNA as a progenitor marker against which to compare these cells. In the future, it would be advantageous to repeat these

experiments using pHH3 and either Pax6 or Tbr2, to assess the proportion of mitotic apical or basal progenitors against their own progenitor population, giving a more accurate measurement of M-phase length. This would also indirectly result in a more accurate measurement of G1-phase length.

### 4.7 Summary

In this chapter, the role of *Gli3* in cell cycle exit and therefore the formation of neurons close to the beginning of neurogenesis has been evaluated. At E11.5 in the lateral cortex, a reduction in *Gli3* resulted in increased cell cycle re-entry, coinciding with an increased apical progenitor proportion at the expense of a decreased neuronal proportion. Furthermore, the basal progenitor proportion was also reduced, indicating not just a failure in apical progenitors to leave the cell cycle but also to form basal progenitors. Here, G1-phase was significantly shorter in the apical progenitor population but unaltered in the basal progenitor population, suggesting *Gli3* directly regulates G1-phase length and cell-autonomously controls the mode of division apical progenitors will undertake. At E12.5, cell cycle exit was increased in the $Gli3^{Xt/Pdn}$ lateral cortex, alongside a reduced apical progenitor proportion compared to E11.5 and increased neuronal proportion. G1-phase, S-phase and M-phase lengths were shorter in the mutant amongst apical progenitors indicating faster cycling through the cell cycle, whilst the mitotic index of basal progenitors was increased, indicating more basal progenitors actively dividing. In the E11.5 medial cortex, cell cycle exit was unchanged in the mutant, as were the proportions of apical and basal progenitors and neurons. Although based on these measurements I am unable to say if G1-phase was significantly altered in the apical progenitor population, G1-phase length was shorter in the total progenitor population, indicating that *Gli3* regulated the cell cycle here but possibly not strongly enough to have a resulting effect on the progenitors and subsequent neurons. By E12.5 in the mutant medial cortex, cell cycle exit was increased and the apical progenitor proportion was decreased whilst the neuronal proportion had increased. G1-phase, S-phase, M-phase and total cell cycle length were reduced in the mutant compared to control, as was seen in the lateral cortex. Therefore, whilst *Gli3* reduction resulted in a shortening of the cell cycle coinciding with increased cell cycle re-entry at E11.5, at E12.5 the reduction in *Gli3* still resulted in a shorter cell cycle whilst cell cycle exit was increased. Additional factors, then, regulating progenitor proliferation or differentiation must surpass the control of the cell cycle as neurogenesis progresses in the $Gli3^{Xt/Pdn}$ cortex.

# Chapter 5: A preliminary investigation into the cellular mechanisms through which *Gli3* may regulate the cell cycle

## 5.1 Introduction

In chapter 4, I showed that the reduction in *Gli3* in $Gli3^{Xt/Pdn}$ embryos results in an increase in cell cycle re-entry in the E11.5 lateral cortex, whilst cell cycle exit is increased laterally and medially at E12.5. Cell cycle lengths were also altered in the mutant, with most often a reduction in G1-, S- and M-phase length as well as total cell cycle length, at both E11.5 and E12.5. In this chapter, I will explore possible mechanisms by which G1-phase and S-phase length were altered.

The mammalian neural progenitor cell cycle is complex. When a parent cell divides, the two progeny enter G1-phase. Here each cell is able to integrate extra- and intra-cellular signals, indicating if it should differentiate and leave the cell cycle, entering G0-phase, or if it should continue on to S-phase and divide again. If the cell is to continue to S-phase, the cyclin-dependent kinases *Cdk4* and *Cdk6* form a complex with the D-type cyclins, predominantly *cyclin-D1* in apical progenitors and *cyclin-D2* in basal progenitors (Glickstein *et al.*, 2007). The Cdk4/6-cyclin D complex hyperphosphorylates pRb, thereby changing the pRb/E2F complex conformation and preventing pRb from actively repressing transcription by the E2F transcription factors. This then allows the cell to progress past the mid G1-restriction point. *Cyclin E* and *Cdk2* expression are then up-regulated, in part by the unrestricted E2Fs, and in complex contribute to further hyperphosphorylation of pRb. This frees the E2F transcription factors from being bound to pRb, enabling transcription of genes required for DNA replication and so transitioning the cell from G1-phase into S-phase (Harbour *et al.*, 1999; Sherr, 1996).

In the $Gli3^{Xt/Pdn}$ dorsal telencephalon I reported a reduction in G1-phase length. *Cdk4/6* and *cyclin D1* are key regulators of progression through G1, and for example when *Cdk4* and *cyclin D1* were overexpressed in cortical progenitors, G1-phase lengthening was inhibited (Lange *et al.*, 2009). Although *Cdk6* has been recently reported to have effects out with its association with the D-type cyclins, for example it can regulate transcription of the Cdk inhibitor $p16^{INK4a}$ (Kollmann *et al*., 2013), with regards to progression past the mid G1-restriction point and into S-phase *Cdk6* and *Cdk4* act in the same way. In the mouse limb bud, a whole-genome chromatin

immunoprecipitation (ChIP)-on-chip identified potential *Gli3* binding sites in the *Cdk6* promoter (Vokes *et al*., 2008). From here, Lopez-Rios *et al*. (2012) conducted further ChIP analysis on control and conditional *Gli3* knockout limb buds and found that endogenous *Gli3* binds to the *Cdk6* promoter region *in vivo*.

I hypothesise, therefore, that the reduction in *Gli3* may result in a dysregulation of *Cdk6* in the developing cortex, promoting faster progression through G1-phase. Indeed, several *Gli3* binding sites were identified up-stream of the *Cdk6* transcription start site, and these were verified *in vitro* through luciferase assay to be functional (Hasenpusch-Theil *et al*., 2018). Under normal physiological conditions, Cdk inhibitors such as $p16^{INK4a}$ and the Cip/Kip families of proteins would be responsible for limiting the activity of Cdks. This allows G1-phase lengthening to take place, and cortical progenitors are able to withdraw from the cell cycle and differentiate into neurons. In recent years, Cdks have become a major focus in cancer therapy, leading to the development of Cdk pharmacological inhibitors. Palbociclib has been identified as a specific inhibitor of Cdk4/6 that shows no significant activity against other Cdks ( Sherr *et al.*, 2016). When used at a high concentration it prevents cells from leaving G1-phase, but at lower concentrations slows progression through G1-phase thereby lengthening it (Toogood *et al.*, 2005; Fry *et al.*, 2004). It therefore represents a useful tool for the artificial lengthening of G1-phase in a *Cdk4/6*-orientated manner.

Following G1-phase, progenitors enter S-phase where DNA replication takes place to ready the cell for division into two new progeny. Whilst it known that progression through S-phase is mediated by Cdk2-cyclin A, the regulation of S-phase length presents a more complicated picture than that of G1-phase. This is primarily as less is known about its regulation and how dysregulation of S-phase length contributes to the way in which a progenitor will divide. In human ESCs, down-regulation of S-phase progression genes prevented pluripotency marker down-regulation (Gonzales *et al.*, 2015). Additionally, treatment of human ESCs with aphidicolin, an inhibitor of DNA replication, resulted in a lengthening of S-phase and an up-regulation of active TGFβ signalling. This is known to promote the pluripotent state in human ESCs and prevent differentiation (Gonzales *et al*., 2015). Furthermore, in the mouse dorsal telencephalon, proliferative cortical progenitors exhibit a longer S-phase length than differentiative progenitors (Arai *et al*., 2011). As no obvious candidate genes by which *Gli3* may regulate S-phase length have been identified by ChIP analysis (Lopez-Rios

*et al.*, 2012; Vokes *et al.*, 2008), it is possible that the shortening of S-phase length measured here represented an increased proportion of differentiative progenitors.

In this chapter, I will begin by analysing microarray analysis data from the E10.5 *Gli3*$^{Xt/Pdn}$ dorsal telencephalon, to look for any obvious candidate genes which may have contributed to the defects in G1- and S-phase length. As alluded to, *Cdk6* was identified in the screen as up-regulated in the *Gli3*$^{Xt/Pdn}$ mutant. I then performed pRb expression analysis at E11.5 and E12.5 to assess if the up-regulation of *Cdk6* had a functional effect on pRb hyperphosphorylation, and found that it was increased. I followed this analysis by culturing control and *Gli3*$^{Xt/Pdn}$ cortical slices *in vitro* for 24 hrs in the presence of palbociclib or DMSO as control to see if G1-phase lengthening could be achieved, and if it would rescue the defect in neuron formation reported at E11.5 in the mutant. However, the culture conditions used were not conducive to cortical slice growth, and so I could not assess the effect of palbociclib on slices. Finally, as no candidate genes for the dysregulation of S-phase length were identified in the microarray screen, I examined *Tis21* expression in apical and basal progenitors of *Gli3*$^{Xt/Pdn}$*;Tis21GFP* embryos to measure the proportion of differentiative divisions. *Tis21* is up-regulated during G1-phase when a progenitor commits to undergoing a differentiative division; apical progenitors into basal progenitors or neurons and basal progenitors into neurons (Arai *et al*., 2011; Iacopetti *et al.*, 1999).

## 5.2 Gene expression profiling of *Gli3* mutants revealed dysregulation of cell proliferation/differentiation genes

In order to investigate how *Gli3* may have regulated cell cycle length in the *Gli3*$^{Xt/Pdn}$ embryo, I examined microarray data from the E10.5 *Gli3*$^{Xt/Pdn}$ dorsal telencephalon, carried out by Thomas Theil and Kerstin Hasenpusch-Theil. E10.5 was used as an early time point preceding the defects observed at E11.5, particularly the reduction in G1- and S-phase and total cell cycle length. Microarray analysis allowed for evaluation of changes in mRNA expression resulting from reduced *Gli3*, which may have resulted in alteration to the cell cycle and ultimately differences in progenitor proliferation/differentiation.

To conduct the microarray analysis, the complete dorsal telencephalon was dissected from E10.5 control and *Gli3*$^{Xt/Pdn}$ embryos. The dorsal telencephalons from two to three littermate embryos were pooled together to form each sample, and three control and mutant littermate samples were compared. The RNAeasy Micro Kit (Qiagen) was used to extract and isolate RNA from the samples, before microarray analysis was performed using Affymetrix GeneChip Mouse Genome 430 2.0 arrays. Analysis of the raw data output from the array was performed at the Sir Henry Wellcome Functional Genomics Facility (Institute of Biomedical and Life Science, University of Glasgow). A cut off value of $p<0.05$ was employed, revealing a total of 262 genes as dysregulated in the *Gli3*$^{Xt/Pdn}$ mutant compared to control, 78 up-regulated and 184 down-regulated.

In support of the reliability of the microarray analyses, a number of genes previously identified as dysregulated in the *Gli3*$^{Xt/Pdn}$ dorsal telencephalon were identified in this screen. *In situ* hybridisation performed by Kuschel *et al*. (2003) revealed an abolition of *Emx1* expression and severe reduction in *Emx2* expression at E10.5. The microarray screen revealed a down-regulation of *Emx1* of 2.94-fold, and a down-regulation of *Emx2* of 2.05-fold. With regards to signalling molecules, Kuschel *et al*. (2003) reported an inability to detect *Wnt3a* and *Bmp6* transcripts via *in situ*, and these showed 2.23-fold and 2.03-fold down-regulations, respectively, in the microarray. At E12.5, Hasenpusch-Theil *et al*. (2015) revealed expanded *Fgf15* and *Fgf17* expression in the *Gli3*$^{Xt/Pdn}$ mutant, transcripts which were up-regulated 1.82-fold and 2.21-fold in the microarray analysis, respectively. Furthermore, in the E11.5 lateral *Gli3*$^{Xt/Pdn}$ cortex I reported a 1.36-fold decrease in the proportion of Tbr2$^{+}$ basal

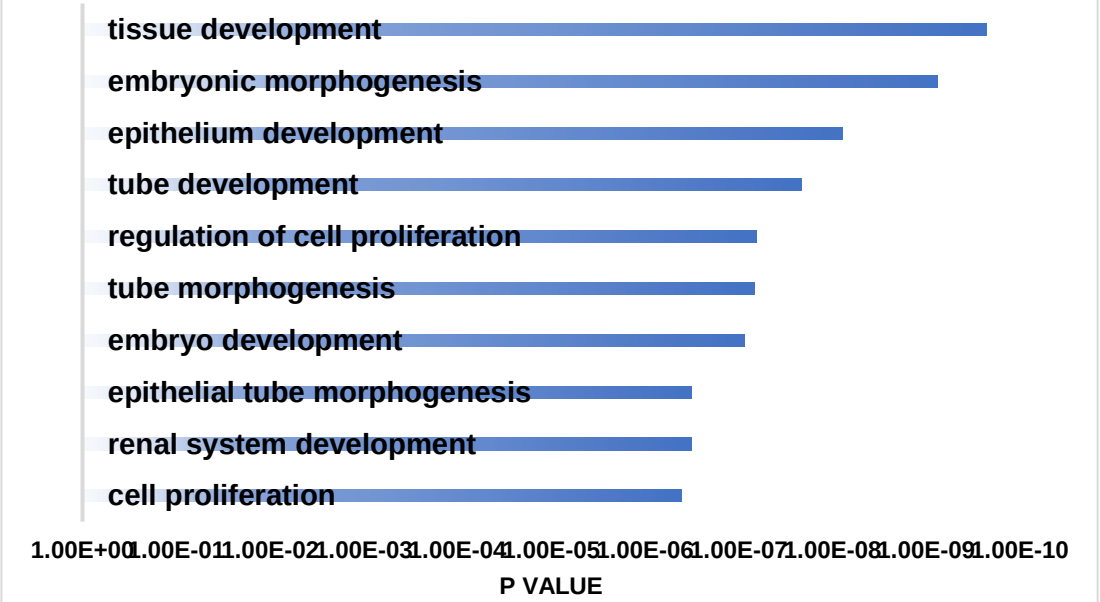


**Figure 5.1: Gene Ontology (GO) analysis of up-regulated genes.** Genes identified as up-regulated by microarray analysis in the E10.5 *Gli3*$^{Xt/Pdn}$ dorsal telencephalon, based on the biological processes associated with each gene. Terms were ranked based upon GO term usage in the list.

progenitors and a 1.98-fold decrease in the proportion of Tbr1$^{+}$ early-born neurons. The microarray analysis revealed a 1.95-fold down-regulation of *Tbr2* and a 2.36-fold down-regulation of *Tbr1* at E10.5. *Pax6* was not identified in the microarray screen, although it may have been dysregulated but not identified due to the cut-off value for fold change used.

To evaluate the microarray data, I conducted Gene Ontology (GO) analysis looking specifically at biological processes. In this analysis, the dysregulated genes are ranked based on the processes in which they have been implicated. The output reveals the number of genes from the submitted gene list which coincide with the total number of genes linked to each process. The Generic Gene Ontology Term Finder tool from Princeton University (Boyle *et al.*, 2011) was used to perform GO analysis on the up- and down-regulated gene lists separately. The biological processes

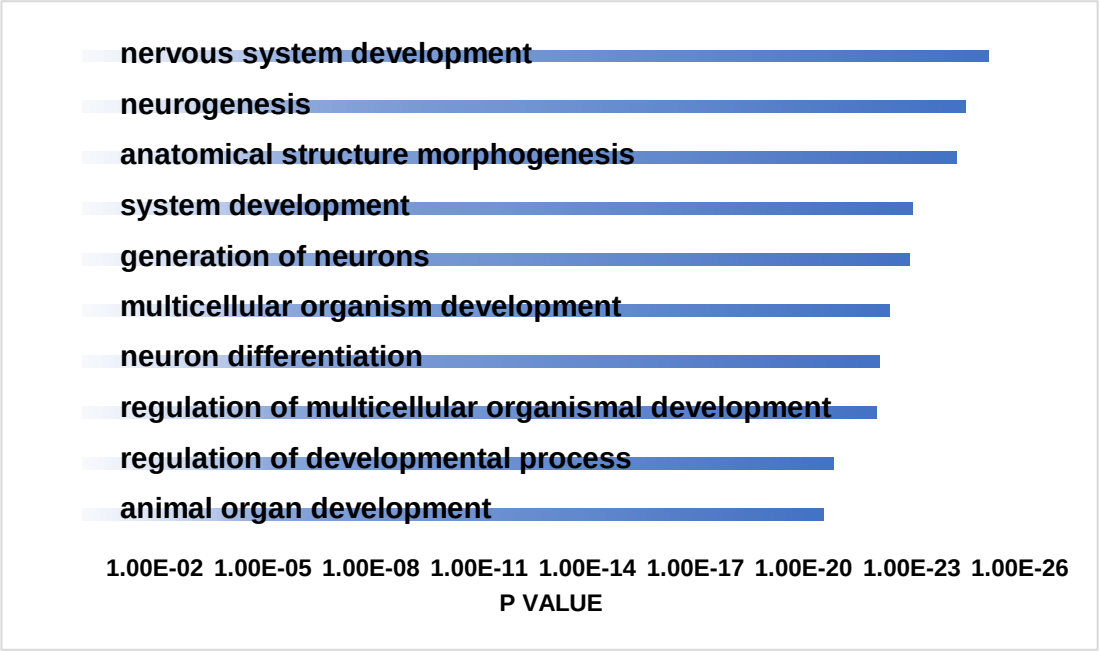


**Figure 5.2: Gene Ontology (GO) analysis of down-regulated genes.** Genes identified as down-regulated in the E10.5 *Gli3*$^{Xt/Pdn}$ dorsal telencephalon, based on the biological processes associated with them. Terms were ranked based upon GO term usage in the list.

identified as linked to each gene set were ranked based on GO term usage in each gene list.

Figures 5.1 and 5.2 show the top 10 results received for up-regulated and down-regulated genes, respectively. Some of the processes identified amongst the up-regulated genes included “regulation of cell proliferation” and “cell proliferation”, whilst the down-regulated processes included “neurogenesis”, “generation of neurons” and “neuron differentiation”. In the E11.5 *Gli3*$^{Xt/Pdn}$ lateral cortex, I reported an increase in cell cycle re-entry and increased apical progenitor proportion with decreased basal progenitor and early-born neuron proportions. I suggested the apical progenitor population was proliferating and re-entering the cell cycle at this age, at the expense of differentiation into neurons. The GO analysis supports this, revealing that 24 hrs before I conducted my immunofluorescent analyses there was already an up-

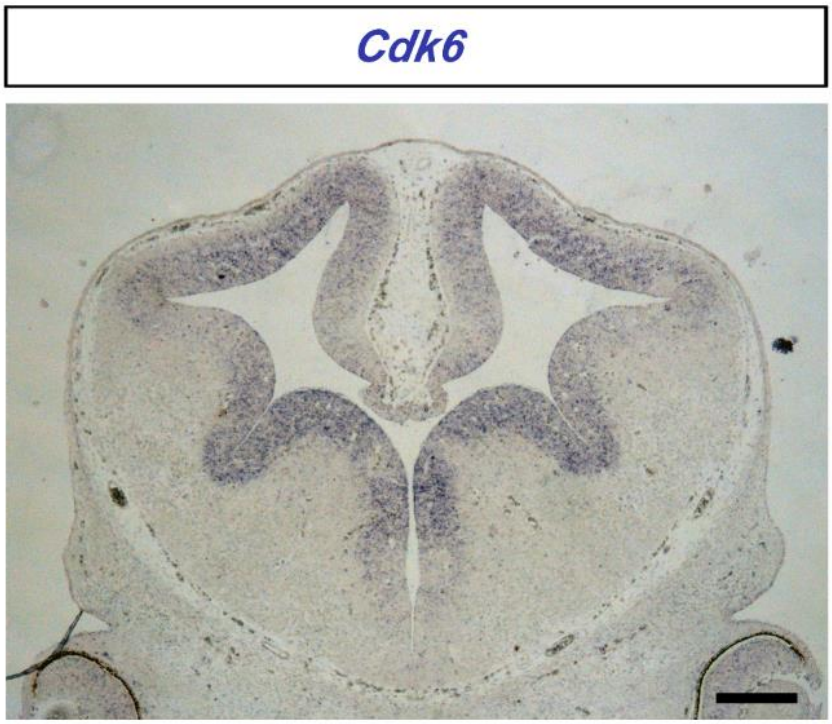


**Figure 5.3: *Cdk6* expression.** *In situ* hybridisation revealing *Cdk6* expression in the E12.5 wild-type cortex. *Cdk6* was expressed in the proliferating zone of the cortex. Image supplied by Kerstin Hasenpusch-Theil. Scale bar = 250μm.

regulation of genes regulating proliferative division at the expense of genes regulating differentiative division.

In regard to the cell cycle length defect observed at E11.5 in the *Gli3*$^{Xt/Pdn}$ cortex, *Cdk6* was identified in the microarray screen as up-regulated 1.59-fold in the mutant compared to control. *Cdk6* is a cyclin dependent kinase which is up-regulated in G1-phase, and in combination with D-type cyclins, progresses a progenitor past the G1 restriction point thereby allowing entry into S-phase (Lim & Kaldis, 2013). The microarray was conducted at the total cell level in the dorsal telencephalon, and G1-phase length was reduced in the *Gli3*$^{Xt/Pdn}$ mutant at the total progenitor level. Figure 5.3 shows *Cdk6* expression in the control E12.5 telencephalon, where it is expressed in the proliferative zone of the cortex (image supplied by Kerstin Hasenpusch-Theil). *Cdk6* therefore represented an interesting candidate gene which may have contributed to the reduction in G1-phase length. Additionally, when this microarray

was conducted, analysis was also carried out on the E10.5 *Gli3*$^{Pdn/Pdn}$ mutant. In this mutant between E11.5 and E12.5, there was no delay in neurogenesis as seen in the lateral *Gli3*$^{Xt/Pdn}$ cortex (Magnani *et al.*, 2010) and no differential expression of *Cdk6*, further suggesting *Cdk6* as a potential candidate gene altering G1-phase length in *Gli3*$^{Xt/Pdn}$.

### 5.3 pRb expression was increased in apical and basal progenitors of the E11.5 lateral *Gli3*$^{XtPdn}$ cortex, whilst at E12.5 it was increased in lateral and medial basal progenitors only

Before focussing on *Cdk6* as a candidate gene reducing the length of G1-phase, I assessed if the up-regulation in *Cdk6* had a consequential effect on the actions of Cdk6. When bound to its catalytic binding partners D-type cyclins, Cdk6 hyperphosphorylates Rb (pRb), releasing its inhibition on the E2F transcription factors and allowing transcription of phase progression genes. I therefore examined pRb expression in the E11.5 and E12.5 *Gli3*$^{Xt/Pdn}$ cortex. As with Pax6 and Tbr2, pRb expression was compared with PCNA expression to give the proportion of progenitors expressing it. Apical and basal progenitors were identified separately based on the position of the pRb$^{+}$ cells, with those along the ventricular surface classified as apical progenitors and those in an aventricular position classified as basal progenitors.

At E11.5, the proportion of pRb$^{+}$ apical progenitors was increased in the *Gli3*$^{Xt/Pdn}$ lateral neocortex compared to control, yet remained unaffected in the medial cortex (lateral: 4.69±0.30% in control and 5.59±0.54% in mutant, n=4, $p<0.05$, medial: 5.05±0.95% in control and 5.99±0.45% in mutant, n=4, $p>0.05$) (figure 5.4 A–E, yellow arrows). In the basal progenitor population, the proportion of pRb$^{+}$ cells was increased laterally but unaltered medially (lateral: 0.33±0.09% in control and 0.91±0.15% in mutant, n=4, $p<0.05$, medial: 0.26±0.18% in control and 0.65±0.36% in mutant, n=4, $p>0.05$) (figure 5.4 A–D, F, white arrows).

At E12.5, the proportion of pRb$^{+}$ apical progenitors in the *Gli3*$^{Xt/Pdn}$ cortex was no different from control in both the lateral and medial cortex (lateral: 4.12±0.55% in control and 5.31±1.07% in mutant, n=4, $p>0.05$, medial: 4.71±0.70% in control and 4.91±0.39% in mutant, n=4, $p>0.05$) (figure 5.5 A–E, yellow arrows). However, the proportion of pRb$^{+}$ basal progenitors was increased in the mutant compared to control

both laterally and medially (lateral: 0.58±0.13% in control and 1.01±0.18% in mutant, n=4, $p<0.05$, medial: 0.13±0.08% in control and 0.74±0.19% in mutant, n=4, $p<0.05$) (figure 5.5 A–D, F, white arrows). Taken together, the reduction in *Gli3* in the mutant cortex did result in an increase in pRb hyperphosphorylation, potentially due to an increase in *Cdk6* expression.

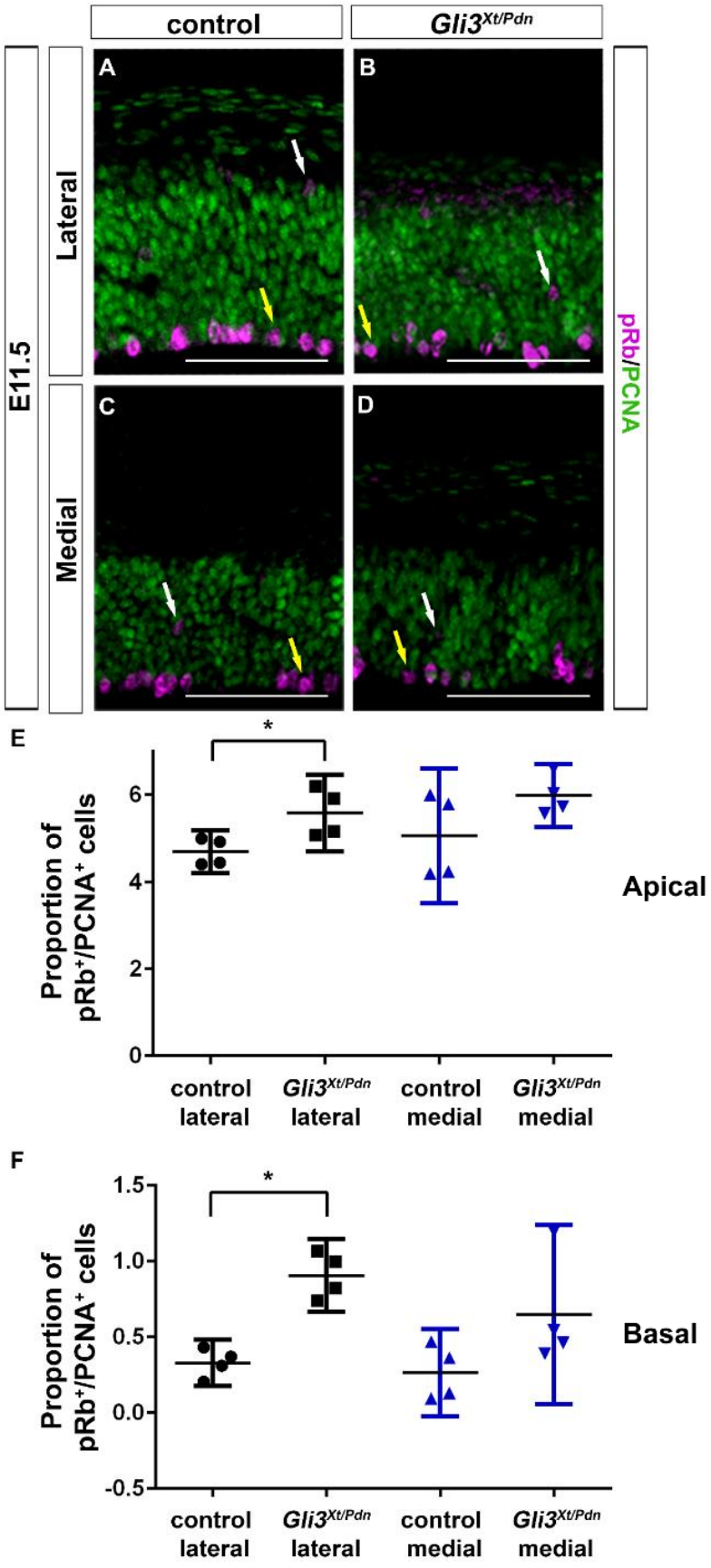
control
Gli3Xt/Pdn
E11.5
Lateral
Medial
A
B
C
D
pRb/PCNA
E
Proportion of pRb+/PCNA+ cells
Apical
control lateral
Gli3Xt/Pdn lateral
control medial
Gli3Xt/Pdn medial
F
Basal
*

**Figure 5.4: pRb S780 expression was increased in the E11.5 lateral cortex. A-D.** pRb/PCNA immunofluorescence on sections of E11.5 cortex from control and *Gli3*$^{Xt/Pdn}$ embryos. Yellow arrows denote apical progenitors, white arrows denote basal progenitors. **E.** The proportion of pRb$^{+}$ cells was increased in the *Gli3*$^{Xt/Pdn}$ apical progenitor population compared to control in the lateral cortex. There was no significant difference between control and mutant in the medial cortex. **F.** The proportion of pRb$^{+}$ cells was significantly increased in the *Gli3*$^{Xt/Pdn}$ basal progenitor population in the lateral cortex. There was no significant difference in the pRb expression between control and mutant in the medial cortex. All statistical data represents mean ± 95% confidence interval; n=4; * = $p<0.05$; Mann-Whitney U-test. Scale bars = 100μm.

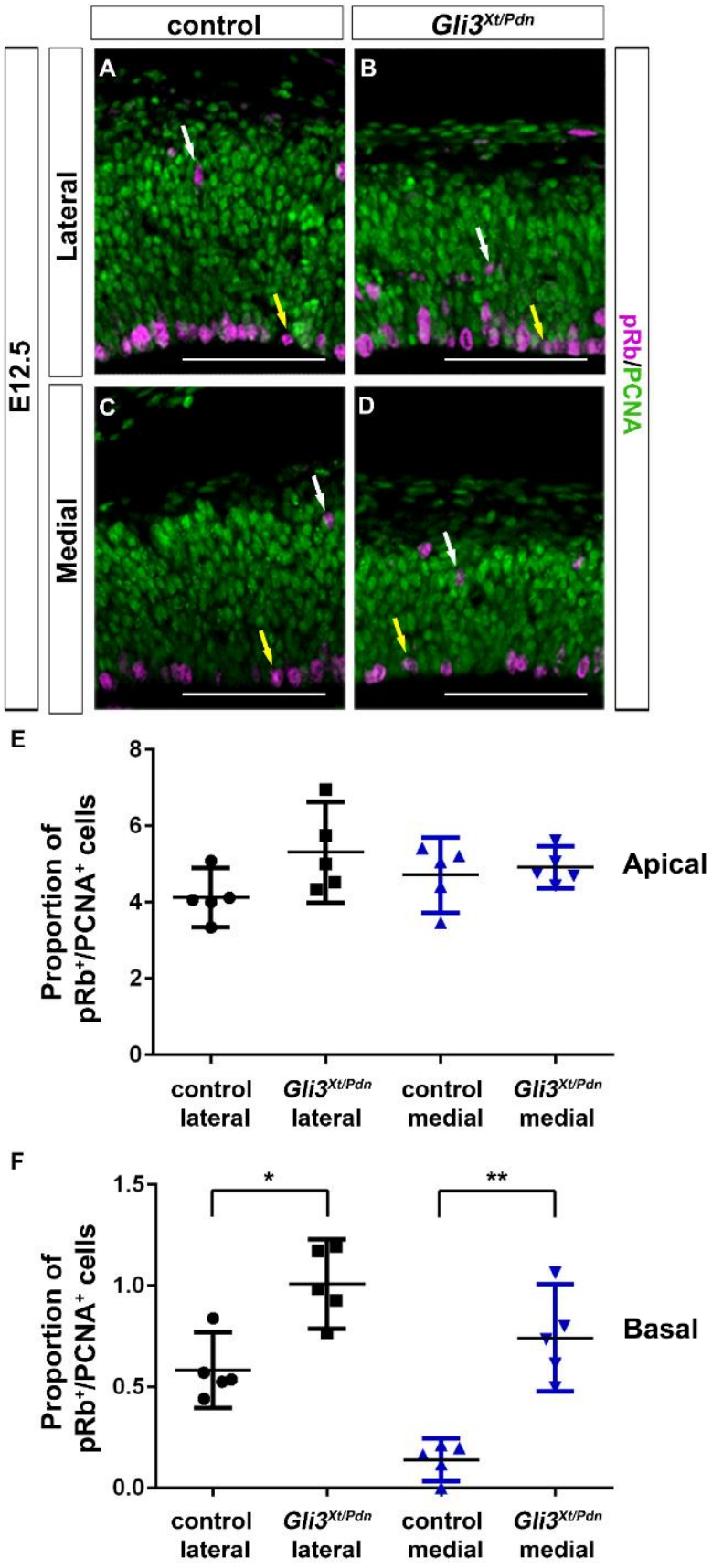
control
Gli3Xt/Pdn
E12.5
Lateral
Medial
A
B
C
D
pRb/PCNA
E
Proportion of pRb+/PCNA+ cells
Apical
control lateral
Gli3Xt/Pdn lateral
control medial
Gli3Xt/Pdn medial
F
Proportion of pRb+/PCNA+ cells
Basal
*
**

**Figure 5.5: pRb S780 expression was increased in basal progenitors of the E12.5 cortex. A-D.** pRb/PCNA immunofluorescence on sections of E12.5 cortex from control and *Gli3*$^{Xt/Pdn}$ embryos. Yellow arrows denote apical progenitors, white arrows denote basal progenitors. **E.** In the lateral cortex, there was no significant difference in the proportion of pRb$^{+}$ apical progenitors in the *Gli3*$^{Xt/Pdn}$ mutant compared to control. Likewise, there was no significant difference between control and mutant in the medial cortex. **F.** The proportion of pRb$^{+}$ cells was significantly increased in the *Gli3*$^{Xt/Pdn}$ basal progenitor population in the lateral cortex. The proportion of pRb$^{+}$ basal progenitors was also increased in the medial mutant cortex compared to control. All statistical data represents mean ± 95% confidence interval; n=5; * = $p<0.05$; ** = $p<0.01$; Mann-Whitney U-test. Scale bars = 100μm.

## 5.4 Palbociclib increased pRb expression in E13.5 CD1 organotypic slice culture

To investigate the link between increased *Cdk6* expression in the E10.5 *Gli3*$^{Xt/Pdn}$ dorsal telencephalon and the reduction in G1-phase length measured at E11.5 and E12.5, a Cdk4/6 specific inhibitor was used to promote rescue of the neurogenesis delay. Developed as a chemotherapy drug, palbociclib specifically inhibits the action of Cdk6 and its counterpart Cdk4. In tumour cell lines, treatment with palbociclib reduces expression of the proliferation marker Ki67 and down-regulated E2F target genes (Sherr *et al.*, 2016). To test the efficacy of palbociclib in cortical slice culture, CD1 embryos were used due to the large litter size of CD1 mice compared to *Gli3*$^{Xt/+}$ and *Gli3*$^{Pdn/+}$ mice. This facilitated evaluation of the concentration of palbociclib to be used in *Gli3*$^{Xt/Pdn}$ slice cultures. The brain was dissected from E13.5 CD1 embryos and embedded in agarose for vibratome sectioning. 300μm coronal sections were incubated for 24 hrs in the presence of either DMSO (control) or palbociclib dissolved in DMSO. Three different concentrations of palbociclib were compared, 1.5μg/ml, 0.75μg/ml and 0.38μg/ml (Fry *et al*., 2004). After culture, the slices were further cryosectioned to 10μm to allow for immunofluorescent analysis. As above, pRb expression was compared against PCNA expression to provide a readout of Cdk6

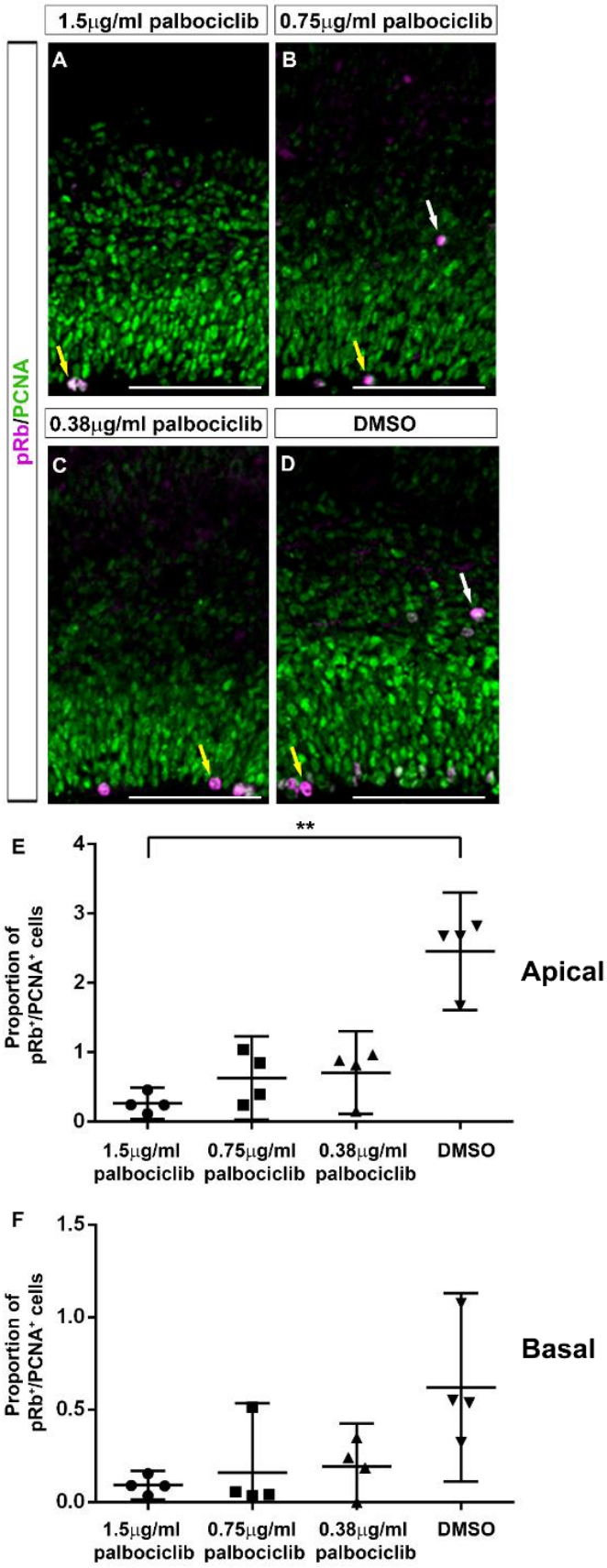
1.5μg/ml palbociclib
0.75μg/ml palbociclib
0.38μg/ml palbociclib
DMSO
A
B
C
D
pRb/PCNA
E
Proportion of pRb+/PCNA+ cells
**
Apical
1.5μg/ml palbociclib
0.75μg/ml palbociclib
0.38μg/ml palbociclib
DMSO
F
Proportion of pRb+/PCNA+ cells
Basal

**Figure 5.6: pRb S780 expression in the lateral cortex of E13.5 CD1 organotypic slice cultures after exposure to DMSO or palbociclib. A-D.** pRb/PCNA immunofluorescence on slice cultures of E13.5 cortex from CD1 embryos. Yellow arrows denote apical progenitors, white arrows denote basal progenitors. **E.** In the apical progenitor population, administration of 1.5μg/ml palbociclib significantly reduced the proportion of $pRb^+$ cells in comparison with DMSO administration. **F.** In the basal progenitor population, administration of all concentrations of palbociclib did not significantly reduced the proportion of $pRb^+$ cells in comparison to DMSO. All statistical data represents mean ± 95% confidence interval; n=4; ** = p<0.01; Kruskal-Wallis test followed by Dunn's post-hoc test. Scale bars = 100μm.

activity. Apical and basal progenitor expression was examined as outlined in the *Gli3*$^{Xt/Pdn}$ cortex, and the lateral and medial cortex were compared.

In the lateral cortex, the proportion of $pRb^+$ apical progenitors was significantly reduced in the presence of 1.5μg/ml palbociclib compared to control, yet 0.75μg/ml and 0.38μg/ml palbociclib did not significantly reduce the proportion of $pRb^+$ apical progenitors (DMSO: 2.46±0.52%, 1.5μml: 0.26±0.14%, 0.75μg/ml: 0.63±0.37%, 0.38μg/ml: 0.71±0.37%. DMSO vs. 1.5μg/ml p<0.01, DMSO vs. 0.75μg/ml p>0.05, DMSO vs. 0.38μg/ml p>0.05, n=4 per condition. Kruskal-Wallis test followed by Dunn's post-hoc test) (figure 5.6 A-E, yellow arrows). In the basal progenitor proportion, the Kruskal-Wallis test revealed there was a significant difference between palbociclib and DMSO treatment, yet the Dunn's post-hoc test was unable to identify between which drug treatment group(s) the significance lay probably due to insufficient power. Subsequent power analysis (conducted using G*Power) revealed a power of 0.43, and a sample size of 12 slices per group would have been required to attain a power of >0.80 (DMSO: 0.62±0.31%, 1.5μml: 0.09±0.05%, 0.75μg/ml: 0.16±0.23%, 0.38μg/ml: 0.19±0.14%. DMSO vs. 1.5μg/ml p>0.05, DMSO vs. 0.75μg/ml p>0.05, DMSO vs. 0.38μg/ml p>0.05, n=4 per condition) (figure 5.6 A-D, F, white arrows).

In the medial cortex, 1.5μg/ml and 0.38μg/ml palbociclib significantly reduced the proportion of $pRb^+$ apical progenitors, whilst 0.75μg/ml did not significantly reduce

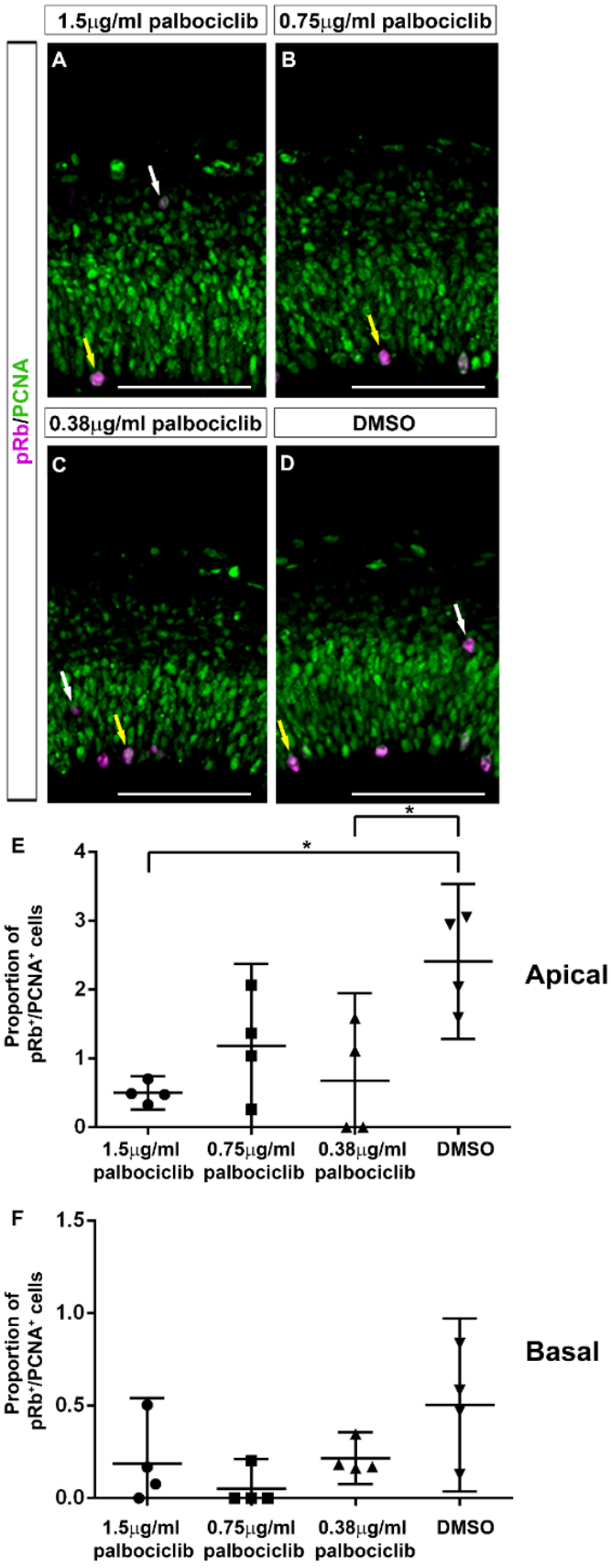
1.5μg/ml palbociclib
0.75μg/ml palbociclib
0.38μg/ml palbociclib
DMSO
A
B
C
D
pRb/PCNA
E
Proportion of pRb+/PCNA+ cells
Apical
1.5μg/ml palbociclib
0.75μg/ml palbociclib
0.38μg/ml palbociclib
DMSO
F
Proportion of pRb+/PCNA+ cells
Basal
1.5μg/ml palbociclib
0.75μg/ml palbociclib
0.38μg/ml palbociclib
DMSO

**Figure 5.7: pRb S780 expression in the medial cortex of E13.5 CD1 organotypic slice cultures after exposure to DMSO or palbociclib. A-D.** pRb/PCNA immunofluorescence on slice cultures of E13.5 cortex from CD1 embryos. Yellow arrows denote apical progenitors, white arrows denote basal progenitors. **E.** In the apical progenitor population, administration of 1.5μg/ml and 0.38μg/ml palbociclib significantly reduced the proportion of $pRb^+$ cells in comparison to DMSO. **F.** In the basal progenitor population, administration of all concentrations of palbociclib did not significantly reduced the proportion of $pRb^+$ cells in comparison to DMSO. All statistical data represents mean ± 95% confidence interval; n=4; * = p<0.05; Kruskal-Wallis test followed by Dunn's post-hoc test. Scale bars = 100μm.

expression (DMSO: 2.41±0.69%, 1.5μml: 0.50±0.15%, 0.75μg/ml: 1.18±0.74%, 0.38μg/ml: 0.67±0.79%. DMSO vs. 1.5μg/ml p<0.05, DMSO vs. 0.75μg/ml p>0.05, DMSO vs. 0.38μg/ml p<0.05, n=4 per condition) (figure 5.7 A-E, yellow arrows). In the medial cortex, no concentration of palbociclib significantly reduced the proportion of $pRb^+$ basal progenitors (DMSO: 0.50±0.29%, 1.5μml: 0.06±0.08%, 0.75μg/ml: 0.05±0.10%, 0.38μg/ml: 0.22±0.09%. DMSO vs. 1.5μg/ml p>0.05, DMSO vs. 0.75μg/ml p>0.05, DMSO vs. 0.38μg/ml p>0.05, n=4 per condition) (figure 5.7 A-D, F, white arrows). Together, palbociclib was able to decrease pRb expression in organotypic cortical slice culture, and so its effect was evaluated in the *Gli3*$^{Xt/Pdn}$ cortex, which showed an increase in pRb expression.

## 5.5 Organotypic slice culture was not conducive to *in vitro Gli3*$^{Xt/Pdn}$ cortical growth

### *5.5.1 E11.5 Gli3*$^{Xt/Pdn}$ *and littermate control slices failed to grow correctly during 24 hrs in vitro*

At E11.5 in the *Gli3*$^{Xt/Pdn}$ lateral cortex, there was a decrease in the proportion of early-born neurons and an increase in apical progenitor proportion, alongside increased cell cycle re-entry. Here, G1-phase length was shorter in the apical progenitor

population alongside an increase in pRb expression, whilst in the basal progenitor population pRb was increased yet G1-phase length was unaltered. *Cdk6* expression was increased in the E10.5 mutant dorsal telencephalon, which could be hypothesised to reduce G1-phase length. Thus the effect of inhibiting the action of Cdk6 and thereby prolonging G1-phase length at this age was evaluated, in order to assess if the reduction in neurogenesis could be rescued.

A concentration of 0.38μg/ml palbociclib was used as it had been shown to decrease pRb expression, and it was very important to prolong G1-phase length whilst not blocking progenitors in G1-phase and causing a failure to progress through the cell cycle. Indeed, the primary use of palbociclib is in breast cancer treatment, where it is used to block tumour cells in G1-phase (DiPippo *et al.*, 2016). To confirm if palbociclib was still able to decrease pRb expression 24 hrs after E11.5 cortical slices had been put into culture, pRb/PCNA expression was evaluated. Telencephalic sections of both control and *Gli3*$^{Xt/Pdn}$ embryos were cultured in the presence of DMSO or 0.38μg/ml palbociclib dissolved in DMSO, with cortical slices from the same embryo used to compare the effects of DMSO and palbociclib.

Under control DMSO conditions, it was apparent that the cortical slices of both control and mutant embryos had failed to grow properly during the 24 hrs in culture. In the control slice shown in figure 5.8 A, whilst most of the midline of the telencephalon has been disrupted, the cortex was still visible at the top of the slice (figure 5.8 A, white arrow). However, the ventricles became filled with tissue which fused in places with the cortical ventricular surface (figure 5.8 A'). Presumably, during culture the slice had flattened and spread outwards, so the ventricular zone either rostral or caudal to the section shown in the figure had fused with that shown. This precluded examination of the slices as it was not clear which cells should be counted. It should also be noted that the images shown in the figures represent the most successful slice cultures. In the *Gli3*$^{Xt/Pdn}$ slices as shown figure 5.8 B, the majority of the midline structures became unidentifiable. It was still possible to identify some cortical tissue, shown on the left of the image, yet clearly growth had been disturbed (figure 5.8 B'). It became difficult to discern a continuous ventricular surface where counting could be conducted.

When cultured in the presence of 0.38μg/ml palbociclib, surprisingly the morphology of the control slice was more recognisable (figure 5.8 C). However, upon closer inspection, the cortex displayed features suggesting growth had been disturbed.

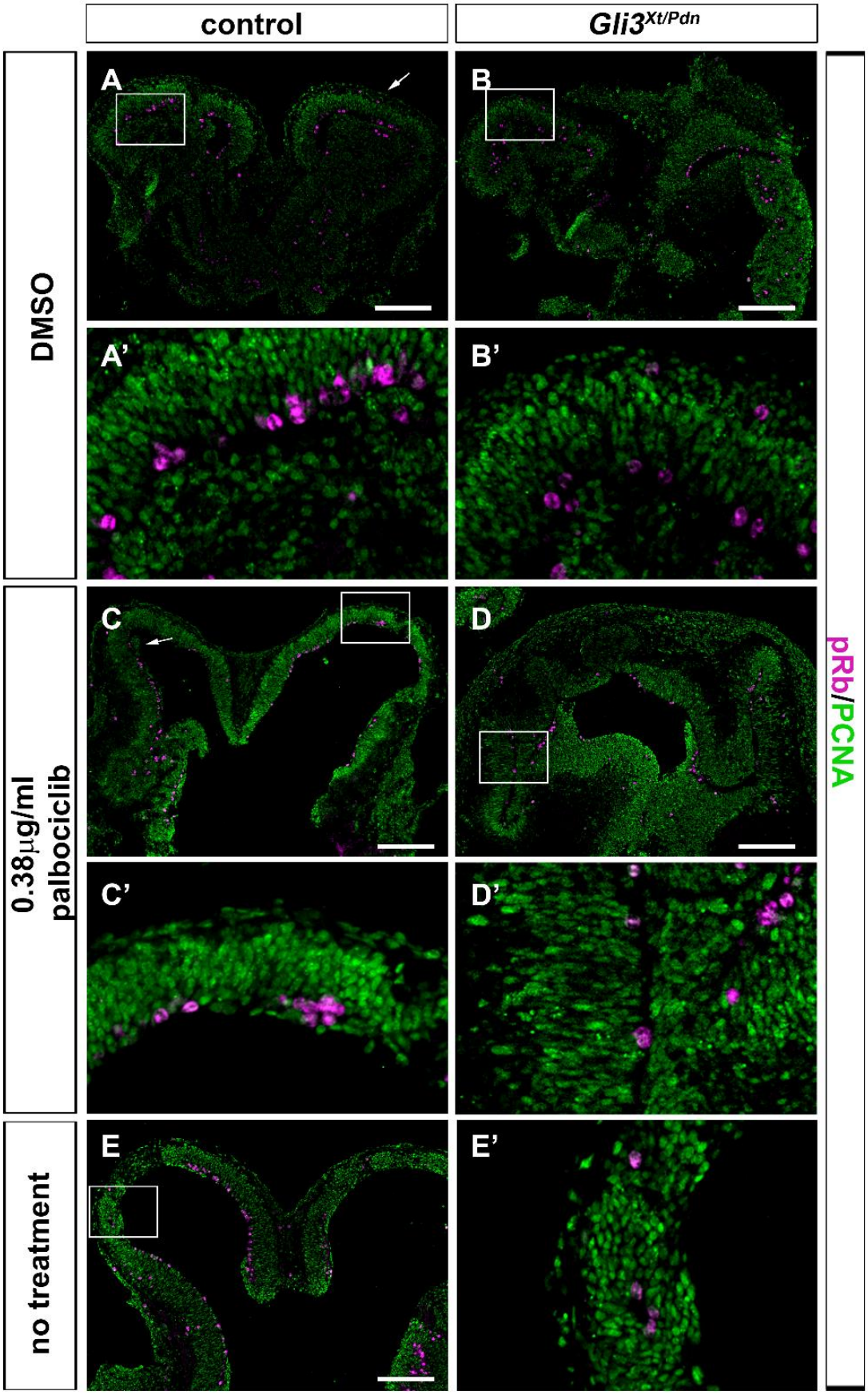
control
Gli3Xt/Pdn
DMSO
0.38µg/ml palbociclib
no treatment
pRb/PCNA
A
B
A'
B'
C
D
C'
D'
E
E'

**Figure 5.8: pRb S780 expression in the cortex of E11.5 control and *Gli3*$^{Xt/Pdn}$ organotypic slice cultures after exposure to DMSO, palbociclib, or neither.** pRb/PCNA immunofluorescence on slice cultures after 24hrs *in vitro*. Boxes in A, B, C, D, E represent area shown in A', B', C', D', E', respectively. **A, A', B, B'.** Control (A, A') and *Gli3*$^{Xt/Pdn}$ (B, B') slices after 24hrs in culture in the presence of DMSO. **C, C', D, D'.** Control (C, C') and *Gli3*$^{Xt/Pdn}$ (D, D') slices after 24hrs in culture in the presence of 0.38μg/ml palbociclib. **E, E'.** Control slice after 24hrs in culture with neither DMSO or palbociclib. Scale bars = 200μm.

There were clumps of cells growing inside the ventricle attached to the ventricular surface (figure 5.8 C, white arrow). pRb$^+$ cells also formed clusters (figure 5.8 C'), instead of lining the ventricle regularly. In the *Gli3*$^{Xt/Pdn}$ slice in the presence of palbociclib, the ventricles had shrunk dramatically in the region of the cortex, so that the presumed ventral and dorsal telencephalon appeared to be in contact (figure 5.8 D') and rosette-like structures formed where the ventricular surface became folded. It therefore became impossible to identify the lateral and medial areas of the cortex.

Collectively, both control and *Gli3*$^{Xt/Pdn}$ cortical slices failed to grow properly in culture when taken at E11.5 and left for 24 hrs, in the presence of either DMSO or palbociclib. The disruption to the cortex meant it was not possible to accurately identify the lateral and medial cortex for counting, and so the effect of palbociclib on pRb expression could not be evaluated.

In order to determine if the presence of DMSO had contributed to the disruption in growth, control cortical slices were cultured without DMSO or palbociclib present (figure 5.8 E). Even when cultured in only supplemented neurobasal medium (table 2.6), growth in the cortex was disturbed. Rosette-like structures formed (figure 5.8 E'), and the regular pattern of pRb$^+$ cells lining the ventricular surface as seen in figure 5.4 was lost. Therefore, at this early stage, the organotypic culture environment was not permissive to the regular growth of the cortex, and so the effect of palbociclib on this stage under these conditions could not be evaluated.

### *5.5.2 E12.5 Gli3$^{Xt/Pdn}$ cortical slices failed to grow properly during 24 hrs in culture*

In the E12.5 *Gli3$^{Xt/Pdn}$* dorsal telencephalon, the proportion of neurons compared to control was increased in both the lateral and medial cortex. This coincided with increased cell cycle exit, indicating progenitor differentiation into neurons. Yet, when the length of G1-phase was measured in the apical progenitor population laterally and the total progenitor population medially, it was reduced in the mutant. Pharmacological G1-phase lengthening has been reported to promote progenitor differentiation (Calegari & Huttner, 2003), and so the effect of artificially lengthening G1-phase in the E12.5 cortex was assessed. E12.5 embryos were harvested and cultured as above for 24 hrs in the presence of either DMSO or 0.38μg/ml palbociclib in DMSO. Control and *Gli3$^{Xt/Pdn}$* littermate embryos were used, with one slice from each embryo being exposed to DMSO and another slice from the same embryo being exposed to palbociclib. As before, pRb expression was used as a measure of Cdk6 activity to assess the effect of the palbociclib.

When slices from control embryos were exposed to DMSO, the structure of the telencephalon remained recognisable (figure 5.9 A). However as with E11.5 slices, rosette-like structures formed albeit to a lesser extent (figure 5.9 A'), and the normally continuous expression of pRb along the ventricular surface was disrupted. In the mutant, the overall structure of the dorsal and ventral telencephalon was again recognisable, but upon closer inspection the cortex displayed severe growth problems. The cortex and LGE/MGE fused at one point (figure 5.9 B'), and the ventricle appeared to become compartmentalised to form multiple smaller ventricles (figure 5.9 B, arrows). The expression of pRb along the ventricular surface was also disrupted, and it was not possible to distinguish where the lateral and medial cortex lay for comparison.

In the presence of palbociclib, slices from control embryos remained identifiable in terms of the dorsal and ventral telencephalon (figure 5.9 C). However, as when exposed to DMSO only, rosettes formed in the cortex and the expression of pRb along the ventricular surface was discontinuous (figure 5.9 C'). In the example slice shown in figure 5.9 C, there was a huge expansion of PCNA$^{+}$ cells basal to the ventricular zone (figure 5.9 C, arrow). Clearly, growth of the cortex was disturbed here. When *Gli3$^{Xt/Pdn}$* slices were exposed to palbociclib, the cortex became thinner (figure 5.9 D). In some areas, the ventricular surface appeared to have split forming two layers of

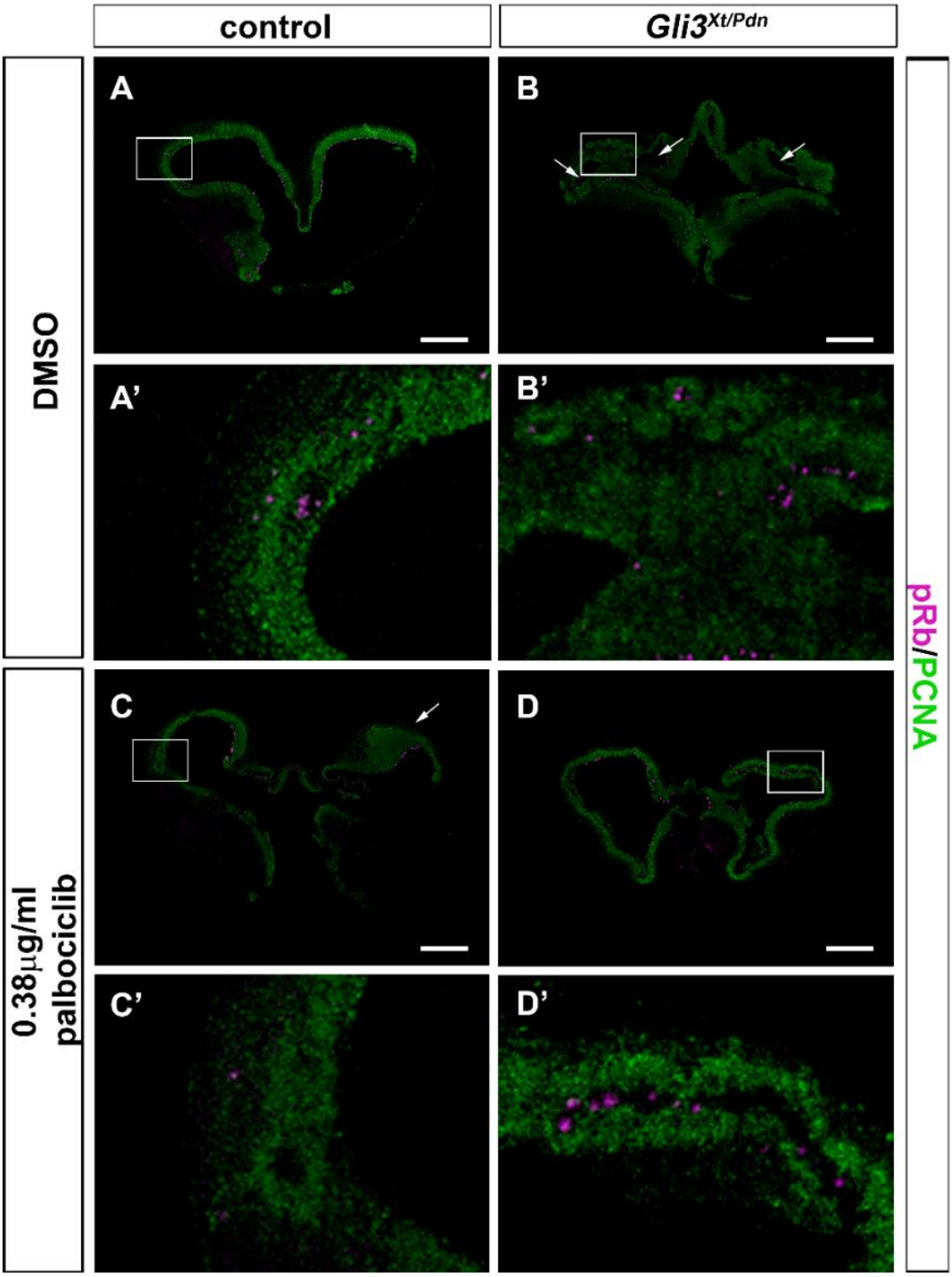
control
Gli3Xt/Pdn
DMSO
0.38μg/ml palbociclib
A
B
A'
B'
C
D
C'
D'
pRb/PCNA

**Figure 5.9: pRb S780 expression in the cortex of E12.5 control and *Gli3*$^{Xt/Pdn}$ organotypic slice cultures after exposure to DMSO or palbociclib.** pRb/PCNA immunofluorescence on slice cultures after 24hrs *in vitro*. Boxes in A, B, C, D represent area shown in A', B', C', D', respectively. **A, A', B, B'.** Control (A, A') and *Gli3*$^{Xt/Pdn}$ (B, B') slices after 24hrs in culture in the presence of DMSO. **C, C', D, D'.** Control (C, C') and *Gli3*$^{Xt/Pdn}$ (D, D') slices after 24hrs in culture in the presence of 0.38μg/ml palbociclib. Scale bars = 250μm.

proliferative cells with pRb$^+$ cells in the middle. This splitting/duplication of the ventricular zone is likely due to flattening of the slice during the culture (figure 5.9 D').

In summary, as with E11.5 slices, at E12.5 slices showed marked disturbance in their growth after 24 hrs of culture. The expression pattern of pRb along the ventricular surface was altered and the formation of rosette-like structures meant a reliable proportion of pRb$^+$/PCNA$^+$ cells could not be calculated. The position of the medial and lateral cortex was also unclear, particularly in the mutant slice exposed to DMSO.

### *5.5.3 At E13.5, growth of Gli3*$^{Xt/Pdn}$ *cortical slices in vitro was defective*

Slice cultures of E13.5 CD1 telencephalon were successful in the presence of either DMSO or palbociclib. In contrast, the uncoordinated growth of E11.5 and E12.5 *Gli3*$^{Xt/Pdn}$ and littermate control slices in culture precluded analysis of the effect of palbociclib. Potentially, the earlier ages were not conducive to this culture technique, or differences between the *Gli3*$^{Xt/Pdn}$ background and CD1 embryos resulted in the ability to study pRb expression in one circumstance but not the other. Therefore, I harvested E13.5 *Gli3*$^{Xt/Pdn}$ and control embryos and cultured cortical slices from them as I did with E13.5 CD1 embryos.

Control cortical slices cultured in the presence of DMSO retained the morphology of the dorsal and ventral telencephalon (figure 5.10 A), although occasionally there was growth of additional cortical-like tissue in the ventricles (figure 5.10 A, arrow). However, importantly, the positioning of pRb$^+$ and PCNA$^+$ progenitors within the cortex replicated that of CD1 embryos in culture and of control embryos that had not been cultured (figure 5.10 A'). As with control slices, it was easier to recognise the

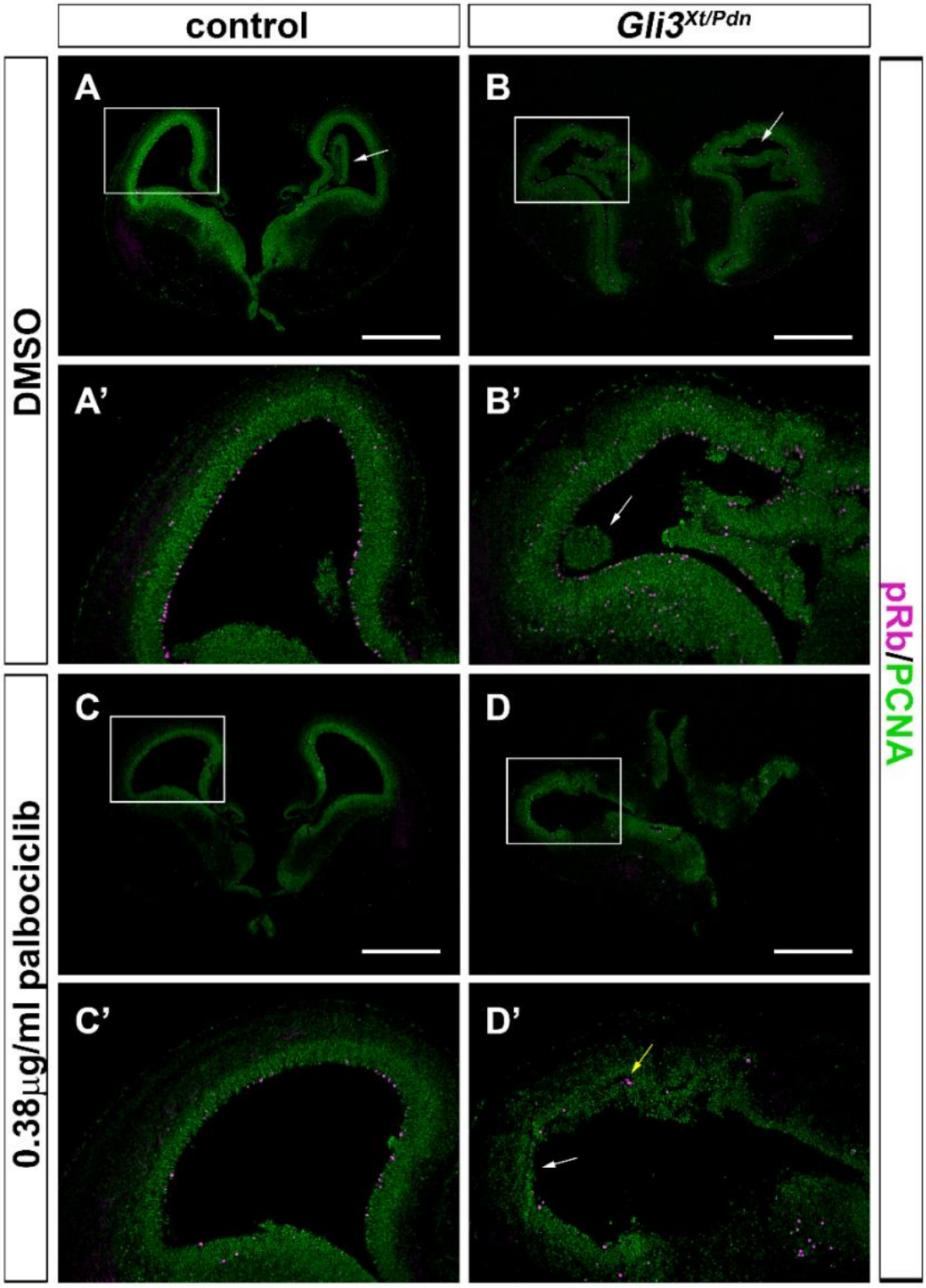
control
Gli3Xt/Pdn
DMSO
0.38µg/ml palbociclib
A
B
A'
B'
C
D
C'
D'
pRb/PCNA

**Figure 5.10: pRb S780 expression in the cortex of E13.5 control and *Gli3*$^{Xt/Pdn}$ organotypic slice cultures after exposure to DMSO or palbociclib.** pRb/PCNA immunofluorescence on slice cultures after 24hrs *in vitro*. Boxes in A, B, C, D represent area shown in A', B', C', D', respectively. **A, A', B, B'.** Control (A, A') and *Gli3*$^{Xt/Pdn}$ (B, B') slices after 24hrs in culture in the presence of DMSO. **C, C', D, D'.** Control (C, C') and *Gli3*$^{Xt/Pdn}$ (D, D') slices after 24hrs in culture in the presence of 0.38μg/ml palbociclib. Scale bars = 500μm.

morphology of *Gli3*$^{Xt/Pdn}$ slices put into culture at E13.5 with DMSO. Nevertheless, there was some compartmentalisation of the ventricle (figure 5.10 B, arrow), and some additional tissue growing inside the ventricle (figure 5.10 B', arrow). The expression pattern of pRb and PCNA appeared mostly normal except where the additional tissue was present in the ventricle.

When palbociclib was added to the cultures, control cortical slices retained the shape of a conventional coronal slice (figure 5.10 C). Again, as with DMSO alone, the expression pattern of pRb and PCNA was as in CD1 embryos, revealing that control slices obtained from a *Gli3*$^{Xt/Pdn}$ litter behaved in culture as the CD1 slices did (figure 5.10 C'). The *Gli3*$^{Xt/Pdn}$ mutant slices retained approximately the correct shape at the whole telencephalon level (figure 5.10 D), however upon closer inspection there was disruption to the positioning of cells (figure 5.10 D'). Expression of pRb along the ventricular surface was reduced (figure 5.10 D', white arrow) and the ventricular zone appeared to have split (figure 5.10 D', yellow arrow). As such, it was not possible to accurately count the proportion of pRb$^{+}$ cells, and so I was unable to determine the effect of palbociclib on *Gli3*$^{Xt/Pdn}$ slices *in vitro*, using this methodology.

## 5.6 Tis21;GFP expression revealed the proportion of apical and basal progenitors undergoing differentiative division in the *Gli3$^{Xt/Pdn}$* mutant

As described in chapter 4, the reduction in *Gli3* in the *Gli3$^{Xt/Pdn}$* mutant resulted in a reduction in S-phase length at E11.5 and E12.5, in both apical and basal progenitors. However, unlike G1-phase length, the microarray analysis did not reveal any obvious candidate genes which might have resulted in *Gli3's* regulation over S-phase length. Arai *et al.* (2011) revealed that in the murine neocortex, S-phase shortening occurs when progenitors being to undergo differentiative division. It is possible that the reduction in S-phase length in the *Gli3$^{Xt/Pdn}$* mutant did not reflect a shortening of S-phase, but a larger proportion of cells undergoing differentiative division, and thus going through a shorter S-phase. Overall, the reduction in S-phase length measured may have reflected an increased proportion of differentiative divisions in the mutant, indicating no regulation of S-phase length by *Gli3*.

To investigate this possibly, *Gli3$^{Xt/Pdn}$;Tis21GFP* embryos were utilised. *Tis21* mRNA is up-regulated during G1-phase in progenitors that will undergo a differentiative division (Iacopetti *et al.*, 1999). Apical progenitors will produce either basal progenitors or neurons, whereas basal progenitors will produce neurons. *Gli3$^{Xt/+}$* mice were crossbred with *Tis21*-GFP reporter mice, where GFP expression is under the control of the *Tis21* promoter (Haubensak *et al.*, 2004). GFP expression thus identified progenitors about to undergo differentiative division. As can be seen in figure 5.11 A, B, the morphology of the E11.5 *Gli3$^{+/+}$* telencephalon, used as control in preceding experiments, was very similar to that of the *Gli3$^{+/+}$;Tis21GFP*, used as control in following experiments, respectively. The gross morphology of E11.5 *Gli3$^{Xt/Pdn}$* telencephalon was slightly different from that of *Gli3$^{Xt/Pdn}$;Tis21GFP* embryos (figure 5.11 C, D, respectively). I therefore examined Pax6 (figure 5.12 B, D) and Tbr2 (figure 5.13 B, D) expression in the cortex of these embryos, and both appeared to be unaffected. So, the proportions of proliferative and differentiative progenitors of these embryos were calculated.

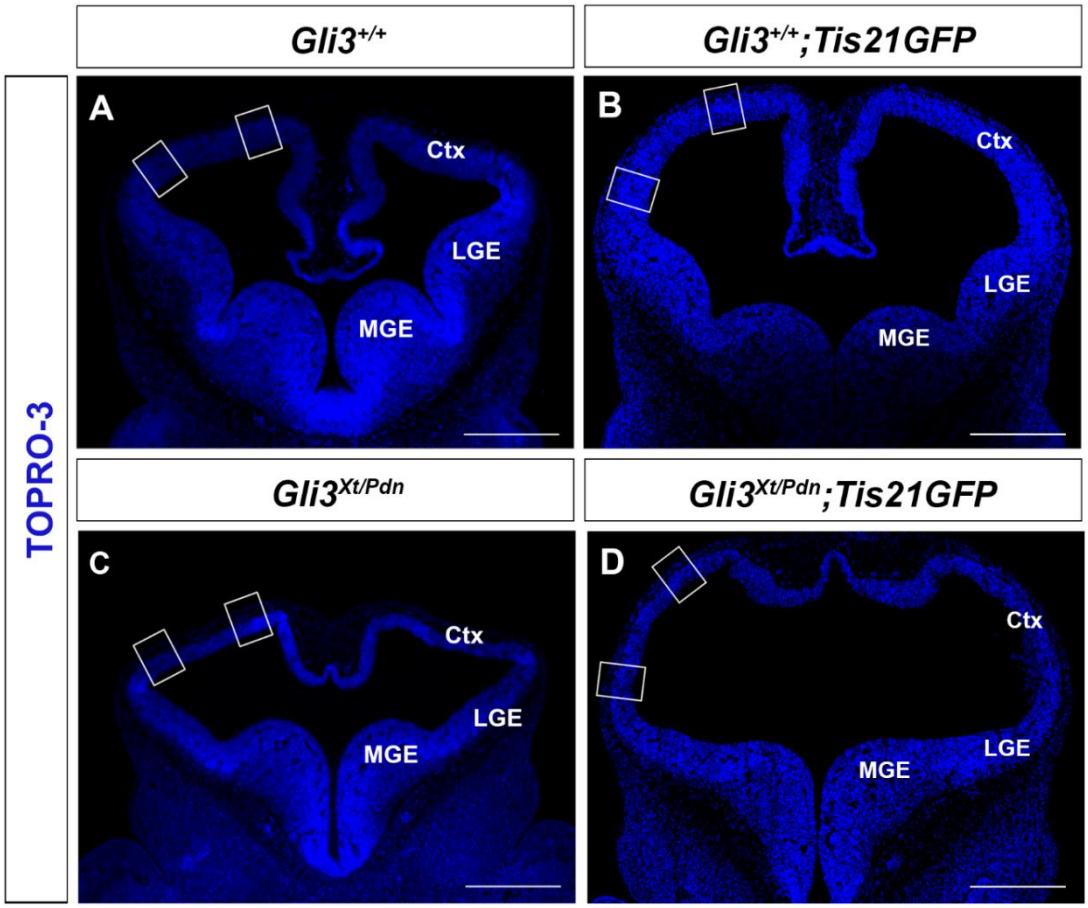


**Figure 5.11: Coronal sections of E11.5 *Gli3*$^{+/+}$, *Gli3*$^{+/+}$*;Tis21GFP*, *Gli3*$^{Xt/Pdn}$ and *Gli3*$^{Xt/Pdn}$*;Tis21GFP* telencephalons.** Boxes overlaid on the lateral and medial cortex indicate the areas used for counting. TOPRO-3 staining was used to identify all nuclei to give a representation of telencephalon morphology. **A, B.** Comparison between control telencephalon (A) used in chapters 3 and 4 and sections 5.2, 5.3 and 5.5, with the control telencephalon of embryos crossed with the *Tis21*-GFP reporter line used in section 5.6. **C, D.** Comparison between *Gli3*$^{Xt/Pdn}$ telencephalon (C) used in chapters 3 and 4 and sections 5.2, 5.3 and 5.5, with the *Gli3*$^{Xt/Pdn}$*;Tis21GFP* telencephalon of embryos crossed with the *Tis21*-GFP reporter line used in section 5.6. Scale bars = 500μm.

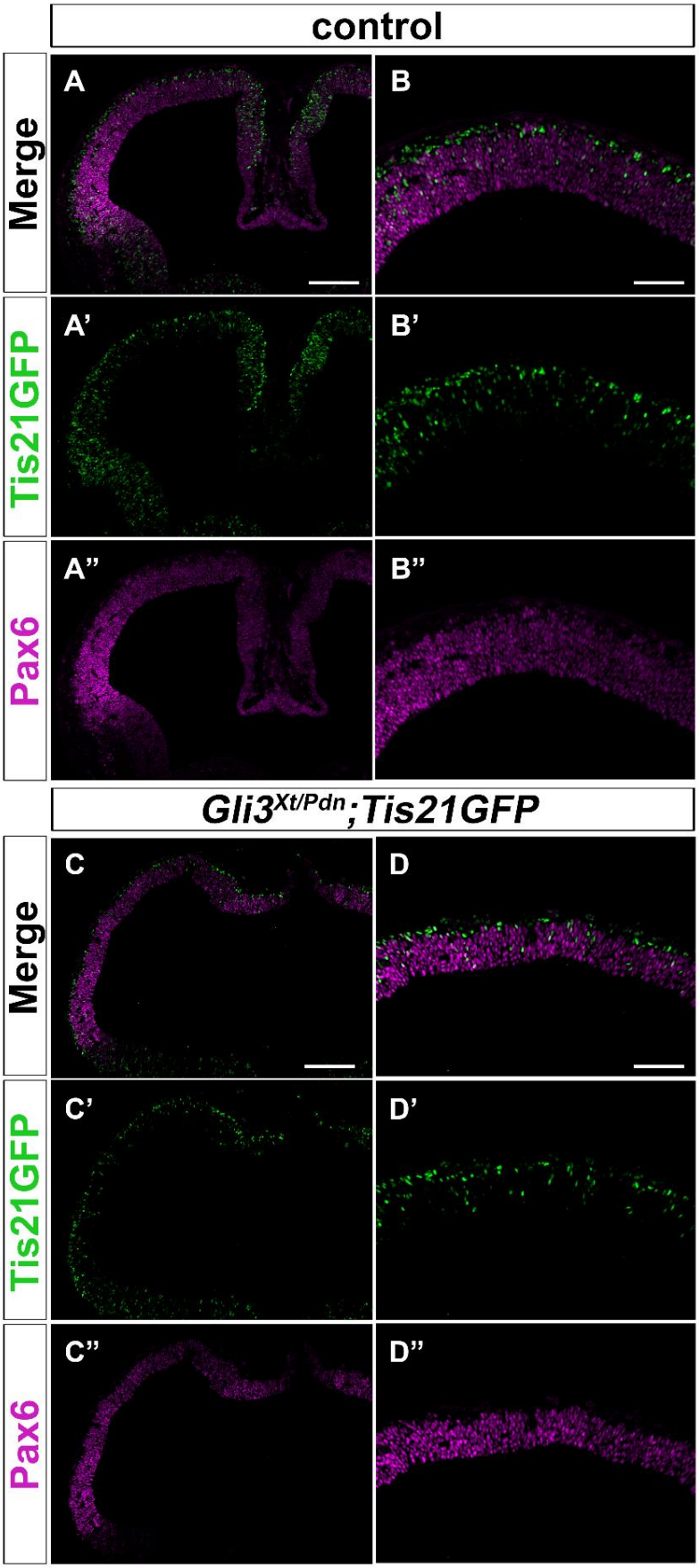
control
Merge
Tis21GFP
Pax6
A
B
A'
B'
A"
B"
Gli3Xt/Pdn;Tis21GFP
Merge
Tis21GFP
Pax6
C
D
C'
D'
C"
D"

**Figure 5.12: Pax6/*Tis21*-GFP immunofluorescence on E11.5 coronal sections of control and *Gli3*$^{Xt/Pdn}$*;Tis21GFP* embryos highlighting differentiative apical progenitors. A, B, C, D.** Merged images showing the overlap between Pax6 and *Tis21*-GFP expression in control (A, B) and mutant (C, D) embryos. **A', B', C', D'.** *Tis21*-GFP expression in control (A', B') and mutant (C', D') embryos. **A", B", C", D".** Pax6 expression in control (A", B") and mutant (C", D") embryos. Scale bars = 100μm (A, C), 200μm (B, D).

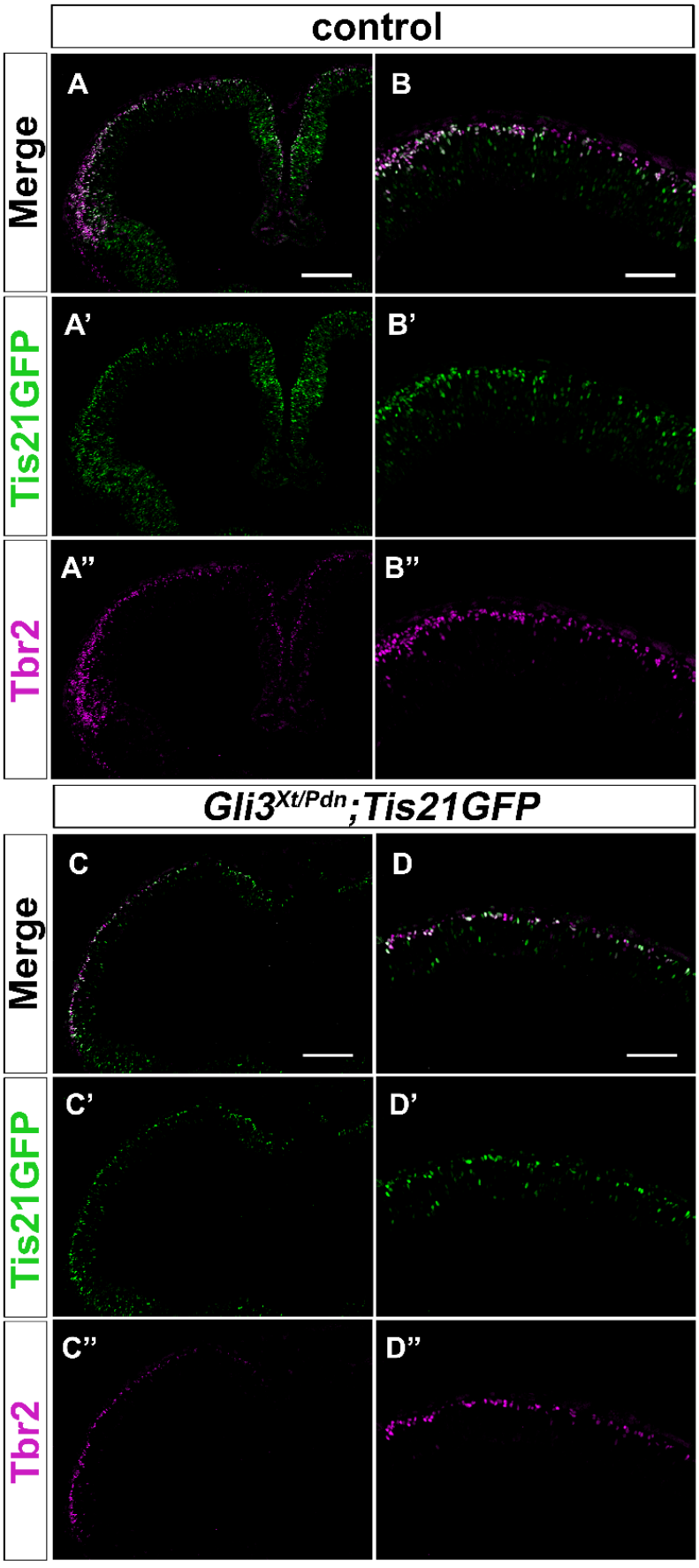
control
Merge
Tis21GFP
Tbr2
A
B
A'
B'
A''
B''
Gli3Xt/Pdn;Tis21GFP
Merge
Tis21GFP
Tbr2
C
D
C'
D'
C''
D''

**Figure 5.13: Tbr2/*Tis21*-GFP immunofluorescence on E11.5 coronal sections of control and *Gli3$^{Xt/Pdn}$;Tis21GFP* embryos highlighting differentiative basal progenitors. A, B, C, D.** Merged images showing the overlap between Tbr2 and *Tis21*-GFP expression in control (A, B) and mutant (C, D) embryos. **A', B', C', D'.** *Tis21*-GFP expression in control (A', B') and mutant (C', D') embryos. **A", B", C", D".** Tbr2 expression in control (A", B") and mutant (C", D") embryos. Scale bars = 100μm (A, C), 200μm (B, D).

### *5.6.1 Apical progenitor differentiation was decreased in the E11.5 medial Gli3$^{Xt/Pdn}$;Tis21GFP cortex, yet it was increased in the E12.5 lateral and medial mutant cortex*

To begin, the proportion of apical progenitors undergoing differentiative division was calculated by dividing the number of *Tis21*-GFP$^+$/Pax6$^+$ double-positive cells against the total number of Pax6$^+$ cells. Conversely, the proportion of *Tis21*-GFP$^-$/Pax6$^+$ cells against the total Pax6$^+$ population gave the proliferative apical progenitor proportion. As before, this proportion was calculated in both E11.5 and E12.5 control and mutant embryos, in the lateral and medial cortex separately.

In the lateral cortex, there was no significant difference in the proportion of differentiative divisions in the E11.5 *Gli3$^{Xt/Pdn}$;Tis21GFP* cortex compared to control (36.43±1.65% in control and 32.14±7.80% in mutant, n=4, p>0.05) (figure 5.14 A, B, E). Consequently, there was also no significant difference in the proportion of proliferative apical progenitors (63.57±1.65% in control and 67.86±7.80% in mutant, n=4, p>0.05) (figure 5.14 A, B, F). However, there was large variance amongst the mutant embryos, with one embryo potentially being anomalous. It would be advantageous to increase the number of embryos examined to determine if the tendency of the other three embryos to display decreased differentiation accurately represented *Tis21* expression in these embryos. Furthermore, the increased proportion of apical progenitors and decreased basal progenitors and neurons, as well as increased cell cycle re-entry would indicate an increase in apical progenitor proliferation at the expense of differentiation. However, in the medial cortex, the proportion of differentiative apical progenitors was significantly decreased in the mutant compared to control (40.98±1.86% in control and 29.43±6.28% in mutant, n=4,

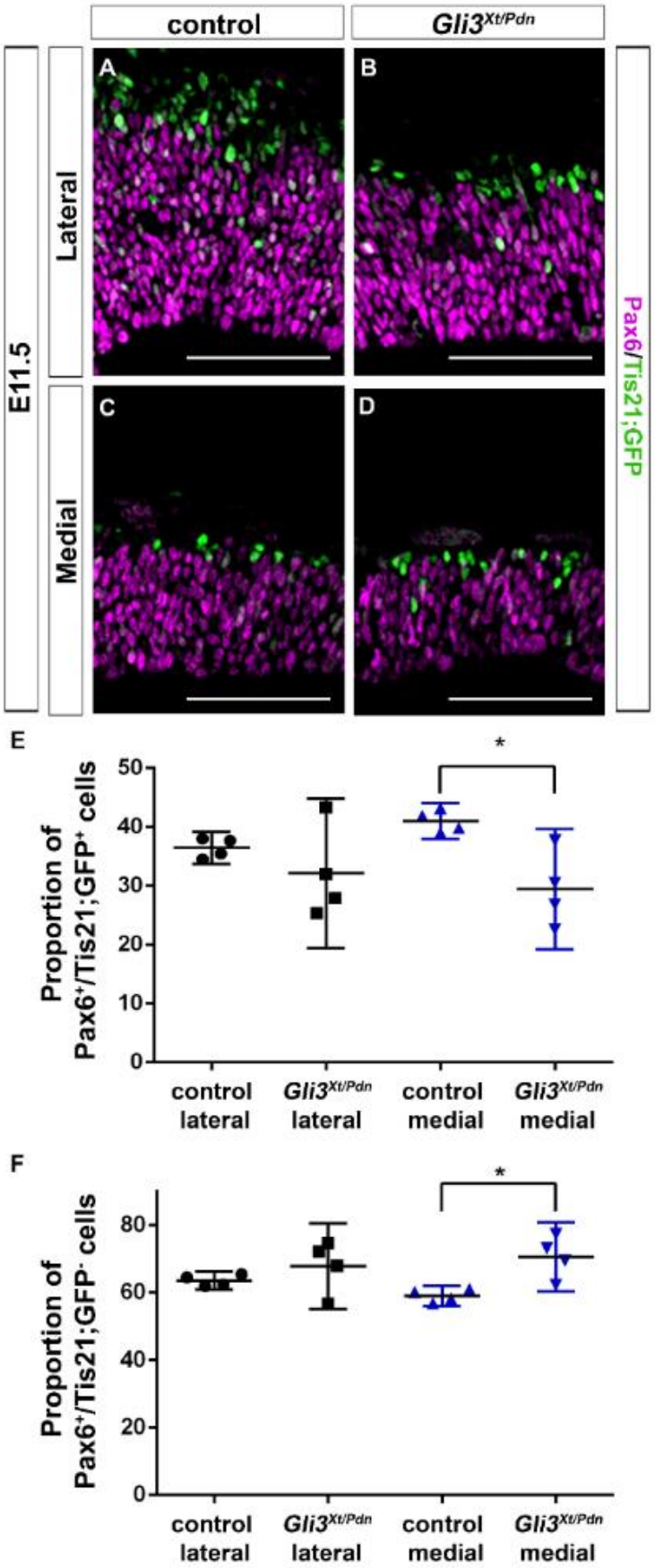
control
Gli3Xt/Pdn
A
B
C
D
E11.5
Lateral
Medial
Pax6/Tis21;GFP
E
Proportion of Pax6+/Tis21;GFP+ cells
50
40
30
20
10
0
*
control lateral
Gli3Xt/Pdn lateral
control medial
Gli3Xt/Pdn medial
F
Proportion of Pax6+/Tis21;GFP- cells
80
60
40
20
0
*
control lateral
Gli3Xt/Pdn lateral
control medial
Gli3Xt/Pdn medial

**Figure 5.14: The proportion of differentiative apical progenitors was decreased in the medial E11.5 cortex. A-D.** Pax6/*Tis21*-GFP immunofluorescence on sections of E11.5 cortex from control and *Gli3*$^{Xt/Pdn}$*;Tis21GFP* embryos. **E.** The proportion of Pax6$^{+}$/*Tis21*-GFP$^{+}$ differentiative apical progenitors showed a tendency to be decreased in the mutant compared to control in the lateral cortex, note the large variance in mutant embryos. The proportion of Pax6$^{+}$/*Tis21*-GFP$^{+}$ differentiative apical progenitors was significantly decreased in the mutant compared to control in the medial cortex. **F.** The proportion of Pax6$^{+}$/*Tis21*-GFP$^{-}$ proliferative apical progenitors showed a tendency to be increased in the mutant compared to control in the lateral cortex. The proportion of Pax6$^{+}$/*Tis21*-GFP$^{-}$ proliferative apical progenitors was significantly increased in the mutant compared to control in the medial cortex. All statistical data represents mean ± 95% confidence interval; n=4; * = p<0.05; Mann-Whitney U-test. Scale bars = 100μm.

p<0.05) (figure 5.14 C, D, E), whilst the proportion of proliferative apical progenitors was significantly increased (59.02±1.86% in control and 70.57±6.28% in mutant, n=4, p<0.05) (figure 5.14 C, D, F). Here, the proportions of apical and basal progenitors and neurons and cell cycle re-entry/exit were unaltered, but may precede changes at E12.5.

At E12.5, in the lateral cortex there was a significant increase in apical progenitors undergoing differentiative division in the mutant (41.25±1.53% in control and 58.54±5.27% in mutant, n=4, p<0.05) (figure 5.15 A, B, E). Simultaneously, the proportion of mutant apical progenitors undergoing proliferative division was decreased (58.75±1.53% in control and 41.46±5.27% in mutant, n=4, p<0.05) (figure 5.15 A, B, F). Likewise, in the medial mutant cortex, the proportion of differentiative apical progenitors was increased (36.36±1.47% in control and 45.82±6.69% in mutant, n=4, p<0.05) (figure 5.15 A, B, E), whilst the proportion of proliferative apical progenitors was decreased (63.63±1.47% in control and 54.18±6.69% in mutant, n=4, p<0.05) (figure 5.15 A, B, F).

Taken together, a change in the proportion of apical progenitors undergoing differentiative division would not account for the difference in S-phase length at E11.5. S-phase length was significantly shorter in the lateral mutant cortex yet the proportion

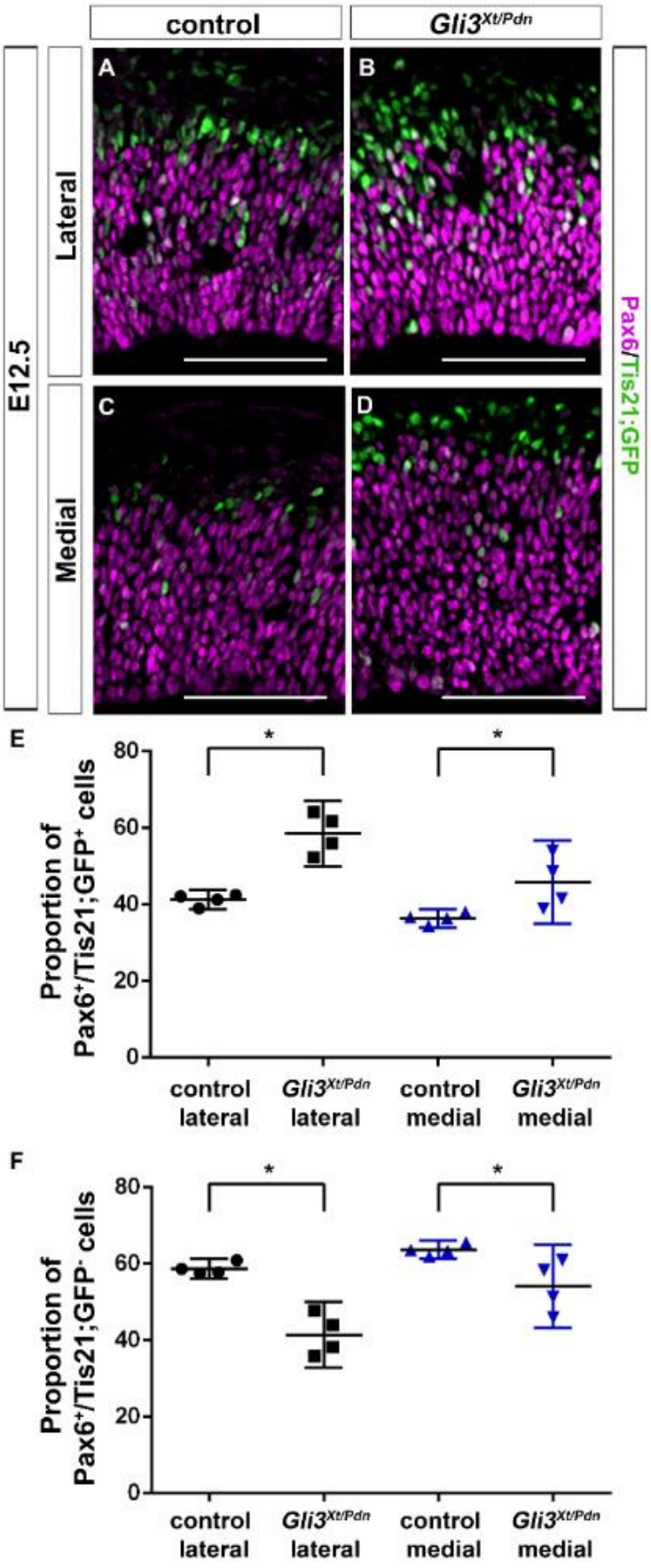
control
Gli3Xt/Pdn
E12.5
Lateral
Medial
A
B
C
D
Pax6/Tis21;GFP
E
Proportion of Pax6+/Tis21;GFP+ cells
0
20
40
60
80
*
*
control lateral
Gli3Xt/Pdn lateral
control medial
Gli3Xt/Pdn medial
F
Proportion of Pax6+/Tis21;GFP- cells
0
20
40
60
80
*
*
control lateral
Gli3Xt/Pdn lateral
control medial
Gli3Xt/Pdn medial

**Figure 5.15: The proportion of differentiative apical progenitors was increased in the E12.5 cortex. A-D.** Pax6/*Tis21*-GFP immunofluorescence on sections of E12.5 cortex from control and *Gli3*$^{Xt/Pdn}$*;Tis21GFP* embryos. **E.** The proportion of Pax6$^{+}$/*Tis21*-GFP$^{+}$ differentiative apical progenitors was significantly increased in the mutant compared to control in the lateral cortex. The proportion of Pax6$^{+}$/*Tis21*-GFP$^{+}$ differentiative apical progenitors was significantly increased in the mutant compared to control in the medial cortex. **F.** The proportion of Pax6$^{+}$/*Tis21*-GFP$^{-}$ proliferative apical progenitors was significantly decreased in the mutant compared to control in the lateral cortex. The proportion of Pax6$^{+}$/*Tis21*-GFP$^{-}$ proliferative apical progenitors was significantly decreased in the mutant compared to control in the medial cortex. All statistical data represents mean ± 95% confidence interval; n=4; * = p<0.05; Mann-Whitney U-test. Scale bars = 100μm.

of differentiative divisions was unaltered, whilst in the medial cortex S-phase length was unaltered in the mutant, yet there was a decrease in differentiative divisions. By E12.5, S-phase length was reduced in the mutant both laterally and medially, and the proportion of apical progenitors undergoing differentiative division was increased. Therefore, at this age, as S-phase length gets shorter in the switch from proliferative to differentiative division, the larger mutant proportion of apical progenitors undergoing differentiative division may account for the reduction measured in S-phase length.

### *5.6.2 Basal progenitor differentiation was increased in the E11.5 lateral Gli3$^{Xt/Pdn}$;Tis21GFP cortex, yet it was unchanged in the E12.5 mutant cortex*

The length of S-phase was decreased in the *Gli3*$^{Xt/Pdn}$ lateral cortex at E11.5, whilst it was not possible to measure S-phase length in the medial cortex. As with the apical progenitor population, the proportion of basal progenitors undergoing differentiative division was also calculated by combining *Tis21*-GFP expression with Tbr2 expression. This was carried out at both E11.5 and E12.5 in the lateral and medial cortex.

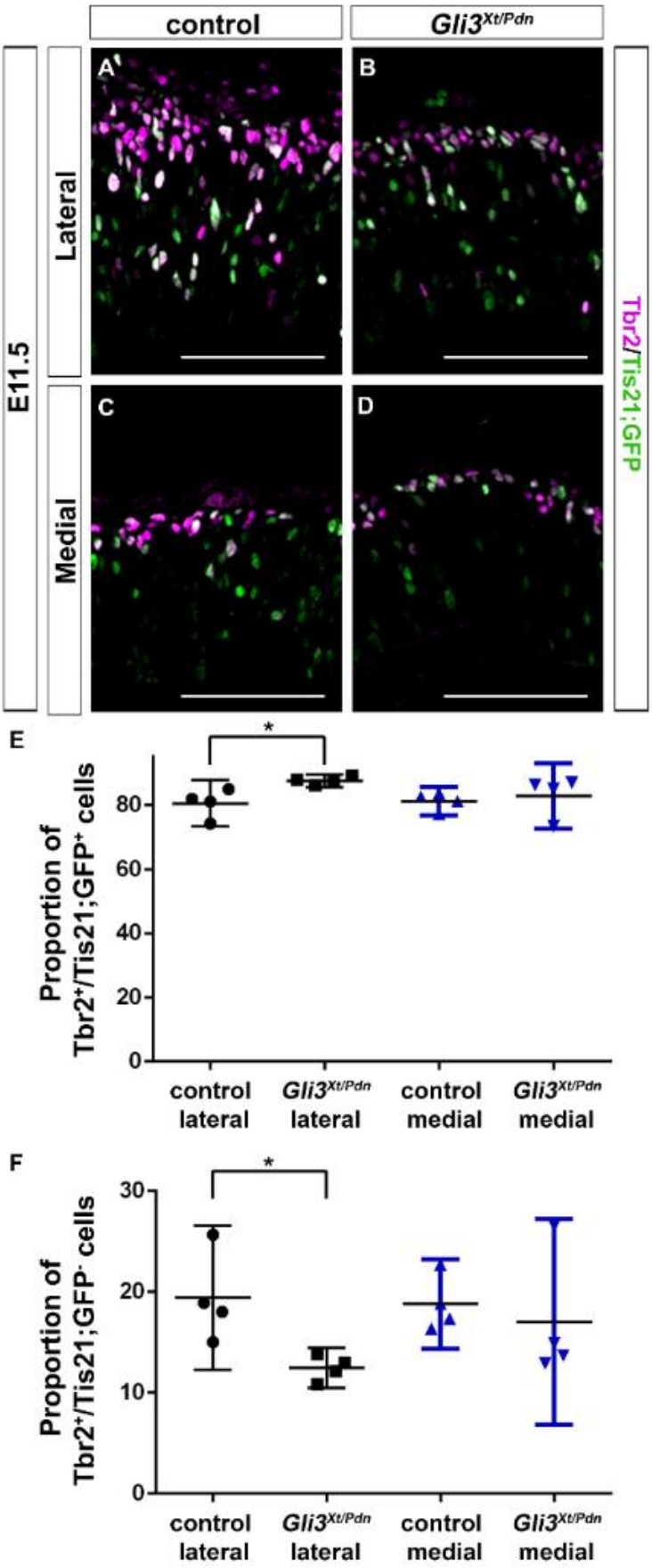
control
Gli3Xt/Pdn
E11.5
Lateral
Medial
A
B
C
D
Tbr2/Tis21;GFP
E
Proportion of Tbr2+/Tis21;GFP+ cells
0
20
40
60
80
*
control lateral
Gli3Xt/Pdn lateral
control medial
Gli3Xt/Pdn medial
F
Proportion of Tbr2+/Tis21;GFP- cells
0
10
20
30
*
control lateral
Gli3Xt/Pdn lateral
control medial
Gli3Xt/Pdn medial

**Figure 5.16: The proportion of differentiative basal progenitors was increased in the lateral E11.5 cortex. A-D.** Tbr2/*Tis21*-GFP immunofluorescence on sections of E11.5 cortex from control and *Gli3*$^{Xt/Pdn}$*;Tis21GFP* embryos. **E.** The proportion of Tbr2$^{+}$/*Tis21*-GFP$^{+}$ differentiative basal progenitors was significantly increased in the mutant compared to control in the lateral cortex. The proportion of Tbr2$^{+}$/*Tis21*-GFP$^{+}$ differentiative basal progenitors was unaltered in the mutant compared to control in the medial cortex. **F.** The proportion of Tbr2$^{+}$/*Tis21*-GFP$^{-}$ proliferative basal progenitors was significantly decreased in the mutant compared to control in the lateral cortex. The proportion of Tbr2$^{+}$/*Tis21*-GFP$^{-}$ proliferative basal progenitors was unaltered in the mutant compared to control in the medial cortex. All statistical data represents mean ± 95% confidence interval; n=4; * = $p<0.05$; Mann-Whitney U-test. Scale bars = 100μm.

Unlike in the lateral apical progenitor population where there was no difference in differentiative division, the proportion of basal progenitors undergoing differentiative division was increased in the mutant at E11.5 (80.58±4.40% in control and 87.54±1.23% in mutant, n=4, $p<0.05$) (figure 5.16 A, B, E). Likewise, the proportion of basal progenitors undergoing proliferative division was decreased (19.42±4.40% in control and 12.64±1.23% in mutant, n=4, $p<0.05$) (figure 5.16 A, B, F). In the medial cortex, the proportion of differentiative basal progenitors was unaltered in the mutant (81.18±2.74% in control and 82.96±6.29% in mutant, n=4, $p>0.05$) (figure 5.16 C, D, E), as was the proportion of proliferative basal progenitors (18.82±2.74% in control and 17.04±6.29% in mutant, n=4, $p>0.05$) (figure 5.16 C, D, F).

By E12.5, in the lateral cortex there was no difference in basal progenitor differentiative division in the mutant (90.18±3.01% in control and 91.50±1.82% in mutant, n=4, $p>0.05$) (figure 5.17 A, B, E) or basal progenitor proliferative division (9.82±3.01% in control and 8.50±1.82% in mutant, n=4, $p>0.05$) (figure 5.17 A, B, F). Similarly, in the medial cortex, there was no change in basal progenitor differentiative division in the mutant compared to control (87.61±2.87% in control and 89.59±2.63% in mutant, n=4, $p>0.05$) (figure 5.17 C, D, E) or in the proportion of proliferative divisions (12.39±2.87% in control and 10.41±2.63% in mutant, n=4, $p>0.05$) (figure 5.17 C, D, F).

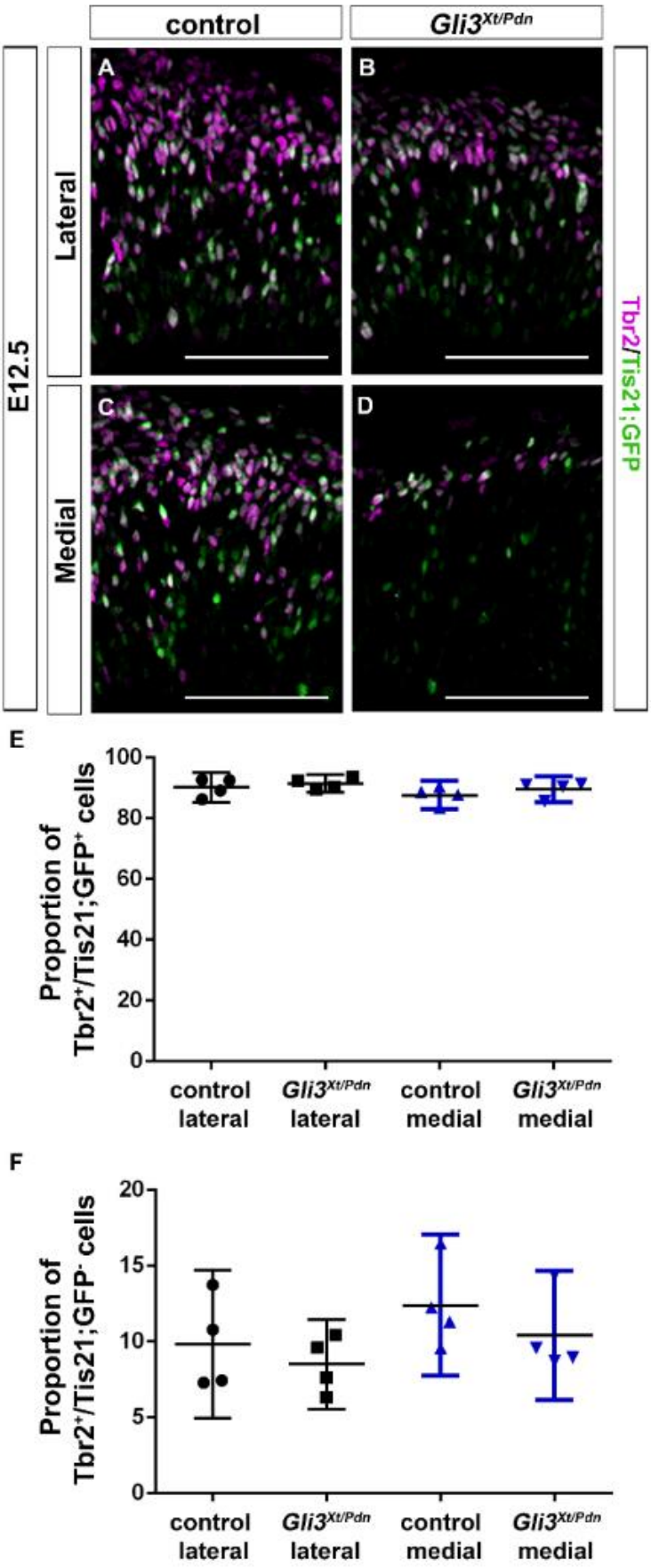
control
Gli3Xt/Pdn
E12.5
Lateral
Medial
A
B
C
D
Tbr2/Tis21;GFP
E
Proportion of Tbr2+/Tis21;GFP+ cells
100
80
60
40
20
0
control lateral
Gli3Xt/Pdn lateral
control medial
Gli3Xt/Pdn medial
F
Proportion of Tbr2+/Tis21;GFP- cells
20
15
10
5
0
control lateral
Gli3Xt/Pdn lateral
control medial
Gli3Xt/Pdn medial

**Figure 5.17: The proportion of differentiative basal progenitors was unaltered in the E12.5 cortex. A-D.** Tbr2/*Tis21*-GFP immunofluorescence on sections of E12.5 cortex from control and *Gli3*$^{Xt/Pdn}$*;Tis21GFP* embryos. **E.** The proportion of Tbr2$^{+}$/*Tis21*-GFP$^{+}$ differentiative basal progenitors was unaltered in the mutant compared to control in the lateral and medial cortex. **F.** The proportion of Tbr2$^{+}$/*Tis21*-GFP$^{-}$ proliferative basal progenitors was unaltered in the mutant compared to control in the lateral and medial cortex. All statistical data represents mean ± 95% confidence interval; n=4; * = $p<0.05$; Mann-Whitney U-test. Scale bars = 100μm.

Although I was unable to measure S-phase length of basal progenitors in the medial E11.5 cortex, in the lateral E11.5 cortex S-phase length was shorter in the mutant. Here, there was an increase in the proportion of basal progenitors undergoing differentiative division, which may account for the difference in S-phase length. By E12.5, S-phase length was no longer altered in mutant basal progenitors compared to control, and the proportion of differentiative divisions was also unaltered.

## 5.7 Discussion

In this chapter, I began to look at the mechanisms by which *Gli3* may regulate the cell cycle, contributing to a defect in early neurogenesis. In *Gli3*$^{Xt/Pdn}$ embryos, at E11.5 and E12.5 G1-phase length is shorter, and microarray analysis revealed that in the E10.5 mutant dorsal telencephalon *Cdk6* was up-regulated. This coincided with an increase in pRb expression at E11.5 and E12.5. In CD1 mouse embryos, it was possible to use the Cdk4/6 specific inhibitor palbociclib in organotypic slice culture to decrease pRb expression. Thus, *Gli3*$^{Xt/Pdn}$ cortical slices were exposed to palbociclib to see if the increase in pRb expression and the delay in neurogenesis could be rescued. However, the mutant cortical slices failed to grow properly under these slice culture conditions, and so it was not possible to evaluate if palbociclib could have rescued the neurogenesis defect. S-phase length was also found to be shorter at E11.5 and E12.5 in the mutant, yet no candidate genes underlying this defect were identified in the microarray analysis. A possible explanation for the shortening of S-phase was an increase in the proportion of differentiative to proliferative divisions. Tis21GFP expression in *Gli3*$^{Xt/Pdn}$*;Tis21GFP* embryos was used to evaluate if this was the case. In the apical progenitor population, a difference in the proportion of progenitors undergoing differentiative division did not account for the changes in S-phase length at E11.5, but could have contributed to the reduction measured in S-phase length at E12.5. In the basal progenitor population, the increase in Tis21GFP$^{+}$ progenitors may have contributed to the reduction in S-phase length at E11.5, but not at E12.5. Taken together, *Cdk6* is a viable candidate through which *Gli3* may regulate G1-phase length, however further experimentation is required to probe this relationship. Based on the data presented here, the mechanism by which *Gli3* regulates S-phase length is more complicated and requires further exploration.

### *5.7.1 Microarray analysis revealed alterations in genes regulating progenitor proliferation/differentiation, and Cdk6 as a possible route through which Gli3 controls G1-phase length*

Microarray analysis was previously conducted on the E10.5 *Gli3*$^{Xt/Pdn}$ dorsal telencephalon to evaluate which genes were up- or down-regulated due to the reduction in *Gli3* function. I carried out GO analysis on these data to gain an

understanding of the biological processes which were dysregulated in the mutant. Genes which were up-regulated in the mutant were associated with processes such as “cell proliferation”, concomitant with down-regulation in genes associated with processes such as “neurogenesis”. Analyses undertaken in the lateral E11.5 *Gli3*$^{Xt/Pdn}$ cortex exposed an increased apical progenitor proportion, alongside decreased basal progenitor and early-born neuron proportions. Cell cycle re-entry was also increased, indicating cell proliferation instead of cell differentiation. Despite the difference in time points between the microarray analyses and analyses of progenitor/neuron proportions, it would appear that at E11.5 there was also an increase in proliferative divisions of apical progenitors, at the expense of differentiative divisions into basal progenitors and neurons. Indeed, as revealed by Tis21GFP expression, there was a tendency towards increased apical progenitor proliferation and decreased differentiation. By E12.5 in the lateral and medial mutant neocortex, the apical progenitor proportion had decreased, whereas the basal progenitor and early-born neuron proportions had increased, indicative of a shift from apical progenitor proliferative to differentiative divisions. This was supported by Tis21GFP expression in the apical progenitor population.

At both E11.5 and E12.5, G1-phase length was shorter in *Gli3*$^{Xt/Pdn}$ apical progenitors. Progression through the mid G1-phase restriction point is regulated by *Cdk4/6* and their association with the D-type cyclins. Indeed, overexpression of *Cyclin D1* and *Cdk4/Cyclin D1* lead to shortening of G1-phase (Lange *et al.*, 2009; Pilaz *et al.*, 2009). Therefore, it was extremely interesting when the microarray screen revealed *Cdk6* as up-regulated 1.59-fold in the mutant compared to control. As well as regulating development of the telencephalon, *Gli3* also regulates the growth of the limb bud. Here, Vokes *et al*. (2008) conducted ChIP-on-ChIP analysis of *Gli3* binding sites and found a potential binding site in the *Cdk6* promoter. Based on this, Lopez-Rios *et al*. (2012) investigated the interaction of *Gli3* with the *Cdk6* promoter region and discovered that *Gli3* does bind to this region. They explored *Gli3;Cdk6* double mutants to evaluate the effect of conditionally inactivating *Cdk6* on the polydactyly phenotype of embryos in which *Gli3* had been conditionally inactivated in the limb bud. The conditional inactivation of *Cdk6* alongside *Gli3* resulted in a partial rescue of the polydactyly phenotype. However, as instead of reducing *Cdk6* levels in the *Gli3* mutant back to control levels they inactivated *Cdk6*, it is difficult to draw conclusions about the partial rescue. It is possible, however unlikely, that the partial rescue of the *Gli3* phenotype was not due to antagonism of *Gli3’s* inhibition on *Cdk6* but was a by-

product of inactivating *Cdk6* and occurred through a *Gli3*-independent mechanism. Yet, electromobility shift assays and luciferase assay confirmed that *Gli3* binds to the *Cdk6* promoter region and inhibits its expression, respectively (Hasenpusch-Theil *et al.*, 2018). Importantly, when the microarray analysis was conducted on $Gli3^{Xt/tPdn}$ dorsal telencephalon, it was also conducted on $Gli3^{Pdn/Pdn}$ dorsal telencephalon. The delay in neurogenesis observed between E11.5 and E12.5 in the $Gli3^{Xt/Pdn}$ cortex was not observed in the $Gli3^{Pdn/Pdn}$ mutant (Magnani *et al*., 2010), and in these embryos *Cdk6* was not differentially expressed in the dorsal telencephalon. *Cdk6* therefore represented a clear target for further investigation.

Conversely, the microarray screen did not identify any obvious candidate genes for the regulation of S-phase length. The reduction in S-phase length may be accounted for by a shift towards differentiative divisions at the expense of proliferative divisions, or by regulation of genes controlling S-phase by *Gli3* which were not identified in this screen. Indeed, when RNA sequencing (RNAseq) was conducted in the $Emx1Cre;Gli3^{fl/fl}$ conditional mutant at E11.5 *Cyclin A2*, which is required for progression through S-phase, was up-regulated, and the Cdk inhibitors $p21^{Cip1}$, $p27^{Kip1}$ and $p57^{Kip2}$ were down-regulated (Hasenpusch-Theil *et al.,* 2018). Progression through each phase of the cell cycle depends on a balance between Cdk/cyclin and Cdk inhibitor expression (Hindley & Philpott, 2012). It is therefore possible that a dysregulation in *Gli3* expression leads to a tip towards increased Cdk expression and decreased Cdk inhibitor expression, leading towards faster progression through S-phase. RNAseq proved to be a more sensitive measure of mRNA dysregulation than the microarray analysis, and I could not discount the possibility that genes regulating S-phase length were dysregulated in the $Gli3^{Xt/Pdn}$ dorsal telencephalon but were not recognised in the microarray screen.

### *5.7.2 Up-regulation of Cdk6 led to increased pRb expression, yet it was not possible to determine if Cdk6 inhibition would rescue the neurogenesis defect*

As *Cdk6* was up-regulated in the E10.5 $Gli3^{Xt/Pdn}$ dorsal telencephalon, it was important to determine if that up-regulation had any output in the E11.5 and E12.5 cortex. *Cdk6* hyperphosphorylates pRb on a number of different serine sites, including serine-780 (S780), phosphorylation of which is inhibited by palbociclib (Fry *et al*., 2004). In certain cancers, Cdks are able to erroneously push cells through the cell cycle to divide proliferatively, and so Cdks have become a major focus in oncology.

In particular, *Cdk4* and *Cdk6* are of great interest due to their strong regulation of Rb, which is often identified as mutated in different cancers. Thus, great effort has been put into developing Cdk4/6 specific inhibitors. Palbociclib has been a successful discovery during this effort and is now licenced in both the United Kingdom and United States for the treatment of breast cancer. It is an orally active, small molecule, reversible Cdk4/6 inhibitor which shows no significant activity against other *Cdks* (Sherr *et al.*, 2016; Choi & Anders, 2014). At high concentrations, it has been shown to block cells in G1-phase and prevent them from entering S-phase in $Rb^+$ cancers, and can cause shrinkage of tumours which is reversible upon drug withdrawal (Toogood *et al.*, 2005; Fry *et al.*, 2004).

In the E11.5 lateral $Gli3^{Xt/Pdn}$ cortex, the proportion of pRb $S780^+$ apical progenitors was increased. In these cells G1-phase length was reduced, indicating that the increase in pRb hyperphosphorylation led to faster progression through that phase. By E12.5, the proportion of $pRb^+$ apical progenitors was unaltered in the mutant compared to control, whilst G1-phase length was reduced. G1-phase length may therefore also be regulated by *Gli3* in a non-*Cdk6* dependent manner.

In the E11.5 and E12.5 lateral basal progenitor populations, the proportions of $pRb^+$ progenitors were increased, whilst G1-phase length was unaltered in these populations. Therefore, this may represent, in support of the E12.5 apical progenitor population, a regulation of G1-phase length not through *Cdk6*. As *Gli3* is primarily expressed in apical progenitors and not in basal progenitors, and the regulation of *Cdk6* was postulated to be direct due to the binding of *Gli3* to the *Cdk6* promoter region, it is possible the reduction in *Gli3* indirectly influenced pRb hyperphosphorylation outside of its control over *Cdk6*. Also, it is possible there was signalling from apical progenitors to basal progenitors thereby altering their $pRb^+$ progenitor proportions, despite their very limited expression of *Gli3*.

In the E11.5 medial cortex, the proportion of $pRb^+$ apical progenitors was unaltered, whilst it was not possible to accurately measure G1-phase length. Here, the proportions of apical and basal progenitors and early-born neurons were also unaffected in the mutant suggesting that the reduction in *Gli3* did not influence the progenitor cell cycle and thereby progenitor/neuronal proportions. By E12.5, G1-phase length was unaltered in the mutant compared to control, as was pRb expression. Yet here the proportion of apical progenitors had decreased in the mutant compared to control whilst the proportion of basal progenitors and neurons had

increased. This would indicate that factors outside of cell cycle regulation, such as alterations in signalling, influenced the decision over the mode of division undertaken in the E12.5 medial *Gli3*$^{Xt.Pdn}$ neocortex. As discussed in section 3.6.2, although the rostro-caudal level examined was chosen to minimise the impact of altered signalling in the *Gli3*$^{Xt/Pdn}$ medial telencephalon (Kuschel *et al.*, 2003), it is still possible these alterations had an impact upon the medial apical progenitor population. Wnt signalling is known to promote apical progenitor proliferative division (Wrobel *et al.*, 2007), and *Wnt* expression in the *Gli3*$^{Xt/Pdn}$ cortical hem is severely reduced. Furthermore, postmitotic neurons have been shown to initiate a feedback mechanism to apical progenitors, promoting a cell fate switch to basal progenitors (Parthasarathy *et al.*, 2014). Potentially, the increased neuronal proportions at E12.5 in the medial and lateral cortex contributed to the reduced and tendency-towards-reduced apical progenitor proportions, respectively.

In the medial E11.5 basal progenitor population, the proportion of pRb$^{+}$ cells was unaltered in the mutant, whilst it was not possible to measure G1-phase length. Here, as above the progenitor/neuronal proportions were unaffected, indicating the reduction in *Gli3* function did not influence progenitor division. By E12.5, the proportion of pRb$^{+}$ cells had increased, whilst again it was not possible to measure G1-phase length. As stated, there was a tip towards increased basal progenitor and neuronal proportions and a decreased apical progenitor proportion. *Gli3* was also not expressed in these progenitors, so it is likely that indirect regulation over progenitor/neuronal proportions outside of *Gli3's* direct regulation over *Cdk6* is relevant here.

Overall, across the two positions measured and the two ages, there were mixed results in terms of how pRb expression, G1-phase length, and progenitor/neuronal proportions related. In the E11.5 mutant lateral cortex, there was an increase in apical progenitor pRb expression, coinciding with G1-phase shortening and an increase in apical progenitor proportion. However, pRb expression was also increased in basal progenitors, whilst G1-phase length was unaffected, yet the proportion of basal progenitors was reduced alongside the proportion of neurons. By E12.5, pRb expression was unaltered in both apical and basal progenitors, whilst G1-phase length was reduced in both populations. The proportion of apical progenitors showed a tendency to be decreased in the mutant compared to control, whilst the basal progenitor and neuronal proportions were increased. In the mutant medial cortex, at

E11.5 pRb expression was unaltered in the apical and basal progenitor populations, and it was not possible to accurately measure G1-phase length. The proportion of apical and basal progenitors and neurons were also unaltered in the mutant. By E12.5, apical progenitor pRb expression was unaltered as was G1-phase length, yet the proportion of apical progenitors was decreased compared to control. The proportion of $pRb^+$ basal progenitors was increased, but I was unable to measure G1-phase length, and the basal progenitor and neuronal proportions were increased. Taken together, it appears that the reduction in *Gli3* also altered G1-phase length outside of its regulation over *Cdk6* via pRb, and altered progenitor proliferation/differentiation into neurons outside of its control over the cell cycle.

To determine if *Gli3's* direct regulation over *Cdk6* contributed to the delay in neurogenesis, the effect of inhibiting Cdk6 by palbociclib was examined *in vitro*. Whilst it was possible to inhibit Cdk6 activity and cause a down-regulation in pRb expression in E13.5 CD1 embryos, it was not possible to conduct the same analyses in $Gli3^{Xt/Pdn}$ embryos. In E11.5 slices which were put into culture for 24 hrs, growth of $Gli3^{Xt/Pdn}$ and control slices were disrupted in the presence of DMSO alone, palbociclib dissolved in DMSO, and without either present. This would indicate that these organotypic slice culture conditions were not amenable to cortical growth of slices at this age. Slices taken at E12.5 and cultured for 24 hrs again showed disrupted growth in both the control and mutant. However, control slices of E13.5 brain appeared normal and showed consistent pRb/PCNA expression patterns as in CD1 cortical slices and embryos which had not been cultured. This would indicate that the earlier the age in which a slice is put into culture, not the background of the embryos, dictates how a slice will behave under these culture conditions. It was therefore not possible to examine the effect of *Cdk6* inhibition in the cortex.

In a number of the slices, rosette-like structures formed across the cortex with a ring of $pRb^+$ cells surrounded by $PCNA^+$ cells. The cortical slices were cultured with the agarose used for embedding still intact around the outside of the slices. It was postulated that *in vivo,* newly generated cells move radially outwards to increase the size of the cortex. Instead in this experimental setup, when these cells moving radially met the agarose barrier at the basal edge of the cortex they turned laterally or medially and created a rosette. With that in mind, the percentage of agarose in which the tissue was embedded was decreased and sections of agarose from around the cortical surface were removed before the slices were cultured (data not shown). This did not

improve the growth of the slices, and so it was concluded that these conditions do not represent a viable *in vitro* tool for measuring palbociclib activity.

In order to test my hypothesis that the increase in *Cdk6* expression contributed to the delayed neurogenesis phenotype in *Gli3*$^{Xt/Pdn}$ mutants, another methodology is required. Since completion of this work, it was shown that palbociclib administered to pregnant females led to effects on the embryonic cortical Tbr1$^{+}$ neuronal population. In the *Emx1Cre;Gli3*$^{fl/fl}$ conditional embryo, the proportion of pRb$^{+}$ cells was increased in the mutant compared to control, as was seen in the lateral *Gli3*$^{Xt/Pdn}$ cortex. In the conditional mutant, *Cdk6* was identified as being up-regulated 1.96-fold at E11.5 by RNAseq and G1-phase length was also shorter, with a decrease in the proportion of Tbr1$^{+}$ early-born neurons. In these mutants, the effect of palbociclib exposure *in vivo* was examined (Hasenpusch-Theil *et al.*, 2018). E10.5 pregnant females were dosed with either sodium lactate buffer (control) or 75mg palbociclib/kg body weight, and embryos harvested 24 hrs later. The proportion of pRb$^{+}$ cells was increased in the mutant compared to control after sodium lactate buffer administration, yet was unaltered after palbociclib exposure. Furthermore, whilst after sodium lactate buffer administration the proportion of Tbr1$^{+}$ cells was decreased in the mutant compared to control, after palbociclib administration there was no difference between control and mutant embryos. This indicated that inhibition of Cdk6 by palbociclib rescued the defect in the proportion of neurons generated in the *Emx1Cre;Gli3*$^{fl/fl}$ mutant. This rescue of delayed neurogenesis strongly supports my hypothesis that *Gli3* controls the onset of cortical neurogenesis by regulating *Cdk6* expression levels. Therefore, it would be very interesting to repeat this experiment in *Gli3*$^{Xt/Pdn}$ embryos.

Taken together, I hypothesise that *Gli3* directly binds to the *Cdk6* promoter and inhibits its expression. During normal cortical development, *Gli3* reduces *Cdk6* expression, allowing a certain level of pRb hyperphosphorylation and transcription of G1- to S-phase progression genes by E2F transcription factors. This allows a progenitor to progress from G1- into S-phase at a certain rate (figure 5.18 A). When *Gli3* expression is reduced, as in the *Gli3*$^{Xt/Pdn}$ embryo, there is less inhibition on the expression of *Cdk6*. Increased *Cdk6* levels lead to increased pRb hyperphosphorylation, and increased transcription of G1- to S-phase progression genes. Cortical progenitors therefore progress through G1-phase at a faster rate (figure 5.18 B). However, this is influenced by the age and location under examination. For example, in the E11.5 mutant medial cortex, the proportions of progenitors and

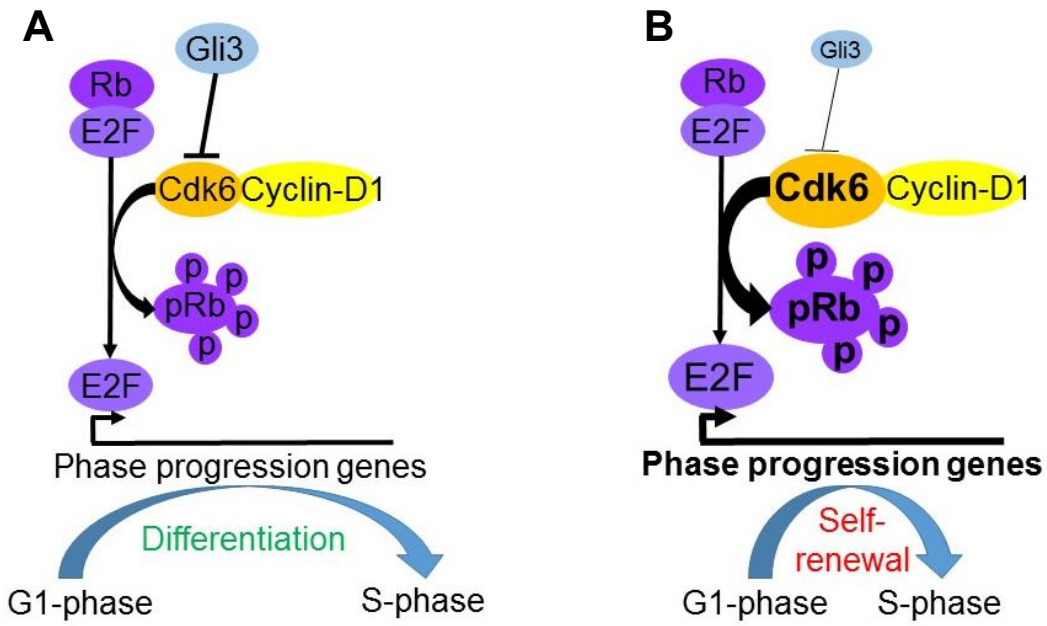


**Figure 5.18: Model summarising my hypothesis of how Gli3 may determine G1-phase length through regulation of *Cdk6*. A.** In control embryos, I propose Gli3 binds to the *Cdk6* promoter region, thereby inhibiting expression of *Cdk6*. A regulated amount of Cdk6 protein is therefore available for binding with cyclin D1, limiting the hyperphosphorylation of pRb. This prevents pRb from disassociating with E2F transcription factors, reducing the level of transcription of phase progression genes. The progenitor remains in G1-phase for longer, and differentiation is promoted. **B.** In *Gli3*$^{Xt/Pdn}$ embryos, I propose the reduced amount of *Gli3* results in an increase in *Cdk6* expression, leading to increased hyperphosphorlyated pRb expression. This promotes disassociation of pRb from E2F transcription factors, allowing them to promote transcription of phase progression genes. The progenitor then proceeds through G1-phase at a faster rate, encouraging self-renewal at the expense of differentiation.

neurons, the proportion of $pRb^+$ cells and G1-phase length were largely unaffected despite a reduction in *Gli3* expression. Yet by E12.5, the proportions of progenitors and neurons and the proportion of $pRb^+$ basal progenitors were altered in the same location. Furthermore, there was a clear difference in the lateral and medial cortex, particularly at E11.5, which may have been related to the rostro-lateral to caudo-medial progression of neurogenesis. These studies have been limited in their scope, as I have been unable to take into account fully the myriad of other factors influencing progenitor proliferation and differentiation in the $Gli3^{Xt/Pdn}$ cortex. For example, as discussed above, signalling plays a key role in influencing neurogenesis and is known to be disturbed in the $Gli3^{Xt/Pdn}$ cortex.

### *5.7.3 Shortening of S-phase length in E12.5 $Gli3^{Xt/Pdn}$ embryos may be due to an increase in the proportion of differentiative progenitors*

The microarray screen conducted on E10.5 $Gli3^{Xt/Pdn}$ dorsal telencephalon did not provide any obvious candidate genes through which *Gli3* may have regulated S-phase length. I therefore hypothesised that perhaps the reduction observed in S-phase length when *Gli3* expression was reduced in the $Gli3^{Xt/Pdn}$ cortex may have been due to an alteration in the proportion of differentiative to proliferative progenitors.

In the E11.5 lateral cortex, the proportion of differentiative apical progenitors was unaltered between the mutant and control as revealed by Tis21GFP expression, whilst S-phase length was shorter in the mutant. By E12.5, the proportion of differentiative apical progenitors was increased in the lateral cortex, whilst S-phase was still reduced in the mutant compared to control. This would indicate that at E11.5 the reduction in S-phase length was not due to an increased proportion of differentiative apical progenitors, which was reflected in the larger proportion of apical progenitors and simultaneously smaller proportions of basal progenitors and neurons. However, at E12.5, the reduction in S-phase length may be accounted for by an increased proportion of differentiative apical progenitors. This would imply that the reduction in *Gli3* had different effects on S-phase length at different time points.

In the E11.5 lateral basal progenitor population, there was an increase in the proportion of differentiative basal progenitors, and a shortening of S-phase length. However, total cell cycle length was also reduced, indicating that an alteration in the

proportion of differentiative basal progenitors did not solely account for the reduction in S-phase length. As *Gli3* was not expressed in this population, the reduction in *Gli3* must have indirectly affected the ratio of differentiative to proliferative divisions. At E12.5, there was no difference in the proportion of differentiative basal progenitors and S-phase length was unaltered, indicating that by this time *Gli3* had no impact upon basal progenitor division in this location.

In the E11.5 medial cortex, there was a decrease in the proportion of apical progenitors dividing differentiatively, whilst S-phase length was unaffected. It would appear then that here the alteration in the ratio of differentiative to proliferative divisions was not great enough to reflect as a change in S-phase length. At E12.5, the proportion of differentiative apical progenitors was increased in the mutant, and S-phase length was reduced. Here, the increase in differentiative apical progenitors may have contributed to the reduction in S-phase length measured. In the basal progenitor population, at both E11.5 and E12.5, the proportion of differentiative basal progenitors in the medial cortex was unaffected in the mutant compared to control, and it was not possible to measure S-phase length.

Taken together, *Gli3* had different spatio-temporal control over the proportions of differentiative versus proliferative apical and basal progenitors. At E11.5, S-phase length was reduced in basal progenitors in the lateral cortex, which could have been accounted for by an increase in differentiative basal progenitor proportion. Further, at E12.5, S-phase length was reduced in lateral apical progenitors and the differentiative proportion of these cells was increased, again possibly underlying the reduction in S-phase length. In contrast, there was a tendency towards a decreased differentiative proportion of E11.5 lateral apical progenitors, whilst S-phase length was reduced, highlighting that the reduction in S-phase length in $Gli3^{Xt/Pdn}$ embryos cannot be fully accounted for by a change in the proportion of differentiative progenitors. Therefore, *Gli3* must somehow affect S-phase length at least indirectly, as the proportion of E11.5 differentiative basal progenitors and basal progenitor S-phase length were altered despite the very low expression of *Gli3*.

As with G1-phase length, it is possible to pharmacologically lengthen S-phase. For example, aphidicolin is a DNA replication inhibitor which can lengthen S-phase and prevent differentiation (Gonzales *et al*., 2015). It would be interesting to test what effect lengthening of S-phase had on progenitor proliferation/differentiation at E11.5 and E12.5 laterally and medially in $Gli3^{Xt/Pdn}$ embryos.

### 5.8 Summary

Taken together, the mechanisms by which *Gli3* regulates the cell cycle are complex and vary based on the age and location under examination. It is likely that *Gli3* directly regulates *Cdk6*, contributing to a reduction in G1-phase length. However, *Cdk6* is likely not the only mechanism by which G1-phase length is controlled by *Gli3*. To further complicate matters, *Gli3* regulates G1-phase length differently between E11.5 and E12.5 through potentially direct and indirect mechanisms. S-phase length was also altered in the $Gli3^{Xt/Pdn}$ mutant at both E11.5 and E12.5. Whilst an alteration in the ratio of proliferative to differentiative divisions may have accounted for the reduction in S-phase length measured at E12.5, this was not the case at E11.5. Therefore, as with G1-phase length, S-phase length must be regulated differently by *Gli3* at E11.5 and E12.5. Finally, in basal progenitors both S-phase length and the proportion of differentiative progenitors were altered, whilst *Gli3* was not expressed in these cells, and so it exhibited non-autonomous control over this population.

## Chapter 6: Final discussion and future work

The focus of this thesis has been the role *Gli3* plays in early neurogenesis. By examining the expression of the Gli3 protein near the onset of cortical neurogenesis, I revealed Gli3's expression in apical progenitors at E11.5 and E12.5 places it in a critical position for influencing the development of the cortex. When *Gli3* is reduced, as in the $Gli3^{Xt/Pdn}$ cortex, the proportions of apical and basal progenitors and early-born neurons are altered at E11.5 and E12.5, indicating an early delay in neurogenesis. A major factor known to influence neurogenesis at this stage is this cell cycle, and *Gli3* was previously implicated in cell cycle regulation in the limb bud (Lopez-Rios *et al*., 2012; Vokes *et al.*, 2008). Based on this, the cell cycle was investigated in the $Gli3^{Xt/Pdn}$ embryo. Cell cycle exit was shown to be affected at E11.5 and E12.5, and G1- and S-phase lengths were critically reduced in the apical progenitor population. Finally, microarray data was examined from the E10.5 $Gli3^{Xt/Pdn}$ dorsal telencephalon to search for potential mechanisms by which *Gli3* may regulate G1- and S-phase length, and preliminary investigations into the regulation of these phases were undertaken. *Cdk6* was revealed as a potential mechanism by which *Gli3* may regulate G1-phase, yet no candidates were identified through which *Gli3* may regulate S-phase.

### 6.1 Gli3 protein expression is primarily confined to apical progenitors and a reduction in *Gli3* results in alterations to the apical and basal progenitor and early-born neuron populations

Whilst the expression of *Gli3* mRNA has been discussed in numerous studies (Pollen *et al*., 2014; Amaniti *et al.*, 2013; Hui *et al.*, 1994), there has been little discussion with regards to Gli3 protein expression. Yabut *et al*. (2016) described Gli3 protein to be expressed in the ventricular and subventricular zones (VZ and SVZ) at E16.5, in both the cytoplasm and nucleus of cells. However, as no cellular subtype markers were used it was not possible to say in which cell types Gli3 was expressed. I investigated this by combining Gli3 immunofluorescence with Pax6 and Tbr2 expression as markers of apical and basal progenitors, respectively, at E11.5 and E12.5. Gli3 protein expression was largely confined to the apical progenitor population with some

expression in a subset of basal progenitors at both ages. Although it was possible to identify some nuclear and cytoplasmic staining in the studies I undertook, it would be advantageous to combine Gli3 immunofluorescence with other cytoplasmic and nuclear markers and use high resolution imaging to fully investigate the subcellular localisation of Gli3 protein.

Furthermore, I conducted Gli3 immunofluorescence analyses on *Gli3*$^{Xt/Pdn}$ embryos at E11.5 and E12.5. The Gli3 expression pattern exhibited in control embryos was replicated in mutant embryos, with expression chiefly in apical progenitors with some in basal progenitors at E12.5. The intensity of the Gli3 staining was reduced in mutant embryos, yet it was not possible to perform a quantitative analysis of this reduction. In the future, a quantification of the reduction of Gli3 protein in the *Gli3*$^{Xt/Pdn}$ cortex using western blotting should be undertaken.

To determine if the reduction in *Gli3* in *Gli3*$^{Xt/Pdn}$ embryos had any effect on the apical and basal progenitor populations I combined Pax6 and Tbr2 immunofluorescence with PCNA, a pan progenitor marker, and quantified the proportion of progenitors which were either apical or basal progenitors compared to the total progenitor population. I then calculated the proportion of early-born neurons using Tbr1, a marker of early-born cortical neurons, and TOPRO-3, as a nuclear marker. At E11.5, in the lateral cortex there was an increase in the proportion of apical progenitors and decreases in the proportion of basal progenitors and neurons in the *Gli3*$^{Xt/Pdn}$ cortex. However, these proportions were unaffected in the medial cortex. By E12.5, there was no difference between the control and mutant apical progenitor proportions laterally whilst the basal and neuronal proportions were increased in the mutant. In the medial mutant cortex, the apical progenitor proportion was decreased and the basal progenitor and neuronal proportions were increased. Taken together, it appeared the reduction in *Gli3* altered the progenitor and neuronal proportions at both ages.

Generally, progenitors are able to undergo two modes of division; proliferative division to form two new progenitors or differentiative division to form one new progenitor of the same subtype and either a basal progenitor (in the case of an apical progenitor division) or neuron (produced from either an apical or basal progenitor). Therefore, the differences in apical and basal progenitor and early-born neuron proportions may have arisen from an imbalance in apical and basal progenitor proliferation/differentiation.

At E11.5 laterally, an increase in apical progenitor proliferation could justify the increased proportion of apical progenitors and decreased proportions of basal progenitors and neurons in the *Gli3*$^{Xt/Pdn}$ cortex. When Tis21, a marker of differentiative division, was investigated there was a tendency in the mutant towards increased apical progenitor proliferative divisions at the expense of differentiative divisions. There was also an increase in basal progenitor differentiative divisions, possibly reflecting the reduced basal progenitor proportion. As apical progenitors constitute the largest progenitor population and give rise to the majority of early-born neurons formed at this age, the reduced early-born neuronal proportion probably reflects the decrease in apical progenitor differentiation. By E12.5, there was no difference between mutant and control in the proportion of apical progenitors, yet the proportions of basal progenitors and early-born neurons were increased in the mutant. Here, both apical and basal mutant progenitors exhibited an increase in differentiative divisions. An interesting future experiment could examine these three cell populations at E13.5 to see if both progenitor populations are decreased due to the increased differentiative divisions and the impact upon the neuronal population. Further, neuronal composition of the E18.5 cortex could be examined, identifying the relative numbers and position of cortical neurons from distinct layers. However, this may be hampered as lamination is disturbed in the mutant. Kuschel *et al*. (2003) reported that at E14.5 there was a dramatic reduction in Pax6 expression, yet this was not quantified, and neither Tbr2 nor Tbr1 were examined. Magnani *et al*. (2013) also reported a near complete loss of subplate neurons in the *Gli3*$^{Xt/Pdn}$ embryo, which may reflect a delay in neurogenesis, and when it finally begins layer VI neurons are formed instead of subplate neurons.

Medially at E11.5 in the *Gli3*$^{Xt/Pdn}$ embryo, there were no differences in the proportions of apical and basal progenitors and early-born neurons or basal progenitor proliferative/differentiative divisions, yet there was an increase in apical progenitor proliferative divisions. One would expect an increase in apical progenitor proliferative division to lead to an increase in the proportion of apical progenitors at E12.5, yet this was not the case. By E12.5, the proportion of apical progenitors in the mutant was decreased compared to control, whilst the proportions of basal progenitors and neurons were increased. In the 24 hrs between analyses apical progenitors could undergo 2-3 full cell cycles (based on total cell cycle length calculated in section 4.4). Potentially medial apical progenitors have begun to divide proliferatively as in the lateral cortex at E11.5 at the time of analysis, but by E12.5 they had begun to divide

differentiatively, as reflected by the increase in differentiative divisions to produce the smaller apical progenitor and larger basal progenitor and neuronal proportions measured. As neurogenesis proceeds laterally to medially, the increase in proliferative apical divisions may have begun first in the lateral hemisphere and resulted in quantifiable changes in progenitor and neuronal proportions by the time of analysis. An increase in proliferative apical divisions may then have begun medially and was measured here but may not have yet produced a perceptible effect on progenitor and neuronal proportions. By E12.5, increased apical progenitor differentiative divisions both medially and laterally reflected the medially decreased apical progenitor proportion and, relative to E11.5, decrease in lateral apical progenitor proportion. Again, an analysis of the proportions of these cells at E13.5 would be of interest.

Due to Gli3 protein being primarily expressed in apical progenitors, and both basal progenitors and early-born neurons arising from apical progenitors, I suggest the alterations in basal progenitor and neuronal proportions were likely in part due to cell autonomous effects in apical progenitors. However, as described, there are also alterations to the signalling centres in *Gli3*$^{Xt/Pdn}$ embryos and so alterations in signalling may have influenced the changes observed in apical and basal progenitor and early-born neuronal proportions. As in the rostral telencephalon there is ectopic *Fgf8* expression and *Wnt2b*, *Wnt3a* and *Bmp4* expression are abolished, I conducted my analyses further caudally in order to circumvent the largest alterations in signalling. Nevertheless, it is likely that signalling changes impacted upon the proportions measured. It would be interesting to repeat the analyses performed here at other rostrocaudal levels in *Gli3*$^{Xt/Pdn}$ embryos to assess the impact of altered signalling.

On the other hand, repeating these analyses in a conditional mutant such as the *Emx1Cre;Gli3*$^{fl/fl}$ mutant, where there is little alteration in signalling, would also be interesting. This has in fact been undertaken (Hasenpusch-Theil *et al.*, 2018); at E11.5, the proportion of basal progenitors and early-born neurons were decreased in the mutant compared to control, whilst at E12.5 there was an increase in the proportion of basal progenitors yet a decrease in the proportion of neurons. The proportion of apical progenitors is increased at both ages. Furthermore, there was no change in apical progenitor proliferative/differentiative divisions at E11.5, yet there was a decrease in apical progenitor proliferative divisions at E12.5. In the basal progenitor population, there was an increase in differentiative divisions at E11.5 but

no change at E12.5. These analyses provide evidence that a mutation in *Gli3* is able to influence progenitor and early-neuronal proportions and differentiative/proliferative division even in the absence of changes to signalling, and so provides further indication that *Gli3* acts cell autonomously on these processes. It is important to note however that these analyses in the conditional mutant were conducted in the rostromedial telencephalon, whereas my analyses were conducted further caudally and further laterally. They were performed there as Wnt signalling is altered in the caudal telencephalon of these embryos and as Gli3 protein is not lost from the lateral telencephalon until E12.5.

### 6.2 Cell cycle kinetics are disturbed in the *Gli3*$^{Xt/Pdn}$ cortex

Cell cycle has long been implicated in determining if a progenitor will undergo a proliferative or differentiative division (Pilaz *et al.*, 2016; Gonzales *et al.*, 2015; Arai *et al.*, 2011; Lange *et al.*, 2009; Pilaz *et al*., 2009; Calegari & Huttner, 2003). *Gli3* has also been reported to regulate the cell cycle in the limb bud (Lopez-Rios *et al.*, 2012; Vokes *et al.*, 2008), and so I focussed on the cell cycle of cortical progenitors.

In the lateral apical progenitor population, there was an increase in cell cycle re-entry at E11.5 and G1- and S-phase and total cell cycle length were decreased in the mutant compared to control. By E12.5 there was an increase in cell cycle exit, yet G1-, S- and M-phase and total cell cycle length remained shorter in the mutant compared to control. G1- and M-phase and total cell cycle length get longer as progenitors undertake differentiative division as opposed to proliferative division, whilst S-phase gets shorter. Therefore, the cell cycle phase lengths measured at both ages appear to be at odds. At E11.5, when cell cycle re-entry is increased one would expect G1-phase and total cell cycle length to be shorter in the mutant, as was recorded. However, S-phase length would be expected to be longer. Conversely, at E12.5 cell cycle exit was increased in the mutant and so S-phase would be expected to be shorter, as was seen, yet G1- and M-phase and total cell cycle length should have been longer in the mutant. Together, I would suggest that perhaps when *Gli3* levels are reduced, G1-phase length is more critical to determining if an apical progenitor will undergo proliferative/differentiative division at E11.5, whilst S-phase length may

be more important at E12.5, as has been reported to be the case in ESCs (Gonzales *et al.*, 2015). However, these results should not be considered in isolation, and again factors other than cell cycle phase length will have contributed to the defects measured in *Gli3*$^{Xt/Pdn}$ apical progenitors.

In the medial apical progenitor population, at E11.5 cell cycle exit was unaltered in the mutant compared to control and S-, G2- and M-phase and total cell cycle length were also unaltered. I was unable to make a measurement for G1-phase, probably due to inaccuracies in measuring other phase lengths. In the future it would be possible to measure the cell cycle phases by other methodologies, such as crossing *Gli3*$^{Xt/Pdn}$ embryos with a FUCCI reporter line to give a direst measurement of G1-phase length in individual cells when using live imagining or time lapse microscopy (Roccio *et al.*, 2013). Alternatively, flow cytometry can be used to measure different cell cycle phases at a single time-point, giving an estimate of G1-, S- and G2/M-phase lengths (Pozarowski & Darzynkiewicz, 2004). It would be interesting to compare the differences in cell cycle phase lengths between the different methodologies. In the E11.5 medial apical progenitors, there was little difference between the *Gli3*$^{Xt/Pdn}$ mutant and control in the measurements conducted. In contrast, in the lateral apical progenitor population there were many differences recorded between *Gli3*$^{Xt/Pdn}$ embryos and control. As neurogenesis proceeds laterally to medially, I would propose the effects on progenitor and neuronal populations resulting from the reduction in *Gli3* increase over time and as neurogenesis proceeds. Perhaps in the E11.5 medial cortex neurogenesis is not advanced enough yet in the mutant for recognisable changes to be measured.

In the E12.5 medial apical progenitor population, there was an increase in cell cycle exit in the mutant compared to control, and S- and M-phase and total cell cycle length were decreased in the mutant. According to Gonzales *et al.* (2015) and Arai *et al*. (2011), S-phase shortens as progenitors transition from proliferative to differentiative divisions as the need for checking DNA fidelity is reduced when progenitors lose their stemness. Here, the proportion of apical progenitors was decreased whilst the proportions of basal progenitors and neurons were increased, again fitting with the notion of apical progenitors dividing differentiatively and/or exiting the cell cycle to form basal progenitors or neurons. Therefore, *Gli3* likely plays a role in maintaining progenitors in active cell cycle in the medial cortex at E12.5.

In E11.5 lateral basal progenitors, S-phase and total cell cycle length were decreased in the *Gli3*$^{Xt/Pdn}$ mutant compared to control. Cell cycle re-entry was also increased here, although I measured cell cycle re-entry/exit in the total progenitor population. In the future this measurement should be repeated using BrdU and Pax6/Tbr2 instead of BrdU and PCNA to differentiate between the two progenitor populations. The proportion of lateral basal progenitors at E11.5 was decreased in the mutant compared to control, and the reduction in S-phase length would indicate basal progenitor differentiative divisions as opposed to proliferative divisions. However, at E12.5 the basal progenitor proportion was increased in the mutant compared to control, so I would suggest the increase in cell cycle re-entry primarily reflected an increase in apical progenitor cell cycle re-entry at the expense of differentiation into basal progenitors. Therefore, the decrease in basal progenitor proportion may reflect (1) an increase in basal progenitor differentiation as suggested by the decrease in S-phase length, (2) a decrease in basal progenitor production due to a decrease in apical progenitor differentiation, or (3) an increase in basal progenitor apoptosis. It is likely the decrease in basal progenitor proportion here was due to decreased basal progenitor production, however an analysis of apoptosis could be conducted to rule out that possibility.

In the lateral E12.5 basal progenitor population, the only cell cycle phase altered in the mutant compared to control was M-phase, which was significantly longer in the mutant. As there was no change in total cell cycle length I would suggest the increase in M-phase instead represented a larger proportion of basal progenitors undergoing mitosis, which could be tested by examining pHH3/PCNA double-expression. The increased proportion of basal progenitors measured at E12.5 could therefore be due to an increase in apical progenitor differentiation into basal progenitors and an increase in basal progenitor proliferative division, triggered by a mechanism other than the cell cycle.

Overall, *Gli3* reduction in the *Gli3*$^{Xt/Pdn}$ embryo had little impact upon the cell cycle in basal progenitors compared to apical progenitors, particularly in the length of G1-phase which was only reduced in the apical progenitor population. Hence, as Gli3 is primarily expressed in apical progenitors, it conceivably regulates the cell cycle directly.

### 6.3 Cellular mechanisms by which *Gli3* may regulate cell cycle length

To begin to understand the mechanisms behind which *Gli3* regulates cell cycle length, I examined microarray gene expression data from E10.5 *Gli3*$^{Xt/Pdn}$ dorsal telencephalon and littermate controls. From this, I identified *Cdk6* as a potential candidate gene which may regulate the length of G1-phase, yet I did not identify any specific genes which may regulate S-phase. To test if G1-phase length was altered by the increase in *Cdk6* levels, I performed organotypic slice cultures in the presence of a *Cdk6* inhibitor, palbociclib, to ameliorate the influence of increased *Cdk6* activity. As no candidate genes were identified to regulate the length of S-phase, I tested the hypothesis that the reduction in S-phase was due to an increase in the proportion of differentiative to proliferative divisions.

As a key regulator of G1-phase length, the increase in *Cdk6* microarray expression provided a viable candidate for *Gli3's* regulation of G1-phase, complimenting other studies providing evidence that *Gli3* regulates *Cdk6* in the limb bud (Lopez-Rios *et al*., 2012; Vokes *et al.*, 2008). To determine if the up-regulation of *Cdk6* at E10.5 in the *Gli3*$^{Xt/Pdn}$ embryo had any measurable output, I examined the level of pRb hyperphosphorylation. In concert with the D-type cyclins, *Cdk6* hyperphosphorylates Rb thereby inhibiting its repression of E2F transcription factors, allowing for expression of G1- to S-phase progression genes. If the increase in *Cdk6* expression had any effect on the cell, I would have expected hyperphosphorylated Rb (pRb) to be increased.

Indeed, in the E11.5 lateral cortex, where I measured a reduction in G1-phase length in apical progenitors, I saw an increase in apical progenitor pRb expression. In the medial cortex, I was unable to accurately measure G1-phase length in the apical progenitor population and unable to measure G1-phase in the basal progenitor population, but there were no differences in the proportions of apical and basal progenitors or early-born neurons, and no change in cell cycle exit, reflecting no difference in pRb expression. At E12.5, the proportion of pRb$^{+}$ cells was unaltered in the mutant lateral apical progenitor population compared to control, whilst G1-phase length was reduced. This suggested that G1-phase length may be regulated in a non *Cdk6*-dependent manner also. Conversely, the proportions of pRb$^{+}$ basal progenitors in the lateral and medial cortex were increased in the mutant compared to control, whilst G1-phase length was unaltered. As *Gli3* shows reduced expression in basal

progenitors, it is likely that *Gli3* also indirectly regulates pRb hyperphosphorylation via a *Cdk6*-independent mechanism.

Besides my finding of an increase in *Cdk6* expression at E10.5 and an increase in pRb expression in the E11.5 mutant lateral cortex coinciding with a reduction in G1-phase length, a *Gli3* binding site has been identified in the *Cdk6* promoter (Lopez-Rios *et al*., 2012; Vokes *et al.*, 2008). Hasenpusch-Theil *et al.* (2018) confirmed that binding of Gli3 to this site results in a decrease in *Cdk6* expression *in vitro*. To test if *Gli3* was able to regulate G1-phase length through *Cdk6* regulation, I attempted to inhibit *Cdk6 in vitro* in organotypic slices cultures using palbociclib, a *Cdk4/6*-specific inhibitor. As a measure of *Cdk6* inhibition, I assessed the proportion of $pRb^+$ cells in the presence of palbociclib compared to in the presence of DMSO, as control. To evaluate the concentration of palbociclib required to alter pRb expression, I used CD1 embryos. In these embryos, a concentration of 0.38μg/ml palbociclib was enough to reduce the proportion of $pRb^+$ cells in slice cultures after 24 hrs. I wanted to use a low concentration of palbociclib to reduce the chance of blocking progenitors in G1-phase and only prolonging the phase length. I subsequently repeated the experiment with palbociclib in $Gli3^{Xt/Pdn}$ mutant slices alongside their littermate controls.

In the E11.5 lateral mutant cortex, I recorded an increase in the proportion of apical progenitors and decreased basal progenitor and neuronal proportions, with a decrease in apical progenitor G1-phase length and increase in $pRb^+$ apical progenitor proportion. Therefore, I first evaluated the effect of palbociclib on slices harvested from E11.5 embryos. When cultured for 24 hrs, both control and mutant slices failed to grow correctly in the presence of either palbociclib or DMSO. Slices from both lost the characteristic shape of coronal brain slices, making it difficult to accurately identify lateral and medial cortex. Furthermore, $pRb^+$ cells began to form rosette-like structures, also making it difficult to stipulate if they represented apical or basal progenitors. To assess if the presence of palbociclib or DMSO or if the slice culture conditions were responsible for the abnormal growth of the slices, I cultured control slices in the absence of palbociclib and DMSO. These slices also showed abnormal growth, indicating that these experimental conditions were not conducive to growth of slices at this age.

Following this, I repeated the slice cultures with slices from embryos harvested at E12.5. As at E11.5, both control and mutant slices failed to grow correctly in the presence of either palbociclib or DMSO, yet growth of control slices was not as

abnormal as at E11.5. Rosette-like formations of $pRb^+$ cells were still present in control and mutant, making quantification of apical and basal $pRb^+$ progenitors not possible.

Finally, I harvested brains from E13.5 control and *Gli3*$^{Xt/Pdn}$ embryos and cultured slices for 24 hrs. Here, slices from control embryos showed normal growth in culture and resembled slices from E13.5 CD1 embryos after 24 hrs in culture. They retained the characteristic shape of a coronal brain slice of this age, and pRb expression retained its *in vivo* pattern, in the presence of DMSO and palbociclib. This showed that the younger a slice was put into culture, the more atypical its growth was, although I cannot rule out that younger CD1 slices would have not grown normally in culture. Therefore, in terms of this technique, it would be noteworthy to repeat the slice cultures at earlier ages to further examine if the background of the embryos or the age of the slices influenced their behaviour *in vitro*. In contrast to control embryos at E13.5, slices from mutant brains exhibited abnormal growth in culture. Additional tissue was present inside the ventricles and the pRb expression pattern was disrupted, with $pRb^+$ cells forming rosette-like rings of cells. Fotaki *et al*. (2006) described neural progenitors forming rosettes in the cortex of *Gli3*$^{Xt/Xt}$ embryos, and so perhaps the slice culture conditions here attenuated that behaviour of *Gli3* deficient progenitors.

Altogether, I am unable to say if the up-regulation of *Cdk6* in the *Gli3*$^{Xt/Pdn}$ cortex contributed to the reduction in G1-phase length. Therefore, additional experiments are required to further investigate this link. G1-phase lengthening has subsequently been shown to rescue delayed neurogenesis in *Emx1Cre;Gli3*$^{fl/fl}$ embryos after administration of palbociclib to pregnant dams 24 hrs before embryo harvesting (Hasenpusch-Theil *et al.*, 2018). In these mutants, *Cdk6* was also up-regulated and there was a reduction in G1-phase length. Additionally, inhibition of *Cdk6* could be achieved by electroporation of RNAi or a dominant-negative construct against *Cdk6* (Mi *et al.*, 2013). Overexpression of *Cdk6*/*cyclin D1* via electroporation of expression plasmids into control embryos to recapitulate the mutant phenotype may also prove attractive (Lange *et al*., 2009; Pilaz *et al.*, 2009), although as this would not be due to alterations in *Gli3* expression it may not provide insight into the role of *Gli3*.

As well as a reduction in G1-phase length, which many have linked to an increased capacity for proliferative division, I recorded a reduction in S-phase length, which has been linked to an increased capacity for differentiative division. The microarray

analyses did not identify any obvious candidate genes dysregulated in the *Gli3*$^{Xt/Pdn}$ dorsal telencephalon which may have accounted for the alteration in S-phase length and which could be further examined. Instead, I hypothesised that the reduction in S-phase length which I measured at E11.5 and E12.5 in the mutant cortex, particularly in apical progenitors, may have been due to an increase in differentiative divisions. At the population level, a larger proportion of progenitors undergoing differentiative division and exhibiting a shorter S-phase would be measured as a reduction in S-phase length using the BrdU/IdU double labelling method. Therefore, I examined Tis21 expression as a measure of the proportion of progenitors undergoing differentiative division.

In the apical progenitor population, at E11.5 there was a decrease in the proportion of differentiative divisions in the mutant compared to control in the medial cortex, with a tendency towards a decrease in the lateral cortex. There was a potential outlier in the lateral mutant data here, and additional embryos should be examined to determine if this was an outlier or if it reflected the mutant population. Here, S-phase length was decreased in the lateral cortex but unchanged in the medial. The reduction in S-phase length in the lateral cortex could not be accounted for by an alteration in the proportion of proliferative to differentiative divisions, whilst the decrease in differentiative divisions medially did not lead to an alteration in S-phase length. Conversely, in the E12.5 apical progenitor population both laterally and medially there was an increase in the proportion of differentiative divisions, whilst S-phase length was decreased in both locations. Consequently, the imbalance in differentiative to proliferative divisions here may account for the decreases recorded in S-phase length at E12.5 but not E11.5.

In basal progenitors, there was an increase in the proportion of differentiative divisions in the mutant lateral E11.5 population, whilst the medial population was unchanged. As in the apical progenitor population, S-phase length was decreased in the mutant laterally, whilst I was unable to measure it medially. Again, the alteration in differentiative divisions could not account for the reduction in S-phase length laterally. At E12.5, there was no change in the proportion of differentiative to proliferative divisions in the mutant laterally or medially, and S-phase length was unaltered in the lateral cortex.

Overall, a disruption in differentiative to proliferative divisions in the mutant could not fully account for the reductions measured in S-phase length. I therefore propose that

*Gli3* could regulate S-phase length. The microarray was performed on E10.5 dorsal telencephalic tissue, and so it is possible that genes regulating S-phase length only became dysregulated at E11.5 or E12.5. Further, the microarray may not have been sensitive enough to identify genes which were not dysregulated at a high level. The analysis was also performed on whole dorsal telencephalons pooled together, and so examination of the cortex alone would be interesting. Other techniques, such as RNAseq, could be performed on the $Gli3^{Xt/Pdn}$ cortex at E11.5 and E12.5 to identify other potential gene candidates regulating the cell cycle. Indeed, RNAseq was performed on the $Emx1Cre;Gli3^{fl/fl}$ dorsal telencephalic midline specifically (Hasenpusch-Theil *et al*., 2018). At E11.5, when S-phase length was also reduced in this mutant in the midline, *Cyclin A2* was up-regulated and $p21^{Cip1}$, $p27^{Kip1}$ and $p57^{Kip2}$ were down-regulated. *Cyclin A2* is responsible for progressing a cell through S-phase, whilst $p21^{Cip1}$, $p27^{Kip1}$ and $p57^{Kip2}$ are cyclin inhibitors which seek to stall progression through the cell cycle. Therefore, an imbalance in the ratio of cyclins to cyclin inhibitors may have tipped towards increased progression through S-phase in this mutant. Possibly, the same situation arises in the $Gli3^{Xt/Pdn}$ mutant, yet the microarray was not sensitive enough or performed at too early an age to identify these changes.

### 6.4 Synopsis and concluding remarks

The aim of this thesis was to further understand the role of *Gli3* in early dorsal telencephalon development. Through immunofluorescent analyses, I revealed that in the cortex Gli3 protein was expressed primarily in apical progenitors between E11.5 and E12.5, and the intensity of that staining was reduced in the $Gli3^{Xt/Pdn}$ mutant. In this mutant the proportions of apical and basal progenitors and early-born neurons were altered at E11.5 and E12.5, indicating a delay in neurogenesis. As in the limb bud *Gli3* had previously been linked to cell cycle regulation, a factor which can also alter the production of progenitors and neurons, I examined the cell cycle in the $Gli3^{Xt/Pdn}$ cortex. In general, the total cell cycle and particularly G1- and S-phase length were reduced in the mutant at both E11.5 and E12.5, indicating *Gli3* also regulates the cell cycle of cortical progenitors. Through examination of $Gli3^{Xt/Pdn}$ microarray expression data, I identified *Cdk6* as a potential target of *Gli3* for the regulation of G1-

phase in the cortex. However, I was unable to test if reducing *Cdk6* levels in the *Gli3*$^{Xt/Pdn}$ cortex would ameliorate the delay in neurogenesis. Finally, I was also unable to identify any candidate genes which may have mediated the reduction in S-phase length. Instead, I examined the ratio of differentiative to proliferative divisions in the mutant to test whether the reduction in S-phase was due to an alteration in this ratio. Potentially, this could have explained the reduction recorded at E12.5.

Whilst there was little Gli3 protein expression in basal progenitors, I recorded alterations in the proportion of basal progenitors in the mutant at E11.5 and E12.5, alongside a reduction in S-phase and total cell length at E11.5 and alterations in hyperphosphorylated pRb expression at E11.5 and E12.5. Finally, the proportion of basal progenitors undergoing differentiative division was increased in the mutant compared to control at E11.5. Taken together, these results suggest *Gli3* likely regulates basal progenitor dynamics non-cell autonomously. A likely candidate through which these features became dysregulated in the *Gli3*$^{Xt/Pdn}$ mutant was alterations in signalling, which requires much further exploration in the context of basal progenitors in this mutant.

On the other hand, as Gli3 was primarily expressed in apical progenitors and the biggest changes in the features examined occurred within this population, it was easier to hypothesise about these cells. G1-phase length was decreased in these cells at E11.5 and *Cdk6*, described previously as a direct *Gli3* target gene (Lopez-Rios *et al.*, 2012; Vokes *et al*., 2008), was identified as up-regulated 1.59-fold in the E10.5 *Gli3*$^{Xt/Pdn}$ mutant dorsal telencephalon compared to control, alongside an increase in pRb hyperphosphorylation in the E11.5 mutant cortex. This therefore became a good starting point for examining cell cycle regulation by *Gli3* in the cortex. I formulated the hypothesis that a decrease in *Gli3* expression would lead to an increase in *Cdk6* expression, resulting in increased pRb hyperphosphorylation. This would lead to a de-repression of the E2F family of transcription factors, allowing for transcription of G1- to S-phase progressing genes. Whilst this hypothesis may well reflect the situation in the lateral E11.5 cortex, it did not fit the medial E11.5 cortex, where pRb expression was not significantly increased in the mutant, or for the lateral and medial E12.5 cortex, where again pRb expression was not significantly increased and G1-phase length was not significantly reduced in the medial cortex. Therefore, considering together all of the analyses performed in this study, I would now suggest that *Gli3* exhibits dynamic temporal and spatial regulation over cortical development.

One reason behind this may be due to the uneven progression of neurogenesis across the cortex, progressing rostro-laterally to caudo-medially, but again differences in signalling across the cortex also likely play a major role.

Overall, this thesis has confirmed the existence of a delay in neurogenesis in the *Gli3*$^{Xt/Pdn}$ cortex between E11.5 and E12.5. It is plausible that alterations in the cell cycle due to the reduction in *Gli3* partially underlie this defect. However, this thesis has also highlighted the complexity of the situation in such a mutant, where many factors are altered by the constitutive reduction of a transcription factor known to play key roles in dorsal telencephalon development. In the future, identification of other *Gli3* gene targets will help in understanding the roles played by *Gli3* in cell cycle regulation, as well as in early cortical neurogenesis.

### 6.5 Overall model

In the E11.5 lateral cortex, the proportion of *Gli3*$^{Xt/Pdn}$ apical progenitors was increased compared to control, alongside reduced proportions of basal progenitors and neurons. G1- and S-phase of the cell cycle were also reduced in *Gli3*$^{Xt/Pdn}$ apical progenitors, and so the increased proportion of apical progenitors combined with the obvious expression of Gli3 protein in those cells (figure 6.1 A, B), may signify *Gli3* acting directly upon apical progenitors at E11.5 to cause them to differentiate and exit the cell cycle. However, there was very little Gli3 protein expressed in basal progenitors at this time yet S-phase length was reduced in the mutant compared to control (figure 6.1 A, B). In these cells, it was likely that *Gli3* was acting indirectly to influence S-phase length, and whilst a reduction in S-phase length corresponds with cell cycle exit, I would propose that the reduced basal progenitor proportion likely reflected a reduced production of basal progenitors from apical progenitors.

In the E11.5 medial cortex, Gli3 was expressed at a lower level compared to laterally in both control and *Gli3*$^{Xt/Pdn}$ embryos (figure 6.1 C, D). In the mutant, I did not measure any difference in apical and basal progenitor and neuronal proportions, or cell cycle measurements, compared to control. It is therefore likely that progenitor cell cycle and

proliferation/differentiation were regulated by factors other than *Gli3*, which is why the reduction in Gli3 protein in *Gli3*$^{Xt/Pdn}$ embryos had little effect.

Taken together, the E11.5 high-lateral to low-medial gradient in Gli3 expression may explain why I measured changes in the progenitor and neuronal proportions and the cell cycle in the lateral *Gli3*$^{Xt/Pdn}$ cortex compared to control, but did not measure any changes medially, where Gli3 would normally be expressed at a low level (figure 6.1 A-D). Gli3 expression was largely confined to the apical progenitor population at this age, and so I propose any changes measured in the basal progenitor and neuronal populations were due to indirect effects upon the apical progenitor population.

By E12.5, there appeared to be more Gli3 expression in basal progenitors in control and mutant embryos than at E11.5, and the high-lateral to low-medial gradient was less apparent (figure 6.1 E-H). In the lateral cortex, the proportion of apical progenitors was unaltered in mutant compared to control, whilst there were larger proportions of both basal progenitors and neurons in the mutant. Further, G1-, S-, and M-phase were shorter in mutant apical progenitors, whilst M-phase was longer in mutant basal progenitors (figure 6.1 E, F). As there was a larger proportion of apical progenitors in the mutant at E11.5, and no difference between control and mutant at E12.5, the apical progenitor population effectively decreased in the mutant between the two time points and there was an increase in cell cycle exit and progenitor differentiation. This links to the increased basal progenitor and neuronal proportions. The reduction in S-phase length would correspond with an increase in apical progenitor differentiation, yet the reduction in G1-phase does not, so in lateral apical progenitors perhaps S-phase length is more important than G1-phase length at E12.5, in contrast to E11.5.

The reduced gradient of Gli3 from lateral to medial cortex at E12.5 could explain why I measured differences between the progenitor and neuronal proportions in control and mutant at E12.5 but not E11.5. In the E12.5 medial cortex, the proportion of apical progenitors was reduced in *Gli3*$^{Xt/Pdn}$ embryos compared to control, whilst the proportions of basal progenitors and neurons were increased. Again, S- and M-phase were shorter in the mutant compared to control in apical progenitors (figure 6.1 G, H). As neurogenesis progresses laterally to medially, the decrease in Gli3 gradient may act as a mechanism to allow the medial cortex to catch up with the lateral cortex in neurogenesis. Gli3 expression may be switched on in basal progenitors at E12.5 to allow them to exit the cell cycle and differentiate into neurons.

Altogether, I propose that under wild type conditions in the E11.5 lateral cortex Gli3 is highly expressed in apical progenitors. Here, it acts to prolong G1-phase of the cell cycle, inducing apical progenitor differentiation into basal progenitors and neurons. This prevents the apical progenitor population from over proliferating and resulting in an increased progenitor population, which would favour an increased production of lower layer neurons, as is seen in the *Gli3*$^{Xt/Pdn}$ embryo (Friedrichs *et al*., 2008). In the medial cortex, Gli3 is lowly expressed in comparison with the lateral cortex, and does not appear to impact as greatly upon the cell cycle and so progenitor proliferation and differentiation. By E12.5, the gradient in Gli3 expression between lateral and medial cortex is reduced, and basal progenitors as well as apical progenitors now express Gli3. The role of *Gli3* in the lateral and medial cortex is now similar, acting to lengthen the cell cycle in apical progenitors. The switching on of Gli3 expression in basal progenitors at this time point might act as a mechanism to induce basal progenitors to undergo differentiation into neurons. In summary, the alterations in progenitor and neuronal proportions combined with the alterations in cell cycle highlight the pleiotropic role of *Gli3* in cortical development, allowing different regions of the cortex to mature at different rates dependent upon the level of protein expression.

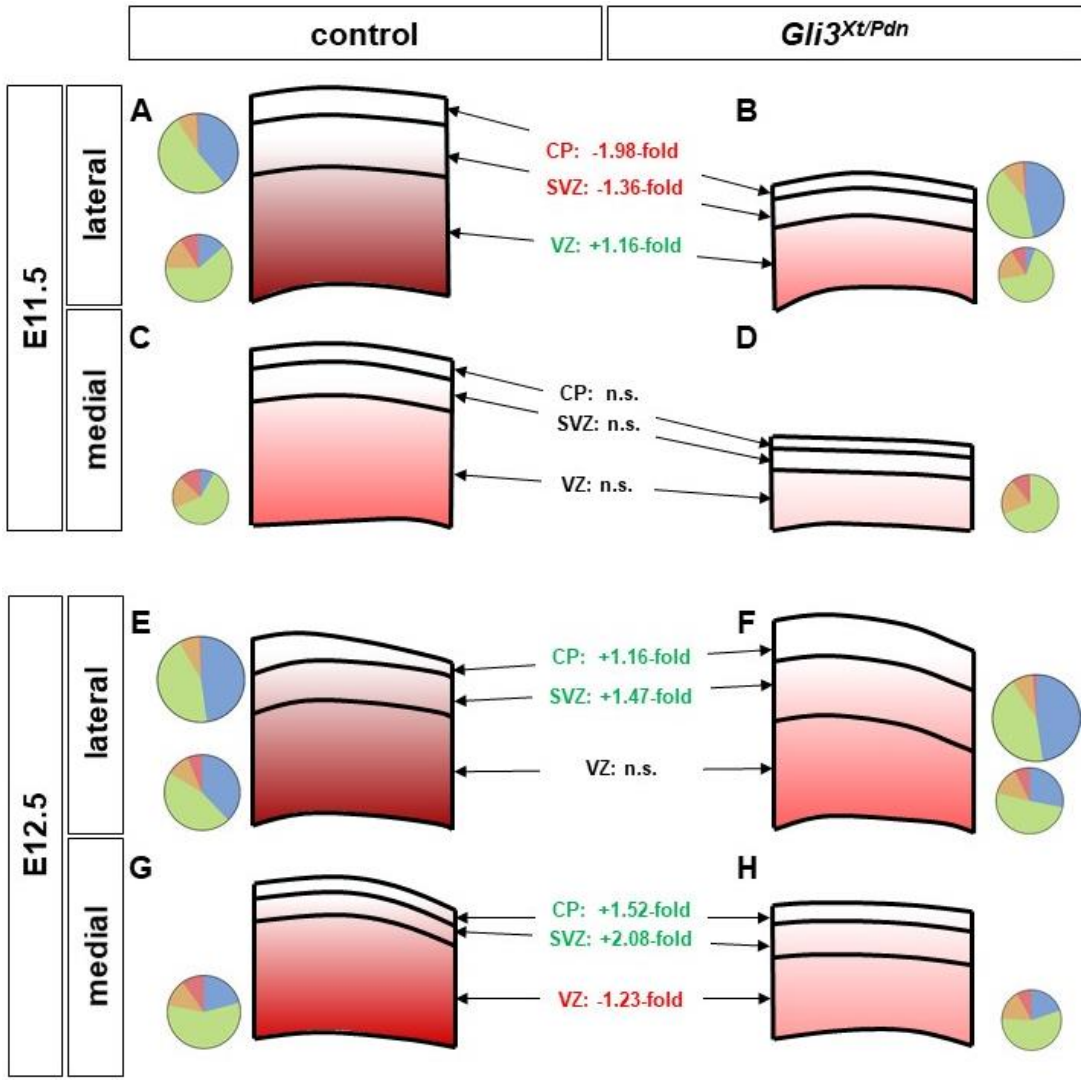


**Figure 6.1: Schematic summarising how differing Gli3 levels across control and *Gli3*$^{Xt/Pdn}$ neocortex impact upon cortical layer proportions and cell cycle phase lengths. A-D.** Representations of E11.5 control (A, C) and *Gli3*$^{Xt/Pdn}$ (B, D) lateral boxes (A, B) and medial boxes (C, D) in which cell counts were performed. The red gradient across boxes shows how the relative level of Gli3 expression differed, although it is important to note that the colour intensity does not represent a quantitative measurement of Gli3 expression. In the control cortex, Gli3 expression was highest laterally in the ventricular zone with little expression in the subventricular zone, and reduced expression in the medial cortex. In the *Gli3*$^{Xt/Pdn}$ cortex, Gli3 expression was reduced compared to control. In the lateral cortex, there was a 1.16-fold increase in the proportion of apical progenitors in the ventricular zone of the mutant, concomitant with 1.36- and 1.98-fold decreases in the proportion of basal progenitors (subventricular zone) and early-born neurons (cortical plate). This was in

alignment with decreases in the cell cycle in both apical and basal progenitors. In the medial cortex, the proportions of apical and basal progenitors and early-born neurons were unaltered in the mutant compared to control, as was the apical cell cycle. **E-H.** Representations of E12.5 control (E, G) and *Gli3*$^{Xt/Pdn}$ (F, H) lateral boxes (E, F) and medial boxes (G, H) in which cell counts were performed. Gli3 expression was highest in the lateral control cortex in the ventricular zone with some expression in the subventricular zone. However, the Gli3 gradient was not as profound between lateral and medial at E12.5 as at E11.5. Gli3 expression was also reduced in the *Gli3*$^{Xt/Pdn}$ cortex compared to control, and although the high-lateral to low-medial gradient was maintained, is was not as apparent as at E11.5. Laterally, the proportion of apical progenitors was unaltered between control and mutant whilst there were 1.47- and 1.16-fold increases in the proportions of basal progenitors and early-born neurons. Here, there was a shortening of the apical progenitor cell cycle. Medially the proportion of apical progenitors was reduced 1.23-fold in the mutant, whilst the proportions of basal progenitors and early-born neurons were increased 2.08- and 1.52-fold, respectively. The apical progenitor cell cycle was reduced in the mutant. CP; cortical plate, SVZ; subventricular zone, VZ; ventricular zone.

## Bibliography


Ali, F., Hindley, C., McDowell, G., Deibler, R., Jones, A., Kirschner, M., Guillemot, F., Philpott, A. (2011). Cell cycle-regulated multi-site phosphorylation of Neurogenin 2 coordinates cell cycling with differentiation during neurogenesis. *Development*, *138*(19), 4267–4277.

Amaniti, E.-M., Hasenpusch-Theil, K., Li, Z., Magnani, D., Kessaris, N., Mason, J. O., & Theil, T. (2013). Gli3 is required in Emx1+ progenitors for the development of the corpus callosum. *Developmental Biology*, *376*(2), 113–124.

Arai, Y., Pulvers, J. N., Haffner, C., Schilling, B., Nüsslein, I., Calegari, F., & Huttner, W. B. (2011). Neural stem and progenitor cells shorten S-phase on commitment to neuron production. *Nature Communications*, *2*, 154.

Assimacopoulos, S., Grove, E. A., & Ragsdale, C. W. (2003). Identification of a Pax6-dependent epidermal growth factor family signaling source at the lateral edge of the embryonic cerebral cortex. *The Journal of Neuroscience : The Official Journal of the Society for Neuroscience*, *23*(16), 6399–6403.

Bielle, F., Griveau, A., Narboux-Nême, N., Vigneau, S., Sigrist, M., Arber, S., Wassef, M., Pierani, A. (2005). Multiple origins of Cajal-Retzius cells at the borders of the developing pallium. *Nature Neuroscience*, *8*(8), 1002–1012.

Bishop, K. M., Goudreau, G., & Leary, D. D. M. (2000). Regulation of Area Identity in the Mammalian Neocortex by Emx2 and Pax6. *Science*, *288*(5464), 344 LP-349.

Blagosklonny, M. V., & Pardee, A. B. (2002). The restriction point of the cell cycle. *Cell Cycle*, *1*(2), 103–110.

Borello, U., Cobos, I., Long, J. E., Murre, C., & Rubenstein, J. L. R. (2008). FGF15 promotes neurogenesis and opposes FGF8 function during neocortical development. *Neural Development*, *3*(1), 17.

Boyle, E. I., Weng, S., Gollub, J., Jin, H., Botstein, D., Michael, J., & Sherlock, G. (2011). GO::TermFinder—open source software for accessing Gene Ontology information and finding significantly enriched Gene Ontology terms associated with a list of genes. *Bioinformatics*, *20*(18), 3710–3715.

Büscher, D., Grotewold, L., & Rüther, U. (1998). The Xt(J) allele generates a Gli3

fusion transcript. *Mammalian Genome*, *9*(8), 676–678.

Calegari, F., & Huttner, W. (2003). An inhibition of cyclin-dependent kinases that lengthens, but does not arrest, neuroepithelial cell cycle induces premature neurogenesis. *Journal of Cell Science*, *116*(24), 4947–4955.

Chenn, A., & Walsh, C. (2002). Regulation of cerebral cortical size by control of cell cycle exit in neural precursors. *Science*, *297*(July), 365–370.

Chiang, C., Litingtung, Y., Lee, E., Young, K. E., Corden, J. L., Westphal, H., & Beachy, P. A. (1996). Cyclopia and defective axial patterning in mice lacking Sonic hedgehog gene function. *Nature*, *383*, 407.

Chizhikov, V. V, & Millen, K. J. (2004). Mechanisms of roof plate formation in the vertebrate CNS. *Nature Reviews Neuroscience*, *5*(10), 808–812.

Choi, Y. J., & Anders, L. (2014). Signaling through cyclin D-dependent kinases. *Oncogene*, *33*(15), 1890–1903.

Colas, J.-F., & Schoenwolf, G. C. (2001). Towards a cellular and molecular understanding of neurulation. *Developmental Dynamics*, *221*(2), 117–145.

Corbin, J. G., Rutlin, M., Gaiano, N., & Fishell, G. (2003). Combinatorial function of the homeodomain proteins Nkx2.1 and Gsh2 in ventral telencephalic patterning. *Development*, *130*(20), 4895 LP-4906.

Crossley, P. H., Martinez, S., Ohkubo, Y., & Rubenstein, J. L. (2001). Coordinate expression of Fgf8, Otx2, Bmp4, and Shh in the rostral prosencephalon during development of the telencephalic and optic vesicles. *Neuroscience*, *108*(2), 183–206.

Danesin, C., Peres, J. N., Johansson, M., Snowden, V., Cording, A., Papalopulu, N., & Houart, C. (2009). Integration of Telencephalic Wnt and Hedgehog Signaling Center Activities by Foxg1. *Developmental Cell*, *16*(4), 576–587.

Dave, R. K., Ellis, T., Toumpas, M. C., Robson, J. P., Julian, E., Adolphe, C., Bartlett, P. F., Cooper, H. M., Reynolds, B. A., Wainwright, B. J. (2011). Sonic hedgehog and notch signaling can cooperate to regulate neurogenic divisions of neocortical progenitors. *PloS One*, *6*(2), e14680.

De Carlos, J. A., & O'Leary, D. D. M. (1992). Growth and Targeting Cortical Pathways of Subplate Axons and Establishment of Major. *The Journal of Neuroscience*,

*12*(4), 1194–1211.

Dehay, C., & Kennedy, H. (2007). Cell-cycle control and cortical development. *Nature Reviews. Neuroscience*, *8*(6), 438–450.

Derynck, R., & Zhang, Y. E. (2003). Smad-dependent and Smad-independent pathways in TGF-β family signalling. *Nature*, *425*, 577.

DiPippo, A. J., Patel, N. K., & Barnett, C. M. (2016). Cyclin-Dependent Kinase Inhibitors for the Treatment of Breast Cancer: Past, Present, and Future. *Pharmacotherapy*, *36*(6), 652–667.

Dou, C. L., Li, S., & Lai, E. (1999). Dual role of brain factor-1 in regulating growth and patterning of the cerebral hemispheres. *Cerebral Cortex*, *9*(6), 543–550.

Dyson, N. (1998). The regulation of E2F by pRB-family?proteins. *Genes and Development*, *12*(617), 2245–2262.

Echelard, Y., Epstein, D., St-Jacques, B., Shen, L., Mohler, J., McMahon, J., & McMahon, A. (1993). Sonic hedgehog, a member of a family of putative signaling molecules, is implicated in the regulation of CNS polarity. *Cell*, *75*, 1417–1430.

Englund, C., Fink, A., Lau, C., Pham, D., Daza, R. a M., Bulfone, A., Kowalczyk, T., Hevner, R. F. (2005). Pax6, Tbr2, and Tbr1 are expressed sequentially by radial glia, intermediate progenitor cells, and postmitotic neurons in developing neocortex. *The Journal of Neuroscience*, *25*(1), 247–251.

Estivill-Torrus, G., Pearson, H., van Heyningen, V., Price, D. J., & Rashbass, P. (2002). Pax6 is required to regulate the cell cycle and the rate of progression from symmetrical to asymmetrical division in mammalian cortical progenitors. *Development*, *129*(2), 455–466.

Favarolo, M. B., & López, S. L. (2018). Notch signaling in the division of germ layers in bilaterian embryos. *Mechanisms of Development*.

Fernandes, M., Gutin, G., Alcorn, H., McConnell, S. K., & Hébert, J. M. (2007). Mutations in the BMP pathway in mice support the existence of two molecular classes of holoprosencephaly. *Development*, *134*(21), 3789 LP-3794.

Fotaki, V., Yu, T., Zaki, P. a, Mason, J. O., & Price, D. J. (2006). Abnormal positioning of diencephalic cell types in neocortical tissue in the dorsal telencephalon of mice lacking functional Gli3. *The Journal of Neuroscience*, *26*(36), 9282–9292.

Frantz, G. D., & McConnell, S. K. (1996). Restriction of late cerebral cortical progenitors to an upper-layer fate. *Neuron*, *17*(1), 55–61.

Friedrichs, M., Larralde, O., Skutella, T., & Theil, T. (2008). Lamination of the cerebral cortex is disturbed in Gli3 mutant mice. *Developmental Biology*, *318*(1), 203–214.

Fry, D. W., Harvey, P. J., Keller, P. R., Elliott, W. L., Meade, M., Trachet, E., Albassam, M., Zheng, X., Leopold, W. R., Pryer, N. K., Toogood, P. L. (2004). Specific inhibition of cyclin-dependent kinase 4/6 by PD 0332991 and associated antitumor activity in human tumor xenografts. *Molecular Cancer Therapeutics*, *3*(11), 1427–1438.

Fuccillo, M., Rallu, M., McMahon, A. P., & Fishell, G. (2004). Temporal requirement for hedgehog signaling in ventral telencephalic patterning. *Development (Cambridge, England)*, *131*(20), 5031–5040.

Fukuchi-Shimogori, T., & Grove, E. A. (2001). Neocortex Patterning by the Secreted Signaling Molecule FGF8. *Science*, *294*(5544), 1071 LP-1074.

Fukuchi-Shimogori, T., & Grove, E. A. (2003). Emx2 patterns the neocortex by regulating FGF positional signaling. *Nature Neuroscience*, *6*(8), 825–831.

Furuta, Y., Piston, D. W., & Hogan, B. L. (1997). Bone morphogenetic proteins (BMPs) as regulators of dorsal forebrain development. *Development*, *124*(11), 2203–2212.

Galceran, J., Miyashita-Lin, E. M., Devaney, E., Rubenstein, J. L., & Grosschedl, R. (2000). Hippocampus development and generation of dentate gyrus granule cells is regulated by LEF1. *Development*, *127*(3), 469 LP-482.

Gámez, B., Rodriguez-Carballo, E., & Ventura, F. (2013). BMP signaling in telencephalic neural cell specification and maturation. *Frontiers in Cellular Neuroscience*, *7*(June), 87.

Garel, S., Huffman, K. J., & Rubenstein, J. L. R. (2003). Molecular regionalization of the neocortex is disrupted in Fgf8 hypomorphic mutants. *Development*, *130*(9), 1903 LP-1914.

Gelman, D. M., & Marín, O. (2010). Generation of interneuron diversity in the mouse cerebral cortex. *European Journal of Neuroscience*, *31*(12), 2136–2141.

Glickstein, S. B., Alexander, S., & Ross, M. E. (2007). Differences in cyclin D2 and D1 protein expression distinguish forebrain progenitor subsets. *Cerebral Cortex*, *17*(3), 632–642.

Goffinet. (1979). An early development defect in the cerebral cortex of the reeler mouse. *Anatomy and Embryology*, *157*(2), 205–216.

Gonzales, K. A. U., Liang, H., Lim, Y. S., Chan, Y. S., Yeo, J. C., Tan, C. P., Gao, B., Le, B., Tan, Z. Y., Low, K. Y., Liou, Y. C., Bard, F., Ng, H. H. (2015). Deterministic Restriction on Pluripotent State Dissolution by Cell-Cycle Pathways. *Cell*, *162*(3), 564–579.

Goodrich, L. V, Johnson, R. L., Milenkovic, L., & Mcmahon, J. A. (1996). Conservation of the hedgehog/patched signalling pathway from flies to mice: induction of a mouse patched gene by Hedgehog. *Genes and Development*, *10*(3), 301–312.

Götz, M., Stoykova, A., & Gruss, P. (1998). Pax6 controls radial glia differentiation in the cerebral cortex. *Neuron*, *21*(5), 1031–1044.

Gratzner, H. G. (1982). Monoclonal antibody to 5-bromo- and 5-iododeoxyuridine: A new reagent for detection of DNA replication. *Science*, *218*(4571), 474–475.

Grove, E. A., Tole, S., Limon, J., Yip, L., & Ragsdale, C. W. (1998). The hem of the embryonic cerebral cortex is defined by the expression of multiple Wnt genes and is compromised in Gli3-deficient mice. *Development*, *125*(12), 2315–2325.

Gupta, S., & Sen, J. (2016). Roof plate mediated morphogenesis of the forebrain: New players join the game. *Developmental Biology*, *413*(2), 145–152.

Hall, P. A., Levison, D. A., Woods, A. L., Yu, C. C., Kellock, D. B., Watkins, J. A., Barnes, D. M., Gillett, C. E., Camplejohn, R., Dover, R. (1990). Proliferating cell nuclear antigen (PCNA) immunolocalization in paraffin sections: an index of cell proliferation with evidence of deregulated expression in some neoplasms. *The Journal of Pathology*, *162*(4), 285–294.

Hanashima, C., Li, S. C., Shen, L., Lai, E., & Fishell, G. (2004). Foxg1 Suppresses Early Cortical Cell Fate. *Science*, *303*(5654), 56–59.

Harbour, J., Luo, R., Santi, A., Postigo, A., & Dean, D. (1999). Cdk phosphorylation triggers sequential intramolecular interactions that progressively block Rb functions as cells move through G1. *Cell*, *98*(6), 859–869.

Harbour, J. W., & Dean, D. C. (2000). The Rb/E2F pathway: Expanding roles and emerging paradigms. *Genes and Development*, *14*(19), 2393–2409.

Hasenpusch-Theil, K., Watson, J. A., & Theil, T. (2015). Direct Interactions Between Gli3, Wnt8b, and Fgfs Underlie Patterning of the Dorsal Telencephalon. *Cerebral Cortex*, *27*(2), 1137–1148.

Hasenpusch-theil, K., West, S., Kelman, A., Kozic, Z., Horrocks, S., McMahon, A. P., Price, D. J., Mason, J. O., Theil, T. (2018). Gli3 controls the onset of cortical neurogenesis by regulating the radial glial cell cycle through Cdk6 expression, 1–12.

Haubensak, W., Attardo, A., Denk, W., & Huttner, W. B. (2004). Neurons arise in the basal neuroepithelium of the early mammalian telencephalon: a major site of neurogenesis. *Proceedings of the National Academy of Sciences of the United States of America*, *101*(9), 3196–3201.

Hayasaka, I., Nakatsuka, T., Fujii, T., Naruse, I., & Oda, S. (1980). Polydactyly Nagoya, Pdn: A new mutant gene in the mouse. *Experimental Animals*, *29*(4), 391–395.

Hébert, J. M., Mishina, Y., & McConnell, S. K. (2002). BMP signaling is required locally to pattern the dorsal telencephalic midline. *Neuron*, *35*(6), 1029–1041.

Hindley, C., & Philpott, A. (2012). Co-ordination of cell cycle and differentiation in the developing nervous system. *The Biochemical Journal*, *444*(3), 375–382.

Holm, P. C., Mader, M. T., Haubst, N., Wizenmann, A., Sigvardsson, M., & Götz, M. (2007). Loss- and gain-of-function analyses reveal targets of Pax6 in the developing mouse telencephalon. *Molecular and Cellular Neuroscience*, *34*(1), 99–119.

Hsieh-Li, H. M., Witte, D. P., Szucsik, J. C., Weinstein, M., Li, H., & Potter, S. S. (1995). Gsh-2, a murine homeobox gene expressed in the developing brain. *Mechanisms of Development*, *50*(2–3), 177–186.

Hui, C. C., & Joyner, A. L. (1993). A Mouse Model of Greig Cephalopolysyndactyly Syndrome - The Extra-Toes(J) Mutation Contains an Intragenic Deletion of the Gli3 Gene. *Nature Genetics*, *3*(3), 241–246.

Hui, C. C., Slusarski, D., Platt, K. A., Holmgren, R., & Joyner, A. L. (1994). Expression

of three mouse homologs of the Drosophila segment polarity gene cubitus interruptus, Gli, Gli-2, and Gli-3, in ectoderm- and mesoderm-derived tissues suggests multiple roles during postimplantation development. *Developmental Biology*, *162*(2), 402–413.

Iacopetti, P., Michelini, M., Stuckmann, I., Oback, B., Aaku-Saraste, E., & Huttner, W. (1999). Expression of the antiproliferative gene TIS21 at the onset of neurogenesis identifies single neuroepithelial cells that switch from proliferative to neuron-generating division. *Proceedings of the National Academy of Sciences*, *96*, 4639–4644.

Ishikawa, Y., Yamamoto, N., Yoshimoto, M., & Ito, H. (2012). The primary brain vesicles revisited: are the three primary vesicles (forebrain/midbrain/hindbrain) universal in vertebrates? *Brain, Behavior and Evolution*, *79*(2), 75–83.

Itoh, N., & Ornitz, D. M. (2004). Evolution of the Fgf and Fgfr gene families. *Trends in Genetics*. Elsevier Current Trends. 20(11), 563-569.

Jacobs, E. C., Campagnoni, C., Kampf, K., Reyes, S. D., Kalra, V., Handley, V., Xie, Y.-Y., Hong-Hu, Y., Spreur, V., Fisher, R. S., Campagnoni, A. T. (2007). Visualization of corticofugal projections during early cortical development in a tau-GFP-transgenic mouse. *The European Journal of Neuroscience*, *25*(1), 17–30.

Johnson, D. R. (1967). Extra-toes: anew mutant gene causing multiple abnormalities in the mouse. *Journal of Embryology and Experimental Morphology*, *17*(June), 543–581.

Jr, V. C., Takahashi, T., & Nowakowski, R. (1995). Numbers, time and neocortical neuronogenesis: a general developmental and evolutionary model. *Trends in Neurosciences*, *18*(9), 379–383.

Kawano, R., Ohta, K., & Lupo, G. (2017). Cadherin-7 enhances Sonic Hedgehog signalling by preventing Gli3 repressor formation during neural tube patterning. *Open Biology*, *7*(12).

Kawano, Y., & Kypta, R. (2003). Secreted antagonists of the Wnt signalling pathway. *Journal of Cell Science*, *116*(13), 2627 LP-2634.

Kiecker, C., & Lumsden, A. (2005). Compartments and their boundaries in vertebrate

brain development. *Nature Reviews Neuroscience*, *6*, 553.

Kohtz, J. D., Baker, D. P., Corte, G., & Fishell, G. (1998). Regionalization within the mammalian telencephalon is mediated by changes in responsiveness to Sonic Hedgehog. *Development*, *125*(24), 5079 LP-5089.

Kollmann, K., Heller, G., Schneckenleithner, C., Warsch, W., Scheicher, R., Ott, R., Schäfer, M., Fajmann, S., Schlederer, M., Schiefer, A. I., Reichart, U., Mayerhofer, M., Hoeller, C., Zöchbauer-Müller, S., Kerjaschki, D., Bock, C., Kenner, L., Hoefler, G., Freissmuth, M., Green, A. R., Moriggl, R., Busslinger, M., Malumbres, M., Sexl, V. (2013). A kinase-independent function of CDK6 links the cell cycle to tumor angiogenesis. *Cancer Cell*, *24*(2), 167–181.

Komada, M., Saitsu, H., Kinboshi, M., Miura, T., Shiota, K., & Ishibashi, M. (2008). Hedgehog signaling is involved in development of the neocortex. *Development*, *135*(16), 2717–2727.

Krawchuk, D., Honma-Yamanaka, N., Anani, S., & Yamanaka, Y. (2013). FGF4 is a limiting factor controlling the proportions of primitive endoderm and epiblast in the ICM of the mouse blastocyst. *Developmental Biology*, *384*(1), 65–71.

Kriegstein, A., & Alvarez-Buylla, A. (2009). The glial nature of embryonic and adult neural stem cells. *Annual Review of Neuroscience*, *32*, 149–184.

Kühl, M., Sheldahl, L. C., Park, M., Miller, J. R., & Moon, R. T. (2000). The Wnt/Ca2+ pathway. *Trends in Genetics*, *16*(7), 279–283.

Kumamoto, T., Toma, K., Gunadi, McKenna, W. L., Kasukawa, T., Katzman, S., Chen, B., Hanashima, C. (2013). Foxg1 Coordinates the Switch from Nonradially to Radially Migrating Glutamatergic Subtypes in the Neocortex through Spatiotemporal Repression. *Cell Reports*, *3*(3), 931–945.

Kuschel, S., Rüther, U., & Theil, T. (2003). A disrupted balance between Bmp/Wnt and Fgf signaling underlies the ventralization of the Gli3 mutant telencephalon. *Developmental Biology*, *260*(2), 484–495.

Lange, C., Huttner, W., & Calegari, F. (2009). Cdk4/cyclinD1 overexpression in neural stem cells shortens G1, delays neurogenesis, and promotes the generation and expansion of basal progenitors. *Cell Stem Cell*, *5*(3), 320–331.

Lee, S. M., Tole, S., Grove, E., & McMahon, A. P. (2000). A local Wnt-3a signal is

required for development of the mammalian hippocampus. *Development*, *127*(3), 457 LP-467.

Lim, S., & Kaldis, P. (2013). Cdks, cyclins and CKIs: roles beyond cell cycle regulation. *Development*, *140*(15), 3079–3093.

Lindsey, B. W., Hall, Z. J., Heuzé, A., Joly, J.-S., Tropepe, V., & Kaslin, J. (2018). The role of neuro-epithelial-like and radial-glial stem and progenitor cells in development, plasticity, and repair. *Progress in Neurobiology*.

Litsiou, A., Hanson, S., & Streit, A. (2005). A balance of FGF, BMP and WNT signalling positions the future placode territory in the head. *Development*, *132*(18), 4051 LP-4062.

Lopez-Rios, J., Speziale, D., Robay, D., Scotti, M., Osterwalder, M., Nusspaumer, G., Galli, A., Holländer, G., Kmita, M., Zeller, R. (2012). GLI3 constrains digit number by controlling both progenitor proliferation and BMP-dependent exit to chondrogenesis. *Developmental Cell*, *22*(4), 837–848.

Magnani, D., Hasenpusch-Theil, K., Jacobs, E. C., Campagnoni, A. T., Price, D. J., & Theil, T. (2010). The Gli3 hypomorphic mutation Pdn causes selective impairment in the growth, patterning, and axon guidance capability of the lateral ganglionic eminence. *The Journal of Neuroscience*, *30*(41), 13883–13894.

Magnani, D., Hasenpusch-Theil, K., & Theil, T. (2013). Gli3 controls subplate formation and growth of cortical axons. *Cerebral Cortex*, *23*(11), 2542–2551.

Maître, J.-L. (2017). Mechanics of blastocyst morphogenesis. *Biology of the Cell*, *109*(9), 323–338.

Mallamaci, A., Muzio, L., Chan, C.-H., Parnavelas, J., & Boncinelli, E. (2000). Area identity shifts in the early cerebral cortex of Emx2−/− mutant mice. *Nature Neuroscience*, *3*, 679.

Marín, O., & Rubenstein, J. L. R. (2001). A long, remarkable journey: Tangential migration in the telencephalon. *Nature Reviews Neuroscience*, *2*(11), 780–790.

Martynoga, B., Drechsel, D., Guillemot, F., Ochoa-espinosa, A., Affolter, M., Fedoriw, A., & Mugford, J. (2012). Molecular Control of Neurogenesis: A View from the Mammalian Cerebral Cortex. *Perspectives in Biology*, *4*, 1–14.

Martynoga, B., Morrison, H., Price, D. J., & Mason, J. O. (2005). Foxg1 is required for

specification of ventral telencephalon and region-specific regulation of dorsal telencephalic precursor proliferation and apoptosis. *Developmental Biology*, *283*(1), 113–127.

McConnell, S. K., Ghosh, A., & Shatz, C. J. (1989). Subplate neurons pioneer the first axon pathway from the cerebral cortex. *Science*, *245*(4921), 978–982.

McConnell, S., & Kaznowski, C. (1991). Cell cycle dependence of laminar determination in developing neocortex. *Science*, *254*(5029), 282–285.

Mi, D., Carr, C. B., Georgala, P. A., Huang, Y. T., Manuel, M. N., Jeanes, E., … Price, D. J. (2013). Pax6 Exerts regional control of cortical progenitor proliferation via direct repression of Cdk6 and Hypophosphorylation of pRb. *Neuron*, *78*(2), 269–284.

Miyata, T., Kawaguchi, A., Okano, H., & Ogawa, M. (2001). Asymmetric inheritance of radial glial fibers by cortical neurons. *Neuron*, *31*(5), 727–741.

Molyneaux, B. J., Arlotta, P., Menezes, J. R. L., & Macklis, J. D. (2007). Neuronal subtype specification in the cerebral cortex. *Nature Reviews. Neuroscience*, *8*(6), 427–437.

Morris, S. A., Teo, R. T. Y., Li, H., Robson, P., Glover, D. M., & Zernicka-Goetz, M. (2010). Origin and formation of the first two distinct cell types of the inner cell mass in the mouse embryo. *Proceedings of the National Academy of Sciences of the United States of America*, *107*(14), 6364–6369.

MuhChyi, C., Juliandi, B., Matsuda, T., & Nakashima, K. (2013). Epigenetic regulation of neural stem cell fate during corticogenesis. *International Journal of Developmental Neuroscience*, *31*(6), 424–433.

Munji, R. N., Choe, Y., Li, G., Siegenthaler, J. A., & Pleasure, S. J. (2011). Wnt Signaling Regulates Neuronal Differentiation of Cortical Intermediate Progenitors. *The Journal of Neuroscience*, *31*(5), 1676 LP-1687.

Naruse, I., Keino, H., Masaki, S., & Yamada, Y. (2000). Mechanism of polydactyly manifestation in mice and its extrapolation to humans. *Congenital Anomalies*, *40*, S25–S33.

Nguyen, L., Besson, A., Heng, J. I.-T., Schuurmans, C., Teboul, L., Parras, C., Philpott, A., Roberts, J. M., Guillemot, F. (2006). p27kip1 independently

promotes neuronal differentiation and migration in the cerebral cortex. *Genes & Development*, *20*(11), 1511–1524.

Nishi, Y., Zhang, X., Jeong, J., Peterson, K. A., Vedenko, A., Bulyk, M. L., Hide, W. A., McMahon, A. P. (2015). A direct fate exclusion mechanism by Sonic hedgehog-regulated transcriptional repressors. *Development*, *142*(19), 3286–3293.

Noctor, S. C., Martínez-Cerdeño, V., Ivic, L., & Kriegstein, A. R. (2004). Cortical neurons arise in symmetric and asymmetric division zones and migrate through specific phases. *Nature Neuroscience*, *7*(2), 136–144.

Nowakowski, R. S., Lewin, S. B., & Miller, M. W. (1989). Bromodeoxyuridine immunohistochemical determination of the lengths of the cell cycle and the DNA-synthetic phase for an anatomically defined population. *Journal of Neurocytology*, *18*(3), 311–318.

Nowakowski, T. J., Fotaki, V., Pollock, A., Sun, T., Pratt, T., & Price, D. J. (2013). MicroRNA-92b regulates the development of intermediate cortical progenitors in embryonic mouse brain. *Proceedings of the National Academy of Sciences*, *110*(17), 7056–7061.

Orenic, T. V, Slusarski, D. C., Kroll, K. L., & Holmgren, R. A. (1990). Cloning and characterization of the segment polarity gene cubitus interruptus Dominant of Drosophila. *Genes & Development*, *4*(6), 1053–1067.

Ornitz, D. M., & Itoh, N. (2015). The Fibroblast Growth Factor signaling pathway. *Developmental Biology*, *4*(3), 215–266.

Panchision, D. M., Pickel, J. M., Studer, L., Lee, S.-H., Turner, P. A., Hazel, T. G., & McKay, R. D. G. (2001). Sequential actions of BMP receptors control neural precursor cell production and fate. *Genes & Development* , *15*(16), 2094–2110.

Paridaen, J., & Huttner, W. (2014). Neurogenesis during development of the vertebrate central nervous system. *EMBO Reports*, *15*(4), 351–364.

Parthasarathy, S., Srivatsa, S., Nityanandam, A., & Tarabykin, V. (2014). Ntf3 acts downstream of Sip1 in cortical postmitotic neurons to control progenitor cell fate through feedback signaling. *Development*, *141*(17), 3324–3330.

Pavletich, N. P., & Pabo, C. O. (1993). Crystal Structure of a GLI-DNA Complex :

Perspectives on Zinc Five-Finger New Fingers. *Science*, *261*(5129), 1701–1707.

Pereira, J. D., Sansom, S. N., Smith, J., Dobenecker, M.-W., Tarakhovsky, A., & Livesey, F. J. (2010). Ezh2, the histone methyltransferase of PRC2, regulates the balance between self-renewal and differentiation in the cerebral cortex. *Proceedings of the National Academy of Sciences of the United States of America*, *107*(36), 15957–15962.

Pilaz, L.-J., Patti, D., Marcy, G., Ollier, E., Pfister, S., Douglas, R. J., Betizeau, M., Gautier, E., Cortay, V., Doerflinger, N., Kennedy, H., Dehay, C. (2009). Forced G1-phase reduction alters mode of division, neuron number, and laminar phenotype in the cerebral cortex. *Proceedings of the National Academy of Sciences of the United States of America*, *106*(51), 21924–21929.

Pilaz, L. J., McMahon, J. J., Miller, E. E., Lennox, A. L., Suzuki, A., Salmon, E., & Silver, D. L. (2016). Prolonged Mitosis of Neural Progenitors Alters Cell Fate in the Developing Brain. *Neuron*, *89*(1), 83–99.

Pollen, A. A, Nowakowski, T. J., Shuga, J., Wang, X., Leyrat, A. a, Lui, J. H., Li, N., Szpankowski, L., Fowler, B., Chen, P., Ramalingam, N., Sun, G., Thu, M., Norris, M., Lebofsky, R., Toppani, D., Kemp, D. W., Wong, M., Clerkson, B., Jones, B. N., Wu, S., Knutsson, L., Alvarado, B., Wang, J., Weaver, L. S., May, A. P., Jones, R. C., Unger, M. A., Kriegstein, A. R., West, J. A A. (2014). Low-coverage single-cell mRNA sequencing reveals cellular heterogeneity and activated signaling pathways in developing cerebral cortex. *Nature Biotechnology*, *32*(10), 1053–1058.

Pozarowski, P., & Darzynkiewicz, Z. (2004). Analysis of Cell Cycle by Flow Cytometry. In A. H. Schönthal (Ed.), *Checkpoint Controls and Cancer: Volume 2: Activation and Regulation Protocols* (pp. 301–311). Totowa, NJ: Humana Press.

Price, D. J., Aslam, S., Tasker, L., & Gillies, K. (1997). Fates of the earliest generated cells in the developing murine neocortex. *The Journal of Comparative Neurology*, *377*(3), 414–422.

Price, D., Jarman, A., Mason, J., & Kind, P. (2011). *Building Brains: An Introduction to Neural Development*. *Building Brains: An Introduction to Neural Development*. Chichester, UK: John Wiley & Sons, Ltd.

Purves, D., Augustine, G. J., Fitzpatrick, D., Hall, W. C., LaMantia, A.-S., McNamara,

J. O., & White, L. E. (2008). *Neuroscience* (4th ed.). Sinauer Associates, Inc.

Quinn, J. C., Molinek, M., Martynoga, B. S., Zaki, P. A., Faedo, A., Bulfone, A., Hevner, R. F., West, J. D., Price, D. J. (2007). Pax6 controls cerebral cortical cell number by regulating exit from the cell cycle and specifies cortical cell identity by a cell autonomous mechanism. *Developmental Biology*, *302*(1), 50–65.

Rallu, M., Corbin, J. G., & Fishell, G. (2002). Parsing the prosencephalon. *Nature Reviews Neuroscience*, *3*(12), 943–951.

Rash, B. G., & Grove, E. A. (2007). Patterning the Dorsal Telencephalon: A Role for Sonic Hedgehog? *Journal of Neuroscience*, *27*(43), 11595–11603.

Rash, B. G., Lim, H. D., Breunig, J. J., & Vaccarino, F. M. (2011). FGF signaling expands embryonic cortical surface area by regulating Notch-dependent neurogenesis. *The Journal of Neuroscience*, *31*(43), 15604–15617.

Roccio, M., Schmitter, D., Knobloch, M., Okawa, Y., Sage, D., & Lutolf, M. P. (2013). Predicting stem cell fate changes by differential cell cycle progression patterns. *Development*, *140*(2), 459–470.

Sansom, S. N., Griffiths, D. S., Faedo, A., Kleinjan, D.-J., Ruan, Y., Smith, J., van Heyningen, V., Rubenstein, J. L., Livesey, F. J. (2009). The Level of the Transcription Factor Pax6 Is Essential for Controlling the Balance between Neural Stem Cell Self-Renewal and Neurogenesis. *PLoS Genetics*, *5*(6), e1000511.

Saxena, M., Agnihotri, N., & Sen, J. (2018). Perturbation of canonical and non-canonical BMP signaling affects migration, polarity and dendritogenesis of mouse cortical neurons. *Development (Cambridge, England)*, *145*(1), dev147157.

Scardigli, R., Bäumer, N., Gruss, P., Guillemot, F., & Le Roux, I. (2003). Direct and concentration-dependent regulation of the proneural gene Neurogenin2 by Pax6. *Development*, *130*(14), 3269 LP-3281.

Seuntjens, E., Nityanandam, A., Miquelajauregui, A., Debruyn, J., Stryjewska, A., Goebbels, S., Nave, K. A., Huylebroeck, D., Tarabykin, V. (2009). Sip1 regulates sequential fate decisions by feedback signaling from postmitotic neurons to progenitors. *Nature Neuroscience*, *12*(11), 1373–1380.

Shen, Q., Wang, Y., Dimos, J. T., Fasano, C. a, Phoenix, T. N., Lemischka, I. R., Ivanova, N. B., Stifani, S., Morrisey, E. E., Temple, S. (2006). The timing of cortical neurogenesis is encoded within lineages of individual progenitor cells. *Nature Neuroscience*, *9*(6), 743–751.

Sherr, C. J. (1996). Cancer cell cycles. *Science (New York, N.Y.)*, *274*(5293), 1672–1677.

Sherr, C. J., Beach, D., & Shapiro, G. I. (2016). Targeting CDK4 and CDK6: From discovery to therapy. *Cancer Discovery*, *6*(4), 353–367.

Shibui, S., Hoshino, T., Vanderlaan, M., & Gray, J. W. (1989). Double labeling with iodo- and bromodeoxyuridine for cell kinetics studies. *Journal of Histochemistry & Cytochemistry*, *37*(7), 1007–1011.

Shimamura, K., Hartigan, D. J., Martinez, S., Puelles, L., & Rubenstein, J. L. (1995). Longitudinal organization of the anterior neural plate and neural tube. *Development*, *121*(12), 3923–3933.

Shimamura, K., & Rubenstein, J. L. (1997). Inductive interactions direct early regionalization of the mouse forebrain. *Development*, *124*(14), 2709–2718.

Shimogori, T., Banuchi, V., Ng, H. Y., Strauss, J. B., & Grove, E. A. (2004). Embryonic signaling centers expressing BMP, WNT and FGF proteins interact to pattern the cerebral cortex. *Development*, *131*(22), 5639–5647.

Shtutman, M., Zhurinsky, J., Simcha, I., Albanese, C., D'Amico, M., Pestell, R., & Ben-Ze'ev, A. (1999). The cyclin D1 gene is a target of the β-catenin/LEF-1 pathway. *Proceedings of the National Academy of Sciences*, *96*(10), 5522–5527.

Silver, D. L., Watkins-Chow, D. E., Schreck, K. C., Pierfelice, T. J., Larson, D. M., Burnetti, A. J., Liaw, H.-J., Myung, K., Walsh, C. A., Gaiano, N., Pavan, W. J. (2010). The exon junction complex component Magoh controls brain size by regulating neural stem cell division. *Nature Neuroscience*, *13*(5), 551–558.

Soufi, A., & Dalton, S. (2016). Cycling through developmental decisions: how cell cycle dynamics control pluripotency, differentiation and reprogramming. *Development*, *143*(23), 4301–4311.

Sultan, K. T., & Shi, S.-H. (2018). Generation of diverse cortical inhibitory interneurons. *Wiley Interdisciplinary Reviews: Developmental Biology*, *7*(2),

e306.

Suryadinata, R., Sadowski, M., & Sarcevic, B. (2010). Control of cell cycle progression by phosphorylation of cyclin-dependent kinase (CDK) substrates. *Bioscience Reports*, *30*(4), 243–255.

Sussel, L., Marin, O., Kimura, S., & Rubenstein, J. L. (1999). Loss of Nkx2.1 homeobox gene function results in a ventral to dorsal molecular respecification within the basal telencephalon: evidence for a transformation of the pallidum into the striatum. *Development*, *126*(15), 3359–3370.

Tam, P. P. L., Williams, E. A., & Chan, W. Y. (1993). Gastrulation in the mouse embryo: Ultrastructural and molecular aspects of germ layer morphogenesis. *Microscopy Research and Technique*, *26*(4), 301–328.

Tempe, D., Casas, M., Karaz, S., Blanchet-Tournier, M.-F., & Concordet, J.-P. (2006). Multisite Protein Kinase A and Glycogen Synthase Kinase 3 Phosphorylation Leads to Gli3 Ubiquitination by SCF TrCP. *Molecular and Cellular Biology*, *26*(11), 4316–4326.

Tetsu, O., & McCormick, F. (1999). β-Catenin regulates expression of cyclin D1 in colon carcinoma cells. *Nature*, *398*(6726), 422–426.

Theil, T. (2005). Gli3 is required for the specification and differentiation of preplate neurons. *Developmental Biology*, *286*(2), 559–571.

Theil, T., Alvarez-Bolado, G., Walter, A., & Rüther, U. (1999). Gli3 is required for Emx gene expression during dorsal telencephalon development. *Development*, *126*(16), 3561–3571.

Theil, T., Aydin, S., Koch, S., Grotewold, L., & Rüther, U. (2002). Wnt and Bmp signalling cooperatively regulate graded Emx2 expression in the dorsal telencephalon. *Development*, *129*(13), 3045–3054.

Thien, H., & Rüther, U. (1999). The mouse mutation Pdn (Polydactyly Nagoya) is caused by the integration of a retrotransposon into the Gli3 gene. *Mammalian Genome*, *10*(3), 205–209.

Tole, S., Ragsdale, C. W., & Grove, E. A. (2000). Dorsoventral patterning of the telencephalon is disrupted in the mouse mutant extra-toes(J). *Developmental Biology*, *217*(2), 254–265.

Toogood, P. L., Harvey, P. J., Repine, J. T., Sheehan, D. J., VanderWel, S. N., Zhou, H., Keller, P. R., McNamara, D. J., Sherry, D., Zhu, T., Brodfuehrer, J., Choi, C., Barvian, M. R., Fry, D. W. (2005). Discovery of a potent and selective inhibitor of cyclin-dependent kinase 4/6. *Journal of Medicinal Chemistry*, *48*(7), 2388–2406.

Vaccarino, F. M., Schwartz, M. L., Raballo, R., Nilsen, J., Rhee, J., Zhou, M., Doetschman, T., Coffin, J. D., Wyland, J. J., Hung, Y.-T. E. (1999). Changes in cerebral cortex size are governed by fibroblast growth factor during embryogenesis. *Nature Neuroscience*, *2*, 246.

Vermeren, M., & Keynes, R. (2010). Vertebrate Central Nervous System: Pattern Formation. In *Encyclopedia of Life Sciences*. Chichester, UK: John Wiley & Sons, Ltd.

Vokes, S. A, Ji, H., Wong, W. H., & Mcmahon, A. P. (2008). A genome-scale analysis of the cis-regulatory circuitry underlying sonic hedgehog-mediated patterning of the mammalian limb. *Genes & Development*, *22*(19), 2651–2663.

Wang, H., Ge, G., Uchida, Y., Luu, B., & Ahn, S. (2011). Gli3 is required for maintenance and fate specification of cortical progenitors. *The Journal of Neuroscience*, *31*(17), 6440–6448.

Wang, L., Hou, S., & Han, Y. G. (2016). Hedgehog signaling promotes basal progenitor expansion and the growth and folding of the neocortex. *Nature Neuroscience*, *19*(7), 888–896.

Wen, X., Lai, C. K., Evangelista, M., Hongo, J.-A., de Sauvage, F. J., & Scales, S. J. (2010). Kinetics of Hedgehog-Dependent Full-Length Gli3 Accumulation in Primary Cilia and Subsequent Degradation. *Molecular and Cellular Biology*, *30*(8), 1910–1922.

Woodhead, G. J., Mutch, C. a, Olson, E. C., & Chenn, A. (2006). Cell-autonomous beta-catenin signaling regulates cortical precursor proliferation. *The Journal of Neuroscience*, *26*(48), 12620–12630.

Wrobel, C. N., Mutch, C. A, Swaminathan, S., Taketo, M. M., & Chenn, A. (2007). Persistent expression of stabilized beta-catenin delays maturation of radial glial cells into intermediate progenitors. *Developmental Biology*, *309*(2), 285–297.

Xuan, S., Baptista, C. A., Balas, G., Tao, W., Soares, V. C., & Lai, E. (1995). Winged

helix transcription factor BF-1 is essential for the development of the cerebral hemispheres. *Neuron*, *14*(6), 1141–1152.

Yabut, O., Ng, H., Fernandez, G., Yoon, K., Kuhn, J., & Pleasure, S. (2016). Loss of Suppressor of Fused in Mid-Corticogenesis Leads to the Expansion of Intermediate Progenitors. *Journal of Developmental Biology*, *4*(4), 29.

Yamanaka, Y., Ralston, A., Stephenson, R. O., & Rossant, J. (2006). Cell and molecular regulation of the mouse blastocyst. *Developmental Dynamics*,

Yip, D. J., Corcoran, C. P., Alvarez-Saavedra, M., DeMaria, A., Rennick, S., Mears, A. J., Rudnicki, M. A., Messier, C., Picketts, D. J. (2012). Snf2l Regulates Foxg1-Dependent Progenitor Cell Expansion in the Developing Brain. *Developmental Cell*, *22*(4), 871–878.

Zarkower, D., & Hodgkin, J. (1992). Molecular analysis of the C. elegans sex-determining gene tra-1: a gene encoding two zinc finger proteins. *Cell*, *70*(2), 237–249.

Zhou, C.-J., Zhao, C., & Pleasure, S. J. (2004). Wnt Signaling Mutants Have Decreased Dentate Granule Cell Production and Radial Glial Scaffolding Abnormalities. *The Journal of Neuroscience*, *24*(1), 121 LP-126.

Zhou, C., Tsai, S. Y., & Tsai, M. J. (2001). COUP-TFI: An intrinsic factor for early regionalization of the neocortex. *Genes and Development*, *15*(16), 2054–2059.